EXPLORATION OF THE BUDDING YEAST KINASE MCK1 IN CELL CYCLE REGULATION

by

Jennifer McQueen

B.Sc., The University of British Columbia, 2005

A THESIS SUBMITTED IN PARTIAL FULFILLMENT OF

THE REQUIREMENTS FOR THE DEGREE OF

DOCTOR OF PHILOSOPHY

in

THE FACULTY OF GRADUATE STUDIES

(Genetics)

THE UNIVERSITY OF BRITISH COLUMBIA

(Vancouver)

August 2012

Abstract

The study of essential cellular processes such as the regulation of the cell cycle and cellular responses to DNA replication stress in model organisms such as the budding yeast *Saccharomyces cerevisiae* (*S. cerevisiae*) benefits our understanding of these processes in human cells. The pathways that govern the response to the DNA replication checkpoint as well as those involved in accurate chromosome segregation are vital to prevent genomic instability, which is a cause of cancer. The yeast cell cycle is governed by one cyclin-dependent kinase, Cdk1, which controls cell cycle transitions by interacting with specific cyclins during G1, S and M phase. Using a combination of genetic and biochemical techniques, I have discovered that Mck1, a homologue of mammalian glycogen synthase kinase 3 (GSK-3), is a novel negative regulator of Cdk1 activity in budding yeast. My thesis also explores a role for Mck1 during the DNA replication checkpoint. Additionally, my work has contributed to the understanding of the mechanisms utilized to restrain spindle elongation during DNA replication stress. My thesis has three main conclusions; 1) The kinase activity of Mck1 is required to inhibit Clb2-Cdk1 activity post-nuclear division. 2) Mck1 kinase activity is required for survival during chronic exposure to DNA replication stress caused by HU in a process other than checkpoint activation. 3) Overexpression of *MCK1* rescues the viability of a kinetochore mutant (*spc24-9*) that is defective in attachment of chromosomes to kinetochore microtubules. In particular, overexpression of Mck1 restrains the precocious spindle elongation that occurs in *spc24-9* strains in response to DNA replication stress. Overall, my thesis demonstrates that the Mck1 kinase contributes to regulation of cell cycle progression in budding yeast. This is important as it demonstrates a conserved function with the mammalian homologue, which has been implicated in several diseases including cancer.

Preface

The work described in Chapter 2 is taken unmodified from the published paper "Ma L., McQueen J., Cuschieri L., Vogel J., Measday V, Spc24 and Stu2 Promote Spindle Integrity When DNA Replication is Stalled, Molecular Biology of the Cell, 18(8): 2805-2816 (2007)". I have renumbered the Figures to fit into the formatting requirements for this thesis. I worked in collaboration with Dr. Lina Ma and Dr. Vivien Measday on this project from the commence of my PhD in September 2005 through to March 2007 (18 months). I performed the microscopy involved in the analysis of spindle expansion during treatment with HU for Figure 2.1B, 2.1C, 2.3, 2.4E, 2.11. I spent a month in the imaging facility of Dr. Jackie Vogel at the University of McGill taking the images for the live cell analysis. The analysis of these images for Figure 2.7 and 2.8 was done by Dr. Laura Cuschieri, Dr. Jackie Vogel and myself. Dr. Lina Ma performed the work in Figure 2.1A, 2.2, 2.4A, 2.4B, 2.4C, 2.4D, 2.5, 2.6, 2.9, 2.10, 2.12, 2.13. Dr. Vivien Measday performed the work for Figure 2.14. Dr. Vivien Measday also wrote the paper. Copyright of the paper belongs to American Society for Cell Biology (ASCB).

The work described in Chapter 3 is in the process of being submitted to the journal Cell Cycle and is work solely performed by myself. Nina Piggott assisted in the creation of strains for Figure 3-9 and 3-10. I had assistance with work performed in Chapter 4 by Perdita Wito and Laura Rose. Perdita worked under my direction as an undergraduate work study student. She performed the experiments for Figure 4.1C, D, 4.2A, B, 4.3B, C, 4.5, 4.6, 4.7A. Another undergraduate student, Laura Rose, performed the work for Figure 4.3A also under my supervision.

Table of contents

List of tables

List of figures

List of symbols and abbreviations

Δ	Delete, null mutant
APC	Anaphase promoting complex
ATP	Adenosine-5'- triphosphate
Ca^{2+}	Calcium ion
CAK	Cdk activating kinase
cAMP	Cyclic adenosine monophosphate
cdk	Cyclin dependent kinase
CEN	Centromere
CPT	Camptothecin
DNA	Deoxyribonucleic acid
dNTP	Deoxynucleoside triphosphate
DSB	Double strand break
FACS	Fluorescence activated cell sorting
FEAR	cdc fourteen early anaphase release
G1	Gap 1 phase of the cell cycle
G2	Gap 2 phase of the cell cycle
GAL	Galactose
GSK-3	Glycogen synthase kinase 3
HCS	High copy suppressor screen
HOG	High osmolarity glycerol

HU	Hydroxyurea
IP	Immunoprecipitation
M	Mitosis phase of the cell cycle
MBF	MCB binding factor
MBP	Myelin basic protein
MEN	Mitotic exit network
MMS	Methyl methanesulfonate
MT	Microtubule
ORF	Open reading frame
PCNA	Proliferating cell nuclear antigen
PKA	Protein kinase A/ cAMP dependent pathway
rDNA	Ribosomal DNA
RFC	Replication factor C (clamp loader complex)
RNR	Ribonucleotide reductase
RPA	Replication protein A
S	Synthesis phase of the cell cycle
S. cerevisiae	*Saccharomyces cerevisiae*/ budding yeast
SAC	Spindle assembly checkpoint
SBF	SCB binding factor
SCF	Ubiquitin ligase complex (Skp1, Cullin/ Cdc53, F-box protein)
SDL	Synthetic dosage lethal
SPB	Spindle pole body/ microtubule organizing centre
ssDNA	Single stranded DNA

TOR	Target of rapamycin
Ts	Temperature sensitive
VFP	Venus fluorescent protein
WCE	Whole cell extract
WT	Wild type
Y	Tyrosine

Nomenclature

Wild type alleles in *S. cerevisiae* are represented by italicized capital letters (e.g. *MCK1)*. Mutant recessive alleles are denoted in lower case italics and represent gene deletions (*mck1*Δ) or point mutations (*mck1D164A*) and disruptions (*mck1-1*). Gene products are written with the first letter capitalized (e.g. Mck1). Genes under transcriptional control by a heterologous promoters have the promoter written prior to the gene as an abbreviation (*GAL-MCK1*).

Acknowledgements

In the making of a scientist, it is important to ensure the proper support so this scientist in-training won't starve, freeze or sleep out in the rain during her training. Thank you to those friends and family that cooked me meals, helped me clean my house and were understanding and patient as I dedicated myself to stealing secrets from the yeasts.

I could not have done this without my family who dried my tears, moved my house multiple times and kept me moving forward in everything I do and who I am. Thank you Mom, Dad, Sarah, Rebecca, and my extended family Todd and KJ. As well, I would like to acknowledge our furry friends that keep us all happy and loved; Denver, Willie and Sam.

To Nana and Papa, who have brought me so many trips to look forward to and supported me in countless ways. I am glad I could carry out this dream.

Omid what are we possibly going to achieve next year to out do this year! I am daily grateful for your love and support.

Thank you Amy, Jessi, Ngaire, PJ, prophecy and Shannon. You have helped share the burden of this degree and have provided me with countless laughs to see me through the darkest parts. Jim, thanks for having been my escape. For being an inspiration and the lady with the most perfect timing, thank you Jessica for always being there when I needed you. For all our midnight talks and walks, I thank you Maria. You are a pillar of strength! Quite literally I

would not have been able to do these experiments without your support. Knowing I had a ride home and a sympathetic ear has meant the world to me.

There have been seven years of people and learning for which to be thankful. I am grateful to the undergraduate students who have been both great pupils as well as substantial help on my project Laura, Dheva and Perdita. To Krystina, with who just a fleeting expression can say everything, thank you for getting it, always! To Jay and Mike, thank you for balancing out the lab and exposing me to the tastier side of yeast. Nina, not many people can do what you do, and you do it so gracefully. Thank you for your endless support. Lina it has been great to see you combining bench science and being a mom so well. I would like to thank my committee Dr. LeAnn Howe, Dr. Chris Loewen, Dr. Ivan Sadowski as well as the Genetics Graduate Program director Dr. Hugh Brock for many years of support and valuable insight into my progress as a doctoral student.

Vivien, there has been so much that I have experienced and explored while in your lab. Thank you for giving me the space to do so.

I would also like acknowledge my funding support from the Michael Smith Foundation of Health Research (MSFHR), the Canadian Institute of Health Research (CIHR) and the Banting and Best Doctoral Research Award.

Dedication

To those who do what they love, with reckless abandon.

Chapter 1: Introduction

1.1 Yeast kinases

A protein kinase is an enzyme that catalyzes the transfer of a phosphate from adenosine-5'-triphosphate (ATP) to a protein substrate. In *S. cerevisiae* there are an estimated 129 protein kinases, 97 of which are shared with metazoans, 23 are shared with *S. pombe* and 9 are unique to *S. cerevisiae* (Manning et al., 2002). Kinases make up 2% of the total number of genes in both yeast and human genomes. Large scale analysis has revealed that there are about ~1000 phosphoproteins of the ~6100 proteins in yeast (Bodenmiller and Aebersold, 2010; Chi et al., 2007; Ficarro et al., 2002; Gnad et al., 2009; Li et al., 2007; Ptacek et al., 2005). Following DNA damage the number of phosphoproteins in yeast increases to ~2278 (Albuquerque et al., 2008). In *S. cerevisiae* ~84% of phosphorylation occurs on serine residues while ~16% of phosphorylation occurs on threonine and tyrosine residues make up only about 0.01% of phosphorylation sites (Gnad et al., 2009). Evolutionary comparisons have found that phosphoproteins are more likely to be conserved from yeast to human than non-phosphorylated proteins (Gnad et al., 2010). However, phosphorylation sites appear to show low conservation from yeast to human (Gnad et al., 2010; Landry et al., 2009). This may be due to the emergence of many kinase families after the divergence of yeast and human (Manning et al., 2002). It has also been noted that many phosphorylation sites occur in unstructured regions of proteins such as turns or loops and thus are expected to evolve more rapidly (Landry et al., 2009). The large proportion of unconserved phosphosites could also represent phosphorylation "noise" from promiscuous kinase activity (Landry et al., 2009; Lienhard, 2008). This would suggest that a large portion of the phosphoproteome does not have an associated function with the phosphorylation event. There is an increased

conservation across species for phosphorylation sites that have associated functions, which explains why phosphoproteins are more likely to be conserved (Ba and Moses, 2010; Boekhorst et al., 2008; Landry et al., 2009; Tan et al., 2009). Conserved phosphosites are enriched in proteins implicated in diseases, emphasizing the importance of studying homologous kinase activity (Tan et al., 2009).

1.2 Mammalian GSK-3 kinase family

The mammalian genome contains two glycogen-synthase kinase (GSK)-3 proteins, GSK-3α and GSK-3β (hereafter referred to as GSK-3). The specific function of these isoforms is not well understood because the majority of research has focused on GSK-3β, while comparative studies with GSK-3α have not been performed. GSK-3 protein kinases were discovered because of their ability to phosphorylate and inhibit glycogen synthase kinases. For many years the ability to block the formation of glycogen was all that was understood about GSK-3. In recent years, however, studies have implicated GSK-3 in protein synthesis, the function of microtubules, cell growth and cellular differentiation (Cohen and Frame, 2001; Frame and Cohen, 2001; Xu et al., 2009). The function of GSK3-β is essential as homozygous GSK-3β mutant mice are inviable (Hoeflich et al., 2000).

The human GSK-3 protein kinases are active in most cells and research has focused on the pathways that negatively regulate GSK-3 kinase activity through inhibitory phosphorylation. Some of these pathways include the mitogen-activated protein kinase cascade (MAPK), which responds to cellular stress, the protein kinase A/ cAMP dependent pathway (PKA), which is involved in cellular communication and the mammalian target of rapamycin (mTOR) signaling pathways which regulate cell growth and nutrient sensing. The activation

of these pathways results in the phosphorylation of residues in the N-terminus of GSK-3 (GSK-3α- Ser21, GSK-3β-Ser9). Upon phosphorylation GSK-3 undergoes a conformational change, which allows the N-terminus to behave as a pseudo substrate, therefore blocking access to substrates (Cohen and Frame, 2001; Frame and Cohen, 2001).

GSK-3 activity is dependent upon phosphorylation of a single tyrosine residue within the activation loop (GSK-3α- Tyr279, GSK-3β-Tyr216) (Hughes et al., 1993). It has not been determined if this phosphorylation is the consequence of GSK-3 autophosphorylation or if another kinase is involved. GSK-3 is a kinase that requires priming phosphorylation on its substrates at a location four residues past the carboxy terminus of its phosphorylation site. The GSK-3 consensus site is Ser/Thr-x-x-x- (Phospho-Ser/Thr), where X is any amino acid and Phospho-Ser/Thr is the primed phosphorylation site (Fiol et al., 1987). As many proteins have been proposed to be GSK-3 substrates there has been established a set of seven criteria to be met in order to consider a protein a real GSK-3 substrate (Table 1-1, Table 1-2) (Frame and Cohen, 2001). Not one proposed substrate has met all the criteria. One of the more substantiated substrates is cyclin D1 (*S. cerevisiae* Cln3). Cyclin D1 is a G1 cyclin, which responds to mitogenic signals to induce entry into the cell cycle. Cyclin D1 is both targeted for ubiquitin degradation and its gene is transcriptionally repressed by the activity of GSK-3β. The transcription of cyclin D1 gene directly correlates to the cellular level of β-catenin. The casein kinase α, primes β-catenin for phosphorylation by GSK-3β, which targets it for destruction. Upon activation of the Wnt pathway both casein kinase α and GSK-3β activity are inhibited thus increasing β-catenin levels and increasing the transcription of cyclin D1. Additionally, GSK-3β can phosphorylate cyclin D1 in a manner that targets if for

ubiquitination and degradation. Cyclin D1 is upregulated in many cancers. The discovery of pharmaceuticals that stimulate GSK-3β activity in order to reduce cyclin D1 would be beneficial for treatment of such cancers (Reviewed in (Takahashi-Yanaga and Sasaguri, 2008)). The study of cell cycle regulation by GSK-3 homologous kinases in such organisms as *S. cerevisiae* will only help expedite our understanding of GSK-3 function.

1.3 Yeast GSK-3 kinase family

The *S. cerevisiae* genome contains four GSK-3 protein kinases; Mck1, Rim11, Ygk3 and Mrk1. Each of the yeast GSK-3 homologues shares sequence similarity to both GSK-3α and GSK-3β. The yeast GSK-3s do not show homology with human GSK-3s in the N-termini, while the GSK-3 activating tyrosine appears to be conserved. Rim11 has specific functions during sporulation and meiosis, while Mck1, Ygk3 and Mrk1 are partially redundant in their transcriptional activation role during stress and PKA signaling. Many studies have focused on Mck1 because of its role in chromosome segregation, calcium stress response, and protein degradation. The work presented in this thesis will further explore the role of Mck1 and the regulation of the cell cycle.

Mck1 is a dual specificity protein kinase and thus is capable of phosphorylating tyrosine, serine and threonine residues (Lim et al., 1993). Mck1 is itself phosphorylated on tyrosine and serine residues (Dailey et al., 1990; Lim et al., 1993). The majority of phospho-tyrosine arises from the action of Mck1 itself, phosphorylating the activation loop (Y199)(Lim et al., 1993; Rayner et al., 2002). Mck1 purified from mutant cells lacking the ability to phosphorylate the Y199 residue, (*mck1Y199F*) are capable of autophosphorylating serine residues (Rayner et al., 2002). However, *in vivo* analysis suggests that the majority of Mck1

phospho-serines occur due to the action of additional kinases (Lim et al., 1993). The kinases that phosphorylate Mck1 are not known at this time. The Y199 phosphorylation within the activation loop is required for the phosphorylation of exogenous substrates such as myelin basic protein (MBP) as well as cell survival upon exposure to caffeine and high temperatures, indicating that it is required for some aspects of Mck1 function (Rayner et al., 2002). Mck1 has been described in many roles such as calcium stress response, sporulation and inhibition of the PKA pathway (Figure 1-1). There have also been several Mck1 substrates identified (Table 1-3).

1.4 Multiple roles for the Mck1 kinase

1.4.1 Mitotic chromosome segregation

Mck1 was identified as an overexpression suppressor of both centromere and kinetochore mutations. Specifically, overexpression of *MCK1* suppresses mutations in the centromere DNA CDEIII region and its protein binding complex, CBF3 (Jiang et al., 1995; Shero and Hieter, 1991). The CBF3 complex is composed of Ndc10/Cbf2 (p110), Cep3 (p64), Ctf13 (p58) and Skp1 (p23) which comprises the central core of the kinetochore (Russell et al., 1999). It was suspected that Mck1 functions in support of mitotic chromosome segregation as *mck1*Δ mutants also exhibited sensitivities to microtubule destabilizing agents such as cold temperature and benomyl treatment (Jiang et al., 1995; Puziss et al., 1994; Shero and Hieter, 1991). Mck1 does not play a role in the spindle assembly checkpoint (SAC) as *mck1*Δ mutants arrested with 2N DNA content in the presence of nocodazole, another microtubule destabilizing drug (Gardner et al., 2001). Mck1 demonstrated the ability to phosphorylate Ndc10 (CBF3 complex) *in vitro* and interact with Ndc10 *in vivo* in a two-hybrid screen

(Jiang and Koltin, 1996). The functional consequence of Mck1's phosphorylation of Ndc10 is not known at this time.

1.4.2 Maintenance of genomic stability

DNA must only be replicated once per cell cycle and many mechanisms exist to prevent DNA re-replication during one cell cycle. This is important to maintain genomic stability. One such mechanism is the destruction of the Cdc6 replication activator; another is through binding of Clb5 to Orc6. Both of these mechanisms are disrupted in a mutant that expresses stabilized Cdc6 (*CDC6*Δ*NT*) as well as mutations in the Clb5 binding domain of Orc6 (*ORC6-rxl*). The combination of both *CDC6*Δ*NT* and *ORC6-rxl* mutants does not cause extensive re-replication but does cause growth difficulties. *MCK1,* along with genes involved in DNA damage response, such as *MEC1* and *RAD53,* when mutated were discovered to be synthetic lethal with the *CDC6*Δ*NT ORC6-rxl* mutant. This suggests that Mck1 has a role in preventing DNA re-replication (Archambault et al., 2005). The laboratory of Dr. Amy Ikui is continuing work on identifying which DNA replication proteins Mck1 may regulate. Additionally, overexpression of *MCK1* was found to rescue lethality of *MEC1* and *RAD53* mutants, which are unable to respond to the DNA replication checkpoint (Desany et al., 1998). The role of Mck1 in the DNA replication checkpoint is unknown at this time.

1.4.3 Calcium stress response

Mck1 is involved in the calcium stress response. Calcium (Ca^{2+}) is a cellular messenger for many processes within the cell. Yeast cells exposed to Ca^{2+} trigger both the calcineurin and the cell wall integrity (Mpk1/Slt2 MAP kinase cascade) pathways. Calcium, when in excess,

is bound by the calmodulin protein (Cmd1), which in turn binds to the phosphatase calcineurin. Calcineurin is a multi-protein complex that is inhibited by Rcn1. Mck1 phosphorylates Rcn1, which leads to promotion of calcineurin activity possibly through targeting Rcn1 for degradation by the ubiquitin ligase complex, SCF^{Cdc4} (Skp1, Cullin/ Cdc53, F-box protein Cdc4)(Figure 1-1A) (Hilioti et al., 2004; Kishi et al., 2007). The cellular response to increased calcium also results in a G2/M arrest, which occurs via stabilization of the Clb2-Cdk1 inhibitory kinase Swe1. Swe1 inhibits Clb2-Cdk1 kinase activity by phosphorylation of Cdk1-tyrosine 19 (Y19). Genetic analysis suggests that the Mpk1/Slt2 pathway activates Mck1 to cause Hsl1 delocalization from the bud neck during calcium stress, thus preventing successful Swe1 degradation (Figure 1-1A) (Mizunuma et al., 2001). Mck1 phosphorylates Hsl1, after which Hsl1 is degraded by SCF^{Cdc4} and is no longer able to recruit Swe1 to the bud neck (Mizunuma et al., 2001). Interestingly, *mck1*Δ mutants unexpectedly have high levels of Slt2/Mpk1 activity suggesting that Mck1 has a role in negative regulation of the Slt2/Mpk1 pathway as well (Griffioen et al., 2003). The lab of Dr. Kellogg has demonstrated that Mck1 is required for the proper phosphorylation of the Mih1 phosphatase, which removes the Swe1-imposed inhibitory phosphorylation on Cdk1-Y19 at G2/M in unstressed cells (Pal et al., 2008). The casein kinases, Yck1 and Yck2 were also implicated in the phosphorylation of Mih1 (Pal et al., 2008). Overall, this data suggests that Mck1 has a role in the regulation and/or phosphorylation of two key Cdk1 regulatory proteins at the G2/M transition – Mih1 and Swe1.

1.4.4 Activation of sporulation

Two GSK-3 homologs in yeast, Mck1 and Rim11, are important for the induction of sporulation. While mutants in the *MCK1* gene have pleiotropic effects, the GSK-3 homolog

Rim11 (*MDS1*) appears to only have defects in sporulation (Puziss et al., 1994). In nutrient rich conditions, Ume6 can act as a meiotic transcriptional repressor through interactions with the histone deacetylases, Sin3 and Rpd3. Upon nitrogen and glucose starvation *IME1* transcription increases and the Ime1 protein binds to the transcription factor Ume6 to promote transcription of meiosis specific genes (Rubin-Bejerano et al., 1996). Mck1 has been implicated in both the activation of Ime1 transcription as well as ascus maturation (Figure 1-1B) (Mitchell and Bowdish, 1992). Rim11 phosphorylates both Ume6 and Ime1, which promotes their interaction and subsequently sporulation (Bowdish et al., 1994; Malathi et al., 1997). Mck1 has also been shown to physically interact with Ume6 through two-hybrid analysis and deletion of both *MCK1* and *RIM11* shows a loss of Ume6 phosphorylation *in vivo* (Xiao and Mitchell, 2000). Both Mck1 and Rim11 appear to have synergistic effects suggesting overlapping roles in different pathways (Puziss et al., 1994; Xiao and Mitchell, 2000).

1.4.5 Downregulation of pyruvate kinase

There have been several description of Mck1's role in the down regulation of pyruvate kinase (Cdc19), which catalyzes the last enzymatic reaction in glycolysis (Figure 1-1C) (Brazill et al., 1997; Griffioen et al., 2003; Rayner et al., 2002). Initially, Mck1 was demonstrated to interact with Cdc19 and phosphorylate it *in vitro* (Brazill et al., 1997). As well, *mck1Δ* strains were shown to have increased pyruvate kinase activity suggesting that Mck1 is a negative regulator of Cdc19 (Brazill et al., 1997). Later studies suggested instead that the relationship between Cdc19 and Mck1 is indirect. It was proposed that Mck1 inhibits the cyclic AMP (cAMP) dependent protein kinase A (PKA) and that PKA phosphorylates Cdc19 to stimulate activation (Rayner et al., 2002). PKA is a heterotetrameric complex

composed of two catalytic subunits (any combination of Tpk1,2,3) and a negative regulatory homodimer (Bcy1). The cAMP messenger associates with Bcy1, thus alleviating the inhibition of the PKA catalytic domain. Mck1 inhibits Tpk1 in a catalytically-dependent manner, but Mck1 does not phosphorylate Tpk1 (Rayner et al., 2002). Interestingly, high levels of PKA activity are correlated with sporulation defects as PKA antagonizes the function of calcineurin (Rayner et al., 2002). Mck1 in addition to other GSK-3 homologues (Mrk1 and Ygk3) have been implicated in the phosphorylation of Bcy1 that promotes relocalization of Bcy1 from the nucleus to the cytoplasm during high temperature, although the reason for Bcy1 relocalization is not clear (Griffioen et al., 2003). During the DNA damage response, Bcy1 relocalization to the cytoplasm was found to be also dependent on Mck1 (Searle et al., 2011).

1.4.6 Transcriptional changes in stress response

A group of 168 genes was determined to be dependent upon Mck1 for maximal expression (Hilioti et al., 2004). Most of these genes are under the control of the stress activated transcription factors Msn2 and Msn4 (Hilioti et al., 2004). Msn2 overexpression can rescue the galactose sensitivity of double (*mck1*Δ *rim11*Δ) or quadruple (*mck1*Δ *rim11*Δ *mrk1*Δ *ygk3*Δ) GSK-3 mutants. During stress induced by high temperatures or high salt, Mck1 is required for proper binding of Msn2 to stress response elements to induce gene expression (Hirata et al., 2003). This is independent of Mck1-Msn2 complex formation or Mck1 dependent phosphorylation (Hirata et al., 2003). The PKA pathway negatively regulates Msn2/Msn4 through phosphorylation-induced retention in the cytoplasm (Gorner et al., 1998).

Aside from stress induced transcriptional regulation by Msn2/Msn4, additional transcription factors such as Yap1 also play a role in regulating transcription in response to oxidative stress. Like Msn2/Msn4, Yap1 is also negatively regulated by the PKA pathway (Fernandes et al., 1997). Together Msn2 and Yap1 regulate the transcription of the transcription factor *YAP4* (Nevitt et al., 2004). Yap4 is thought to play a role downstream of the High Osmolarity Glycerol (HOG) pathway, and may induce genes involved in glycerol metabolism (Nevitt et al., 2004). Phosphorylation of the Yap4 transcription factor appears to promote its stability but not its activity under stress conditions, such as osmotic, oxidative, high temperature and DNA damage caused by methyl methanesulfonate (MMS). The *in vivo* phosphorylation of Yap4 is dependent on the GSK-3 kinases Mck1, Rim11, Ygk3 as well as PKA (Pereira et al., 2009).

The Target of Rapamycin (TOR) signaling pathway positively regulates cell growth in response to nutrients. The TOR pathway is inhibited through starvation or treatment with rapamycin. During such treatment, the production of ribosomes and tRNA synthesis is reduced through inhibition of RNA polymerase III, which transcribes all nuclear tRNA genes, the 5S rRNA, and other small RNA genes. RNA polymerase III is inhibited through several mechanisms, including phosphorylation of some of its subunits. Phosphorylation of the RNA polymerase III subunit Rpc53 by the priming kinase Kns1, followed by Mck1, was recently shown to be one mechanism for RNA polymerase III inhibition upon rapamycin treatment (Lee et al., 2012). Interestingly, PKA promotes activity of RNA polymerase III, therefore Mck1 once again has an antagonistic role to PKA.

1.4.7 Protein degradation

Besides the involvement of Mck1 in the phosphorylation and subsequent degradation of Rcn1 and Hsl1, Mck1 has also been implicated in the targeted degradation of Rog1 and in the N-end rule pathway (Andoh et al., 2000; Hwang and Varshavsky, 2008). Little is known about Rog1 except that it forms a complex with the Rsp5 E3 ubiquitin ligase, in a GSK-3 (Mck1, Rim11, Ygk3, Mrk1) dependent manner (Andoh et al., 2000). Mutation of Rog1 rescues the temperature sensitivity of *GSK-3* null mutants, suggesting that the temperature sensitivity of *mck1*Δ strains may be due to accumulation of Rog1 (Andoh et al., 2000).

Mck1, but not other GSK-3s, has also been found to phosphorylate the ubiquitin ligase Ubr1, which functions in the N-end rule degradation pathway (Hwang and Varshavsky, 2008). The phosphorylation of Ubr1 by Mck1 requires first a priming phosphorylation by the casein kinase proteins, Yck1 and Yck2. Ubr1 phosphorylation has a stimulatory effect and Ubr1 activity increases the degradation of the transcriptional repressor Cup9, allowing transcription of the peptide transporter gene *PTR2*. Ptr2 is required for transport of di/tri-peptides and is induced by glucose.

Mck1 has functions in common with the GSK-3 human homologues such as targeting proteins for degradation and transcriptional regulation. Like the human homologue, Mck1 substrates may require a priming phosphorylation and the Mck1 activation loop (Y199) must be phosphorylated for some of Mck1 functions. In yeast, Mck1 appears to act in a positive manner towards stress induced pathways, such as those that occur during high calcium stress or nutrient limitation. In many instances, Mck1 acts antagonistically to the PKA pathway

which is triggered through glucose rich conditions. It is interesting to note that in yeast Mck1 has been shown to directly inhibit the PKA pathway, while in human cells the PKA pathway has been shown to inhibit GSK-3. An understanding of the pathways, conditions and regulations under which Mck1 and the other yeast GSK-3 protein kinases function is far from complete.

1.5 The cell cycle

The timing of the mitotic cell cycle in *S. cerevisiae* is governed by one cyclin dependent kinase (Cdk), Cdk1 (*CDC28*). Cdk1 is a proline directed kinase that phosphorylates the consensus sequence Ser/Thr*-Pro-x-Lys/Arg (x is any amino acid and * is the phosphorylated serine or threonine). The regulation of Cdk1 differentiates the events of chromosome replication and segregation. Cdk1 is regulated by activators such as its nine associated cyclins (Cln1-3 and Clb1-6) and Cks1 as well as activating phosphorylation. Cdk1 is negatively regulated through inhibitory phosphorylation as well as binding of inhibitors such as Far1 or Sic1 (Reviewed in (Mendenhall and Hodge, 1998)). The level of Cdk1 remains constant throughout the cell cycle and it has been long thought that transcriptional or translational regulation of Cdk1 does not contribute to Cdk1 regulation (Morgan, 1997).

1.5.1 Activation of Cdk1

On their own, Cdks have very little kinase activity and require both cyclin binding and activating phosphorylation to become active. The Cdk kinases have two conformational problems that cause their low activity - these are the misalignment of key catalytic residues involved in the phosphate transfer and the blocking of the substrate-binding site by the T-

loop. Binding of cyclins results in major conformational changes of Cdk that facilitate substrate binding and catalytic activity. Furthermore, phosphorylation of the T-loop at Thr 169 in Cdk1 opens up the substrate-binding site and increases the number of contacts with cyclins. In budding yeast Thr 169 phosphorylation is dependent on a Cdk-activating kinase (CAK), Cak1, while in higher eukaryotes CAK is a protein complex (reviewed (Mendenhall and Hodge, 1998)). It has been recently suggested that Cak1 also aids in stabilizing Cdk1 complexes (Kim et al., 2009). A highly conserved Cdk interacting protein, Cks1, appears to assist in the functioning of Cdk1. Although its absolute requirement has been disputed, Cks1 has been implicated in conjunction with Cdk1 for transcriptional control of genes such as *CDC20* and as an assembly factor of cyclin-Cdk1 complexes (Mendenhall and Hodge, 1998; Morris et al., 2003; Yu et al., 2005; Yu and Reed, 2004). The nine cyclins in budding yeast are grouped into two classes - one that is required for entry into the cell cycle (G1 cyclins) and the other for the mitotic events of the cell cycle (chromosome replication and segregation) (B-type cyclins). The three G1 cyclins (*CLN3, CLN1, CLN2*) have overlapping functions at Start, as only one of the three is required for viability (Futcher, 1991; Hadwiger et al., 1989; Richardson et al., 1989). The B-type, or mitotic cyclins, are expressed in waves during S (*CLB5,6*), G2 (*CLB3,4*) and M (*CLB1,2*) phase. All the cyclins demonstrate redundancy and have some overlapping functions, as described below.

CLN3 is the Cdk1 cyclin that demonstrates the least periodicity during the cell cycle, with only a slight increase in abundance at M/G1 (McInerny et al., 1997; Tyers et al., 1993). Cln3-Cdk1 inhibits the transcriptional repressor Whi5, thereby permitting the transcription of Start specific genes such as *CLN1* and *CLN2* (Costanzo et al., 2004; de Bruin et al., 2004).

The mating factor pathway inhibits Cln3-Cdk1 function through the binding of Far1 (Jeoung et al., 1998). Cln3-Cdk1 activity also has to overcome the presence of Far1 at the commence of an unperturbed cell cycle (Alberghina et al., 2004). Cln3 is a low abundant protein with low Cdk1 activity compared to Cln1 and Cln2, therefore it seems reasonable that Cln3-Cdk1 activity is quickly replaced by a sharp increase in Cln1 and Cln2 (Tyers et al., 1993). Cln3 is rapidly phosphorylated by the activity of Cdk1, and thus targeted for degradation by the ubiquitin conjugating enzyme Cdc34 (Tyers et al., 1992; Yaglom et al., 1995).

The transcription of *CLN1* and *CLN2* commences at Start under control of the SBF (SCB-binding factor) heterodimeric transcription factor, peaking sharply in late G1 and decreasing through S-phase (Nasmyth and Dirick, 1991; Ogas et al., 1991). Although *CLN1* and *CLN2* expression is positively regulated by a feedback loop, *CLN3* is all that is required to drive maximal transcription (Stuart and Wittenberg, 1995). SBF transcription is negatively regulated by Clb2-Cdk1, thus allowing increasing Clb2 levels to turn off Cln1/2 production (Amon et al., 1993). Cln2-Cdk1 is responsible for growth polarization and budding, spindle pole body duplication, inhibition of Sic1 and inhibition of the mating response pathway through phosphorylation of Ste5 and Far1. As well, Cln2-Cdk1 inactivates the anaphase promoting complex (APC) which promotes B-type cyclin accumulation (Henchoz et al., 1997; Queralt and Igual, 2004; Strickfaden et al., 2007). Cln1-Cdk1 has a minor role as compared to Cln2-Cdk1. Both Cln1 and Cln2 are highly unstable (half-life of 5-10 minutes) as their Cdk1 activity targets them for destruction in a negative feedback loop (Deshaies et al., 1995; Lanker et al., 1996; Skowyra et al., 1999). This high degree of instability of G1

cyclins is beneficial to the cell as it allows for a sharp peak of expression of genes required to pass the Start transition.

CLB5 and *CLB6* encode S-phase B-type cyclins that are expressed in late G1, similar to *CLN1* and *CLN2*, but under the control of the MBF (MCB-binding factor) transcription factor. Clb5 and Clb6 initiate S-phase, prevent re-replication, and inhibit the G1 cyclin-Cdk1 complexes. Some major targets of Clb5-Cdk1 are the DNA replication proteins Sld2, Cdc6, Orc6, Mcm3 and the activator of the APC, Cdh1(Loog and Morgan, 2005). Clb5-Cdk1 appears to play the major role, as deletion of *CLB5* but not *CLB6*, delays replication (Donaldson et al., 1998). Clb5 persists through S phase and disappears as cells enter anaphase (Schwob et al., 1994; Schwob and Nasmyth, 1993). The stability of Clb5 is dependent upon the cell cycle phase. Clb5 is highly unstable in alpha factor arrested cells (half-life 5 minutes), but shows increasing stability in S or M phase (half-life 20 minutes) (Seufert et al., 1995). Clb6 is highly unstable (half-life <5 minutes) and is rapidly degraded at the G1/S border providing a reason as to why Clb5 has the larger role during replication (Jackson et al., 2006). The hydrophobic patch of Clb5 has been suggested to function in binding to the RXL motif of Cdk1 substrates such as Orc6. After commence of replication, Clb5-Cdk1 binds to Orc6 and is thought to prevent re-initiation of replication from origins (Wilmes et al., 2004).

The transcription of *CLB3* and *CLB4* commences at the beginning of S-phase and continues through anaphase (Richardson et al., 1992). Clb3/Clb4-Cdk1 are responsible for spindle formation although Clb1/2-Cdk1 can perform this task in the absence of Clb3 or Clb4 (Ikui

and Cross, 2009; Richardson et al., 1992). Additionally, Clb3/4-Cdk1 can compensate for the activity of Clb5/6 during S-phase.

CLB1 and *CLB2* are transcribed 10 minutes before anaphase and 20 minutes after *CLB3* and *CLB4* (Fitch et al., 1992). *CLB2* transcription is controlled by the Mcm1 and the Swi5 Factor (SFF) transcription factor complex (Fkh2, Ndd1)(Amon et al., 1993; Maher et al., 1995; Pic-Taylor et al., 2004). *CLB2* has the more prominent role in mitosis as only the deletion of *CLB2* and not that of *CLB1* results in accumulation of G2 cells. The activation of Clb2-Cdk1 is important for spindle elongation while the inhibition of Clb2-Cdk1 is required for mitotic exit (Ghiara et al., 1991; Surana et al., 1991). Clb2-Cdk1 activity governs the switch from apical to isotropic bud growth although its direct target is unknown (reviewed in (Enserink and Kolodner, 2010)). Inhibition of Clb2-Cdk1 results in elongated buds due to prolonged apical growth (Surana et al., 1991). The hydrophobic patch of Clb2 has been suggested to target it to subcellular localizations such as the bud neck through binding with Bud3 (Bailly et al., 2003). The activity of Clb2-Cdk1 can repress transcription of *CLN*s through phosphorylation mediated inhibition of the transcription factor SBF (Swi4) (Amon et al., 1993). The transcription of *CLB5/6* is under the control of the MBF transcription factor, and is thus unaffected by Clb2-Cdk1 activity (Schwob and Nasmyth, 1993).

The degradation of cyclins is also important for the control of the cell cycle. As cells enter early G1 phase there are high levels of APC^{Cdh1}, which actively degrades any remaining mitotic cyclins. Cln1/2/3 are immune to degradation by APC^{Cdh1}, being degraded instead by the SCF complexes (Barral et al., 1995). As Cln levels rise, the Cln-Cdk1 complex

inactivates APC^{Cdh1}, facilitating the accumulation of B-type cyclins (Zachariae et al., 1998). Clb6 is the exception, as it is the only B-type cyclin degraded by the SCF as opposed to the APC (Jackson et al., 2006). Cln2 is targeted for degradation by the SCF through Cdk1 dependent phosphorylation (Lanker et al., 1996). Through negative feedback, Clb2-Cdk1 phosphorylates and activates APC^{Cdc20}, which then degrades a portion of Clb2 as well as Clb5 (Rudner and Murray, 2000; Shirayama et al., 1999; Wäsch and Cross, 2002). During mitosis APC^{Cdh1} is activated, and completes the degradation of mitotic cyclins.

A lot of work has been done to understand what determines cyclin specificity (Archambault et al., 2004; Cross et al., 1999; Loog and Morgan, 2005). Cyclin specificity is created by their transcriptional profile, substrate preferences, subcellular localization and ability to be inhibited by various cell cycle inhibitors such as Sic1 and Swe1 (Reviewed in (Bloom and Cross, 2007)). A recent report suggests that cyclins not only provide some level of specificity through docking sites with substrates, but also alter the active site specificity of Cdk1(Kõivomägi et al., 2011). Despite the specificity of the cyclins during unperturbed growth, it is interesting to note that under particular conditions some cyclins can perform the tasks of other cyclins, alluding to a possible lack of substrate specificity for each cyclin. Clb5-Cdk1 can compensate for the activity of G1 cyclins, and with the removal of the inhibitor Swe1, Clb2-Cdk1 can perform the actions of Clb5-Cdk1 (Hu and Aparicio, 2005; Schwob et al., 1994; Schwob and Nasmyth, 1993). This suggests that Clb2-Cdk1 may have the least specific activity and that additional cyclins have evolved with more specificity.

1.5.2 Inhibition of Cdk1

There are two major inhibitors of cyclin-Cdk1 function - Far1 and Sic1. Not only is Far1 an important inhibitor of cyclin-Cdk1 during response to mating factor but it also sets a limit for the amount of Cln3-Cdk1 activity required to enter the cell cycle under unperturbed growth conditions (Alberghina et al., 2004). Far1 is able to inhibit the activity of all three Cln1/2/3-Cdk1 complexes (Jeoung et al., 1998; Tyers and Futcher, 1993). Sic1, on the other hand, inhibits Clb-Cdk1 complexes. Sic1 has two main roles; firstly, the prevention of replication through inhibition of Clb5-Cdk1. This persists until the phosphorylation of Sic1 by Cln-Cdk1 and subsequent destruction of Sic1 in G1/S (Schneider et al., 1996; Schwob et al., 1994; Verma et al., 1997). Secondly, Sic1 is involved in the inhibition of Clb-Cdk1 in late mitosis (Donovan et al., 1994; Schwob et al., 1994). Both Far1 and Sic1 bind tightly to Cdk1 and are thought to prevent substrate binding (Mendenhall, 1993; Peter and Herskowitz, 1994).

Cdk1 also undergoes inhibitory phosphorylation on tyrosine 19 (Y19). This phosphorylation is important for spindle pole body separation and nuclear division as the phospho-mimic Cdk1-Y19E is unable to fulfill these tasks (Lim et al., 1996). The control of Cdk1-Y19 phosphorylation falls under the responsibility of Swe1, a kinase that directly phosphorylates Y19, and Mih1, a phosphatase that dephosphorylates Y19 (Booher et al., 1993; Russell et al., 1989). Swe1 preferentially inhibits Clb2-Cdk1 over the other cyclin-Cdk1 complexes (Keaton et al., 2007). Swe1 inhibits Clb2-Cdk1 by both phosphorylation as well as direct binding (Booher et al., 1993; Keaton et al., 2007; McMillan et al., 1999b).

1.6 Overview of select cell cycle events

1.6.1 Start

In budding yeast Start is defined as the commitment to the cell cycle. It represents the point of no return. Start can be prevented through addition of mating factor or stresses such as heat shock (Cross, 1995). It is marked by an immense (>200 genes) surge in transcription, which is initiated by the activity of Cln3-Cdk1 (Skotheim et al., 2008; Tyers et al., 1993). The promoters of genes required for DNA replication and growth are occupied by antagonistic factors. These factors either promoting transcription, such as the SBF or MBF transcription factors and others inhibiting transcription such as the Rpd3 histone deacetylase complex, and transcriptional inhibitor Whi5 (Huang et al., 2009; Takahata et al., 2009; Wang et al., 2009). There appears to be three ways in which gene transcription can be activated to induce start. The prominent way is through the export of Whi5 from the nucleus, which is induced by Cln3-Cdk1 phosphorylation (Costanzo et al., 2004; de Bruin et al., 2004; Wittenberg and Reed, 2005). Secondly, Cln3-Cdk1 also inhibits Rpd3, which assists in activating transcription (Wang et al., 2009). Thirdly, there is evidence to suggest the involvement of another cyclin dependent kinase, Pho85, in promoting G1 transcription (Huang et al., 2009; Wysocki et al., 2006). Once SBF and MBF activate gene expression, the cells have passed Start.

1.6.2 Initiation of DNA replication

The beginning of replication is divided into two stages. The first occurs in M/G1 and involves the loading of pre-replicative complexes (pre-RC's) onto origins of replication This process is called licensing and involves the replicative helicase (Mcm2-7), origin recognition complex (ORC), Cdc6 and Cdt1. The pre-RC requires loading of the pre-initiation complex

(pre-IC) for activation. This involves proteins required for helicase activity such as; Cdc45, GINS (Sld5, Psf1, Psf2, Psf3), Sld2 and Dpb11 (reviewed in (Diffley, 2010)). While assembly of the pre-RC requires low Cdk1 activity and high APC activity, origin firing requires high Cdk1 activity and low APC activity. This ensures that origins of replication are fired only once per cell cycle. Clb5-Cdk1 prevents pre-RC assembly through both phosphorylation dependent and independent means. The interaction between Cdk1 and Orc6 sterically prevents the recruitment of Cdt1/Mcm2-7. Furthermore, Clb5-Cdk1 phosphorylation of Orc6 prevents Cdt1 binding (Chen and Bell, 2011). Replication initiation requires the activity of both Cdk1 and the Dbf4/Drf1-dependent CDC7 kinase, DDK. Clb5-Cdk1 activates Sld2 and Sld3 by phosphorylation, while DDK activates Mcm2, 4, and 6 (reviewed in (Labib, 2010)). Activated helicase unwinds double stranded DNA and the exposed single stranded DNA (ssDNA) is bound by replication protein A (RPA). The pre-IC loads the DNA polymerases (α, δ, ε). Once the primase polymerase-α has synthesized the first primers it is replaced by the clamp loader complex (replication factor C; RFC) and the sliding clamp (proliferating cell nuclear antigen; PCNA). The majority of the pre-IC travels along with the replication fork in what is termed the replisome, leaving behind Orc1-6 at the origins of replication. Replication continues through the activity of polymerase δ/ε until replication forks coalesce and the DNA ends are joined through ligation (reviewed in (Morgan, 2007)).

1.6.3 Morphogenic checkpoint

Defects in actin polarization or bud formation trigger the morphogenesis checkpoint. The checkpoint results in the accumulation of the Swe1 kinase and thus the inhibition of Clb2-

Cdk1 due to phosphorylation of Cdk1 Y19 (Keaton and Lew, 2006; Lew, 2003). The degradation of Swe1 requires the activity and controlled localization of at least four kinases (Cla4, Hsl1, Cdk1, Cdc5) in addition to the localization of Swe1 at the bud neck (Asano et al., 2005; Keaton et al., 2008). The order of the events is disputed but what is known is that localization of Hsl1 at the bud neck is required for both the phosphorylation and recruitment of Hsl7, which is also required for Swe1 degradation, as well as the re-localization of Cdc5 from the spindle pole bodies to the bud neck (Asano et al., 2005; Cid et al., 2001; McMillan et al., 1999a; Shulewitz et al., 1999). Swe1 is also recruited to the bud neck in an Hsl1/Hsl7 dependent manner and is subsequently phosphorylated multiple times by both Cdc5 and Cdk1/Clb2 (Asano et al., 2005; Cid et al., 2001; Longtine et al., 2000; McMillan et al., 1999a; McMillan et al., 2002; Sakchaisri et al., 2004; Shulewitz et al., 1999). Additionally, Swe1 is phosphorylated by the septin filament assembly protein kinase Cla4 (Sakchaisri et al., 2004). Once heavily phosphorylated, Swe1 is then ubiquitinated by SCF^{met30} (Kaiser et al., 1998). It has been suggested that Hsl1 and Hsl7 monitor the geometry of the budneck, and if the bud neck is malformed, degradation of Swe1 is prevented (Keaton and Lew, 2006; Lew, 2003).

1.6.4 Spindle formation and chromosome segregation

In budding yeast, the mitotic spindle is created by the separation of the microtubule organizing centres, or spindle pole bodies (SPBs), which are embedded in the nuclear envelope throughout the cell cycle. At the start of each cell cycle, the SPB duplicates, the new SPB is inserted into the nuclear envelope and in late S phase the SPBs separate to form a short bipolar spindle (Crasta and Surana, 2006). Immediately following replication, cohesion

is established between sister chromatids which holds them together until metaphase. After replication of the centromere the kinetochore assembles on the centromeric DNA. The kinetochore is a multi-subunit trilaminar structure. The inner kinetochore is composed of the centromere binding complex CBF3 and the histone variant Cse4, the central kinetochore is composed of multiple complexes (Ndc80, Mtw1, Spc105 and Ctf19) and the outer kinetochore contains the Dam1 complex which interacts with the microtubule (Westermann et al., 2007). The Dam1 complex forms a ring around each microtubule emanating from the SPBs and allows the kinetochore to track along with depolymerizing or growing microtubules (Westermann et al., 2005). Also localized to the kinetochore are several microtubule motor proteins such as Cin8 as well as many microtubule associated proteins such as Stu2, which assist in kinetochore-microtubule attachment and tracking.

Prior to sister chromatid segregation, sister chromatids must form bipolar attachments, where the kinetochore on each chromatid must bind a microtubule from opposite SPBs. Tension is created by the force of poleward movement of captured kinetochores to opposite poles. This is countered by the cohesive forces between sister chromatids. If the kinetochores of sister chromatids have attached to microtubules from the same SPB, no tension exists, and the highly conserved Ipl1 Aurora-B protein kinase phosphorylates the kinetochore, which encourages detachments of kinetochores from microtubules so that proper bipolar attachment can be attained (Biggins and Murray, 2001). Unattached kinetochores trigger spindle assembly checkpoint (SAC). The SAC proteins Bub1 and Bub3 are located at kinetochores during early mitosis, whereas Mad1, 2 and 3 are recruited by unattached kinetochores. Mad1,

2, and 3 form a complex with Cdc20 thus preventing APC activation and chromosomal segregation until bipolar spindles have been formed (reviewed in (Amon, 1999)).

Once all sister chromatids have attained bipolar attachment, the cell is ready to progress from metaphase to anaphase. The APC^{Cdc20} is activated by elevated Clb2-Cdk1 levels and targets the protein Pds1, otherwise known as securin, for degradation. Removal of Pds1 releases its binding partner Esp1 from inhibition (Visintin et al., 1997). Esp1 is the budding yeast separase, and cleaves the cohesion protein, Scc1, allowing dissolution of sister chromatid cohesion and segregation of sister chromatids to opposite SPBs during anaphase (Uhlmann et al., 1999).

1.6.5 Completion of mitosis

Mitotic exit occurs in two steps. Both these steps require the activation of the Cdc14 phosphatase that counteracts the activities of Cdk1 (Visintin et al., 1998). The first step in Cdc14 release is called the cdc Fourteen Early Anaphase Release (FEAR) pathway, the second is the Mitotic Exit Network (MEN) (Jaspersen et al., 1998; Stegmeier et al., 2002). It has been proposed that the two mechanisms lead to the dephosphorylation of two distinct groups of substrates that control separate events.

1.6.5.1 FEAR

The Cdc14 phosphatase is kept sequestered in the nucleolus by its binding partner Net1 (Visintin et al., 1999). The phosphorylation of Net1 by Clb2-Cdk1 reduces its binding capacity for Cdc14, and results in the partial release of Cdc14 from the nucleolus (Azzam et

al., 2004). Esp1, in a combined effort with Slk19, Spo12 and Cdc5, down regulates the phosphatase $PP2A^{Cdc55}$, which regulates Net1 phosphorylation (Queralt et al., 2006). This permits the accumulation of Net1 phosphorylation and the first release of Cdc14 from the nucleolus. This first wave of Net1 activity is responsible for four main activities. Firstly, it stabilizes the anaphase spindle through establishment of a spindle midzone and altering spindle dynamics (Higuchi and Uhlmann, 2005; Khmelinskii et al., 2007). Secondly, it regulates spindle positioning (Ross and Cohen-Fix, 2004). Thirdly, it is involved in the segregation of ribosomal DNA (rDNA) (Sullivan et al., 2004). Lastly, it triggers the activation of the MEN.

1.6.5.2 MEN

The MEN involves the recruitment of the Cdc15 kinase to the SPB, where Cdc15 activates Dbf2-Mob1, which is required for full Cdc14 release (Lee et al., 2001; Mohl et al., 2009; Rock and Amon, 2011). This is done by at least two documented ways. Firstly, through the spindle positioning checkpoint, where a SPB bound GTPase, Tem1 is poised to sense the entrance of the nucleus into the daughter cell. Tem1 is kept in an inactive hydrolysed state indirectly through the activity of a mother cell specific kinase, Kin4. Kin4 activates Bub2-Bfa2 (GTPase activating protein) promoting Tem1 hydrolysis. Once the SPB enters the daughter cell, the bud specific protein Lte1 promotes the formation of active Tem1 (Tem1-GTP), and Cdc5 inhibits the activity of Bub2-Bfa2. Activated Tem1 now recruits Cdc15 to the spindle pole body. Cdc5, independent of its role in inhibiting Bub2-Bfa2, also promotes the association of Cdc15 with the spindle pole body (Reviewed in (Lew and Burke, 2003; Segal, 2011). Secondly, early release of Cdc14 dephosphorylates Cdc15 promoting its role in

mitotic exit through an unknown mechanism (Jaspersen and Morgan, 2000). Following the final release of Cdc14, the Cdk1 inhibitor Sic1 is activated both transcriptionally and post-translationally. Cdc14 also dephosphorylates the APC specificity factor Cdh1 which promotes its binding to the APC. Degradation of Clb-Cdk1 by APC^{Cdh1} is a prerequisite for cytokinesis. As well, several components of the MEN (Dbf2, Cdc5) are subsequently involved in the successful completion of cytokinesis (reviewed in (Howell and Lew, 2012)).

1.7 The DNA replication checkpoint

Many cancers have been linked to defects in DNA replication and repair (Hoeijmakers, 2001; Kastan and Bartek, 2004). The cellular methods used to detect and repair such defects appear to be conserved from yeast to man (reviewed in (Lisby and Rothstein, 2004; Zhou and Elledge, 2000)). DNA damage is monitored due to external assaults on DNA by agents such as UV irradiation, or by internal errors that arise which slow replication fork progression (Reviewed in (Branzei and Foiani, 2009)). There are two checkpoints that function during S-phase. They contain many overlapping components and targets but respond to different types of DNA defects. The first is the intra-S checkpoint or DNA damage checkpoint. This checkpoint responds to DNA damage such as double strand breaks and is not dependent on replication. The second is the DNA replication checkpoint, which is also referred to as the S-phase checkpoint. This checkpoint is dependent on the formation of replication forks and the development of ssDNA. Mutations in components of the DNA replication checkpoint lead to increased genome instability in yeast and as genome instability plays a role in human cancer development, a complete understanding of this checkpoint is of great interest ((Myung et al., 2001), reviewed in (Lengauer et al., 1998)).

During replication, replication forks may slow for both exogenous and endogenous reasons. Experimentally, forks can be stalled by treatment with hydroxyurea (HU), which specifically inhibits ribonucleotide reductase (RNR) (reviewed in (Davies et al., 2009)), thus depleting deoxynucleoside triphosphate (dNTP) pools and slowing or pausing the replication fork. The DNA replication checkpoint has also been referred to as the HU checkpoint (W. Caldecott, 2004). Another agent commonly used to induce this checkpoint is methyl methanesulfonate (MMS). MMS causes slowed replication forks by modifying guanine and adenines to methyl derivatives, which causes mismatch base pairing (Beranek, 1990; Paulovich and Hartwell, 1995). Slowed replication forks also occur due to repetitive sequences or aberrant DNA structures. However, natural pause sites such as rDNA replication fork barriers, are dealt with in a checkpoint independent manner (reviewed in (Branzei and Foiani, 2009)). As replication forks slow, ssDNA becomes exposed as the helicase (MCM) continues to unwind double stranded DNA in the absence of replication (Byun et al., 2005; Nedelcheva et al., 2005; Sogo et al., 2002). RPA, is a heteromeric complex comprised of three essential protein subunits - Rpa1, Rpa2, Rpa3. RPA binds both the ssDNA of Okazaki fragments produced during lagging strand replication as well as ssDNA produced during replication stress. RPA bound ssDNA is recognized by Ddc2, which in turn recruits Mec1 (Longhese et al., 1996; Zou and Elledge, 2003). Mec1 is an essential phosphoinositide (PI)-3-kinase related protein kinase that is required to initiate signal transduction in response to DNA damage and stalled replication forks. Similar to the process of replication, where the RFC complex recognizes the 3’ end of primer DNA and assists the loading of the circular PCNA structure which encircles DNA, during DNA replication stress an RFC like complex (Rad24- Rfc2-5) recruits the PCNA like (Ddc1-Mec3-Rad17) complex to ssDNA sites (Branzei and Foiani, 2009;

Putnam et al., 2009; Zou et al., 2003). The loading of these complexes onto ssDNA, in addition to the protein Dpb11, also assists in the recruitment and activation of Mec1 (Figure 1-2).

DNA double strand breaks (DSB), if they occur during replication, can activate the DNA damage checkpoint as well as the DNA replication checkpoint. The MRX complex senses this signal and activates the Tel1 [homologue of human ataxia-telangiectasia mutated (ATM) gene] checkpoint protein kinase. If the DSB is not repaired by non-homologous end joining, long stretches of ssDNA are produced by nuclease degradation of the 5' end, which triggers the DNA replication checkpoint (Reviewed in (Harrison and Haber, 2006; Lisby and Rothstein, 2004)). Once activated, the signal from Mec1 is amplified through the transducers Mrc1 or Rad9, which in turn activate the checkpoint effector kinase Rad53. Mec1 and Rad9 also activate an additional effector kinase Chk1, although its role in yeast is much less prominent than that of Rad53 (Reviewed in (Branzei and Foiani, 2009; Harrison and Haber, 2006; Segurado and Tercero, 2009)). Certain iterations of this pathway are preferred during different points in the cell cycle, or by different types of replication stress. What is important to note is that many of the functions are at least partially redundant (Kolodner et al., 2002). For example although Mrc1, not Rad9, is the preferred signal transduction amplifier during replication stress, in the absence of Mrc1, Rad9 can promote Rad53 activation (Alcasabas et al., 2001).

Cells that are met with challenges in replication, whether caused exogenously or endogenously, carry out six important functions in order to maintain genomic integrity and

complete replication in the face of adversity. These functions are G2/M arrest, prevention of origin firing, stimulation of RNR activity, change in transcription to induce genes involved in DNA replication and repair, fork stabilization and chromatin remodeling (Figure 1-2).

1.7.1 Cell cycle arrest

Checkpoints were first described as pathways that delay mitosis in response to DNA damage (Hartwell and Weinert, 1989; Weinert and Hartwell, 1988). The cell carries out a different set of responses depending on if the DNA defects are detected in S-phase or G2/M. Although cells arrested due to HU-induced replication stress in S-phase or DNA damage in G2/M both share the same morphological characteristics such as a large bud and undivided nucleus the exact mechanism of their checkpoint response is quite different.

DNA defects detected in G2/M trigger a checkpoint response that prevents precocious mitosis in three ways (Gardner et al., 1999; Sanchez et al., 1999). Firstly, the Chk1 kinase inhibits Pds1 cleavage, thus preventing Esp1 activation and anaphase (Wang et al., 2001). Secondly, Rad53 inhibits the Cdc5 kinase, thereby preventing activation of the MEN. Thirdly, APC^{Cdc20} is phosphorylated and inhibited in a Mec1 and PKA dependent manner, thus preventing mitotic progression (Searle et al., 2004; Searle et al., 2011). The DNA replication checkpoint, arrests cells prior to spindle elongation not by targeting components of anaphase as the G2/M DNA damage checkpoint does, but by regulating spindle dynamics, and ensuring bipolar attachment (Bachant et al., 2005; Krishnan et al., 2004; Ma et al., 2007). For example during HU treatment overexpression of the microtubule motor protein Cin8 can cause spindle elongation, and removal of Cin8 can rescue the spindle defects of checkpoint

deficient cells (Krishnan et al., 2004). This demonstrates that the regulation of spindle dynamics is quite different between S-phase and G2/M phase checkpoint arrest, where only non-degradable forms of Cin8 can cause spindle elongation (Zhang et al., 2009).

Prevention of mitosis does also not appear to be an essential function of the DNA replication checkpoint nor the DNA damage response, as treatment with agents that prevent mitosis such as benomyl, does not rescue the replication stress sensitivity of checkpoint mutants (Desany et al., 1998). The situation in budding yeast is different than in *S. pombe* or mammalian cells, where both DNA damage in G2/M as well as DNA replication stress causes inhibition of the mitotic CDK complex by phosphorylation of Cdk1 on Y15 (Abraham, 2001; Amon et al., 1992; Rhind et al., 1997; Sorger and Murray, 1992). The equivalent Cdk1 phosphorylation in *S. cerevisiae* (Y19) is not required to arrest cells upon DNA damage stress or DNA replication stress (Amon et al., 1992; Sorger and Murray, 1992).

1.7.2 Prevention of origin firing

Unlike wild type cells, checkpoint deficient cells (*rad53* and *mec1*) during replication stress initiate replication from late replication origins (Santocanale and Diffley, 1998; Santocanale et al., 1999; Shirahige et al., 1998). Two different classes of kinases involved in replication initiation, Cdk1 and DDK are regulated by the Rad53 kinase activity. Cdk1 targets the protein Sld3, to initiate replication. Yet, in response to DNA replication stress, Rad53 inhibits Sld3 through phosphorylation. Similarly, a component of the replication initiation kinase complex DDK, Dbf4 is targeted for inhibition by Rad53 (Zegerman and Diffley, 2010). Recent work has shown that during DNA replication stress all replication origins do

fire but at a delayed rate (Alvino et al., 2007). This suggests that the checkpoint is involved in the proper temporal regulation of origin firing. The blocking of late replication origins however, is also not an essential function of the checkpoint. Making use of a *MEC1* mutant, *mec1-100*, which cannot block the firing of late replication origins, it was discovered that *mec1-100* is neither HU sensitive nor MMS sensitive (Tercero et al., 2003). The authors put forth the idea that it is the replication fork stability, which is the essential function of the checkpoint.

1.7.3 Stimulation of RNR

Ribonucleotide reductase (RNR) controls the level of dNTP in the cell. Increased levels of RNR can rescue the lethality of *mec1*Δ or *rad53*Δ strain (Desany et al., 1998). RNR is regulated in three ways. First, the increased transcription of RNR genes, is controlled by the activation of the kinase Dun1 and Mec1. Dun1 along with Mec1 and Rad53 phosphorylates and inhibits Crt1, a RNR gene transcriptional repressor therefore increasing RNR transcription (Huang et al., 1998). Second, RNR's activity is regulated by binding the Sml1 inhibitor, which is negatively regulated by Dun1. Third, a subunit of RNR is sequestered in the nucleus by the protein Dif1, which in turn is negatively regulated by the checkpoint (reviewed in (Labib and De Piccoli, 2011)). RNR is not the only gene that is controlled during the DNA replication checkpoint. Many genes required for DNA repair and DNA replication are under the control of the transcriptional activator MBF. In order for these genes to remain actively transcribed during the DNA replication checkpoint, Rad53 directly phosphorylates the transcriptional inhibitor Nrm1, which prevents Nrm1 binding to MBF thereby increasing transcription of MBF regulated genes (Bastos de Oliveira et al., 2012;

Travesa et al., 2012). Transcriptional changes however are not the essential function of the checkpoint as addition of cycloheximide to wild type cells during replication stress does not cause a loss of viability (Tercero et al., 2003).

1.7.4 Fork stabilization

Upon exposure to replication stress, *rad53* mutant strains exhibit broken or collapsed replication forks, replisome dissociation, a failure to complete replication and an accumulation of long stretches of ssDNA (Desany et al., 1998; Lopes et al., 2001; Sogo et al., 2002). Fork rate progression is independent of the checkpoint (Tercero and Diffley, 2001). A clear understanding of how the DNA replication checkpoint impacts the replication fork is unknown. There has been evidence to suggest that the checkpoint promotes replication fork stability through direct regulation of replication fork components (polymerase α,ε**,** MCM's, Tof1) (Reviewed in (Segurado and Tercero, 2009)). Recent work by the Labib lab, suggests that the replication fork machinery is stably associated with the DNA in the absence of checkpoint proteins Mec1 and Rad53, but that its function may be impaired (De Piccoli et al., 2012).

1.7.5 Chromatin remodeling

Chromatin remodeling and histone regulating enzymes have emerged as an important function of the checkpoint. Mec1 phosphorylates the deacetylase, Hst3 during replication stress (MMS), which targets Hst3 for degradation and thereby increases the level of histone H3K56 acetylation (Thaminy et al., 2007). This accumulation of histone H3 acetylation has been previously observed and is important in viability during HU stress (Ozdemir et al.,

2005). Additionally, Mec1 also targets Ies4 of the chromatin remodeling complex Ino80 where it is thought to modify histones ahead of stalled and defective forks thus easing fork progression (Morrison et al., 2007; Papamichos-Chronakis and Peterson, 2008; Shimada et al., 2008). Mec1 has also been reported to phosphorylate histone H2A upon DNA replication stress (Cobb et al., 2005).

1.7.6 Recovery from DNA replication stress

Successful recovery from HU induced replication stress is thought to require activation of the DNA replication checkpoint activation, active Cdk1 and degradation of the Cdk1 inhibitor Swe1. As indicated above, which DNA replication checkpoint function is essential for survival in HU is still debated. Most evidence suggests a role in replication fork stability. As well the pre-replication complex components, Cdc45 and MCM2-7 have been shown to be required for continued replication following HU treatment (Diffley et al., 2000). Cdk1 activity is required to prevent re-initiation of replication as well as to prevent gross chromosomal rearrangements during acute HU treatment (Diffley et al., 2000; Enserink et al., 2009). Interestingly, there is also evidence to suggest that the inhibitor of Cdk1 activity, Swe1 accumulated initially during HU arrest but its subsequent degradation is required for recovery from HU (Liu and Wang, 2006; Matmati et al., 2009; Raspelli et al., 2011; Tripathi et al., 2011). The degradation of Swe1 is important to ensure proper bud morphology as cells deficient in Swe1 degradation demonstrate elongated buds (Liu and Wang, 2006).

Table 1-1 GSK-3 potential substrates (Frame and Cohen, 2001; Sutherland, 2011).

GSK3 targets	Yeast homologue	No. of Criteria Met	Biological Process	Cellular Process	Function proposed for phosphorylation
Glycogen synthase	Gsy2	5	Glycogen Synthesis	Endocrine control	Inactivates
eIF2B	eIF2B complex	5	Protein synthesis	Cell growth	Inactivates
Axin	none	4	Wnt signalling		Stabilizes protein Recruits B-catenin
β-Catenin	none	4	Wnt signalling	Development	Targets for degradation
Cyclin D1	Cln3	4	Cell division cycle		Targets for degradation Nuclear export
Jun	Gcn4	4	Transcription factor	Growth and survival	Inhibits DNA binding and activation
Myc	none	4	Transcription factor	Growth and survival	Targets for degradation
C/EBPα	none	4	Transcription factor		
Tau		4	Microtubule binding protein	Neurobiology	Inhibits binding to microtubules
C/EBPβ	none	3	Transcription factor	Endocrine control Growth and survival	Inhibits DNA binding and activation
MAP1B	none	3	Microtubule binding protein	Neurobiology	Maintains microtubule instability

Table 1-2 Criteria for identification of GSK-3 substrates (Frame and Cohen, 2001).

Criteria
• The substrate should be shown, by phosphopeptide mapping and sequence analysis, to be phosphorylated by GSK-3 in vitro at the same reside(s) that is (are) phosphorylated in vivo.
• Phosphorylation should be abolished by mutagenesis of this (these) site(s) to (a) non-phosphorylatable residue(s).
• The phosphorylation of the endogenous protein in cells should decrease in response to one or more signals known to inhibit GSK-3; dephosphorylation should occur with similar kinetics as the inhibition of GSK-3.
• The endogenous protein should become dephosphorylated at the relevant site(s) in vivo when cells are incubated with cell permeant inhibitors of GSK-3.
• Phosphorylation of the residues targeted by GSK3 should affect the function of the protein in a manner consistent with physiological effects of the agonist(s) that regulate(s) GSK-3 activity.
• Phosphorylation of the protein at the GSK-3 site(s) should not occur in cells that carry targeted disruptions of the genes encoding GSK-3, and be restored when GSK-3 is replaced.
• Dephosphorylation of the protein at the GSK-3 site(s) should not occur in response to the appropriate signal signals in cells that do not express one of the protein kinases that lies upstream of GSK-3; for example, in PDK-/- embryonic stem cells, PKB, MAPKAP-K1 and p70 S6 kinase are not activated, and GSK-3 is not inhibited, in response to IGF-1 tumour - promoting phorbol esters.

Table 1-3 Mck1 substrates

Mck1 Substrates	Reference	Additional Information
Cbf2/Ndc10	(Jiang et al., 1995)	
Cdc19 (Pyk1)	(Brazill et al., 1997)	Disputed by (Rayner et al., 2002)
Hsl1	(Mizunuma et al., 2001)	GST-Hsl with HA-Mck1
MAP-2	(Lim et al., 1993)	Recombinant purified
MBP	(Rayner et al., 2002)	Also confirmed by (Lim et al., 1993) and (Dailey et al., 1990)
pCREB2	(Puziss et al., 1994)	Contains priming phosphorylation
Rcn1	(Hilioti et al., 2004)	Required priming phosporylation by p42
Rpc53	(Lee et al., 2012)	Requires priming phosphorylation by Kns1.
tau	(Lim et al., 1993)	Recombinant purified
Ubr1	(Hwang and Varshavsky, 2008)	Requires priming phosphorylation Yck1/Yck2
Ume6	(Xiao and Mitchell, 2000)	Suspected (not shown directly)

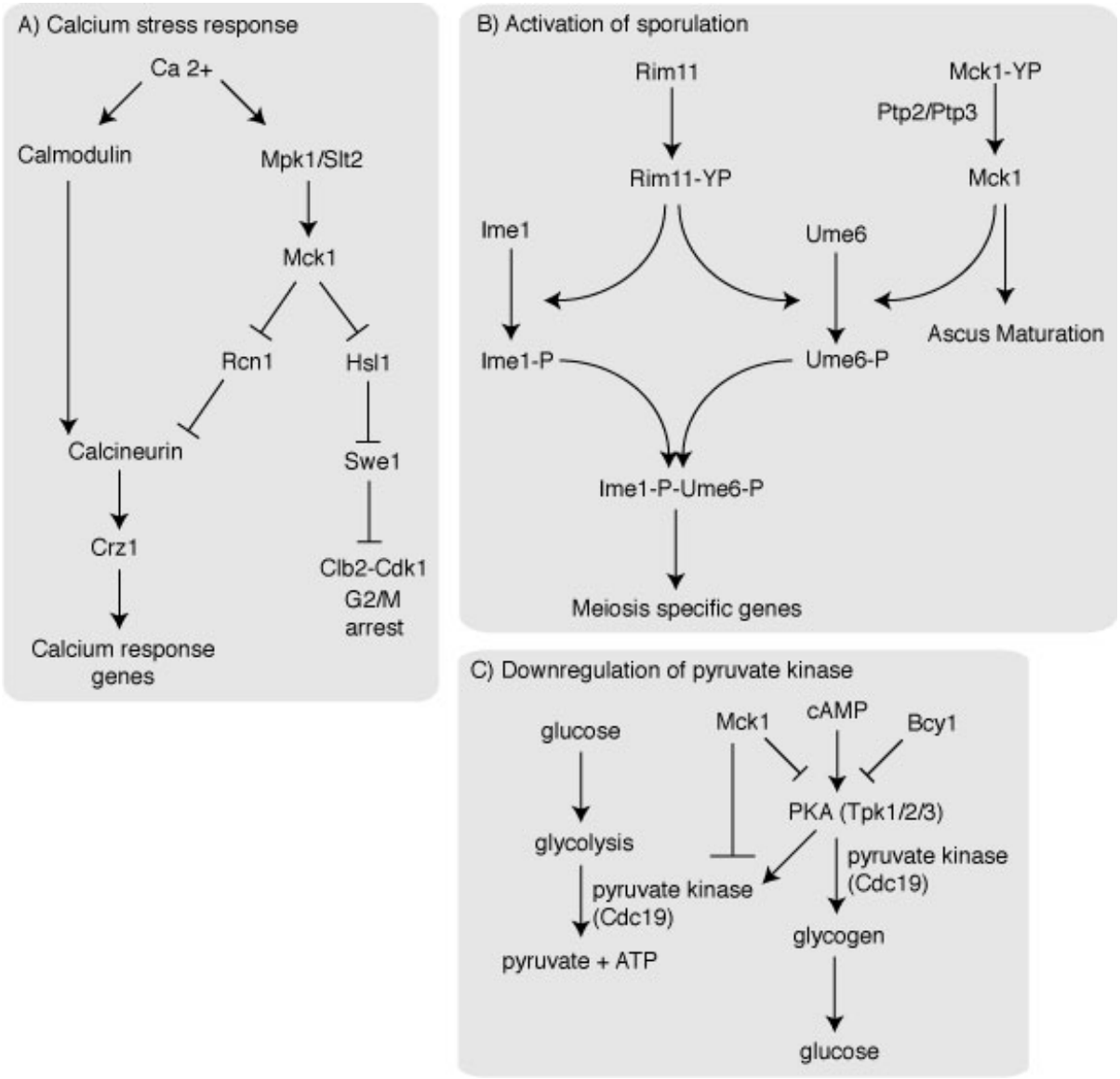

Figure 1-1 Some pathways in which Mck1 is implicated.

Table 1-4 Regulation and function of *S. cerevisiae* cyclins (Mendenhall and Hodge, 1998).

	Main function	Transcription			Inhibited by	Localization	Degraded by
		Initiates	Peaks	Factors			
CLN3	START	Throughout cell cycle	M/G1	Mcm1	Far1, Sic1 poorly	Nuclear	SCF (Grr1/Cdc4?)
CLN1	START	At Start	Late G1	SBF	Far1		SCF^{Grr1}
CLN2	START	At Start	Late G1	SBF	Far1	Cytoplasmic and sites of polarized growth	SCF^{Grr1}
CLB5	DNA replication	At Start	Late G1	MBF	Sic1	Nuclear	APC^{Cdc20}
CLB6	DNA replication	At Start	Late G1	MBF	Sic1		SCF^{Cdc4}
CLB3	SPB Separation	mid S to G2	S-phase			Nucleus, SPB, Mitotic spindle	
CLB4	SPB Separation	mid S to G2	S-phase			Nucleus, SPB, Mitotic spindle	
CLB2	Nuclear Division	G2/M	Late G2	Fkh2/Ndd1/ Mcm1	Swe1, Sic1	Nucleus, SPB, Mitotic spindle, Bud neck	APC^{Cdc20} APC^{Cdh1}
CLB1	Nuclear Division	G2/M	Late G2	Fkh2/Ndd1/ Mcm1		Nucleus, SPB, Mitotic spindle	

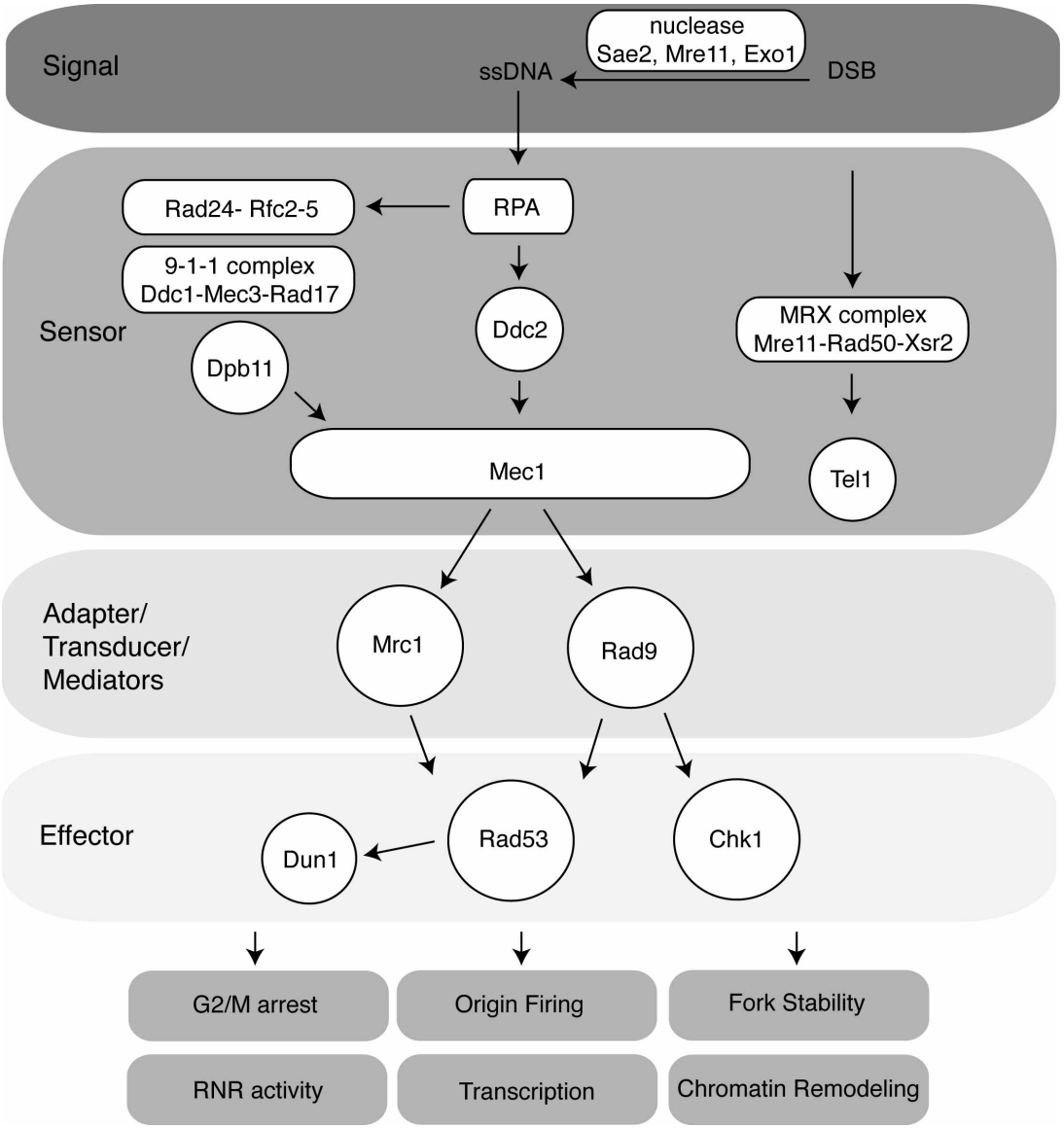

Figure 1-2 DNA replication and S-phase DNA damage checkpoint pathways.

Chapter 2: Spc24 and Stu2 promote spindle integrity when DNA replication is stalled.

Chapter 2 is a modified version of a published paper: Ma L., McQueen J., Cuschieri L., Vogel J., Measday V, Spc24 and Stu2 Promote Spindle Integrity When DNA Replication is Stalled, Molecular Biology of the Cell, 18(8): 2805-2816 (2007). By permission © The American Society for Cell Biology. See details in Preface.

2.1 Introduction

Preserving the integrity of the genome is a fundamental requirement for eukaryotic cell viability. DNA replication must be completed prior to segregation of the chromosomes to prevent the transmission of partially replicated chromosomes to daughter cells. In the budding yeast *Saccharomyces cerevisiae*, cells undergo a closed mitosis and the microtubule (MT) organizing centres, or spindle pole bodies (SPBs) are embedded in the nuclear envelope. SPB duplication begins at the end of anaphase and spindle formation begins during S phase when duplicated SPBs separate from each other (Adams and Kilmartin, 1999; Jaspersen and Winey, 2004). Because chromosomes remain attached to kinetochore MTs throughout the cell cycle, spindle expansion must be restrained until all sixteen chromosomes have duplicated and kinetochores on sister chromatids have formed bipolar MT attachments. When DNA replication is stalled by HU treatment, cells arrest with a large bud, an undivided nucleus positioned at the mother-bud neck and a short bipolar spindle (Allen et al., 1994). Maintaining a short spindle is crucial for cell survival during HU induced arrest, which activates the DNA replication checkpoint effectors Mec1 and Rad53 (Kolodner et al., 2002).

When *mec1* and *rad53* mutants are treated with HU, the DNA replication checkpoint is not activated and as a result replication forks are not stabilized, the spindle expands and unequal division of incompletely replicated nuclear material occurs – all of these events contribute to cell lethality (Allen et al., 1994; Lopes et al., 2001; Weinert et al., 1994).

In human cells, stalled replication forks activate the ATM (ataxia telangiectasia mutated) and Chk2 kinases, which are Mec1 and Rad53 homologs respectively, and arrest the cell cycle by inhibiting mitotic entry (Canman, 2001). Until recently, it was presumed that *mec1* and *rad53* mutants enter mitosis prematurely upon HU treatment. However, two recent studies have shown that this is not the case, suggesting that spindle expansion is actively restrained when DNA replication is stalled (Bachant et al., 2005; Krishnan et al., 2004; Krishnan and Surana, 2005). Two mechanisms, which are not mutually exclusive, have been proposed for how spindle expansion is prevented during the DNA replication checkpoint. One mechanism suggests that spindle associated proteins are regulated in a Mec1/Rad53-dependent manner (Krishnan and Surana, 2005). Spindle expansion and nuclear division of *mec1-1* mutants is reduced in cells carrying mutations of the kinesin-5/BimC ortholog Cin8 and XMAP215 ortholog Stu2 (Krishnan et al., 2004). The second mechanism proposes that tension imposed by the bipolar attachment of kinetochores to MTs emanating from opposite SPBs is responsible for maintaining a short spindle upon inhibition of DNA replication (Bachant et al., 2005).

In budding yeast, each kinetochore, a multi-protein complex that resides on centromere (*CEN*) DNA, attaches to a single MT (McAinsh et al., 2003). After chromosome replication,

kinetochores on sister chromatids must attach to MT emanating from opposite SPBs in order to achieve bipolar attachment. The SPB pulling force opposes the cohesion holding sister chromatids together and creates tension that physically separates *CEN* regions during metaphase (Goshima and Yanagida, 2000; He et al., 2000; Pearson et al., 2001). The kinetochore not only attaches to spindle MTs but is also capable of regulating MT dynamics and spindle stability before and during mitosis. Firstly, MT associated proteins such as Stu2 and kinesin-related motor proteins localize to and function at kinetochores (He et al., 2001; McAinsh et al., 2003; Tanaka et al., 2005; Tytell and Sorger, 2006). Secondly, the Dam1 outer kinetochore complex encircles MTs and mutations in Dam1 components severely affect MT dynamics (Cheeseman et al., 2001; Miranda et al., 2005; Shimogawa et al., 2006; Westermann et al., 2005). Thirdly, a group of kinetochore proteins called chromosome passenger proteins relocalize from kinetochores to the spindle midzone during anaphase and regulate spindle stability and cytokinesis (Bouck and Bloom, 2005).

We have identified an HU sensitive *spc24-9* kinetochore mutant that prematurely elongates its spindle upon HU treatment. By performing a high copy suppressor (HCS) screen, we have identified ten genes that when over-expressed rescue the HU sensitivity and spindle expansion defect of the *spc24-9* mutant strain. We characterized the rescue function of two of these genes –Stu1, a MT associated protein that shares a region of similarity to the CLASP/Mast/Orbit sub-family of MT plus-end tracking proteins and Stu2 which is a member of the conserved Dis1/XMAP215 family of MT plus end binding proteins (Gard et al., 2004; Inoue et al., 2000; Yin et al., 2002). We demonstrate that both Stu1 and Stu2 are localized to the kinetochore early in the cell cycle and that Stu2 kinetochore binding depends

on Spc24. By performing quantitative and time-lapse analysis of Stu2 fluorescence on spindles during HU treatment, we show that spindle expansion in *spc24-9* cells correlates with mis-localization of Stu2. We propose that localization of Stu2 to the kinetochore in cells when DNA replication is stalled is imperative for maintaining a short spindle and preventing separation of incompletely replicated DNA.

2.2 Results

2.2.1 Spc24 is required for viability and preventing spindle expansion during HU arrest

The budding yeast Ndc80 central kinetochore complex, which is composed of the four coiled-coil proteins, Ndc80, Nuf2, Spc24 and Spc25, is required for proper attachment of chromosomes to spindle MTs and activation of the spindle checkpoint in the presence of defects in attachment (Janke et al., 2001; Le Masson et al., 2002; Montpetit et al., 2005; Pinsky et al., 2006; Wigge and Kilmartin, 2001). It has recently been shown that the kinetochore has a role in maintaining a short (1.5-2μm) spindle when DNA replication is stalled by treatment of cells with HU (Bachant et al., 2005). Previously, we created two mutants in the coiled-coil region of Spc24 (*spc24-8* and *spc24-10*) and one mutant in the C-terminus of Spc24 (*spc24-9*) (Montpetit et al., 2005). We tested these alleles for viability in the presence of HU at semi-permissive temperature (30^{o}C) and found that the growth of the *spc24-9* mutant is sensitive to levels of HU that do not inhibit the growth of *spc24-8* and *spc24-10* mutants and the wild type strain (Figure 2-1A). Next, we monitored the spindle length and bulk segregation of DNA in *spc24* mutants arrested in G1 and released into 0.2M HU media. This analysis revealed that 100% of wild type and 98% of *spc24-8* and *spc24-10*

mutants maintain a short spindle and undivided nuclei after 3 hours exposure to HU, however the majority (76%) of *spc24-9* mutants displayed elongated spindles and segregated nuclei (Figure 2-1B, 2-1C). Our data suggests that the *spc24-9* mutation results in a defect in the function of the Ndc80 complex in preventing expansion of the spindle in cells with partially replicated DNA.

2.2.2 Characterization of the kinetochore in *spc24-9* mutants

The Ndc80 complex is composed of two subcomplexes - Nuf2/Ndc80 and Spc24/Spc25 – that are linked via their coiled-coil domains (Wei et al., 2005). The C-terminal mutation in *spc24-9* lies within the Spc24 globular domain (Montpetit et al., 2005; Wei et al., 2005). To determine the state of the kinetochore and the Ndc80 complex in *spc24-9* mutants, we performed chromatin immunopreciptation (ChIP) assays using a member of the inner kinetochore CBF3 complex, Ndc10 and the Ndc80 protein. We found that Ndc10 was able to interact with centromere (*CEN*) DNA in *spc24-9* cells at both restrictive temperature (37^{o}C) and after three hours of 0.2M HU treatment at 30^{o}C, suggesting that the core kinetochore is still intact in *spc24-9* mutants (Figure 2-2A, lanes 10 and 12). Ndc80, however, showed a clear defect in its ability to associate with *CEN* DNA in *spc24-9* cells both at 37^{o}C and after three hours of 0.2M HU treatment at 30^{o}C (Figure 2-2B, lanes 10 and 12). In corroboration with our ChIP data, we found that Ndc80-VFP localization was also perturbed in *spc24-9* mutants at 37^{o}C and is even more affected in HU arrested cells (Figure 2-9). 80% of HU treated *spc24-9* mutants showed diffuse and weak Ndc80-VFP staining suggesting that the Ndc80 complex is disrupted when *spc24-9* cells are exposed to 0.2M HU (Figure 2-9).

2.2.3 Bipolar attachment is not a requirement for maintaining a short spindle in HU treated cells

Previous studies have suggested that specific kinetochore mutants display inappropriate spindle expansion during HU exposure due to their inability to establish kinetochore-MT bipolar attachment and thus appropriate tension on the spindle (Bachant et al., 2005). Using a *CEN15*-GFP marked strain, we found that a similar percentage of wild type, *spc24-9* and *spc24-10* cells displayed bipolar attachment in cells released from a G1 block to 30^{o}C (Figure 2-3A). Thus, *spc24-9* kinetochores are capable of bipolar attachment to spindle poles during a normal cell cycle at the same temperature (30^{o}C) that results in *spc24-9* HU lethality. Whether or not kinetochores attain bipolar attachment in a wild type strain in the presence of partially duplicated DNA (as a result of treatment with HU) is unclear. We reasoned that exposing cells to increasing concentrations of HU would increase replication fork stalling (.05M-0.3M HU) and impact the number of *CENs* that were replicated (Clarke et al., 2001). We monitored *CEN15* separation as a sign of bipolar attachment using *CEN15*-GFP and Spc29-CFP tagged wild type and *spc24-9* mutant strains. Wild type cells treated with the lowest concentration of HU (.05M HU) exhibited *CEN15* bipolar attachment in 60% of cells after 3hours (Figure 2-3B). Importantly, *spc24-9* mutants displayed the same percentage of separated *CEN15* foci suggesting once again, that *spc24-9* mutants are capable of bipolar attachment (Figure 2-3B). Similar to previous studies, we found that separated *CEN15* foci were detected in 23% of wild type cells exposed to 0.1M HU yet only 4% of separated *CEN15* foci were seen in 0.2M HU treated wild type cells (Goshima and Yanagida, 2000; Krishnan et al., 2004). The majority of wild type cells treated with the highest concentration of HU (0.3M HU) contained one *CEN15* foci that colocalized with one SPB

suggesting either that *CEN15* had not yet replicated or had replicated but not yet established bipolar attachment (Figure 2-3C). Previous work has demonstrated that unreplicated monocentric minichromosomes also remain in the close vicinity of one SPB (Dewar et al., 2004). Thus the ability of *CEN15* to attain bipolar attachment is not correlated with maintaining a short spindle during the DNA replication checkpoint.

2.2.4 Identification of HCS genes that rescue *spc24-9* HU lethality

To understand why Spc24 is required for viability when DNA replication is stalled, we performed a HCS screen to identify genes that, when overexpressed, could suppress the lethality of *spc24-9* cells exposed to HU. Ten genes were identified in our HCS screen (Table 2-2). Multiple isolates of *SPC24* and its interacting partner *SPC25* were recovered (Janke et al., 2001; Wigge and Kilmartin, 2001). We also identified four genes encoding proteins that regulate spindle dynamics – MT associated proteins Stu1 and Stu2, the kinesin-related motor protein Kip2 and a protein involved in spindle positioning called Dma1 (Fraschini et al., 2004; Pasqualone and Huffaker, 1994; Roof et al., 1992; Wang and Huffaker, 1997). Two protein kinases were isolated – Mck1, which has a role in chromosome segregation and Rck2 which has a role in the osmotic stress response pathway (Bilsland-Marchesan et al., 2000; Neigeborn and Mitchell, 1991; Shero and Hieter, 1991). We identified Gic1 which has roles in cell polarity and mitotic exit (Brown et al., 1997; Chen et al., 1997; Hofken and Schiebel, 2004). Finally, we identified the Hcm1 transcription factor which has also been isolated in a variety of synthetic lethal screens pertaining to the cell division cycle and chromosome segregation (Daniel et al., 2006; Horak et al., 2002; Montpetit et al., 2005; Sarin et al., 2004; Zhu and Davis, 1998). Interestingly, Hcm1 has been shown to activate expression of spindle

and chromosome segregation proteins specifically in S phase (Pramila et al., 2006). None of the HCS genes were able to rescue the inviability of a *mec1* mutant on HU plates (data not shown) suggesting that they were suppressing the specific defect of *spc24-9* mutants.

2.2.5 HCS rescue occurs through restraining spindle expansion

We next determined if the HCS genes rescued *spc24-9* HU lethality by restraining spindle expansion and thus premature chromosome segregation. *spc24-9* mutants carrying the HCS rescue plasmids were synchronized in G1 phase, released into HU for 3 hours and immunofluorescence was performed to analyze chromosome segregation and spindle morphology. All of the HCS genes were able to restore a single nucleus phenotype to *spc24-9* HU treated cells (Figure 2-4D). The *STU1* and *STU2* rescue clones that we identified in our screen lacked the N-terminal 97 and 252 amino acids of Stu1 and Stu2, respectively (herein referred to as *STU1ΔN* and *STU2ΔN*). We tested if high copy full length *STU1* or *STU2* expression plasmids were capable of rescuing *spc24-9* HU lethality. Expression of full length *STU2* was clearly not able to rescue either the HU lethality or chromosome segregation defects of *spc24-9* mutants suggesting that the N-terminal truncation is an important feature of the *STU2ΔN* rescue activity (Figure 2-4A, 2-4D). Expression of full length *STU1* was able to rescue *spc24-9* HU lethality and chromosome separation at levels above vector alone, but not as well as the *STU1ΔN* clone (Figure 2-4A, 2-4D).

We reasoned that expression of *STU2ΔN* might be rescuing the spindle expansion defect in HU treated *spc24-9* mutants by destabilizing MTs. Consistent with this hypothesis, *STU2ΔN* clone lacks the TOG1 domain of Stu2 which binds tubulin heterodimers (Al-Bassam et al.,

2007; Al-Bassam et al., 2006). Previous work has shown that expression of Stu2 lacking its TOG1 domain, which still binds MTs, results in decreased mitotic spindle length and slows down anaphase spindle elongtion (Al-Bassam et al., 2006). We asked if Stu2ΔN localization is similar to endogenous Stu2 by tagging Stu2ΔN with VFP (which still retains its *spc24-9* HU rescue activity) and endogenous Stu2 with CFP. Indeed we found that Stu2ΔN-VFP localization overlapped with Stu2-CFP in both wild type and *spc24-9* mutants in log phase or HU treated cells, consistent with previous data demonstrating that Stu2ΔTOG1-GFP still binds MT plus ends (Figure 2-10, (Al-Bassam et al., 2006)). To test if depletion of Stu2 activity using another mutant form of Stu2 is also capable of preventing spindle expansion in *spc24-9* cells, we combined *spc24-9* with the *stu2-10* Ts mutation (Severin et al., 2001) and tested the double mutant for separation of nuclei upon HU treatment. Only 8% of *stu2-10 spc24-9* mutants segregated nuclei after 3 hours of HU treatment compared to 59% of *spc24-9* mutants (Figure 2-4E). Therefore, functional Stu2 is required for the spindle expansion defect in *spc24-9* mutants. Although *stu2-10 spc24-9* double mutants maintained a short spindle during HU treatment, they were lethal on HU plates at 30^{o}C (Figure 2-4B) suggesting that the defects in both Stu2 and Spc24 prevent cell cycle recovery after HU exposure.

Stu2 interacts with two other MT plus-end tracking proteins, Bim1 and Bik1 (Chen et al., 1998; Lin et al., 2001; Wolyniak et al., 2006). Since we had previously shown that *bim1 spc24-9* mutants have a synthetic growth defect (Montpetit et al., 2005), we deleted *BIK1* in *spc24-9* cells and analyzed growth phenotypes. The *bik1 spc24-9* double mutant rescued the nuclei separation defect of HU treated *spc24-9* mutants and both the HU (at 30^{o}C) and Ts (at 33^{o}C) lethality of *spc24-9* mutants (Figure 2-4C, 2-4E). Therefore the activity of Stu2 and

Bik1 is responsible for the spindle expansion and subsequent nuclei separation and lethality of *spc24-9* cells upon HU exposure.

We also determined if Stu1 is required for the spindle expansion activity in *spc24-9* HU treated cells by creating a *stu1-5 spc24-9* double mutant (Yin et al., 2002). The *stu1-5 spc24-9* mutant behaved in a similar manner to *spc24-9* mutants and elongated their spindles when treated with HU suggesting that, unlike Stu2 and Bik1, Stu1 activity is not required for spindle expansion in HU exposed *spc24-9* mutants. Although both *spc24-9* and *stu1-5* individual mutants grow well at 30^{o}C on rich media (YPD), the double mutant is synthetically lethal at 30^{o}C (Figure 2-4D). In addition, the *spc24-9 stu1-5* double mutant is viable at 25^{o}C in rich media but inviable when grown on HU plates (Figure 2-4D). The sensitivity of *spc24-9 stu1-5* double mutants to HU and the synthetic lethal interaction between *spc24-9* and *stu1-5* mutants suggests that Stu1 and Spc24 have a joint or parallel role in restraining spindle expansion during the DNA replication checkpoint.

2.2.6 Stu1 localizes to kinetochores prior to anaphase

Stu1, which was originally isolated as a suppressor of a *tub2* (β-tubulin) mutation, interacts with Tub2 and localizes to the spindle midzone in anaphase spindles (Pasqualone and Huffaker, 1994; Yin et al., 2002). However, the localization of Stu1 in relation to a SPB marker has not been assessed. We imaged Stu1 fused to VFP in relation to the Spc29-CFP SPB protein by synchronizing cells in G1 phase with mating pheromone, then releasing into the cell cycle and fixing cells every 30min. The budding yeast spindle reaches a length of 1.5-2μm prior to entering anaphase (Pearson et al., 2001). Prior to anaphase, we detected

three evenly distributed patterns of Stu1-VFP localization in fixed cells - a bilobed distribution pattern inbetween the Spc29-CFP foci which is a hallmark localization pattern for a kinetochore protein (Figure 2-5, top row) (He et al., 2001; Measday et al., 2002), a single foci located closer to one of the SPBs (Figure 2-5, second row) and a continuous signal in between SPBs (Figure 2-5, third row). In agreement with previous results, we also found that Stu1-VFP localized to the midzone of anaphase spindles (Figure 2-5, fourth row) (Yin et al., 2002). Finally, in telophase, we observed a dispersed Stu1 signal near the SPBs (Figure 2-5, bottom row).

Our localization data suggests that Stu1 may interact with the kinetochore. We tested if Stu1 localizes to the kinetochore by performing Stu1-Myc chromatin immunoprecipitation (ChIP) assays from logarithmically growing cells. Stu1-Myc specifically associated with *CEN1* and *CEN3* DNA but not with a non-*CEN* loci, *PGK1* (Figure 2-6A, lane 4). We performed a Stu1-Myc ChIP assay in a *spc24-9* mutant strain at both permissive (25^{o}C) and restrictive (37^{o}C) temperature (Figure 2-6B). Stu1-Myc is still able to associate with *CEN* DNA at restrictive temperature suggesting that Stu1 does not require Spc24 to bind kinetochores (Figure 2-6B, lane 4). In summary, our localization and ChIP data demonstrate that Stu1 localizes to kinetochores early in the cell cycle in an Spc24 independent manner and relocalizes to the spindle around the time of the metaphase to anaphase transition.

2.2.7 Stu2 localizes to kinetochores early in the cell cycle

In anaphase cells, Stu2-GFP localizes to the cytoplasmic side of the SPB and along the spindle MTs as determined by immunoelectron microscopy (Kosco et al., 2001). In addition,

Stu2 has been shown to colocalize with kinetochores and SPBs and bind *CEN* DNA in metaphase cells (He et al., 2001). We analyzed Stu2-VFP localization in short (<1.5μm) spindles (acquired at the time of bud emergence) and during normal spindle expansion using time-lapse microscopy (Figure 2-11). We observed that Stu2-VFP signal displayed a bilobed pattern between Spc29-CFP foci in short spindles (Figure 2-11, image 10b). Time-lapse microscopy using longer exposures (which saturate Stu2-VFP spindle fluorescence) revealed that Stu2-VFP also tracks on astral microtubules and transiently associates with SPBs as astral MT shorten (data not shown). Our imaging data is consistent with Stu2 localizing primarily to kinetochores and/or the nuclear spindle prior to metaphase. Once spindles had lengthened (>2μm), we detected co-localization of Stu2-VFP with Spc29-CFP as well as Stu2-VFP at the spindle midzone as previously described (Figure 2-11, image 0c) (He et al., 2001; Kosco et al., 2001). The localization of Stu2 to kinetochores early in the cell cycle suggests that defects in kinetochore function when DNA replication is stalled by HU treatment may significantly affect Stu2 activity.

2.2.8 Stu2 is mislocalized in HU treated *spc24-9* cells

We tested if Stu2 localization to the kinetochore depends on functional Spc24 by using both ChIP and microscopy analyses. Stu2-Myc displayed a decreased ability to interact with *CEN* DNA in *spc24-9* cells as we increased the temperature from permissive (25^{o}C) to semi-permissive (30^{o}C) conditions (Figure 2-6D, lanes 8 and 10). Stu2-Myc did not co-precipitate with *CEN* DNA in *spc24-9* mutants shifted to restrictive temperature (37^{o}C) suggesting that Stu2 requires Spc24 to interact with the kinetochore (Figure 2-6D, lane 12). Although Stu2 requires Spc24 for proper *CEN* localization in logarithmically growing cells, this does not

necessarily reflect the situation when cells are exposed to HU. We performed a Stu2-Myc ChIP assay in wild type and *spc24-9* cells after treating cells with HU for three hours at 30°C. Stu2 interaction with *CEN* DNA was highly reduced in *spc24-9* mutants compared to wild type cells (Figure 2-6C, compare lanes 2 and 4). Thus Spc24 is required for Stu2 to efficiently interact with *CEN* DNA in both log phase and HU treated cells. To test if Stu2 localization is perturbed in *spc24-9* cells, we performed a quantitative analysis of Stu2-VFP fluorescence during HU exposure. Cells were released from a G1 pheromone block into HU at 25°C, shifted to 30°C and fixed after 60min of incubation. At this time point, spindle expansion had clearly begun in *spc24-9* cells as spindle lengths averaged 2.5μm in mutant cells compared to 1.8μm in wild type cells (Figure 2-7B). Analysis of individual cells revealed that Stu2 remained as bilobed foci in wild type cells whereas Stu2 signal was clearly mis-localized along the spindle midzone (cs) or next to one pole (monopolar) in *spc24-9* cells (Figure 2-7A, 3-dimensional render, rotated). Analysis of Stu2-VFP fluorescence on the spindle indicated that Stu2-VFP fluorescence intensity decreased significantly in the *spc24-9* mutant relative to wild type (Figure 2-7C). Stu2-VFP also re-distributed from discrete foci to diffuse fluorescence along the length of the spindle (Figure 2-7A); thus Stu2-VFP fluorescence on the spindle per unit length (μm; see Materials and Methods for details) was used for the comparison of Stu2-VFP in wild type versus *spc24-9* cells. In general, this analysis revealed that spindles in the *spc24-9* mutant had decreased Stu2-VFP fluorescence and were longer, suggesting that spindle expansion correlates with mis-localization of Stu2 (Figure 2-7C). However, we noticed that low levels of Stu2-VFP fluorescence were found on both long and short spindles in *spc24-9* cells suggesting that the relationship between spindle length and Stu2 levels was not absolute. More specifically, we

wondered if the observed spindle expansion observed in *spc24-9* cells was permanent or represented oscillations in spindle length.

To further explore the dynamics of Stu2 interaction with the spindle and spindle expansion, we analyzed dynamic changes in Stu2-VFP fluorescence and spindle length in living cells using time-lapse microscopy. For this analysis, HU-arrested wild type and *spc24-9* mutant cells were shifted to 30^{o}C on the microscope stage and the HU arrest maintained throughout the time-lapse by mounting the cells in FP medium supplemented with HU. This analysis revealed that spindle length remains relatively static in wild type cells, with an average net change (either shrinking or elongating) in length of 0.40±0.125 μm during the time-lapse for all cells (n=4) analyzed (Figure 2-8A and 2-8C). Spindle length at the start of the time-lapse was not significantly different between wild type and *spc24-9* cells, and was similarly static in *spc24-9* cells (n=4 cells/strain) during the first 5 min. of the time-lapse (Figure 2-8B). In contrast with wild-type cells, spindle length increased significantly (1.45±0.638 μm) in the *spc24-9* mutant over time (Figure 2-8B and 2-8C). At 18 min. after the shift to 30˚C, a net increase in spindle length occurred in all four *spc24-9* cells; in each cell spindle length had increased (0.9 – 2.3 μm; mean length increase of 1.3.± 0.66 μm) relative to length at the start of the time lapse and relative to all four wild-type cells (Figure 2-8B and 2-8D). For this reason, we chose to compare the intensity of Stu2-VFP fluorescence on the spindle at time 0 and at 18 min. Stu2-VFP fluorescence was significantly decreased in *spc24-9* cells compared to wild type cells (Figure 2-8E), suggesting that mis-localization of Stu2 is correlated with the spindle expansion observed (Figure 2-8D). Finally, we detected significant oscillation of spindle length between 10- 28 min. in *spc24-9* cells (Figure 2-8B), suggesting that mis-

localization of Stu2 results in transient spindle expansion. The transient nature of this defect is consistent with our observation of a sub-population of *spc24-9* cells with short spindles and mis-localized or low Stu2-VFP levels.

2.3 Discussion

The kinetochore is required to restrain spindle expansion in budding yeast when DNA replication is stalled however the mechanism by which kinetochores maintain spindle length in this state is not well understood. We identified genes that when over-expressed, rescue the lethality and spindle expansion defects of the *spc24-9* kinetochore mutant when exposed to HU. Two MT plus end binding proteins, the CLASP related protein Stu1 and XMAP215 homologue Stu2, were identified and their interactions with the kinetochore were explored further. We find that Stu1 localizes to kinetochores early in the cell cycle and relocalizes to the spindle midzone after metaphase and that Stu2 binds to the kinetochore in a Spc24 dependent manner. In addition, inappropriate spindle expansion in HU treated *spc24-9* cells can be prevented by inhibiting Stu2 activity. We propose that mislocalization of Stu2 in *spc24-9* cells enables spindle expansion during the DNA replication checkpoint.

2.3.1 Kinetochore-MT bipolar attachment and the DNA replication checkpoint

DNA microarray studies have suggested that most *CENs* are replicated upon exposure to HU (Feng et al., 2006; Yabuki et al., 2002). Thus budding yeast *CENs* may be capable of attaining bipolar attachment during HU treatment. However, our data suggests that bipolar attachment may not be the only mechanism by which kinetochores maintain short spindles during HU arrest. Firstly, wild type and *spc24-9* cells display similar percentages of *CEN15*-

GFP bipolar foci when treated with different concentrations of HU yet only *spc24-9* spindles expand (Figure 2-3B). Secondly, when wild type cells are treated with high concentrations of HU, we detect a single *CEN15*-GFP focus that clearly colocalizes with one SPB (Figure 2-3C). This data is similar to previous studies demonstrating that a GFP marked unreplicated minichromosome colocalizes with one SPB after SPB separation (Dewar et al., 2004). Although our data does not distinguish between replicated and unreplicated *CEN15*, *CEN15* is clearly attached to one pole, yet the spindle remains short. Thus we propose that the ability to attain bipolar attachment during HU treatment is not correlated with restraining spindle expansion.

2.3.2 Stu2 activity enables spindle expansion in *spc24-9* HU treated cells

We isolated a truncated version of the XMAP215 homologue, *STU2* (*STU2ΔN*), in our *spc24-9* HCS screen that lacks the N-terminal 252 amino acids of Stu2 (Table 2-2). We propose that over-expression of *STU2ΔN* rescues *spc24-9* HU lethality by restraining MT dynamics induced by mis-localization of Stu2. *STU2ΔN* lacks the N-terminal TOG1 domain that binds tubulin heterodimers but retains the TOG2 domain that binds MT plus ends (Al-Bassam et al., 2006). Previous studies have shown that Stu2 lacking its TOG1 domain binds MT plus ends but cannot promote plus end MT growth suggesting that *STU2ΔN* inhibits *spc24-9* HU spindle expansion via the same mechanism (Al-Bassam et al., 2006). The *spc24-9* mutant and the resultant mislocalization of Stu2 (see next section) is an important feature of *STU2ΔN*'s rescue function because overexpression of *STU2ΔN* does not inhibit spindle expansion in a wild type cell cycle (Figure 2-12). Another possible Stu2ΔN rescue mechanism, which is not mutually exclusive with the previous mechanism, is that over-

expression of *STU2ΔN* is titrating out a Stu2 interacting protein that is mediating spindle expansion in *spc24-9* HU cells. Stu2 interacts with the CLIP-170 ortholog, Bik1, at the C-terminus of Stu2 (Wolyniak et al., 2006). We find that deletion of the Stu2 interacting protein Bik1 rescues the *spc24-9* spindle expansion defects and HU lethality at 30^{o}C and that the *bik1 spc24-9* double mutant grows at a higher temperature than the *spc24-9* mutant alone (Figure 2-4C, 2-4E). Thus, inhibition of Stu2 or Bik1 plus end MT activity prevents spindle expansion when *spc24-9* mutants are under HU arrest.

2.3.3 Stu2 retention at the kinetochore is important for maintaining a short spindle when DNA replication is stalled

Our data suggests that Stu2 activity is required for spindle expansion in *spc24-9* HU treated cells. The *stu2-10 spc24-9* double mutant no longer displays inappropriate spindle expansion when exposed to HU (Figure 2-4E). Why is Stu2 able to promote spindle expansion in HU treated *spc24-9* cells but not wild type cells? We propose that the inability to recruit and retain Stu2 at the kinetochore in *spc24-9* mutants enables Stu2 to promote MT dynamics. Our ChIP data suggest that the interaction of Stu2 with *CEN* DNA is perturbed in *spc24-9* mutants both in log phase cells and during HU treatment (Figure 2-6C and 2-6D). In agreement with our studies, Stu2 does not associate with *CEN* DNA at restrictive temperature in an *ndc80-1* Ts mutant (He et al., 2001). Thus the Ndc80 complex is required for recruitment of Stu2 to the kinetochore.We performed a detailed analysis of Stu2-VFP fluorescence and spindle length in both live and fixed *spc24-9* HU treated cells. Shortly after shift to restrictive temperature (30^{o}C for *spc24-9* cells exposed to HU), we detected spindle expansion and mis-localization of Stu2-VFP as well as its diffusion along the axis of the

spindle (Figure 2-7). Stu2-VFP also displayed variable localization patterns including movement to one pole and to the spindle midzone in these cells (Figure 2-7A). Our time-lapse analysis revealed that HU treatment induces *spc24-9* mutants to undergo oscillations in spindle length, unlike wild type cells where relatively little change in spindle length is detected (Figure 2-8). We identified a window of time when the spindle was at an average maximum length in these analyses and quantitated Stu2-VFP fluorescence levels at this time. Stu2-VFP fluorescence was significantly reduced compared to wild type cells suggesting a correlation between reduction in Stu2-VFP fluorescence and spindle expansion (Figure 2-8E). The oscillations observed also explain why short spindles with decreased Stu2 are observed in populations of *spc24-9* cells. Finally, oscillations in spindle length were also detected in HU exposed *rad53* mutants, suggesting that activation of the DNA replication checkpoint regulates spindle dynamics and in the absence of the checkpoint this restraint is compromised (Bachant et al., 2005). Our studies have uncovered the role of an effector of the checkpoint, Stu2, in restraining spindle dynamics while localized at the kinetochore.

2.3.4 The role of Stu2 during the DNA replication checkpoint

Does Spc24 participate in regulating spindle expansion only during the DNA replication checkpoint or also during an unperturbed cell cycle? To address this question we measured spindle length in a wild type versus *spc24-9* mutant after release from a G1 block to restrictive temperature (Figure 2-13). We found that early in the cell cycle, *spc24-9* mutants had longer spindles than wild type cells consistent with a defect in the S phase checkpoint during a normal cell cycle. As cells progressed, *spc24-9* spindle expansion lagged behind wild type cells suggesting a delay in anaphase. This data is consistent with our analysis of

DNA content during a synchronous cell cycle at restrictive temperature which demonstrated that *spc24-9* cells progress more rapidly through S phase than wild type cells (compare 60 min. time point between wild type and *spc24-9*, Figure 2-14). However, once DNA has replicated in *spc24-9* cells, a 2N content of DNA is maintained for two hours before 1N DNA content is once again detected [Figure 2-14, (Montpetit et al., 2005)]. Thus *spc24-9* cells accelerate through S phase but are delayed in anaphase.

2.3.5 Mechanism of spindle expansion in *rad53* and *mec1* mutants

The results shown here suggest that the kinetochore regulates spindle integrity during an HU induced DNA replication checkpoint by sequestering proteins such as Stu2 that regulate MT dynamics. Why then do *mec1* and *rad53* mutants elongate their spindles during the DNA replication checkpoint? A previous study used a *CEN* transcription read through assay to demonstrate that the kinetochore is still capable of blocking access to the transcription machinery in a *rad53-21* strain suggesting that the inner CBF3 kinetochore complex that binds DNA is still intact (Bachant et al., 2005). Ndc10, a CBF3 component, is also present on *CEN* DNA in *spc24-9* cells suggesting that the spindle expansion is not due to defects in inner kinetochore assembly (Figure 2-2A). Not all central kinetochore mutants display *CEN* transcription read through thus the central kinetochore may be compromised in *rad53* or *mec1* mutant strains (Doheny et al., 1993). *mec1-1* HU treated cells display upregulation of *STU2* and *CIN8* mRNA and protein levels suggesting that increased levels of MT regulatory proteins may contribute to spindle expansion in *mec1-1* cells (Krishnan et al., 2004). Our data suggests that mis-localization of Stu2 by disruption of a central kinetochore complex also causes spindle expansion during the DNA replication checkpoint.

By using HU as a method to stall cells in the process of DNA replication, we have uncovered a role for the kinetochore in regulating spindle dynamics in S phase. We have discovered a role for Spc24 in recruiting Stu2 to the kinetochore to mediate MT dynamics prior to metaphase. Mutation of Spc24 results in mis-localization of Stu2 and deregulation of spindle dynamics when DNA replication is stalled and likely during an unperturbed S phase as well. We propose that the kinetochore regulates spindle integrity during an HU induced DNA replication checkpoint by sequestering proteins such as Stu2 that play central roles in controlling spindle MT dynamics.

2.4 Materials and methods

2.4.1 Strain construction

Standard methods for yeast culture and transformation were followed (Guthrie and Fink, 1991). Rich medium (YPD), and supplemental minimal medium (SC) were used (Kaiser et al., 1994) as well as FPM (minimal media supplemented with adenine and 6.5g/L sodium citrate) for microscopy analysis (Pot et al., 2005). Yeast strains used in this study are described in Table 2-1. Genes were deleted or epitope tagged using standard yeast methods (Longtine et al., 1998).

2.4.2 HCS screen

We transformed a 2μ yeast genomic DNA library carrying 6-8kb genomic DNA fragments (Connelly and Hieter, 1996) into the *spc24-9* strain and plated 40,000 colonies onto SC-URA plates to select for the presence of the library plasmid. We then replica plated the colonies to 0.1M HU (Sigma) SC-URA plates and incubated at 30^{o}C to identify colonies that could

rescue the HU lethality of *spc24-9* mutants. Library plasmids were rescued from colonies growing on the 0.1M HU SC-URA plates and transformed back into *spc24-9* mutants to confirm the HU rescue phenotype. Plasmids were then sequenced using T3 and T7 primers to identify the flanking sequences of the genomic insert.

2.4.3 Plasmid construction - subcloning of HCS genes

The coordinates of the genomic DNA identified in the HCS screen rescue plasmids and their subsequent subclones to confirm identity of the gene are as follows:

STU1ΔN: Chr.II, 151363-158219; *STU1ΔN* subclone: Chr.II, 153753-158219; *STU2ΔN*: Chr.XII, 230442-237078; *STU2ΔN* subclone: Chr.XII 233569-237078; *KIP2*: Chr.XVI, 252390-259933; *KIP2* subclone: Chr.XVI, 257172-259933; *GIC1*: Chr.VIII, 220246-228530; *GIC1* subclone: Chr.VIII, 220246-222771; *RCK2*: Chr.XII, 634230-640397; *RCK2* subclone: Chr.XII, 634230-636611; *HCM1*: Chr.III, 224203~231351; *MCK1*: Chr. XIV, 52447-58767; *DMA1*; Chr.VIII, 337353-344031; *DMA1* subclone: Chr. VIII, 337353-342008. *DMA1* was confirmed as the gene responsible for rescue by digesting the *DMA1* subclone with EcoRI followed by Klenow treatment to create a frameshift in the *DMA1* gene. Full length *MCK1* was a gift from Dr. Phil Hieter (Shero and Hieter, 1991), full length *HCM1* was a gift from Dr. Trisha Davis (Zhu et al., 1993), and full length *STU1* and *STU2* were gifts from Dr. Tim Huffaker (Pasqualone and Huffaker, 1994; Wang and Huffaker, 1997).

2.4.4 Microscopic analyses

2.4.4.1 Immuno-fluorescence

Cells shown in Figures 2-1, 2-3, 2-4 and 2-5 were imaged using a Zeiss Axioplan 2 microscope equipped with a CoolSNAP HQ camera (Photometrics, Tucson, AZ) and Metamorph (Universal Imaging, West Chester, PA) software. The indirect immunofluorescence microscopy studies in Figures 2-1 and 2-4 were performed as described previously (Hyland et al., 1999) with the following modifications. Cells were synchronized in G1 at 25°C using α-mating factor (5μg/ml) (BioVectra), released into 0.2M HU for 3 hours at 30˚C and fixed with a final concentration of 3.7% formaldehyde for 1 hour. Spindles were visualized by staining with Yol 1-34 rat antitubulin antibody (1:50) (Serotec, Oxford) followed by fluorescein-conjugated goat anti-rat secondary antibody (1:2000). Single focal plane images were acquired with a 100X objective.

2.4.4.2 Analysis of GFP-centromeres, Stu1-VFP and Stu2-VFP localization in fixed cells

CEN15-green fluorescent protein (GFP) tagged [Figure 2-3, (Goshima and Yanagida, 2000)], cells were synchronized with α-mating factor and LacI-GFPHIS LacO::URA3-*CEN15*(1.8) was activated with 30mM 3-aminotriazole in SC–HIS media. Cells were released into indicated concentrations of HU in FPM media for 3 hours. Cells were washed and fixed in a total concentration of 2% formaldehyde for 15 min. Image stacks were acquired with a 100X objective at a step of 0.2 μm to span the entire cell. Stu1-VFP fluorescence (Figures 2-5) was imaged as described above with the following alterations. Cells were grown in FPM media at 30°C, synchronized with α-mating factor and released to 30°C. After 30 min., samples were

taken every 15 min. and fixed in 70% ethanol. Stu2-VFP in fixed cells (Figure 2-7) was imaged with a WaveFX spinning disc confocal microscope (Quorum Technologies) as previously described (Cuschieri et al., 2006) without agar pads. Optical sections (0.5 μm) were acquired through a ±2.5 μm z-plane (total of 5.0 μm stack) using Volocity 3DM acquisition software (Improvision, UK).

2.4.4.3 Live cell analysis

For live-cell imaging of Stu2-VFP fluorescence intensities and spindle length measurements (Figure 2-8 and Figure 2-11), overnight cultures were grown in YPD (containing 2X adenine sulfate) at 25˚C to a cell density of ~0.3-0.4 OD_{600} units ml^{-1}. Cultures were then diluted to 0.2 OD_{600} units ml^{-1} and grown for an additional generation. Cells were arrested with 5 ug/ml of alpha factor for 1.5 hr at 25˚C, washed and then released into media containing 0.2 M HU for 1.5 hours at 25˚C. 1 ml samples of each strain were taken and re-suspended in ~ 50 μl of 30˚C pre-warmed media containing 0.2 M HU. Cells were mounted on a pre-warmed 30˚C heated stage and allowed to equilibrate for 15 min prior to imaging.

Multi-channel 4D imaging of Spc29-CFP and Stu2-VFP fluorescent fusion proteins was performed using a WaveFX spinning disc confocal system (Quorum Technologies, Guelph ON) as previously described (Cuschieri et al., 2006). A Tokai Hit stage warmer was used to shift cells from 25˚C to 30˚C, image acquisition commenced 15 min. after the stage reached 30˚C. Optical sections (0.5 μm) were acquired through a ±2.5 μm z-plane (total of 5.0 μm stack) at 2 min. intervals for 30 min. using Volocity 3DM acquisition software (Improvision, UK).

2.4.4.4 Spindle length measurements

Calculation of spindle lengths in fixed and live cell analyses shown in Figures 2-7 and 2-8 was performed using Volocity Classification (Improvision, UK). Spindle lengths (in μm) were measured in triplicate for each time point and the average value and standard error of the mean determined. Lengths were determined by measuring the linear distance (μm; in x, y, z) between the mid-point of one SPB (Spc29-CFP channel) to the midpoint of the opposite SPB. All spindle lengths were measured in the XYZ plane view using the line length measurement tool. Average spindle lengths and standard errors were calculated using Excel software. Spindle length measurements for Figures 2-12 and 2-13 were calculated using MetaMorph software by measuring the distance between Spc29CFP foci as described (Montpetit et al., 2005).

2.4.4.5 Stu2-VFP fluorescence measurement

For Stu2-VFP fluorescence measurements shown in Figures 2-7 and 2-8, image stacks were acquired using an exposure of 91 msec/frame (providing an un-saturated image). For both fixed and live cell analyses, fluorescence intensity was measured by rastering a 4x4 voxel volume along the length of the long axis of the spindle (4x4 voxel: spindle fluorescent unit), including both SPBs. Background subtraction as performed as follows: the fluorescence in a 4x4 voxel volume positioned in the cytoplasm was measured, and subtracted from each fluorescence units acquired along the spindle resulting in corrected spindle fluorescence units (arbitrary units). For live cell analyses, background fluorescence was determined for each time point. The corrected fluorescence per unit length (fluorescence/μm) was calculated.

Background subtractions, corrected fluorescence values and standard deviations were calculated using Excel software.

2.4.5 ChIP assays

ChIP experiments and primers used for PCR analysis were performed as described previously (Measday et al., 2002; Pot et al., 2003). The linear range for PCR analysis was determined and dilutions used for Figure 2A were T (total chromatin,1:200), immunoprecipitation (IP, 1:1); Figure 2-2B, T (1:200), IP (5:1); Figure 2-2C, T (1:200), IP (5:1). Dilutions used for Figure 2-6A were T (1:780), IP (1:6); Figure 2-6B, T (1:780), IP (1:2.5); Figure 2-6C and 2-6D T (1:125), IP (1:1).

2.4.6 Flow cytometry

Flow Cytometry was performed as described (Haase and Lew, 1997).

Table 2-1 Yeast strains used in this study

Strain	Genotype	Source
CU1000	*MATa stu1-5 his3D200 leu2-3,112 ura3-52*	(Yin et al., 2002)
CUY1088	*MATa stu2-10::URA3 his3D200 leu2-3,112 ura3-52*	(Kosco et al., 2001)
TWY308	*MATa mec1-1 ura3 trp1*	(Weinert et al., 1994)
YLM79	MATa *ura3-52, lys2-801, ade2-101, his3D200, leu2D1, trp1D63 STU1-MYC::TRP1*	This study
YLM185	MATa *ura3-52, lys2-801, ade2-101, his3D200, leu2D1, trp1D63 STU1-VFP::kanMX6 SPC29-CFP:: hphMX4*	This study
YLM187	MATa *ura3-52, lys2-801, ade2-101, his3D200, leu2D1, trp1D63 STU2-VFP::kanMX6 SPC29-CFP:: hphMX4*	This study
YLM288	MATa *ura3-52, lys2-801, ade2-101, his3D200, leu2D1, trp1D63 STU2-VFP::kanMX6 SPC29-CFP:: hphMX4 spc24-9::natMX4*	This study
YLM400	MATa *ura3-52, lys2-801, ade2-101, his3D200, leu2D1, trp1D63 STU2-MYC::TRP1 spc24-9::natMX4*	This study
YLM451	MATa *ura3-52, lys2-801, ade2-101, his3D200, leu2D1, trp1D63 STU1-MYC::TRP1 spc24-9::natMX4*	This study
YLM533	MATa *ura3-52, lys2-801, ade2-101, his3D200, leu2D1, trp1D63 NDC80-VFP::kanMX6 SPC29-CFP:: hphMX4*	This study
YLM535	MATa *ura3-52, lys2-801, ade2-101, his3D200, leu2D1, trp1D63 NDC80-VFP::kanMX6 SPC29-CFP:: hphMX4 spc24-9::natMX4*	This study
YLM542	MATa *ura3-52, lys2-801, ade2-101, his3D200, leu2D1, trp1D63 NDC80-13MYC::His3MX6 SPC24::natMX4*	This study
YLM544	MATa *ura3-52, lys2-801, ade2-101, his3D200, leu2D1, trp1D63 NDC80-13MYC::His3MX6 spc24-9::natMX*	This study
YLM557	MATa *ura3-52, lys2-801, ade2-101, his3D200, leu2D1, trp1D63 NDC10::13MYC::kanMX spc24-9::natMX4*	This study
YLM609	MATa *ura3-52, lys2-801, ade2-101, his3D200, leu2D1, trp1D636 STU2-CFP:: hphMX4 pSTU2DN-VFP::kanMX*	This study
YLM610	MATa *ura3-52, lys2-801, ade2-101, his3D200, leu2D1, trp1D636 STU2-CFP:: hphMX4 spc24-9::natMX4 pSTU2DN-VFP::kanMX*	This study
YM234	MATa *ura3-52, lys2-801, ade2-101, his3D200, leu2D1, TRP1+ stu2-10::URA3 spc24-9::kanMX6*	This study
YM406	MATa *ura3-52, lys2-801, ade2-101, his3D200, leu2D1, trp1D63 STU2-MYC::TRP1*	This study
YM480[a]	*MATa LacI-GFP::HIS3 LacO::URA3-CEN15(1.8) Spc29-CFP::kanMX6 SPC24::natMX4*	This study
YM482[a]	*MATa LacI-GFP::HIS3 LacO::URA3-CEN15(1.8) Spc29-CFP::kanMX6 spc24-9::natMX4*	This study

Strain	Genotype	Source
YM487[a]	*MATa LacI-GFP::HIS3 LacO::URA3-CEN15(1.8) Spc29-CFP::kanMX6 spc24-10::natMX4*	This study
YM836	MATa *ura3-52, lys2-801, ade2-101, his3D200, leu2D1, trp1D63 bik1::kanMX6*	This study
YM903	MATa *ura3-52, lys2-801, ade2-101, his3D200, leu2D1, TRP1+ stu1-5 spc24-9::kanMX6*	This study
YM935	MATa *ura3-52, lys2-801, ade2-101, his3D200, leu2D1, trp1D63 bik1::kanMX6 spc24-9::natMX4*	This study
YPH499	MATa *ura3-52, lys2-801, ade2-101, his3D200, leu2D1, trp1D63*	P. Hieter
YPH1734	MATa *ura3-52, lys2-801, ade2-101, his3D200, leu2D1, trp1D63 NDC10::13MYC::kanMX6*	(Measday et al., 2002)
YVM1363	MATa *ura3-52, lys2-801, ade2-101, his3D200, leu2D1, trp1D63 spc24-10::kanMX6*	(Montpetit et al., 2005)
YVM1370	MATa *ura3-52, lys2-801, ade2-101, his3D200, leu2D1, trp1D63 SPC24::kanMX6*	(Montpetit et al., 2005)
YVM1380	MATa *ura3-52, lys2-801, ade2-101, his3D200, leu2D1, trp1D63 spc24-9::kanMX6*	(Montpetit et al., 2005)
YVM1448	MATa *ura3-52, lys2-801, ade2-101, his3D200, leu2D1, trp1D63 spc24-8::kanMX6*	(Montpetit et al., 2005)
YVM1591	MATa *ura3-52, lys2-801, ade2-101, his3D200, leu2D1, trp1D63 spc24-9::natMX4*	This study

[a]These strains were created by mating a W303 strain derivative (Goshima and Yanagida, 2000) with an S288C strain derivative hence the precise genotype is not known.

Table 2-2 HCS screen of *spc24-9* HU lethality.

HU rescue[a]	Gene Name	ORF	Biological Process[d]
+	*DMA1*	YHR115C	Spindle position and orientation
+	*RCK2*	YLR248W	Oxidative and osmotic stress signaling
+	*STU1* truncated[b]	YBL034C	MT dynamics
+ +	*GIC1*	YHR061C	Cell polarity
+ + +	*KIP2*	YPL155C	Mitotic spindle positioning
+ + +	*MCK1*	YNL307C	Mitotic and meiotic chromosome segregation
+ + + +	*HCM1*	YCR065W	Transcription
+ + + + +	*STU2* truncated[c]	YLR045C	MT dynamics
+ + + + +	*SPC24*	YMR117C	Chromosome Segregation
+ + + + +	*SPC25*	YER018C	Chromosome Segregation

[a]growth of *spc24-9* mutant carrying rescue clone struck on .05M HU plates at 30^{o}C

from weak (+) to strong (+++++) growth

[b]the *STU1* rescue clone is missing the N-terminal 97 amino acids

[c]the *STU2* rescue clone is missing the N-terminal 252 amino acids

[d]GO Annotation from *Saccharomyces* Genome Database

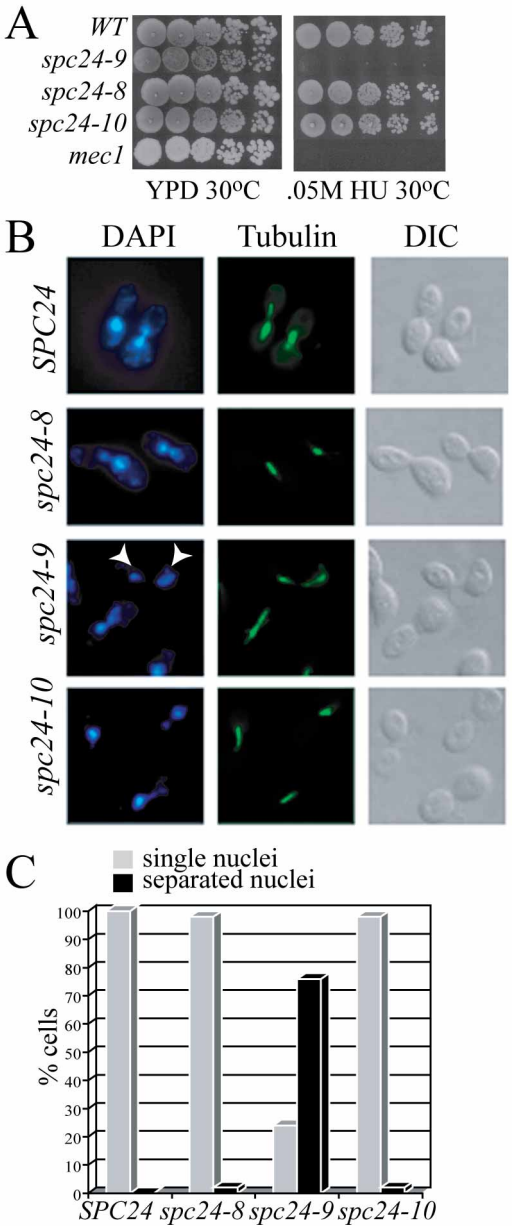

Figure 2-1 *spc24-9* mutants are sensitive to HU due to inappropriate spindle expansion.

(A) Cell dilution assay of indicated strains grown on YPD and .05M HU at 30°C for 3 days. (B) Immunofluorescence analysis of wild type (*SPC24*), *spc24-8*, *spc24-9* and *spc24-10* cells synchronized in G1 phase with α-factor, then released into 0.2M HU for 3 hours at 30°C. Shown are representative cells after 3 hours HU treatment imaged for DNA (DAPI), MTs (Tubulin) and cell morphology (DIC). White arrowheads point to separated nuclei in the *spc24-9* mutant. (C) Percentage of cells (100 cells counted) described in (B) displaying single (grey bars) or separated (black bars) nuclei.

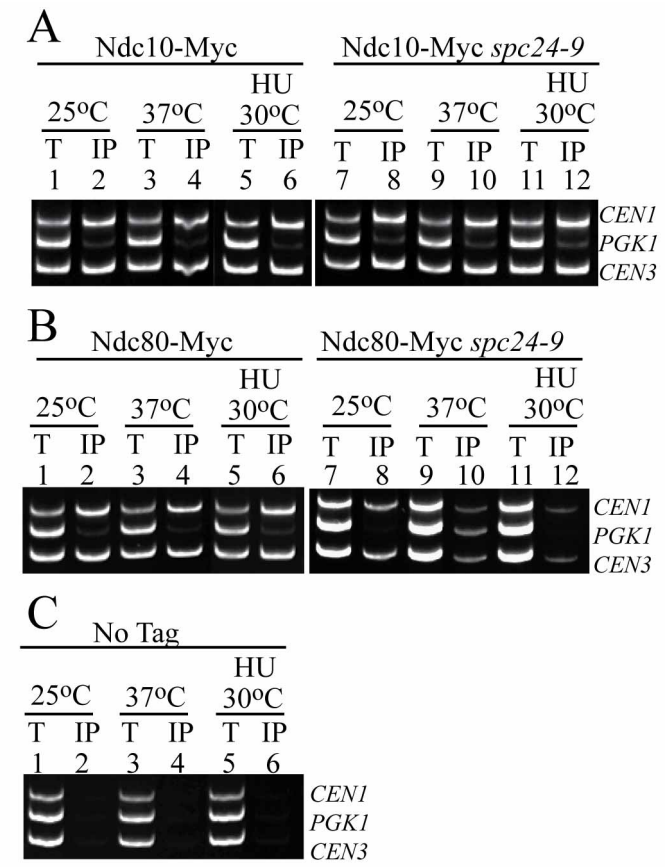

Figure 2-2 Ndc80 CEN association is disrupted in *spc24-9* mutants.

Multiplex PCR analysis of *CEN1*, *PGK1* and *CEN3* loci was performed with total chromatin (T) or immunoprecipitate (IP) as PCR templates. Strains were grown at 25°C to log phase, then either shifted to 37°C for three hours, or incubated in 0.2M HU at 30°C for three hours. (A) Ndc10-Myc wild type (lanes 1-6) or *spc24-9* cells (lanes 7-12). (B) Ndc80-Myc wild type (lanes 1-6) or *spc24-9* cells (lanes 7-12). (C) Wild type strain carrying no epitope tag (No Tag, lanes 1-6) shown as a control. An untagged *spc24-9* mutant was also used as a control and showed similar results (data not shown).

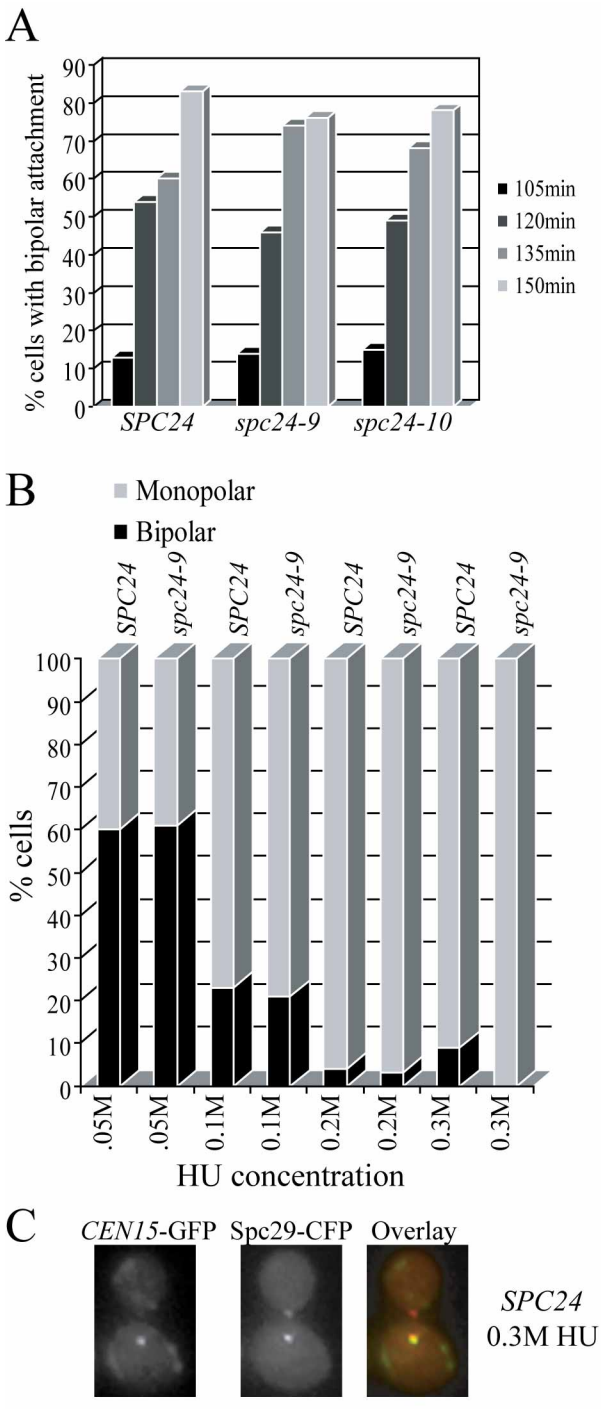
A
% cells with bipolar attachment
90
80
70
60
50
40
30
20
10
0
105min
120min
135min
150min
SPC24
spc24-9
spc24-10
B
Monopolar
Bipolar
SPC24
spc24-9
SPC24
spc24-9
SPC24
spc24-9
SPC24
spc24-9
% cells
100
90
80
70
60
50
40
30
20
10
0
.05M
.05M
0.1M
0.1M
0.2M
0.2M
0.3M
0.3M
HU concentration
C
CEN15-GFP
Spc29-CFP
Overlay
SPC24
0.3M HU

Figure 2-3 *spc24-9* mutants are capable of establishing bipolar attachment.

(A) Wild type (*SPC24*), *spc24-9* and *spc24-10* strains carrying LacO repeats integrated 1.8kb from *CEN15*, LacI-GFP and Spc29-CFP were synchronized in G1 phase with α-factor and released at 30°C. Samples were taken every 15 min. and imaged using fluorescence microscopy for the presence of the *CEN15*-GFP and Spc29-CFP signal. Shown are the time points (105 min. onwards) at which the cells began to display bipolar attachment (separation of *CEN15*-GFP signals). Duplicate experiments were performed with similar results. Shown is the result of one experiment in which 100 cells containing a spindle of 0.5μm or larger were counted for each time point. (B) Wild type (*SPC24*) and *spc24-9 CEN15*-GFP Spc29-CFP strains were synchronized in G1 phase with α-factor, split into four cultures and indicated concentrations of HU were added for 3 hours at 30°C. Similar results were seen with duplicate experiments thus data from one experiment is shown (100 cells counted). (C) Example of a wild type (*SPC24*) cell from (B) after 3 hours of 0.3M HU treatment that displays monopolar *CEN15* attachment. In the overlay, *CEN15*-GFP is green and Spc29-CFP is red.

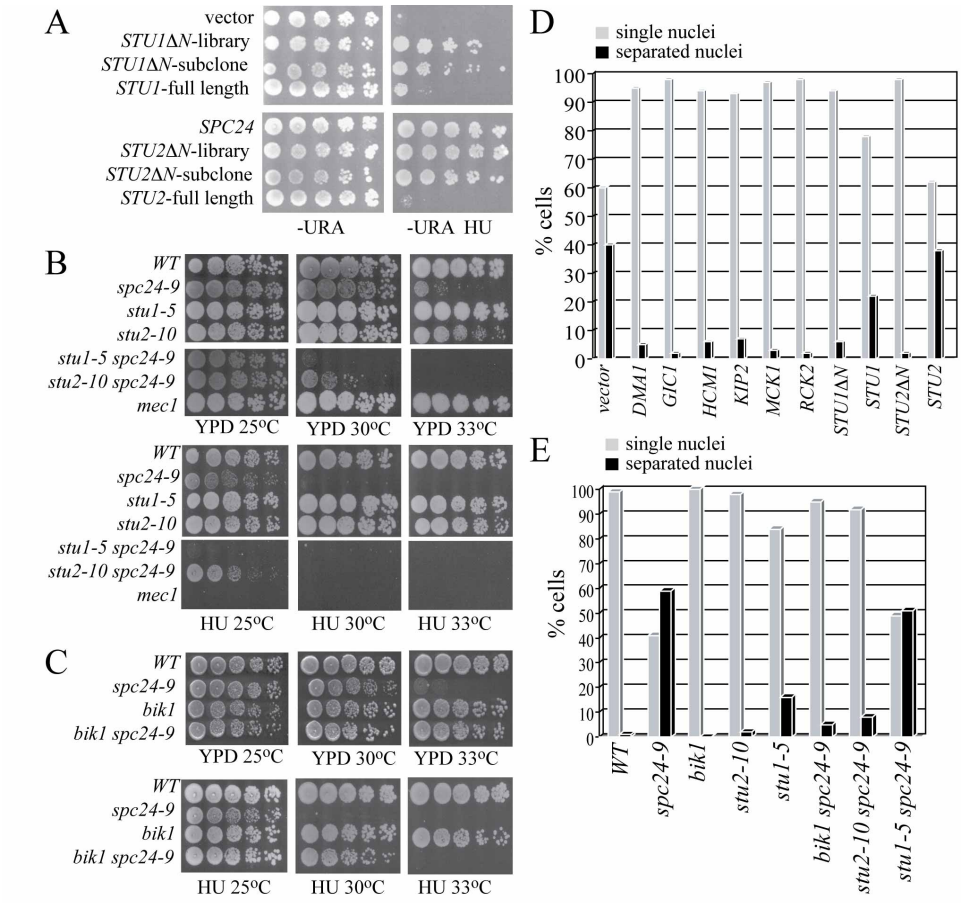

Figure 2-4 Spindle expansion in *spc24-9* mutants depends on active Stu2.

(A) Cell dilution assay of *spc24-9* mutants carrying the following 2μ plasmids: vector (pRS202), *STU1ΔN*-library (HCS clone identified in screen), *STU1ΔN*-subclone (subclone of *STU1ΔN*-library containing only the *STU1* gene), *STU1* full length (gift of T. Huffaker), full length *SPC24*, *STU2ΔN*-library (HCS clone identified in screen), *STU2ΔN*-subclone (subclone of *STU2ΔN*-library containing only the *STU2* gene), *STU2* full length (gift of T. Huffaker) were grown on -URA plates at 30°C for 4 days or –URA .05M HU at 30°C for 5 days. (B) and (C) Cell dilution assay of indicated strains grown on YPD at 25°C (2 days), 30°C and 33°C (3 days) and .05M HU at 25°C, 30°C and 33°C (3 days). (D) Immunofluorescence analysis of *spc24-9* mutants carrying the indicated HCS plasmids synchronized in G1 phase with α-factor, then released into 0.2M HU for three hours at 30°C. Cells were counted (100 per sample) for single nuclei (grey bars) or separated nuclei (black bars) by DAPI staining. Duplicate experiments were performed with similar data and shown is the result of one experiment. (E) Immunofluorescence analysis of indicated strains treated and analyzed as described in (D).

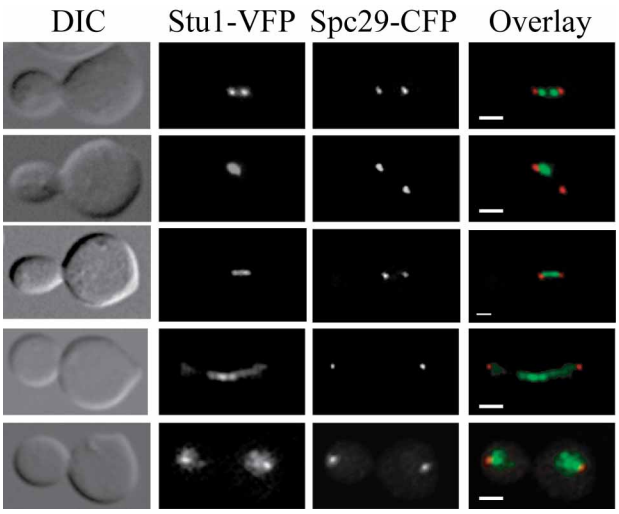

Figure 2-5 Stu1 localizes to kinetochores and the spindle midzone.

Wild type Stu1-VFP Spc29-CFP cells were synchronized in G1 phase with α-factor and released into the cell cycle at 30°C. Cells were fixed in 70% ethanol every 15 min. for 90 min. and imaged as described in the Material and Methods. In the overlay, green is VFP signal and red is CFP. Scale bar is 2μm for all images.

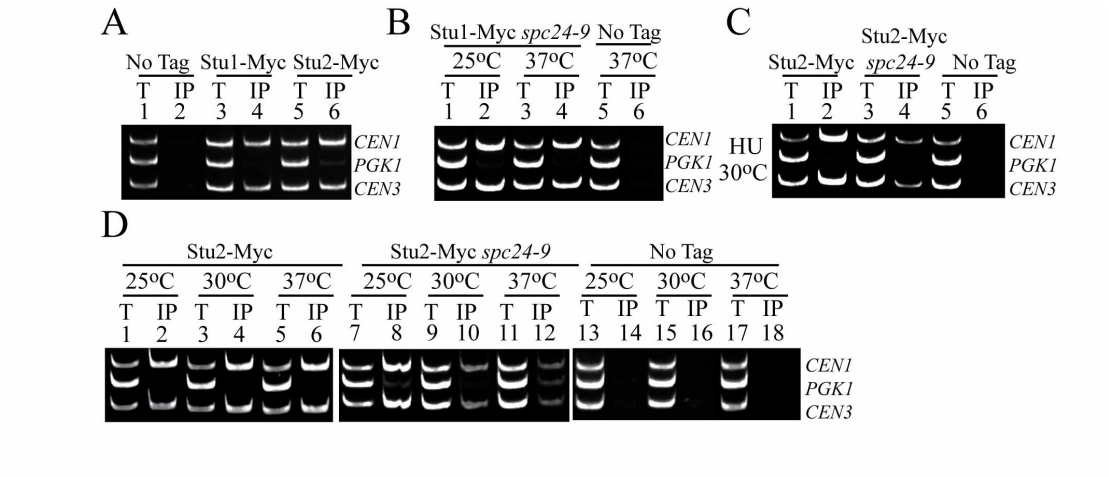

Figure 2-6 Stu2 CEN binding is abolished in *spc24-9* mutants whereas Stu1 is still able to associate with CEN DNA.

Multiplex PCR analysis of *CEN1*, *PGK1* and *CEN3* loci was performed with total chromatin (T) or immunoprecipitate (IP) as PCR templates. Strains were grown at 25ºC to log phase, then either kept at 25ºC or incubated at 30ºC or 37ºC for three hours. (A) Wild type log phase cells grown at 30ºC and carrying no epitope tag (No Tag), (lanes 1-2), Stu1-Myc (lanes 3-4) and Stu2-Myc (lanes 5-6). (B) *spc24-9* mutants carrying Stu1-Myc (lanes 1-4) and a wild type strain with no tag at 37ºC (lanes 5-6). (C) Stu2-Myc in a wild type (lanes 1-2), *spc24-9* (lanes 3-4) and an untagged wild type strain (NoTag, lanes 5-6). Strains were grown to log phase at 25ºC, HU was added to a final concentration of 0.2M HU and cells were shifted to 30ºC for three hours. (D) Stu2-Myc in a wild type (lanes 1-6) and *spc24-9* (lanes 7-12) strains. No Tag strain (lanes 13-18) is an untagged wild type strain. For all ChIP assays where the *spc24-9* mutant was used, we included both a wild type and *spc24-9* untagged control and saw similar results thus only the wild type untagged control is presented.

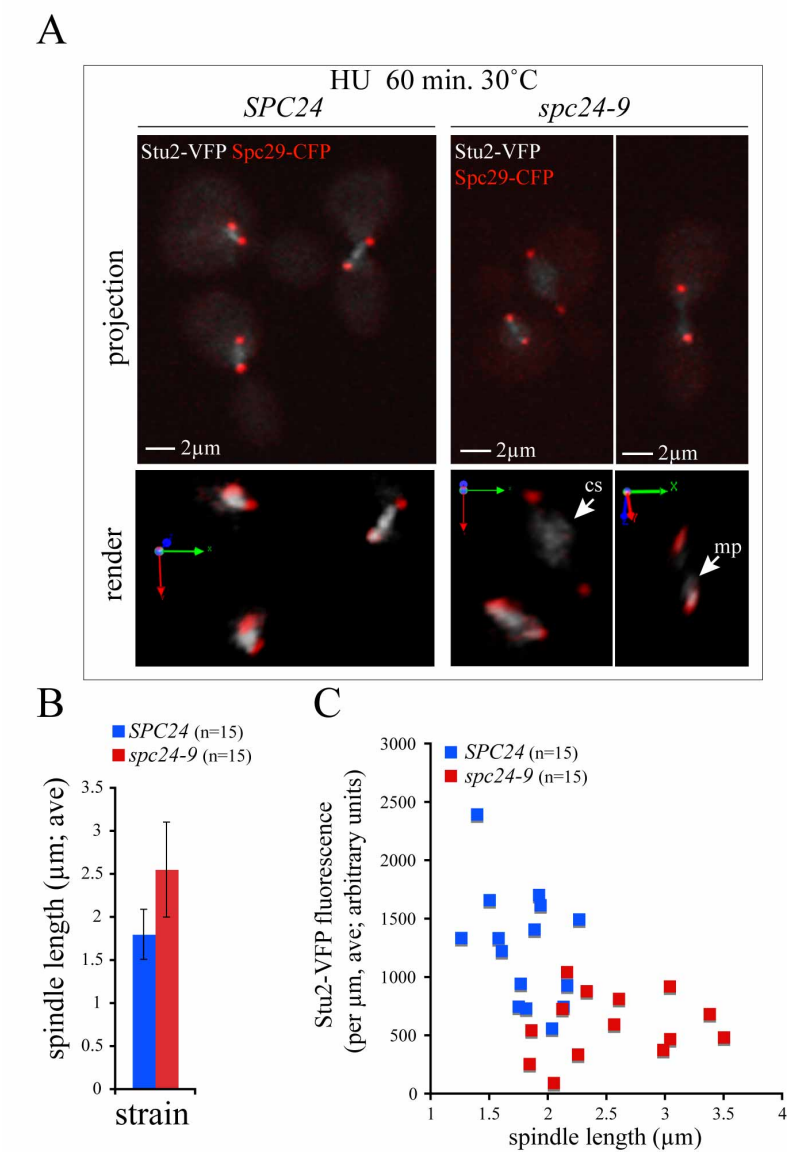

Figure 2-7 Increased spindle length correlates with Stu2 mislocalization and reduction.

Wild type (*SPC24*) and *spc24-9* cells expressing Stu2-VFP Spc29-CFP were synchronized in G1 phase with pheromone, released into 0.2M HU at 25°C for 1.5h and shifted to 30°C in HU for 60 min., then fixed. (A) Representative images (extended focus and 3-dimensional render) of Stu2-VFP (greyscale) and Spc29-CFP (red) fluorescence in wild type and *spc24-9* cells at 60 min. after shift to 30°C are shown; mp indicates monopolar localization (near the SPB), whereas cs indicates localization to the central spindle. (B) Average (ave) spindle length of wild type (*SPC24*) and *spc24-9* cells after a 60 min. incubation in 0.2M HU at 30°C (n=15). (C) Quantitative analysis of Stu2-VFP fluorescence per µm plotted as a function of spindle length.

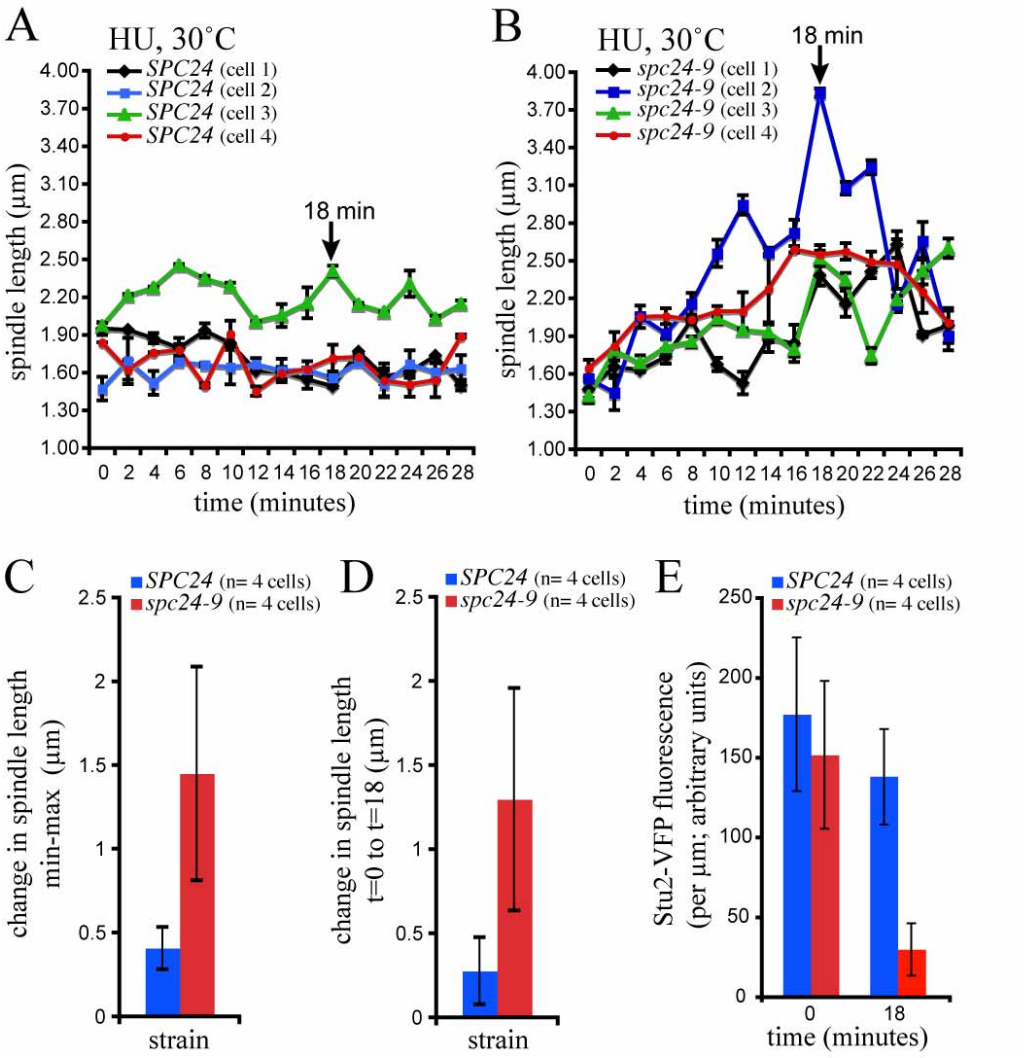

Figure 2-8 Decreased Stu2 in the *spc24-9* mutant results in oscillation of spindle length.

Wild type (*SPC24*) and *spc24-9* cells carrying Stu2-VFP Spc29-CFP were synchronized in G1 phase with pheromone, released into 0.2M HU at 25°C for 1.5h, mounted in FP supplemented with HU, shifted to 30°C on a heated stage and time-lapse microscopy performed. Time zero is time in HU at 30°C after equilibration on the stage at 30°C for 15 min. Spindle length is plotted for four cells of each strain (A, *SPC24*; B, *spc24-9*) as a function of time, each depicted with a different colour, and shows oscillation with a net increase in length observed in all four *spc24-9* cells at 18 min. (C) In contrast with wild-type cells, spindle length increases in *spc24-9* cells. (D) Spindle length is significantly increased in all four *spc24-9* cells at 18 min. relative to length at t=0. (E) At 18 min., Stu2-VFP fluorescence on the spindle is significantly decreased in all *spc24-9* mutant cells relative to wild-type cells.

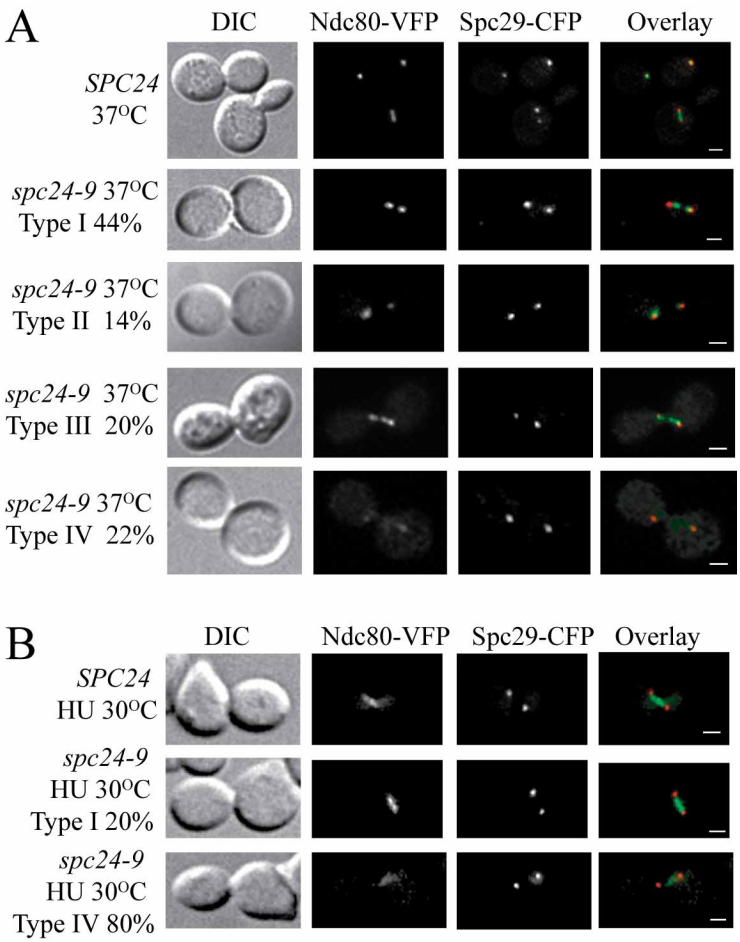

Figure 2-9 Ndc80 is mislocalized in *spc24-9* mutants.

(A) Ndc80-VFP Spc29-CFP wild type (*SPC24*) and *spc24-9* cells were grown at 25°C to log phase, then incubated at 37°C for three hours, fixed in 70% ethanol and imaged. Four types of Ndc80 localization patterns were detected in *spc24-9* mutants: Type I: Wild type Ndc80, 44% of cells; Type II: Ndc80 localized to one SPB (14% of cells); Type III: Multiple Ndc80 foci (20% of cells); Type IV: Little or no Ndc80-VFP signal (22% of cells). (B) Ndc80-VFP Spc29-CFP wild type (*SPC24*) and *spc24-9* cells were grown at 25°C to log phase, then incubated at 30°C in 0.2M HU for three hours, fixed in 70% ethanol and imaged. In *spc24-9* cells, Ndc80-VFP localization either resembled wild type cells (20% of cells) or Ndc80-VFP levels were very low and barely detectable (80% of cells). In the overlay, green is VFP signal and red is CFP. Scale bar is 2μm for all images.

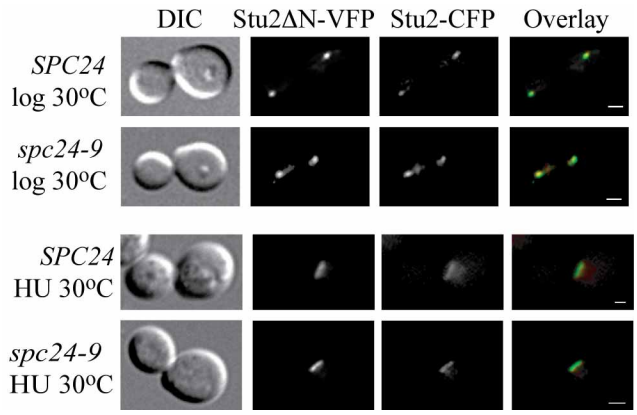

Figure 2-10 Stu2ΔN-VFP localization overlaps with endogenous Stu2-CFP.

Wild type (*SPC24*) and *spc24-9* strains carrying Stu2ΔN-VFP on a 2μ plasmid and endogenous Stu2-CFP were either grown at 30°C to log phase or incubated in 0.2M HU for three hours, fixed in 70% ethanol and imaged. In the overlay, green is VFP signal and red is CFP. Scale bar is 2μm for all images.

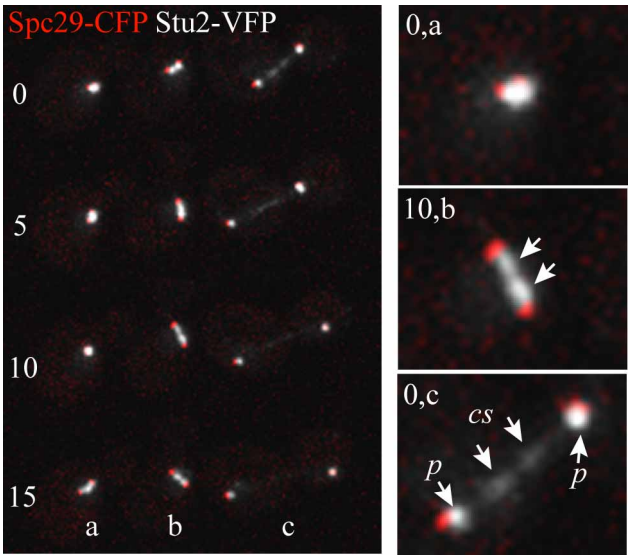

Figure 2-11 Time-lapse analysis of Stu2-VFP.

Stu2-VFP Spc29-CFP cells were imaged using time-lapse microscopy at 30°C as described in the Materials and Methods. Stu2-VFP is represented in greyscale and Spc29-CFP in red. Arrows in Image 10,b point to Stu2-VFP bilobed foci on the nuclear side Spc29-CFP. Arrows in Image 0, c point to Stu2-VFP localization on the central spindle (cs) and poles (p).

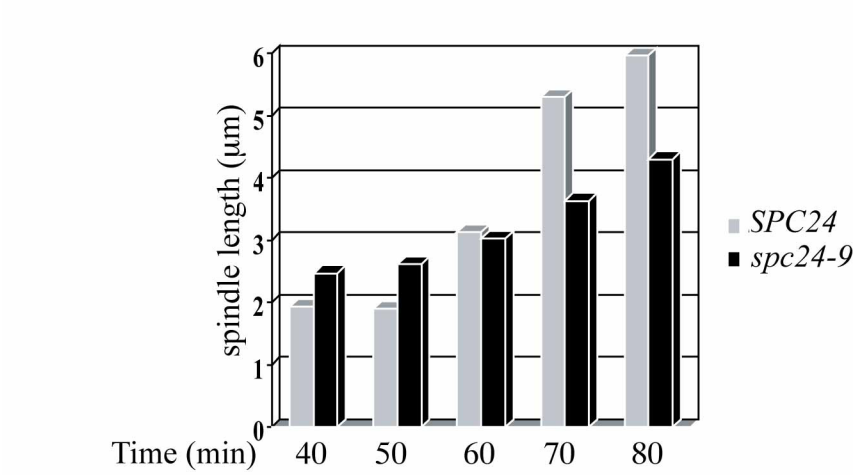

Figure 2-12 Overexpression of *STU2ΔN* does not affect wild type spindle length in an unperturbed cell cycle.

Vector control (pRS326) and *STU2ΔN* were expressed in cells carrying Stu2VFP Spc29CFP. Cells were grown to log phase at 30°C, arrested with α-factor for 1.5hours at 30°C, released to 30°C and time points taken every 15min. Spindle length was calculated as described in the Materials and Methods. Thirty cells were counted for each time point.

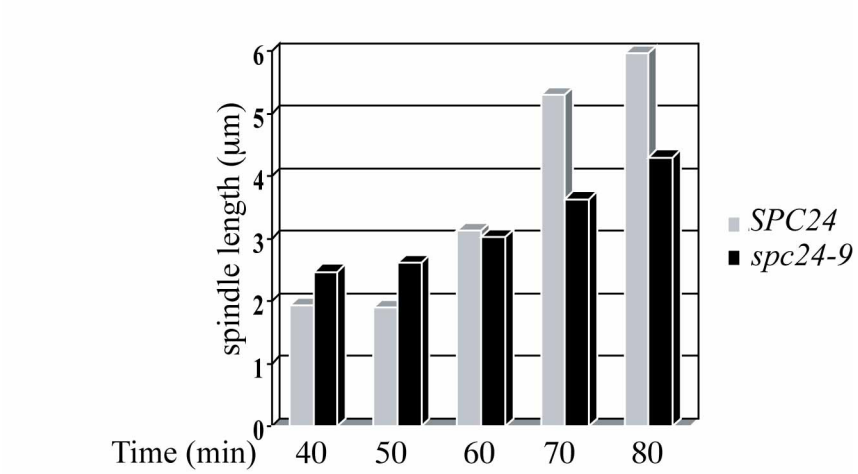

Figure 2-13 *spc24-9* mutants display spindle expansion early in the cell cycle but a delay in anaphase.

Wild type (*SPC24*) and *spc24-9* cells carrying Stu2VFP Spc29CFP were grown at 25°C to log phase, incubated with α-factor for 1hour at 25°C, resuspended in prewarmed 37°C media with new α-factor and incubated for 2 hours at 37°C. Cells were then released from the G1 arrest into 37°C and time points taken every 10min. Spindle length was measured by calculating the distance from Spc29-CFP foci to Spc29-CFP foci. Fifty cells were counted per time point.

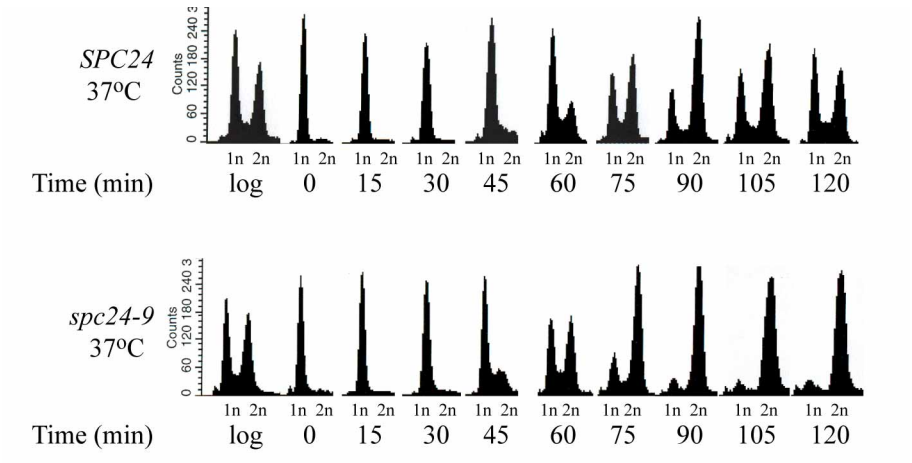

Figure 2-14 ***spc24-9*** **mutants accelerate through S phase and delay at anaphase at restrictive temperature.**

Wild type (*SPC24*) and *spc24-9* cells were grown at 25°C to early log phase, arrested in G1 phase with pheromone, released to 37°C and time points taken every 15 min. DNA content was measured by flow cytometry as described in the Materials and Methods.

Chapter 3: Mck1 inhibits the activity of Clb2-Cdk1 post nuclear division.

3.1 Introduction

Mck1 is a GSK-3 protein kinase that in budding yeast has been implicated in calcium response (Mizunuma et al., 2001), kinetochore function (Jiang and Koltin, 1996; Jiang et al., 1995; Shero and Hieter, 1991), sporulation (Neigeborn and Mitchell, 1991; Zhan et al., 2000), transcription during stress response (Hirata et al., 2003) and nutrient sensing (Brazill et al., 1997; Griffioen et al., 2003; Pereira et al., 2009; Rayner et al., 2002). Through phosphorylation, Mck1 can target its substrates for degradation (Hwang and Varshavsky, 2008; Mizunuma et al., 2001). Mck1 also inhibits the activity of targets through its physical association with the target (Rayner et al., 2002) or by indirectly causing re-localization of the target (Griffioen et al., 2003; Mizunuma et al., 2001).

Cells possess tightly controlled mechanisms to replicate and segregate chromosomes accurately into daughter cells. To achieve this, cyclin dependent kinases (CDK) control events particular to each step of the cell cycle. In budding yeast there is only one major CDK that controls cell cycle progression, Cdk1 *(CDC28)*. Cells fluctuate between a period of high Cdk1 activity, whereby chromosomes are replicated and segregated and periods of low Cdk1 activity required for mitotic exit and licensing of origins of replication (Chen et al., 2000; Nasmyth, 1996). This oscillation of Cdk1 activity helps to ensure that one cell cycle is completed before the subsequent one begins. Throughout S-phase and G2, protein levels of both Swe1 (Sia et al., 1996) and the mitotic cyclin Clb2 rise (Surana et al., 1991). Clb2-Cdk1 is inhibited by Swe1's inhibitory phosphorylation on Y19 (Booher et al., 1993). Once Swe1 is degraded by a concerted effort of many proteins (Cla4, Hsl1, Cdk1, Cdc5, Clb2-Cdk1)

Clb2-Cdk1 is fully activated. Any remaining inhibitory phosphorylation (Y19) can then be removed through the action of the Mih1 phosphatase (Asano et al., 2005; Sakchaisri et al., 2004). Once active, Clb2-Cdk1 promotes the assembly of the mitotic spindle and entry into anaphase (Chee and Haase, 2010; Rahal and Amon, 2008).

These aforementioned mechanisms controlling Cdk1 activity upon mitosis are themselves subject to regulation. Swe1's activity is monitored through the morphogenic checkpoint, while Mih1's regulation is less well understood. The morphogenic checkpoint oversees bud neck assembly through specific placement of regulatory kinases at the bud neck (Lew and Burke, 2003). Only when the neck is properly assembled is Swe1 degraded and mitotic Clb2-Cdk1 activated. The morphogenic checkpoint is well documented to respond to septin collar or actin cytoskeleton disturbances (reviewed (Lew, 2003)) but also responds to increased calcium levels (Miyakawa and Mizunuma, 2007) and DNA replication stress (Enserink et al., 2006; Liu and Wang, 2006). Mih1 shows both cell cycle dependent phosphorylation and localization patterns (Keaton et al., 2008; Pal et al., 2008). The control of Mih1 phosphorylation appears dependent on several kinases and phosphatases including Clb2-Cdk1, $PP2A^{CDC55}$, Yck1 and Yck2 (Pal et al., 2008).

Cells exposed to Ca^{2+} trigger the calcineurin as well as the cell integrity (Mpk1 MAP kinase cascade) pathways. Both of these pathways control Swe1 levels, calcineurin through transcriptional control and Mpk1 through post translational changes. The Mpk1 pathway triggers the protein kinase Mck1 which is required for Hsl1 delocalization from the bud neck thus preventing Swe1 degradation (Mizunuma et al., 2001). It has previously been reported

that Mck1 could also impact Mih1 phosphorylation status in unperturbed cells (without calcium stress) although direct phosphorylation was not shown (Pal et al., 2008). This chapter describes my studies demonstrating that Mck1 indeed has a role in mitotic cell cycle progression and likely inhibits the Clb2-Cdk1 kinase.

3.2 Results

3.2.1 The *MCK1* deletion mutant is sensitive to changes in gene expression that increase Clb2-Cdk1 activity.

To discover novel roles for the Mck1 protein kinase, I collaborated with Dr. Dewald van Dyk, a post doctorate fellow in Dr. Brenda Andrew's laboratory, who was performing a genome wide synthetic dosage lethality (SDL) screen with all known non-essential yeast kinases (Sharifpoor et al., 2012). The premise of SDL screening is based on the theory that a gene expressed at high levels may not affect wild type cells, but may be detrimental in strains deleted for proteins that interact, regulate or oppose the function of the overexpressed gene (Boone et al., 2007; Measday and Hieter, 2002; Sopko et al., 2006). Dr. van Dyk performed a SDL screen with 92 kinase deletion mutants against 5380 open reading frames (ORF) overexpressed on a 2μ *pGAL1/10-GST-6XHIS -ORF-URA* plasmid. The screen identified several SDL genetic interactions in strains lacking *MCK1*. To confirm potentially interesting genes, I transformed several of the same 2μ *pGAL-GST-ORF* inducible plasmids used in the initial screen into *mck1*Δ strains and plated serial dilutions of each strain onto both dextrose (control) and galactose media. I confirmed that overexpression of *pGAL-GST-MIH1* on galactose media is lethal to a *mck1*Δ strain but not a wild type strain (Figure 3-1A). Additional hits were confirmed by Dr. Dewald van Dyk but are not of interest to this study

(Sharifpoor et al., 2012). Studies have shown that Mih1 preferentially dephosphorylates Clb2-Cdk1 over other cyclin bound Cdk1 complexes (Keaton et al., 2007). To determine if the SDL phenotype is specific to a particular cyclin-Cdk1 complex, I created *cyclin*Δ and *mck1*Δ double mutants, transformed them with the *GAL-GST-MIH1* plasmid and performed serial dilution assays. The *GAL-GST-MIH1 mck1*Δ SDL phenotype was completely rescued only by the deletion of the mitotic cyclin, *CLB2* (Figure 3-1C). This raises the possibility that the lethality caused by overexpression of *pGAL-GST-MIH1* in a *mck1*Δ strain was due to hyper-active mitotic Clb2-Cdk1. To test this, I transformed a *pGAL-CLB2-HA* plasmid into *mck1*Δ and performed serial dilution assays (Figure 3-1B). I observed that over expression of *CLB2* in the absence of *MCK1*, caused lethality. Both the SDL phenotypes suggest that high Clb2-Cdk1 activity is not well tolerated in the absence of *MCK1*.

3.2.2 *MIH1,* when overexpressed, is active regardless of the presence of *MCK1*.

Although the rescue of the SDL phenotype of *pGAL-GST-MIH1 mck1*Δ strain by removal of *CLB2* suggests that Mih1 is active within this context, further evidence came from examining the effect of *pGAL-GST-MIH1* on Cdk1-Y19 phosphorylation. I transformed *pGAL-GST-MIH1* into *CLB2-HA* and *CLB2-HA mck1*Δ strains. I immunoprecipitated Clb2 with anti-HA beads and probed the bound Cdk1 for inhibitory phosphorylation using a Y19 phosphorylation specific antibody [anti-phospho-Cdc2 (tyr15)]. Overexpression of *GAL-GST-MIH1* caused loss of Cdk1 inhibitory phosphorylation in the presence or absence of *MCK1* indicating that Mih1 is active and that *MCK1* is not required for Mih1 phosphatase activity (Figure 3-2).

3.2.3 The hindered growth rate of *MCK1* deletion mutants is ameliorated in the absence of *MIH1* and deteriorated in the absence of *SWE1*.

A contrasting approach to SDL gain of function screens is the analysis of genetic interactions between loss of function double mutants. To more thoroughly examine the relationship between Mck1 and the regulators of Cdk1-Y19 phosphorylation (*SWE1* and *MIH1*), I looked for genetic interactions between deletion mutants. I did not observe any growth defects in the single (*mck1*Δ*, mih1*Δ*, swe1*Δ) or double mutants (*swe1*Δ *mck1*Δ and *mih1*Δ *mck1*Δ) by serial dilution at 30˚ C on YPD agar plates (data not shown). To analyze the double mutants in more detail I performed growth curve analysis on both the single and double mutants. Each strain was grown to log phase and diluted into a 96-well plate in replicates of eight. Optical density (OD_{600nm}) measurements were averaged across the eight replicates (Figure 3-3A and 3-3B). Qualitatively, the *mck1*Δ strains' growth curve was not as steep as the wild type strain, indicating a slower growth rate. Removal of *MIH1*, improved the growth rate by increasing the slope of the curve, while removal of *SWE1* augmented the growth defect by decreasing the slope of the curve.

To quantify the growth curves, growth rates were determined for the exponential growth phase of each replicate. Averages and standard deviations are shown (Figure 3-3C). To determine if the double mutant growth rates were statistically different from the single mutants, *p*-values were calculated (Figure 3-3D). With a *p*-value of < 0.1, the *mck1*Δ*mih1*Δ double mutant growth rate was significantly decreased from the growth rate of *mih1*Δ and significantly improved over the *mck1*Δ strains. The growth rate of the *mck1*Δ*swe1*Δ strain was significantly decreased from both that of the *swe1*Δ and *mck1*Δ mutants.

An additional approach used to examine genetic interactions makes use of the multiplicative model, which states that in the absence of genetic interactions, the phenotype of a double mutant is the product of the phenotypes for the two individual mutants (Reviewed (Boone et al., 2007). Using this model, I made predictions for the growth rate of the double mutants if no genetic interaction occurred, and compared that to what was observed experimentally. Growth rates relative to wild type were calculated for each of the single and double mutants. Averages and standard deviations are shown (Figure 3-3E and 3-3F). Neutral predictions indicating no genetic interaction are plotted. Removal of *MIH1* improved the growth rate (Figure 3-3E) and removal of *SWE1* hindered the growth rate (Figure 3-3F) of *mck1*Δ strains when compared to the prediction. These results suggest that in the absence of *MCK1,* Clb2-Cdk1-Y19 phosphorylation is beneficial. Two possible explanations for this are, firstly, that *mck1*Δ cells on their own have increased amounts of mitotically active Clb2-Cdk1 and any additional increase in Clb2-Cdk1 activity overburdens cellular mechanisms required for viability. Secondly, *mck1*Δ cells may have difficulties in cell cycle phases prior to G2/M transition and that promotion of mitosis through Clb2-Cdk1 activation is detrimental.

3.2.4 *MCK1* deletion mutants show delays in replication.

To differentiate between these hypotheses, I examined *mck1*Δ strains for perturbations in the cell cycle by analysis of DNA content, nuclear division and budding. Both wild type and *mck1*Δ cells were synchronized with the mating pheromone alpha factor, released from the G1 arrest into fresh media and time points were taken for both fluorescence activated cell sorting (FACS) analysis and microscopy every 10 minutes. Alpha factor was added to the culture at 80 minutes to prevent a second round of DNA replication. FACS analysis was

performed on six replicates and one representative is shown in Figure 3-4A. By comparing the 40 minute time points, I observed that wild type cells had almost completed replication whereas the *mck1*Δ cells were only half way through replication, suggesting a replication delay in *mck1*Δ cells. A more detailed analysis was performed by gating the FACS data for separate 1N and 2N populations in each of the six replicates in both strains. An averaged percentage of 1N and 2N populations throughout the time course is shown in Figure 3-4B with standard deviations. This analysis reveals that *mck1*Δ mutants take an increased amount of time to complete replication judged by the time required to go from the peak levels of 1N to 2N (Figure 3-4B, as indicated by the bars). Wild type cells completed replication within 60 minutes (Figure 3-4B, minutes 10-70) whereas *mck1*Δ cells needed an additional 10 minutes. (Figure 3-4B, minutes 10-80). Therefore, Mck1 plays a role in the proper timing of replication. It has been published previously that *mck1*Δ mutants are synthetic lethal when combined with a deletion mutant of the S phase cyclin *CLB5,* suggesting a role in replication (Ikui and Cross, 2009). Additionally, I will discuss in Chapter 4 the characterization of *mck1*Δ mutants sensitivity to replication stress. This data supports the hypothesis that *mck1*Δ strains are sensitive to increased activity of Clb2-Cdk1 possibly because of defects prior to G2/M, but does not eliminate the possibility of *mck1*Δ strains have increased levels of Clb2-Cdk1.

3.2.5 *MCK1* deletion mutants delay in the completion of the cell cycle.

Using fluorescence microscopy, I analyzed budding and nuclear division in wild type and *mck1*Δ cells during the synchronous cell cycle experiment described above. There are two findings from the microscopy analysis. The first confirmed the replication delay of about 10 minutes, as seen by the shift of G1, S/G2, M (Dividing), M (Divided) curves to the right by

10 minutes in the *mck1*Δ strain (Figure 3-4C). The second finding is that after nuclear division, *mck1*Δ cells did not exit the cell cycle and re-enter into G1, as demonstrated by the persistence of M phase (Divided) levels from 80-160 minutes (Figure 3-4C). These results reveal that *mck1*Δ cells are delayed in replication, and have difficulties completing the cell cycle.

3.2.6 In the absence of *MCK1*, Clb2 protein levels persist past nuclear division.

To further investigate the intolerance of the *mck1*Δ strain to increased activity of Clb2-Cdk1, I determined if there was a change in Clb2 protein levels and regulation in the absence of *MCK1*. I also examined changes in the protein level or regulation of the Clb2-Cdk1 regulators Mih1 and Swe1 in wild type and *mck1*Δ strains. Cells were arrested in G1 phase with mating pheromone, released and time points taken every 15 minutes starting at 30 minutes post pheromone release. In wild type cells, the Clb2 mitotic cyclin appears in G2 and its protein levels reach a maximum just before anaphase and disappear as cells enter anaphase (Surana et al., 1991). Clb2 persisted longer in the absence of *MCK1* when compared to wild type (Figure 3-5A and 3-B). Previous data from Dr. Kellogg has shown that in wild type cells Mih1 exists in several phospho-isoforms that are distinguished by SDS PAGE as slower migrating bands (Pal et al., 2008). A heavily phosphorylated, and presumed to be inactive form of Mih1 is present throughout G1 and S phase. As cells enter mitosis, Mih1 is subsequently de-phosphorylated and presumably activated. Upon exit of mitosis Mih1 appeared again mainly in its phosphorylated form. In the absence of *MCK1,* I observed a decrease in the top phospho-isoform protein band at 45 and 60 minutes (Figure 3-5C and 3-5D, Top Band). I also observe an accumulation of the dephosphorylated form (bottom band)

of Mih1 at the end of mitosis in *mck1*Δ cells (Figure 3-5C and 3-5D, bottom band, see 90 and 105 minutes). The accumulation of dephosphorylated Mih1 (bottom band) was only transient as *mck1*Δ enter the cell cycle with heavily phosphorylated Mih1 (top band) similar to wild type (Figure 3-5C and 3-5D, bottom band, see 30 minutes). It has been previously reported that the removal of *MCK1* results in an accumulation of dephosphorylated Mih1 in logarithmic phase cells (Pal et al., 2008). My results support this data and additionally demonstrate that Mck1 effects Mih1 phosphorylation in a cell cycle dependent manner. Protein levels of the negative regulator of Clb2-Cdk1, Swe1 peak during S/G2 in wild type cells. Swe1 is phosphorylated on multiple residues by many kinases, which eventually results in its degradation during nuclear division (Asano et al., 2005; McMillan et al., 1998). This phosphorylation shift or subsequent degradation remained unchanged in the absence of *MCK1* (Figure 3-5E). In summary, cell cycle protein analysis has revealed that Mck1 positively influences Mih1 phosphorylation, while negatively impacting Clb2 protein levels. Interestingly, Clb2-Cdk1 has been previously shown to promote Mih1 de-phosphorylation (Pal et al., 2008). This suggests the possibility that the increase in the de-phosphorylated form of Mih1 in *mck1*Δ cells is a by-product of higher Clb2 levels. This data supports the hypothesis that *mck1*Δ strains are sensitive to any increased amount of Clb2-Cdk1 activity due to abnormally high levels of Clb2-Cdk1 that they possess.

Since *mck1*Δ cells exhibit a cell cycle delay as demonstrated both in Figure 3-4 and again in the FACS analysis of this experiment (Figure 3-5F and 3-5G), it was important to determine if this caused the observed change in Clb2 protein levels. As Clb2 protein levels are cell cycle regulated, there is a strong correlation between the amount of Clb2 in a cell population

and the cell cycle phase of that same population. If the change in Clb2 abundance was solely due to the observed cell cycle delay in *mck1*Δ cells, I would expect that Clb2 protein levels would correlate to appropriate cell cycle phases, in both *WT* and *mck1*Δ cells. Any deviation from this would suggest a role for Mck1 in the proper regulation of Clb2. In wild type cells, Clb2 protein level peaked at 60 minutes (Figure 3-5B). The corresponding microscopy revealed that at 60 minutes ~12% of wild type cells are in the process of, or finished, nuclear division (M-phase) whereas by 75 minutes ~60% of cells have completed mitosis (Figure 3-5H and I, Graph M). Clb2 accumulated pre-anaphase and therefore the correlation between western blot and microscopy analysis is as expected (Surana et al., 1991). In the absence of *MCK1,* there was a 15 minute delay in Clb2 accumulation (Figure 3-5B, 75 minutes). When Clb2 levels peaked in *mck1*Δ (75 minutes), ~37% of cells had already undergone nuclear division (Figure 3-5H and I, Graph M) and by 90 minutes the population had increased to ~67%. The inappropriate correlation of Clb2 levels and cell cycle phases, suggests that the change in Clb2 observed in *mck1*Δ is not simply a result of the cell cycle delay, but indicates a role for Mck1 in Clb2 regulation.

Following nuclear division, which occurs at 75 minutes in wild type and 90 minutes in *mck1*Δ (Figure 3-5I, graph M) I observed an increased level of Clb2 in the absence of *MCK1* (Figure 3-5B). This increased Clb2 level at 105 minutes in *mck1*Δ cells, correlated to an accumulation of large budded, bi-nucleate cells indicating a delay in cell cycle completion (either in mitotic exit or cytokinesis). High levels of Clb2 have been previously associated with delays in mitotic exit (Cross et al., 2005). This suggests that Mck1 may play a role in regulating Clb2 post-nuclear division.

3.2.7 *MCK1* deletion mutants exhibited an increase in Clb2-Cdk1 kinase activity post nuclear division.

To determine if *mck1*Δ strains have increased levels of Clb2-Cdk1 activity, I performed a cell cycle Cdk1 kinase assay (Figure 3-6). Clb2-HA was immunoprecipitated during a synchronized cell cycle and assayed for activity against the known Cdk1 substrate Histone H1 (Wittenberg and Reed, 1988). In wild type cells (*CLB2-HA*), Clb2-Cdk1 activity peaked at 65 minutes, which is after the completion of DNA replication (Figure 3-6C, 65 minutes) and before nuclear division (Figure 3-6D, 65 minutes). Nuclear division occurred at 85 minutes, which correlated with a reduction in Clb2-Cdk1 activity (Figure 3-6A, 85 minutes). Cells entered the subsequent cell cycle at 105 minutes when Clb2-Cdk1 is inactive (Figure 3-6A, 105 minutes). Once wild type cells had nearly completed the second round of replication at 125 minutes, Clb2-Cdk1 activity increased again (Figure 3-6A, 125 minutes). In the absence of *MCK1* (*CLB2-HA mck1*Δ), Clb2-Cdk1 activity is similar to wild type cells up until 65 minutes, but remained active past the point of nuclear division (Figure 3-6A, 85 and 105 minutes). The persistent activity of Clb2-Cdk1 in the *mck1*Δ strain can also be visualized by measuring protein band intensities of the Histone H1-P band relative to that of Cdk1 from the whole cell extract (WCE) (Figure 3-6E). In this manner, I also examined levels of immunoprecipitated Clb2 and its association with Cdk1 and Cdk1-Y19 phosphorylation (Figure 3-6E). Again, there is an increased amount of Clb2 post nuclear division at 105 and 125 minutes in *mck1*Δ cells (Figure 3-6E, Graph Clb2-HA). There also appears to be a general increased level of Cdk1-Y19 phosphorylation bound to Clb2 throughout the cell cycle in *mck1*Δ strains, although this does not appear to inhibit the activity of Clb2-Cdk1 as

indicated by the ability to phosphorylate Histone H1 throughout the cell cycle. Mck1 plays a role in the negative regulation of Clb2-Cdk1 activity post nuclear division.

3.2.8 *MCK1* is not involved in the degradation of Clb2.

An increased abundance of active Clb2-Cdk1 in *mck1*Δ cells post nuclear division could indicate that Mck1 is involved in either the inhibition of Clb2-Cdk1 activity or Clb2 degradation. To test the latter possibility, I expressed HA-tagged *CLB2* from the *GAL* promoter on a plasmid *(pGAL-CLB2-HA)* in wild type and *mck1*Δ cells for 30 minutes. Cells were washed and re-suspended in media containing dextrose to turn off expression of *CLB2*. Clb2-HA degradation was followed by western analysis for two hours. Clb2-HA was degraded within two hours regardless of the presence of Mck1 suggesting that Mck1 is not required for Clb2 turn-over (Figure 3-7). Additionally, Mck1 may inhibit Clb2 activity, but not protein stability.

3.2.9 Mck1 co-immunoprecipitated with Clb2 and Mih1.

As both genetic and protein data suggest, Mck1 plays a role in Clb2-Cdk1 inhibition, I next investigated whether this action could be through direct interaction. Firstly, I performed co-immunoprecipitations with transformed wild type and Myc tagged Mck1 strains with a *pGAL-CLB2-HA* plasmid (a gift from M. Tyers). Transformed strains were grown in galactose media to allow the expression of Clb2. Mck1 was immunoprecipitated with anti-Myc beads and co-purifying Clb2 was detected with anti-HA antibody, indicative of an interaction between Mck1 and Clb2 (Figure 3-8A, Far right lane). The increased amount of de-phosphorylated Mih1 in *mck1*Δ strains suggests the possibility that Mih1 is phosphorylated by Mck1. Therefore, I looked for an interaction between Mck1 and Mih1

proteins. I transformed *pGAL-GST-MIH1* into both wild type and *mck1*Δ strains, expressed Mih1 by growth in galactose and subsequently immunoprecipitated Mck1 and looked for interaction with Mih1 by western blotting with anti-GST. Mck1 also shows interaction with Mih1 (Figure 3-8C, lane 4). I also examined if the interaction of Mih1 with Mck1 depended on Clb2 and vice versa. There was no change in binding of Clb2 (Figure 3-8B, Lane 4) or Mih1 (Figure 3-8C, Lane 6) to Mck1 in either case. I was unable to detect the presence of Cdk1 in these immunoprecipitations suggesting that Mck1 may interact with Clb2 but not the Clb2-Cdk1 complex (Data only shown for Mih1, Figure 3-8C). As both Mih1 and Clb2 were expressed from the GAL promoter, their interaction with Mck1 may be an artifact of overexpression.

3.2.10 Mck1 did not co-immunoprecipitate with Cdk1 activity.

To further investigate if the Mck1 protein could co-immunoprecipitate with Clb2-Cdk1 I used Cdk1 kinase assays, which may be more sensitive than Western blotting to determine if the Mck1protein could immunoprecipitate with Cdk1 activity. I made use of the analog sensitive kinase allele for Cdk1 (*cdc28-as1*) and performed Mck1 immunoprecipitations and kinase assays in this strain background. I first tested Mck1 kinase activity, by performing immunoprecipitations with varying amounts of protein lysate incubated with affinity matrix antibodies. After immunoprecipitating Mck1, I added Histone H1 as an exogenous substrate and gamma labeled ^{32}P-ATP (γ-^{32}P-ATP). Mck1 is known to auto-phosphorylate at tyrosine 199 and this was used as a positive control for Mck1 activity (Rayner et al., 2002). I detected phosphorylation of both Mck1 and Histone H1 in Mck1 immunoprecipitations (Figure 3-9A). A previous publication stated that Mck1 is unable to phosphorylate histones (Dailey 1990). Therefore, I hypothesized that the observed H1 phosphorylation may be due

to a co-purifying kinase such as Cdk1, with known activity towards histone H1. The analog sensitive kinase allele for Cdk1 (*cdc28-as1*) is completely inhibited by addition of 10 μM 1NM-PP1 (Figure 3-9B). Strains were constructed that had wild type function for Mck1 and Cdk1 (*MCK1-myc CDC28*), a kinase dead version of Mck1 (*mck1D164A-myc CDC28*), an analog sensitive allele of Cdk1 (*MCK1-myc cdc28-as1*) or double kinase mutants (*mck1D164A-myc cdc28-as1)*. Immunoprecipitations of Mck1 were isolated from each strain and half of each purification was incubated with the inhibitor, 1NM-PP1, and the other half incubated with solute only, prior to incubation with γ-^{32}P-ATP and Histone H1. A large reduction of Mck1 and Histone H1 phosphorylation was detected when kinase dead Mck1 was immunoprecipitated compared to active Mck1 (Figure 3-9C, compare Lanes 2 and 4). Neither Histone H1 nor Mck1 phosphorylation was further decreased upon removal of Cdk1 activity (Figure 3-9C, compare Lanes 9 and 10). These results suggest that phosphorylation of H1 in the Mck1 immunoprecipitation is not due to co-precipitating Cdk1 activity and reveals the novel ability of Mck1 to phosphorylate Histone H1.

3.2.11 Clb2-Cdk1 activity is inhibited by Mck1 kinase activity but independent of phosphorylation.

Thus far, my data suggests that Clb2-Cdk1 activity is elevated in *mck1*Δ strains suggesting that Mck1 may inhibit Clb2-Cdk1 activity. Therefore, I investigated whether the potential inhibition by Mck1 could be caused by direct phosphorylation of Clb2. I performed Mck1 kinase assays with Clb2 added as a substrate (Figure 3-10A). Clb2-HA was immunoprecipitated from the *cdc28-as1* strain to be added as a substrate. The Cdk1 allele in the *cdc28-as1* strain is less active, and Clb2-HA runs at a lower mobility on polyacrylamide gels as seen in Figure 3-9B (compare 0 μm 1NM-PP1 CDC28 versus *cdc28-as1* lanes). This

version of Clb2-HA was required to distinguish the Mck1-myc autophosphorylation band from Clb2-HA as they migrate at a similar mobility on polyacrylamide gels. One half of the Clb2-HA *cdc28-as1* immunoprecipitate was incubated with the inhibitor 1NM-PP1 while the other half was incubated with solute alone. Both inhibited and uninhibited forms of Clb2-HA bound to affinity matrix anti-HA beads were added to three unique kinase reactions. The first kinase reaction consisted of untagged cells incubated with myc beads to control for background proteins precipitating with beads (empty), the second contained immunoprecipitated Mck1-myc, the third an immunoprecipitated kinase dead allele of Mck1 (mck1D164A-myc). Phosphorylated Clb2 is observed in the Clb2-HA IP with no inhibitor added (Figure 3-10A, Lane 8) whereas no phosphorylated Clb2 is detected upon addition of 1NM-PP1 (Figure 3-10A, Lane 7). Mck1-myc did not phosphorylate inhibited (+1NM-PP1) Clb2-HA *cdc28as1* as I did not observe a band in lane 2 of the expected size, although I observed the auto-phosphorylation of Mck1 (Figure 3-10A Lane 2). When uninhibited (-1NM-PP1) Clb2-HA was added to the kinase reactions I could clearly detect Clb2 in lanes 4 where there is no kinase added and in Lane 6 where there is no Mck1 kinase activity. Interestingly, I did not observe phosphorylated Clb2 in lane 5, which is the reaction with Mck1 kinase activity. This suggests that Mck1 kinase activity may prevent Clb2 phosphorylation via inhibition of Clb2-Cdk1 activity. Mck1 has been previously shown to inhibit protein kinases through means other than phosphorylation (Rayner et al., 2002).

I have used this kinase reaction method previously to identify Mck1 substrates. Two forms of the phosphatase Pah1 (Pah1-HA and a phosphatase dead version, Pah1-D398E-HA) involved in lipid synthesis were immunoprecipitated with anti-HA beads and added to wild

type Mck1 immunoprecipitations *(MCK1-myc*) or kinase dead (*mck1D164A-myc*) immunoprecipitations. Phosphorylation of both forms of Pah1 by a co-precipitating kinase is seen in Figure 3-10B (lane 2 and lane 3). However, when either Pah1 or Pah1-D398E is added to Mck1 immunoprecipitations, Pah1 phosphorylation is greatly increased (Figure 3-10A, lane 7). Phosphorylation of Pah1 and Pah1-D398E is dependent on Mck1 kinase activity as addition of either protein to kinase dead Mck1 results in background levels of protein phosphorylation (Figure 3-10, Lane 12). This indicates that Pah1 is a substrate for the Mck1 kinase. In contrast, when the cyclin Cln2 was added as a substrate there was no observed Mck1 dependent phosphorylation, even though like Pah1, Cln2 possesses Mck1 (GSK-3) consensus sites (PhosphoGrid www.phosphogrid.org). This positive control for the *in vitro* kinase assay supports the idea that Clb2 is not a substrate for Mck1 kinase activity.

3.2.12 Overexpression of *MCK1* leads to *SWE1* dependent bud elongation indicative of inactive Clb2-Cdk1.

I obtained additional data to support the hypothesis that Mck1 inhibits Clb2-Cdk1 activity from Mck1 overexpression studies. Wild type cells were transformed with *pGAL-GST-MCK1* and grown in galactose for a total of 16 hours. Logarithmic growth was maintained throughout the time course. Samples were taken for FACS and microscopy every 2 hours up until 12 hours and then one time point at 16 hours was taken. FACS and microscopy samples were analyzed in comparison to vector alone. Upon eight hours of *MCK1* over-expression cells began to exhibit elongated morphologies (Figure 3-11A) and a 2N accumulation (Figure 3-11B), indicative of Clb2-Cdk1 inactivity (Reviewed in (Lew, 2003). Removal of *SWE1,* the kinase that inhibits Clb2-Cdk1, partially rescues the elongation morphology (Figure 3-11C and 3-11D).

3.2.13 Mih1 is not a substrate for Mck1 kinase activity.

The interaction between Mih1 and Mck1 as well as the change in Mih1 phospho-isoforms in the absence of *MCK1* suggests Mih1 as a target for Mck1 phosphorylation. To test if Mih1 is a possible substrate for Mck1, I performed immunoprecipitations of *pGAL-GST-MIH1* grown in galactose. I concentrated the protein and ran samples on a coomassie gel (Figure 3-12A, right panel). I then added *GST-MIH1* and γ-^{32}P-ATP to Mck1 immunoprecipitates (Figure 3-2 B). I was unable to see any phosphorylation at the molecular weight expected for Mih1, although I can see Mck1 autophosphorylation indicating that Mck1 is active in this assay (Figure 3-12B). Therefore, under these conditions it does not appear that Mih1 is a substrate for the kinase activity of Mck1.

3.3 Discussion

There are two main findings in this work. Firstly, that *mck1*Δ strains experience a delay in replication, which will be discussed further in the following chapter. Secondly, Mck1 inhibits Clb2-Cdk1 activity in late mitosis. Without having examined the spindle, I cannot say if the spindle has disassembled indicating a cytokinesis defect or whether it remains intact suggesting a mitotic exit defect. However, both the NoCut pathway mutants (Norden et al., 2006) and cytokinesis mutants (Song and Lee, 2001) are capable of Clb2 degradation. The degradation of Clb2 is a prerequisite for cytokinesis, as overexpression of non-degradable Clb2 results in a telophase arrest and not a cytokinesis arrest (Surana et al., 1993). Therefore, I believe that the cell cycle completion delay I observe in *mck1*Δ cells is due to defects in mitotic exit and not cytokinesis. There are three documented mechanisms to inhibit Clb2-Cdk1 during the exit from mitosis. Firstly, the anaphase promoting complex ($APC^{Cdc20/Cdh1}$)

degrades the mitotic cyclin, Clb2. Secondly, Sic1 acts as a potent Cdc28 inhibitor. Lastly, the phosphatase Cdc14 antagonizes the kinase activity of Clb2-Cdk1. There is biphasic release of Cdc14 controlled by the FEAR pathway in early anaphase, and then the MEN in late anaphase (reviewed in (de Gramont and Cohen-Fix, 2005; Sullivan and Morgan, 2007)). Mck1 may either promote or be an effector of one of these pathways or it may act through an alternative pathway.

Evidence that Mck1 inhibits Clb2-Cdk1 is five-fold. (1) Cells devoid of *MCK1* do not tolerate excess Clb2-Cdk1 activity, either through removal of *SWE1* or overexpression of either *MIH1* or *CLB2* (Figure 3-1A, 3-1B and 3-3). This is also observed in *sic1*Δ and APC mutant strains (Cross et al., 2005; Kramer et al., 1998; Schwab et al., 1997; Toyn et al., 1997). (2) Similar to mutations in genes involved in the MEN, FEAR pathway and the APC (Deshaies, 1997; Schwab et al., 1997; Stegmeier et al., 2002), *mck1*Δ cells have a prolonged presence of active Clb2-Cdk1 post nuclear division (Figure3-6). (3) I have shown that Mck1 and Clb2 can physically interact (Figure 3-8A). Physical interactions between Clb2 and components of degradation machinery such as Cdh1(Schwab et al., 2001) and Sic1 (Archambault et al., 2004) have previously been described. (4) Mck1 kinase activity can inhibit the ability of Clb2-Cdk1 to phosphorylate Clb2 *in vitro* (Figure 3-10A). Potent inhibitors of Cdk1 such as Sic1(Mendenhall, 1993) and Swe1 (Booher et al., 1993) have both been shown to inhibit Cdk1 kinase activity *in vitro*. (5) The switch from apical growth to isotropic depends on functional Clb1/Clb2-Cdk1 (Lew and Reed, 1993). Cells defective in Clb2-Cdk1 activity exhibit an elongated bud phenotype that is rescued by loss of *SWE1*

(Barral et al., 1999). Overexpression of *GAL-GST-MCK1* results in *SWE1* dependent bud elongation, which is a hallmark sign of Clb2-Cdk1 inhibition (Figure 3-11).

3.3.1 Does Mck1 inhibit Clb2-Cdk1 through one of the known pathways?

3.3.1.1 Mck1 does not share a pathway with the APC.

The APC plays a large role in the degradation of Clb2 in early anaphase with the activator Cdc20 (APC^{Cdc20}) and again in late anaphase with the activator Cdh1 (APC^{Cdh1}). Although both *MCK1* and APC mutants share similar phenotypes such as prolonged Clb2 activity and negative genetic interactions with additional mutants that elevate Clb2 levels (eg. *sic1*Δ), I do not believe my data supports Mck1 being part of an APC pathway as *mck1*Δ mutants do not share more specific phenotypes with APC mutants. For example, APC mutants arrested in G1 with alpha factor have high Clb2 protein levels (Kramer et al., 1998; Schwab et al., 1997). I do not observe an increase in Clb2 early in the *mck1*Δ cell cycle (Figure 3-5A, 30 minutes and Figure 3-6A, 25 minutes). APC mutants arrest in G2, with a large bud and a single nucleus as they struggle to activate the proteins required for anaphase such as Esp1 (Zachariae et al., 1996). I do not observe such an arrest or delay in a *mck1*Δ mutant (Figure 3-4). Finally, Clb2 turnover is not affected in *mck1*Δ cells suggesting that the APC is active (Figure 3-7).

3.3.1.2 Mck1 inhibition through Sic1 or inhibitory process similar to Sic1.

Another possibility is that Mck1 either acts through Sic1 to inhibit Clb2-Cdk1 or, similar to Sic1, binds and inhibits Clb2-Cdk1 (Mendenhall, 1993). *SIC1* deletion mutants have phenotypes at many stages of the cell cycle (Donovan et al., 1994; Mendenhall, 1993; Toyn et al., 1997) owing to Sic1-mediated inhibition of both Clb5/6-Cdk1 and Clb2-Cdk1 activity

(reviewed in (Barberis, 2012)). However, unlike a *mck1*Δ mutant, a *sic1*Δ mutant commences replication prematurely due to its role in inhibition of Clb5/6-Cdk1 (Lengronne and Schwob, 2002). Sic1 was initially identified as a co-purifying protein with Cdk1, however I have not been able to demonstrate an interaction between Mck1 and Cdk1 (Mendenhall, 1993) (Figure 3-9). As a potent inhibitor of Clb2-Cdk1 activity, Sic1 has many genetic interactions with additional components of the Clb2-Cdk1 machinery (MEN and APC). It acts as a dosage suppressor to those mutants that arrest with high Clb2-Cdk1 levels such as (MEN) *dbf2, cdc5, cdc15, tem1, lte1, cdc15, mob1* (Donovan et al., 1994; Hofken and Schiebel, 2004; Jaspersen et al., 1998; Luca et al., 2001; Toyn et al., 1997; Visintin et al., 1998) and has been found to be synthetic lethal with components of both the APC (*cdc23*, *apc2*; (Kramer et al., 1998) and MEN (Toyn et al., 1997)). I have not tested whether overexpression of *MCK1* can rescue any of the aforementioned mutants. The only negative genetic interaction between *mck1*Δ mutants and components of the Clb2 inhibition machinery reported by the yeast community is a synthetic sick phenotype in *mck1*Δ*sic1*Δ double mutants (SGD, http://www.yeastgenome.org, (Collins et al., 2007; Fiedler et al., 2009; Pan et al., 2006)). As *mck1*Δ mutants do not share many phenotypes with *sic1*Δ mutants, it is unlikely that they share a common pathway.

Alternatively, like Sic1, Mck1 may be a stoichiometric inhibitor, as it does not appear to inhibit through phosphorylation of Clb2-Cdk1. Evidence that Mck1 can function in this way has been described previously (Rayner et al., 2002). The requirement of Mck1 kinase activity for Clb2-Cdk1 inhibition may demonstrate the need for Mck1 autophosphorylation, and perhaps conformational changes that might ensue.

3.3.1.3 Mck1 may share pathways with FEAR or MEN.

As *MCK1* deletion mutants lack the characteristic phenotypes that would support its role in either an APC or Sic1 pathway, I believe Mck1 could act through either the FEAR or MEN pathway. Large-scale phosphorylation studies have found that Mck1 binds to the FEAR components Cdc14 and Net1 (Breitkreutz et al., 2010) suggesting a possible role for Mck1 in the early stages of anaphase. There are several Mck1 (GSK-3) consensus sites on Net1 (PhosphoGRID). Further evaluation of this hypothesis is required and work is suggested in the future directions.

3.3.2 Mck1 may be involved in pheromone induced Clb2 inactivation.

Synchronization with alpha factor induces an APC^{Cdh1} triggered degradation of Clb2 (Oikonomou and Cross, 2011; Zachariae et al., 1996). Consistently in *mck1*Δ cultures treated with alpha factor there are 20% of cells that remain bi-nucleate in M phase compared to 7% in WT (Figure 3-4C, Graph M). When *mck1*Δ cells are synchronized with alpha factor they don't completely arrest in G1, having a subpopulation of large budded binucleate cells. The delayed exit from mitosis may be due to high levels of Clb2 blocking cytokinesis. However, this is disputed by western blot analysis that showed Clb2 protein levels at 25 mins (Figure 3-6A) or 30 minutes (Figure 3-5A) past alpha factor arrest are equal between the wild type and *mck1*Δ strains. When alpha factor is added back into media following release from synchronization to prevent subsequent cell cycles, I observed a stronger mitotic exit phenotype than when no alpha factor is added back, compare Figure 3-5I (Graph M, 90-105 minutes) to Figure 3-6D (85-125 minutes). Budding yeast only responds to alpha factor during a short window of time in G1 pre-Start (Reid and Hartwell, 1977). Many of the large binucleate cells observed in the *mck1*Δ strains during mating pheromone arrest appear to

have formed mating projection (shmoo) (Data not shown). This suggests that despite not having completed cytokinesis, the cell behaves in a G1 manor. The delay in mitotic exit of 13% of cells in alpha factor block may also contribute to the delay in replication observed.

3.3.3 Mck1 is not involved in Clb2-Cdk1 regulation prior to mitosis in an unperturbed cell cycle.

There are many pathways and proteins that restrain Clb2-Cdk1 activity to the G2/M transition. Tightly regulated Clb2 transcription and potent Cdk1 inhibitors such as Sic1 and Swe1 prevent premature Clb2-Cdk1 activity before mitotic entry. After mitotic entry, Clb2-Cdk1 activity is rapidly inhibited, thereby creating a tight window where mitotic Clb2-Cdk1 can function. It has been previously published that Mck1 plays a role in Swe1 activation and thus Clb2-Cdk1 inhibition in response to calcium stress (Mizunuma et al., 2001). I have not found any evidence that *mck1*Δ cells have difficulties in restraining Clb2-Cdk1 activity prior to the G2/M transition in an unperturbed cell cycle. I do not observe premature Clb2-Cdk1 protein or activity (Figure 3-5A and 3-6A). As well, *mck1*Δ strains do not seemingly enter mitosis prematurely as one would suspect with increased levels of Clb2-Cdk1 (Oikonomou and Cross, 2011).

3.3.4 An alternative hypothesis; Mck1 inhibits Mih1.

An alternative interpretation of the results is that Mck1 inhibits Mih1 directly. This is supported by the *pGAL-GST-MIH1 mck1*Δ SDL phenotype (Figure 3-1) as well as the *mih1*Δ*mck1*Δ partial rescue of *mck1*Δ slow growth phenotype (Figure 3-3), which suggests that in the absence of *MCK1*, Mih1 is misregulated. This is confirmed by changes in Mih1 phospho-isoforms in *mck1*Δ strains (Figure 3-5C). I additionally observe a physical

interaction between Mck1 and Mih1 (Figure 3-8C) that is independent of Clb2. I was unable to observe Mih1 phosphorylation by Mck1. It has been previously noted that Mck1 requires a preceding or "priming" phosphorylation (Hilioti et al., 2004; Hwang and Varshavsky, 2008; Lee et al., 2012). In an effort to preserve any priming signals I made use of yeast purified Mih1, yet there may still have been insufficient priming. The phosphorylation of Mih1 has been shown to be partially dependent on Yck1/2, which are known priming kinases for Mck1 activity (Hwang and Varshavsky, 2008; Pal et al., 2008). Additional kinase assays would need to be performed to determine whether Mck1 could phosphorylate Mih1, with priming phosphorylation by Yck1/2 or other kinases.

There is also conflicting evidence to the hypothesis that Mck1 inhibits Mih1. For example, *mck1*Δ strains exhibit higher than average Cdk1-ptyr levels throughout the cell cycle (Figure 3-6E, graph Cdk1-ptyr) indicating that Mih1 is less active in the absence of *MCK1*. This suggests that Mck1 may promote Mih1 activity. However, over expressed Mih1 does not require Mck1 to promote Cdk1-Y19 dephosphorylation (Figure 3-2). Although metazoan Mih1 homologues (Cdc25A,B,C) have roles in the promotion of CDK activity at both the G1/S and G2/M transition, deletion of budding yeast *MIH1* only hinders the G2/M transition, suggesting Mih1 promotes Cdk activity only in mitosis (reviewed in (Boutros et al., 2006; Pal et al., 2008; Russell et al., 1989). If Mck1 functions to inhibit Mih1 activity, it is difficult to explain why I do not observe mitotic entry changes in *mck1*Δ strains. Also it would be pure speculation as to how a change in Mih1 activity could lead to the late accumulation of Clb2-Cdk1 and the cell cycle completion delays as observed in *mck1*Δ strains. The only evidence to suggest a role for Mih1 in cell cycle completion is a transient re-localization of

Mih1 from the cytoplasm into the nucleus at telophase (Keaton et al., 2008). The biological reason for Mih1 re-localization is not understood.

It is possible that the phenotypes observed in this chapter, are the result of different Mck1 functions, such as both the inhibition of Mih1 and Clb2-Cdk1. However, the majority of my data supports the explanation that Mck1 inhibits Clb2-Cdk1 activity in late mitosis.

3.4 Materials and methods

3.4.1 Strains, plasmids and media

Yeast strains and plasmids used in this study are described in Table 3.1 and Table 3.2 respectively. I found that the S288C-YPH499 strain did not grow well in galactose media therefore the S288C- BY4742 background was used for experiments that required galactose induction. The kinase reactions were done with the W303 background as the *CLB2-HA* and *cdc28as1* strains have been well cited in the literature. Figure 3-1, Figure 3-2, Figure 3-7, Figure 3-8A, 3-8B and Figure 3-11 were done with S288C- BY4742 derived strains. Figure 3-3, Figure 3-4 and Figure 3-8 were done with the S288C-YPH499 derived strains. Figure 3-5 A, 3-5B and 3-5C were done with *SWE1-myc, SWE1-myc mck1*Δ strains. Figure 3-6, 3-9, 3-10 were done in the W303 background. In Figure 3-12 the Mck1-myc strains is S288C-YPH499 while the GST and the GST-Mih1 protein was purified from a S288C- BY4742 background strain. Figure 3-8C is a mixed background S288C (YPH499/BY4742). Genes were deleted or epitope tagged by using standard PCR-based homologous recombination yeast methods (Longtine et al., 1998). To construct the *mck1D164Amyc* strain the *pmck1D164A* plasmid was transformed into a *mck1*Δ strain, and was epitope tagged with MYC:TRP using standard methods. The tagged plasmid was checked by both PCR and

epitope tag expression. The plasmid was subsequently digested to remove the *mck1D164Amyc:TRP* insert and transformed into a *mck1*Δ*KanMX6* strain. Desired recombinants were selected and checked for epitope expression and by flanking PCR. Standard methods for yeast culture and transformation were followed (Guthrie and Fink, 1991). Media for yeast growth was either yeast peptone with 2% dextrose (YPD) or supplemental minimal media (SC) lacking the amino acid uracil (SC^{-URA}) with either dextrose, raffinose or galactose as carbon sources (Kaiser et al., 1994).

3.4.2 Spot assays

Cultures were grown in minimal SC^{-URA} media (2% raffinose, 0.1% dextrose) overnight. Cell concentration was measured as optical density (OD_{600nm}) by spectrometer and cultures diluted to allow for doubling at least twice in Sc^{-URA} (2%raffinose). Serial dilutions were performed by first diluting the cultures to an optical density of 10^6 cells mL^{-1} (OD_{600nm} 0.1), then subsequently diluting 5 fold. Cultures (4 μL) were spotted on both SC^{-URA} (2% dextrose) and SC^{-URA} (2% galactose) plates.

3.4.3 Growth curves

All strains were grown overnight in YPD. Cultures were diluted to an OD_{600nm} of 0.05 to allow for two doublings. Cultures were then diluted to an OD_{600nm} of 0.1 and 200 μL was added to each well of a BD Falcon 96-well flat bottom plate (BD Biosciences) with eight technical replicates. OD_{600nm} measurements were taken on an Infinite® Pro microplate reader (Magellan v7.0™ Software; Tecan Group Ltd.) every 20.8 minutes for 16 hours. Every 14 minutes, the plate underwent orbital rotation for 5 minutes, rested for 30 seconds and then the OD_{600nm} was measured. Each time point was averaged amongst replicates and the mean

values were plotted versus time. The mean growth rate was calculated for each replicate. The growth rate was taken as the slope of the line at exponential growth. Exponential growth was defined as the time between 50% OD_{600nm} max and 75% OD_{600nm} max. OD_{600nm} max was taken as the average of the last three time points. The growth rate was averaged for the eight replicates and the mean value and standard deviation calculated. Two-sample *t*-test were performed on growth rates, and *p*-values recorded. Growth rate was calculated as a percentage of WT for each of the strains. Neutral predications for the double mutants were calculated as the product of the two single mutants, their standard deviation was the product of the single mutants standard deviation. All calculations were done with Numbers '09 (Apple Inc. Version 2.1 (436)).

3.4.4 Synchronization

Cells were grown to early-logarithmic phase in YPD at 30 °C, arrested with 5 µg/ mL alpha-mating factor (BioVectra) for 1 hour followed by a second dose for an additional hour. Cells were washed twice and resuspended in media lacking alpha-mating factor. In order to prevent subsequent cell cycles, alpha-mating factor was added back to cultures at 80 minutes except in Figure 3-5E and Figure 3-6.

3.4.5 Flow cytometry

Cells were fixed in 70% ethanol (EtOH), 30% 1 M sorbitol overnight at 4 ˚C. Fixed cells were pelleted and resuspended in 1 mg/ mL RNAse A, 0.2 M TrisHCl pH 7.5 and incubated overnight at 37 ˚C. Proteinase K (5 µL of 20 mg/mL) was added and incubated for at least 1 hour at 50 ˚C. Cells were pelleted and re-suspended in 400 µL of 0.2 M Tris pH7.5. Cell clumps were disrupted by sonication and stained with 600 µL of 1 µg/ µL propidium iodide,

0.2 M Tris pH 7.5 for at least one hour. Flow cytometry was performed by a BD FACScan (BD Biosciences) with BD Cell Quest Pro software (BD Biosciences) and analyzed using FlowJo software (Version 9.4.10). Data was gated for 1N, 2N and >2N populations.

3.4.6 Microscopy

Cells were fixed in 3.7% formaldehyde for 10 minutes. To avoid microtubule destruction, cells were centrifuged at 2,500 rpm, washed and resuspended in 1X PBS. Membranes were permeabilized by addition of 70 % EtOH and incubated at room temperature for 30 minutes. Following resuspension in PBS, cells were sonicated, pelleted and re-suspended in 50 ng/mL DAPI solution. Microscopy analysis of samples was performed on a Zeiss Colibri LED illuminator with a Zeis Axiocam Ultra High Resolution Monochrome Digital Camera Rev3.0). Images were analyzed using ImageJ software (version 1.45b, http://imagej.nih.gov.ij). Graphs were produced using Numbers ’09 Apple Inc. (Version 2.1 (436)).

3.4.7 Western blot

Cells collected in Figure 3-6 were lysed by resuspending pellets in 600 µL of kinase lysis buffer and 100 µL of glass beads then vortexing for 5 x 1min in a FastPrep homogenizer (MP Biomedicals). Protein concentrations were measured by Bradford assay and equal amounts of protein lysate (80 µg) was loaded on the polyacrylamide gels.

In Figure 3-5, 2 mL samples were taken for each time point. Cells were pelleted and supernatant removed. Cold sample buffer (100 µL) (0.065 M Tris HCl pH 6.8, 3% SDS, 10% glycerol, 5% beta-mercaptoethanol, 1X Phosphatase Cocktail 2 SIGMA-Aldrich, 2 mM

PMSF, 0.01% bromophenol blue) was added to each pellet with 100 µL glass beads prior to freezing in liquid nitrogen. Cell pellets were lysed by vortexing (4X 30 seconds at 5 m/s) in the FastPrep Homogenizer (MP Biomedicals). Samples were centrifuged (20 seconds at 10,000 rpm) to reduce suds, boiled for 5 minutes, centrifuged (5 minutes at 10,000 rpm) and 10 µL was loaded onto a poly-acrylamide gel (12% Acrylamide/ Bis, 78:1). Proteins were transferred onto a nitrocellulose membrane by wet transfer. Membranes were blocked for 1 hour in 1X PBS 5% dry milk at room temperature.

Endogenous untagged Clb2 was detected using a rabbit polyclonal antibody (Y-180 Santa Cruz, sc-9071) (1:2000), Cdk1 was detected using monoclonal mouse anti-PSTAIR (Sigma Aldrich P 7962) (1:7500), Swe1-myc was detected using monoclonal mouse anti-myc (Roche) (1:5000). All primary antibodies were incubated with blocking buffer overnight at 4˚C. To detect Mih1, blots were blocked in Mih1 block (1X PBS, 0.5 M NaCl, 0.1% Tween 20, 3% dry milk) for one hour. Polyclonal rabbit anti-Mih1 antibody (gift from Dr. Kellogg) was diluted to a working concentration of 4 µg/ µL in Mih1 block and incubated at 4 ˚C for at least 20 hours. Detection of phosphorylated tyrosine 19 Cdk1 in Figure 3-2 and 3-6 was performed by first blocking the membrane in 1X TBS, 0.1% Tween 20, 5% dry milk for an hour at room temperature, then incubating with the phospho-specific antibody P-cdc2 Y15 (Cell signaling 9111S) (1:1000) dilution in 1X TBS, 0.1% Tween 20, 5% BSA overnight at 4˚C. Epitope tagged Clb2-HA in Figure 3-6, 3-7, 3-8 and 3-12, was detected using mouse monoclonal anti-HA antibody (Roche) (1:2500 in either 1X PBS 5% dry milk, or 1X TBS 5% BSA) incubated overnight at 4˚C. Epitope tagged Mih1-GST in Figure 3-8 and 3-12 was

detected using anti-GST antibodies (GE Healthcare RPN1236) at a dilution of 1:5000 in either 1X PBS 5% dry milk, or 1X TBS 5% BSA, incubated overnight at 4 ˚C.

Horseradish peroxidase (HRP) conjugated secondary antibodies were used to visualize and amplify the primary signal. Secondary antibodies were goat-anti-mouse (Roche) (1:5000) or Goat anti-rabbit (Roche) (1:5000) and were incubated in blocking buffer with the membranes for 1 hour at room temperature. All proteins were imaged by chemilluminesence on film. Band intensity analysis in Figure 3-5 and 3-6 were done by measuring pixel intensity in ImageJ (version 1.45b, http://imagej.nih.gov.ij). Relative intensities were calculated using Numbers ’09 Apple Inc. (Version 2.1 (436)).

3.4.8 Kinase assays

Cells were lysed in kinase lysis buffer (0.25 M NaCl, 0.05 M Tris pH7.5, 2.5 mM NaF, 12 μM 6DMAP, 0.1% NP-40, 5 μM EDTA, 1 mM PMSF, 1μg/mL Leupeptin, 10 μg/ mL TLCK, 0.98 μg/ mL Pepstatin, 1 mM DTT, 10 μg/mL TPCK, 10 μg/mL SBTI, 1 μg/mL Aprotinin). All IP’s were performed at 4 ˚C for at least an hour. The IP’s in Figure 3-8 were done overnight. All myc epitope IP’s were done with Covance affinity matrix monoclonal mouse antibody 9E10 (Covance AFC-150P). HA epitope IP’s were done with Covance affinity matrix monoclonal antibody HA.11. For the Clb2-HA/Cdk1 kinase assay in Figure 3-6, following synchronization, 100 mL samples were pelleted and frozen on dry ice. Samples were lysed in 600 μL of kinase lysis buffer. Protein quantification was done on a NanoDrop. Protein lysate (18 mg) was incubated with affinity matrix HA beads (40 μL of a 50% solution), before proceeding with the washes. Half the beads were prepared for kinase reactions, while the other half was prepared for western blot analysis. Whole cell extract (160

μg) was also used for western blot analysis. Additional Clb2-HA/Cdk1 IP's in Figure 3-9B and Figure 3-10A were performed with 10 mg of protein lysate to 20 μL of 50% slurry of affinity matrix anti-HA and 8 mg of protein lysate to 20 μL of 50% slurry of affinity matrix anti-HA, respectively. In Figure 3-12, Clb2-HA/Cdk1 was immunoprecipitated (IP'd) from 4.5 mg protein lysate with 20 μL of 50% slurry of affinity matrix anti-HA. Figure 3-9C and 3-10A, both *MCK1-myc* and *mck1D164A-myc* were IP'd at 20 mg protein lysate per 20 μL of 50% affinity-matrix anti-myc beads. *PAH1-HA*, *PAH1-D398E-HA* and *CLN2-HA* in Figure 3-10B was IP'd from 7.5 mg protein lysate per 20 μL of 50% affinity matrix anti-HA. After the IP's beads with bound protein were washed four times in 1 mL wash buffer (0.25 M NaCl, 0.05 M Tris pH 7.5, 0.1% NP-40, 5 μM EDTA, and 1 mM DTT) and twice in 1 mL kinase buffer (10 mM $MgCl_2$, 5 mM $MnCl_2$, 0.05 M Tris pH7.5, 0.5 μM ATP, 1 μM DTT). Kinase reactions were run with the addition of 4 μL Υ-^{32}P-ATP in kinase buffer, with the exception of Figure 3-10 where 1μL of Υ-^{32}P-ATP was added. A variety of substrates were added in kinase assays. Where indicated (Figure 3-6, 3-9, 3-10, 13-2) 1 μg of Histone H1 (Roche) was added as a substrate. Concentrated GST-Mih1 or GST (1.75 μL of protein prepared as described below) were added as substrates in Figure 3-12. Protein IP's (prepared as described below) were also added as substrates in Figure 3-10. Inhibitor 1NM-PP1 (Toronto Research Chemicals) was prepared according to manufacturer's instructions in DMSO. Inhibitor or control (DMSO) was incubated with Clb2-HA preparations for 10 minutes at 30 ˚C for Figure 3-9 (B and C), and Figure 3-10A. Clb2-HA kinase reactions for Figure 3-6 and 3-9 were incubated for 30 minutes at 30 ˚C, while Figure 3-10 were incubated for 45 minutes at 30 ˚C until addition of 2X SDS loading buffer. Kinase reactions were run on polyacrylamide gels, dried on a gel dryer and imaged using film.

3.4.9 Co-immunoprecipitations

Mck1-myc was IP'd in Figure 3-8A from 30 mg of protein lysate incubated with 10 μL of 50% affinity-matrix anti-myc beads. In Figure 3-8B, 15 mg of protein lysate was incubated per 10 μL of a 50% affinity-matrix anti-myc beads. Figure 3-9A concentrations of protein lysate per 20 μL of 50% affinity-matrix anti-myc beads are shown.

3.4.10 Galactose induced over expression

All strains were grown in SC^{-URA} (2% raffinose, 0.1% dextrose) overnight. OD_{600nm} was measured and strains diluted in SC^{-URA} (2% raffinose) to obtain logarithmically growing cultures of sufficient quantity for experiments. To express genes under the control of the *GAL1* promoter, cultures were pelleted and washed once and re-suspended in SC^{-URA} (2% galactose) for the indicated amount of time.

3.4.11 GST and GST-MIH1 purification

Cultures were grown (500 mL) overnight in SC^{-URA} (2% raffinose, 0.1% dextrose) to an OD_{600nm} of 1.0. Cells were pelleted, washed and re-suspended in SC^{-URA} (2% galactose) for 3 hours at 30 ˚C. Cells were pelleted again and washed in cold dH_2O and divided amongst 10 flat bottom microcentrifuge tubes. Cells in each tube were lysed in 300 μL of kinase lysis buffer and 200 μL of glass beads. Lysates were cleared by centrifugation at 14,000 rpm for 10 minutes at 4 ˚C. Cleared lysates were pooled and concentrations measured by NanoDrop. Protein lysate (400 mg) was incubated with 50% glutathione sepharose beads (1.6 mL) overnight at 4˚C. Protein bound beads were washed 4X 1mL kinase washing buffer 2X 1 mL elution buffer (10% glycerol, 1 μM DTT, 50 μM Tris pH 8.0, 150 mM NaCl) and eluted with 1 mL of 30 mM glutathione in elution buffer for 1 hour at room temperature. Half the eluate

(500 μL) was heated at 75 ˚C for 10 minutes then concentrated by centrifugation (10,000 rpm for 10 minutes at room temperature) in a Centricon centrifugal filter unit (Millipore). The eluate (eluate 1) was resuspended in 20 μL of H_2O, 2 μL was saved to run on coomassie gel and the rest concentrated again for 2 minutes at 14,000 rpm. A second eluate (eluate 2) was resuspended in 20 μL of H_2O and 2 μL was run out on a coomassie gel.

Table 3-1 Yeast strains used in this study

Strain	Genotype	Source
YJM561	BY4742/S288C, MATα *ura3Δ::NAT^{R}can1Δ::STE2pr-Sp_HIS5 lyp1Δ his3Δ1 leu2Δ0 ura3Δ0 met15Δ0 LYS2+*	(Tong et al., 2001)
YJM562	BY4742/S288C, *MATα YNL307CΔNatR can1Δ::STE2pr-Sp_his5 lyp1Δ his3Δ1 leu2Δ0 ura3Δ0 met15Δ0 LYS2+*	(Tong et al., 2001)
YM1761	YPH499/S288C, MATa *his3Δ200 ade2-101 ura3-52 lys2-801 leu2Δ1 trp1-Δ63*	Phil Hieter
YJM336	YPH499/S288C, MATa *his3Δ200 ade2-101 ura3-52 lys2-801 leu2Δ1 trp1-Δ63, mck1Δ::KanMX6*	This study
YJM881	BY4741/S288C, MATa *his3Δ1 leu2Δ0 met15Δ0 ura3Δ0 ura3Δ::NAT^R cln3ΔkanMX*	This study
YJM879	BY4741/S288C, MATa *his3Δ1 leu2Δ0 met15Δ0 ura3Δ0 cln3ΔkanMX mck1ΔNAT^R*	This study
YJM945	BY4741/S288C, MATa *his3Δ1 leu2Δ0 met15Δ0 ura3Δ0 ura3Δ::NAT^R cln1ΔkanMX*	This study
YJM947	BY4741/S288C, MATa *his3Δ1 leu2Δ0 met15Δ0 ura3Δ0 cln1ΔkanMX mck1ΔNAT^R*	This study
YJM949	BY4741/S288C, MATa *his3Δ1 leu2Δ0 met15Δ0 ura3Δ0 ura3Δ::NAT^R cln2ΔkanMX*	This study
YJM951	BY4741/S288C, MATa *his3Δ1 leu2Δ0 met15Δ0 ura3Δ0 cln2ΔkanMX mck1ΔNAT^R*	This study
YJM875	BY4741/S288C, MATa *his3Δ1 leu2Δ0 met15Δ0 ura3Δ0 ura3Δ::NAT^R clb6ΔkanMX*	This study
YJM877	BY4741/S288C, MATa *his3Δ1 leu2Δ0 met15Δ0 ura3Δ0 clb6ΔkanMX mck1ΔNAT^R*	This study
YJM1087	BY4741/S288C, MATa *his3Δ1 leu2Δ0 met15Δ0 ura3Δ0 ura3Δ::NAT^R clb1ΔkanMX*	This study
YJM1089	BY4741/S288C, MATa *his3Δ1 leu2Δ0 met15Δ0 ura3Δ0 clb1ΔkanMX mck1ΔNAT^R*	This study
YJM892	BY4741/S288C, MATa *his3Δ1 leu2Δ0 met15Δ0 ura3Δ0 ura3Δ::NAT^R clb2ΔkanMX*	This study
YJM887	BY4741/S288C, MATa *his3Δ1 leu2Δ0 met15Δ0 ura3Δ0 clb2ΔkanMX mck1ΔNAT^R*	This study
YJM953	BY4741/S288C, MATa *his3Δ1 leu2Δ0 met15Δ0 ura3Δ0 ura3Δ::NAT^R clb3ΔkanMX*	This study
YJM956	BY4741/S288C, MATa *his3Δ1 leu2Δ0 met15Δ0 ura3Δ0 clb3ΔkanMX mck1ΔNAT^R*	This study
YJM1080	BY4741/S288C, MATa *his3Δ1 leu2Δ0 met15Δ0 ura3Δ0 ura3Δ::NAT^R clb4ΔkanMX*	This study
YJM1082	BY4741/S288C, MATa *his3Δ1 leu2Δ0 met15Δ0 ura3Δ0 clb4ΔkanMX mck1ΔNAT^R*	This study
YJM97	S288C, MATa *his3Δ200 ade2-101 ura3-52 lys2-801 leu2Δ1 trp1-Δ63, swe1-13myc::HIS3*	This study
YJM99	S288C, MATa *his3Δ200 ade2-101 ura3-52 lys2-801 leu2Δ1 trp1-Δ63, swe1-13myc::HIS3, mck1ΔkanMX6*	This study
YJM871	W303, MATa *ura3Δ, trp1-1, ade2-1, his3-11, 15 Leu2-3, 112 can1-100 GAL+, clb2-HA*	Mike Tyers
YJM1029	W303 MATa *ura3Δ, trp1-1, ade2-1, his3-11, 15 leu2-3, 112 can1-100, mck1ΔkanMX6 clb2-HA*	This study
YLM91	YPH499/S288C, MATa *his3Δ200 ade2-101 ura3-52 lys2-801 leu2Δ1 trp1-Δ63, MCK1-13myc::TRP1*	This study
YJM889	YPH499/S288C, MATa *his3Δ200 ade2-101 ura3-52 lys2-801 leu2Δ1 trp1-Δ63, MCK1-13myc::TRP1, mih1Δ::TRP1*	This study

Strain	Genotype	Source
YJM1143[a]	YPH499/BY4742 S288C MATα *ade2-101 lys2-801 MCK1-13myc::TRP1 clb2ΔkanMX*	This study
YM2169 (DK186)	W303, MATa *leu2-3, 112 trp1-1 can1-100 ura3-1 ade2-1 his3-11,15 GAL+ bar1*	Doug Kellogg
YJM1157	W303, MATa *leu2-3, 112 trp1-1 can1-100 ura3-1 ade2-1 his3-11,15 GAL+ bar1 MCK1-13myc:KanMX6*	This study
YJM1158	W303, MATa *leu2-3, 112 trp1-1 can1-100 ura3-1 ade2-1 his3-11,15 GAL+ bar1 MCK1-13myc:KanMX6 cdc28::cdc28-as1*	This Study
YJM1243A	W303, MATa *leu2-3, 112 trp1-1 can1-100 ura3-1 ade2-1 his3-11,15 GAL+ bar1 mck1D164A-13-myc:TRP*	This study
YJM1246C	W303, MATa *leu2-3, 112 trp1-1 can1-100 ura3-1 ade2-1 his3-11,15 GAL+ bar1 mck1D164A-13-myc:TRP cdc28::cdc28-as1*	This study
YJM1211A	W303, MATa *leu2-3, 112 trp1-1 can1-100 ura3-1 ade2-1 his3-11,15 GAL+ bar1 CLB2-HA:HIS cdc28::cdc28-as1*	This study

[A] These strains were created by mating a BY4742 strain to a YPH499 strain hence the precise genotype is not known.

Table 3-2 Plasmids used in this study.

Plasmid Name	Plasmid	Description	Reference or Source
BVM392	*pGAL-CLB2-HA*	*pWS945, CEN4, GAL10-CLB2-3xHA, LEU2, URA3*	Mike Tyers, Wolfgang Seufert
BVM389	*Empty vector*	*pRS316, CEN6, URA3*	Mike Tyers, R Nash
BVM391	*CLN-2HA*	*CEN, pGAL-CLN2-3HA, URA*	Mike Tyers
PGH312	*PAH1HA*	*Yep351, 2μ, PAH1-HA, LEU2*	Carman Lab (Han et al., 2007)
pGH312-D398E	*PAH1-D398E HA*	*Yep351, 2μ, PAH1-D398E-HA, LEU2*	Carman Lab (Han et al., 2007)
BVM311	*pGAL-GST-MIH1*	*pEGH, 2μ, GAL1/10-GST-6xHIS-MIH1, URA3*	Open biosystems
Not yet designated	*pGAL-GST-MCK1*	*pEGH,2μ, GAL1/10-GST-6xHIS-MCK1, URA3*	Open biosystems
BVM288	*Empty vector*	*pEGH, 2μ*	Open biosystems

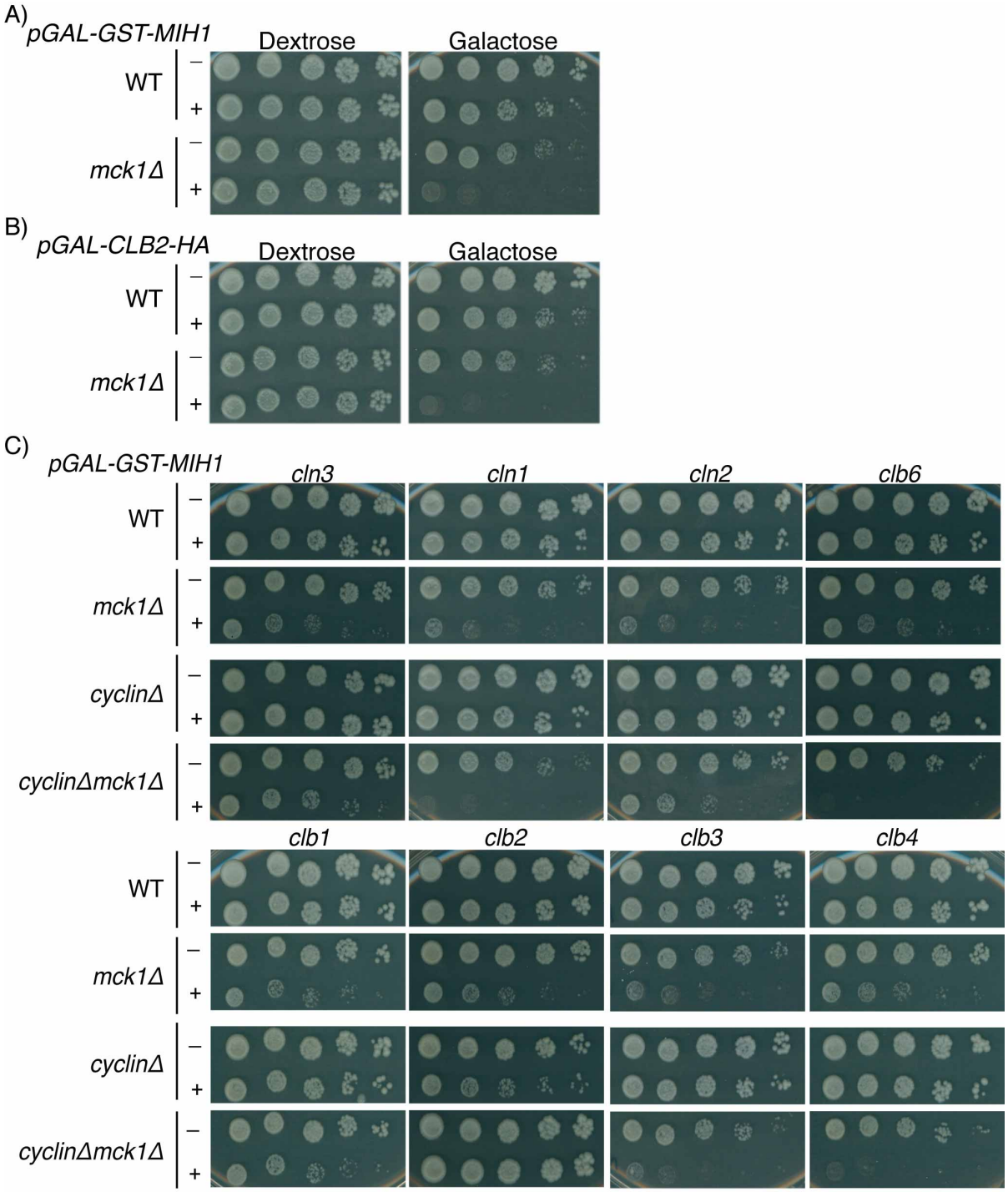
A)
pGAL-GST-MIH1
Dextrose
Galactose
WT
mck1Δ
B)
pGAL-CLB2-HA
Dextrose
Galactose
WT
mck1Δ
C)
pGAL-GST-MIH1
cln3
cln1
cln2
clb6
WT
mck1Δ
cyclinΔ
cyclinΔmck1Δ
clb1
clb2
clb3
clb4
WT
mck1Δ
cyclinΔ
cyclinΔmck1Δ

Figure 3-1 Overexpression of *MIH1* is toxic to *mck1*Δ mutants in a *CLB2* dependent fashion.

Wild type, *mck1*Δ*, cyclin*Δ and *mck1*Δ *cyclin*Δ double mutant strains were serially diluted onto the indicated media and grown for 4 days at 30 ˚C. A) Over expression of *pGAL-GST-MIH1* (+) or vector alone (-) in a wild type (WT) or *mck1*Δ strain. B) Over expression of *pGAL-CLB2-HA* (+) or vector alone (-) in a wild type (WT) or *mck1*Δ strains. C) The gene at the top of the column represents the cyclin gene that is deleted for that column; *cyclin*Δ. *pGAL-GST-MIH1* (+) or vector alone (-) were over expressed in wild type (WT), *mck1*Δ*, cyclin*Δ or *cyclin*Δ *mck1*Δ double mutants and plated onto galactose media.

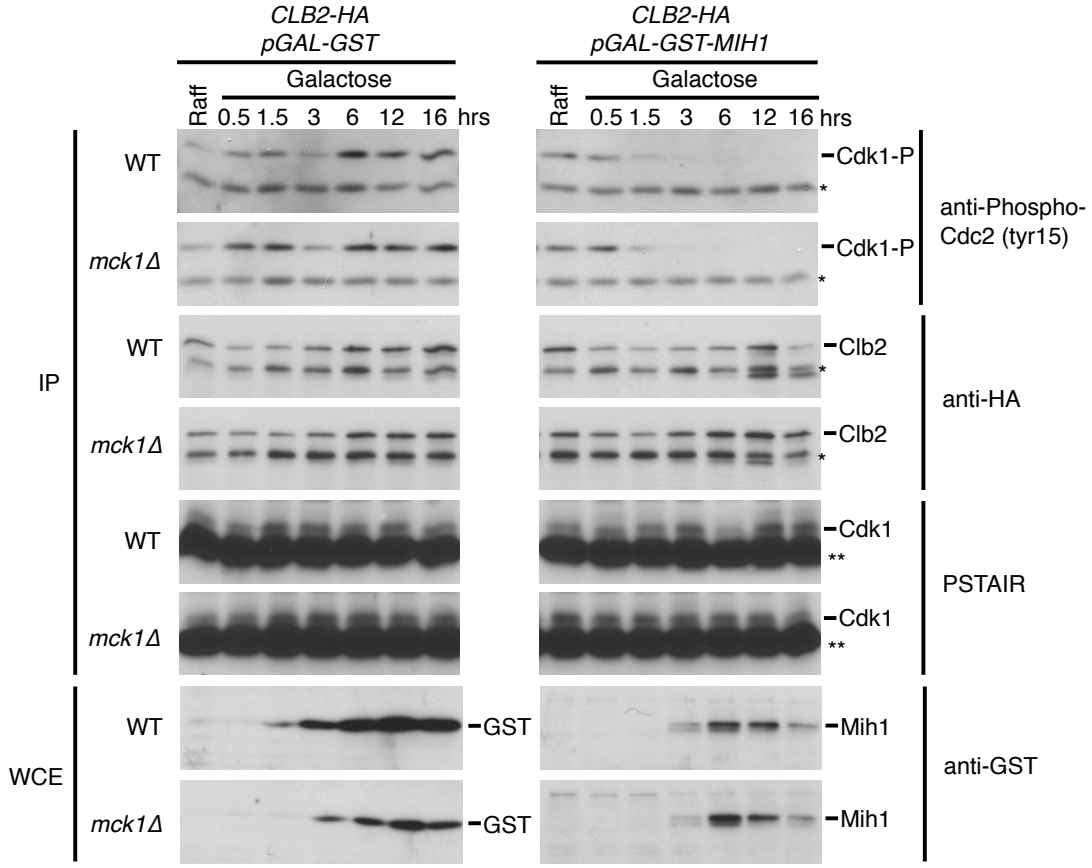

Figure 3-2 Mih1 is active in the absence of Mck1.

The following strains were grown in SC^{-URA} raffinose (Raff) overnight re-suspended in galactose media for indicated times; *CLB2-HA pGAL-GST, CLB2-HA pGAL-GST-MIH1, CLB2-HA mck1Δ pGAL-GST, CLB2-HA mck1Δ pGAL-GST-MIH1.* Clb2-HA was immunoprecipitated (IP'd) and analyzed by western blot with anti-phospho-Cdc2(tyr15), anti-HA and anti-PSTAIR (Cdk1) antibodies. Whole cell extracts (WCE) were analyzed with anti-GST antibodies. (*) Indicates background bands as determined by use of mutant analysis. (**) Indicates light chain immunoglobulin.

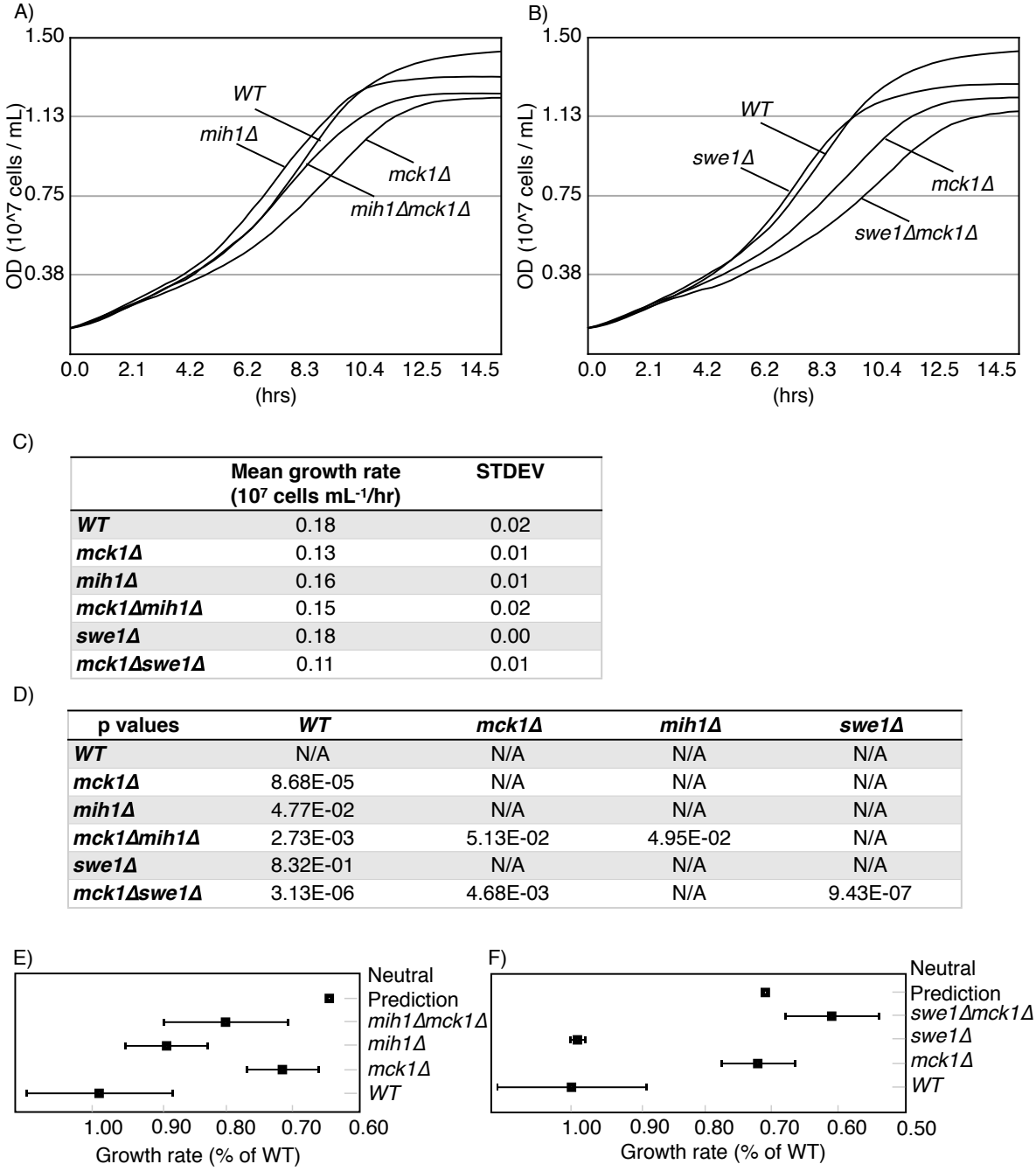

C)

	Mean growth rate (10^7 cells mL^{-1}/hr)	STDEV
WT	0.18	0.02
mck1Δ	0.13	0.01
mih1Δ	0.16	0.01
mck1Δmih1Δ	0.15	0.02
swe1Δ	0.18	0.00
mck1Δswe1Δ	0.11	0.01

D)

p values	*WT*	*mck1Δ*	*mih1Δ*	*swe1Δ*
WT	N/A	N/A	N/A	N/A
mck1Δ	8.68E-05	N/A	N/A	N/A
mih1Δ	4.77E-02	N/A	N/A	N/A
mck1Δmih1Δ	2.73E-03	5.13E-02	4.95E-02	N/A
swe1Δ	8.32E-01	N/A	N/A	N/A
mck1Δswe1Δ	3.13E-06	4.68E-03	N/A	9.43E-07

Figure 3-3 The slow growth rate of *mck1*Δ strains is ameliorated by *mih1*Δ and worsened by *swe1*Δ.

A and B) The indicated strains were grown in a 96 well plate and OD_{600nm} measurements were taken every 20.8 minutes. The average of 8 replicate growth curves per strain is plotted. C) Average calculated growth rates were determined by the slope of the line of exponential growth with standard deviations. D) Calculated *p*-values for growth rates of strains in rows compared to those in columns. E and F) Growth rates relative to WT plotted with standard deviation. Neutral prediction indicates no genetic interaction. Error bars represent standard deviation. Error bars for neutral predication are too small to observe.

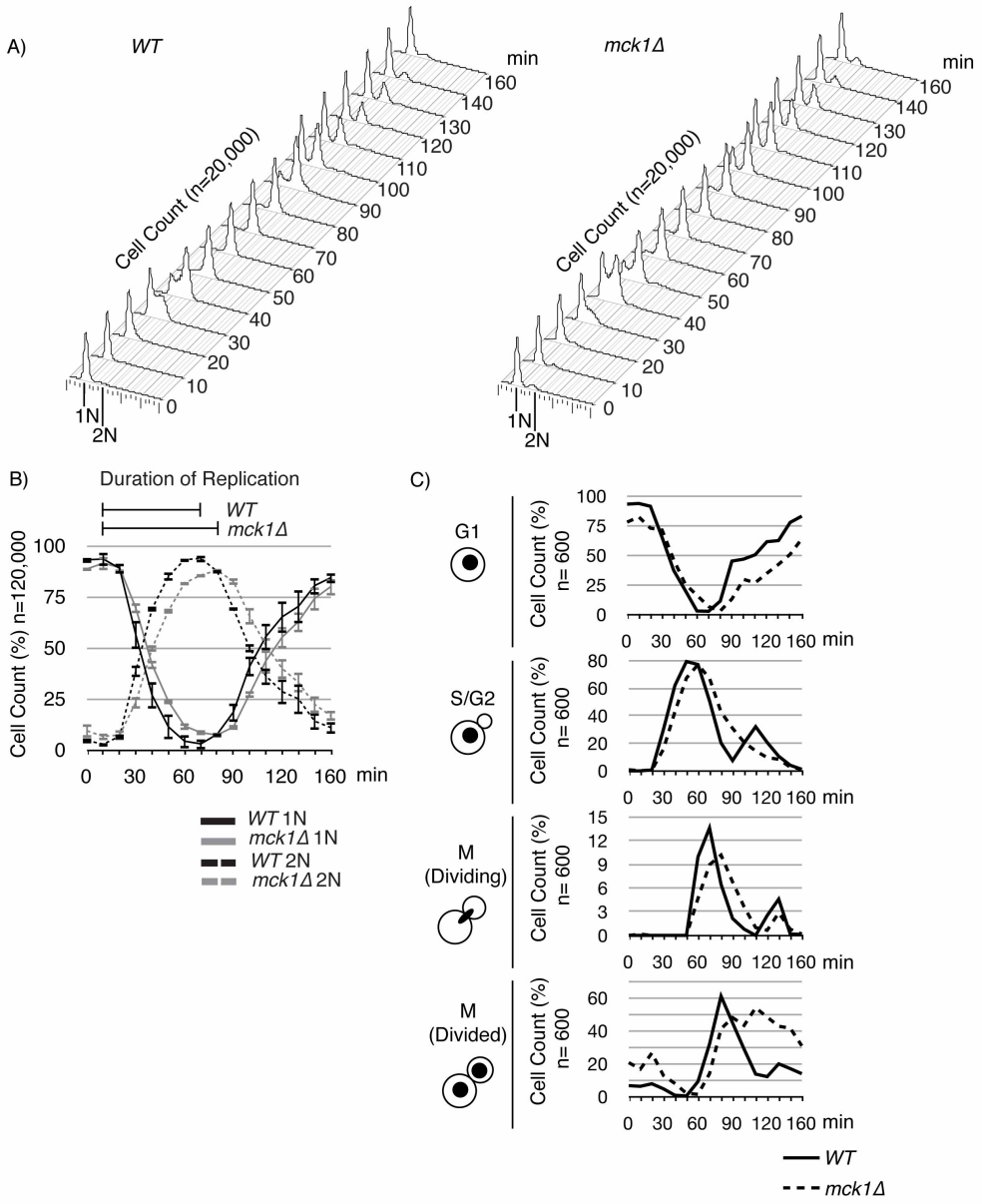
A)
WT
mck1Δ
min
160
140
130
120
110
100
90
80
70
60
50
40
30
20
10
0
Cell Count (n=20,000)
1N
2N
B)
Duration of Replication
WT
mck1Δ
Cell Count (%) n=120,000
100
75
50
25
0
0 30 60 90 120 160 min
WT 1N
mck1Δ 1N
WT 2N
mck1Δ 2N
C)
G1
S/G2
M
(Dividing)
M
(Divided)
Cell Count (%)
n= 600
0 30 60 90 120 160 min
WT
mck1Δ

Figure 3-4 *mck1*Δ strains are delayed in replication and cell cycle completion.

WT and *mck1*Δ strains were synchronized in G1 with mating pheromone. After release from G1 arrest, cell cycle time points were taken every 10 minutes from two independent cultures in replicates of three and processed for FACS and microscopy. A) A representative DNA content profile analyzed by FACS from one replicate of wild type (WT) and *mck1*Δ strains. B) FACS data gated for 1N and 2N populations. Population numbers were averaged from the 6 samples taken (replicates of three from two independent cultures) for each time point. Average population size as a percentage of total cells counted is shown. Error bars represent the standard deviation. Bars above the graph indicate the time required for replication. C) Cell cycle analysis by microscopy of budding index and nuclear division by DAPI staining was performed on duplicate samples from the same culture in both strains.

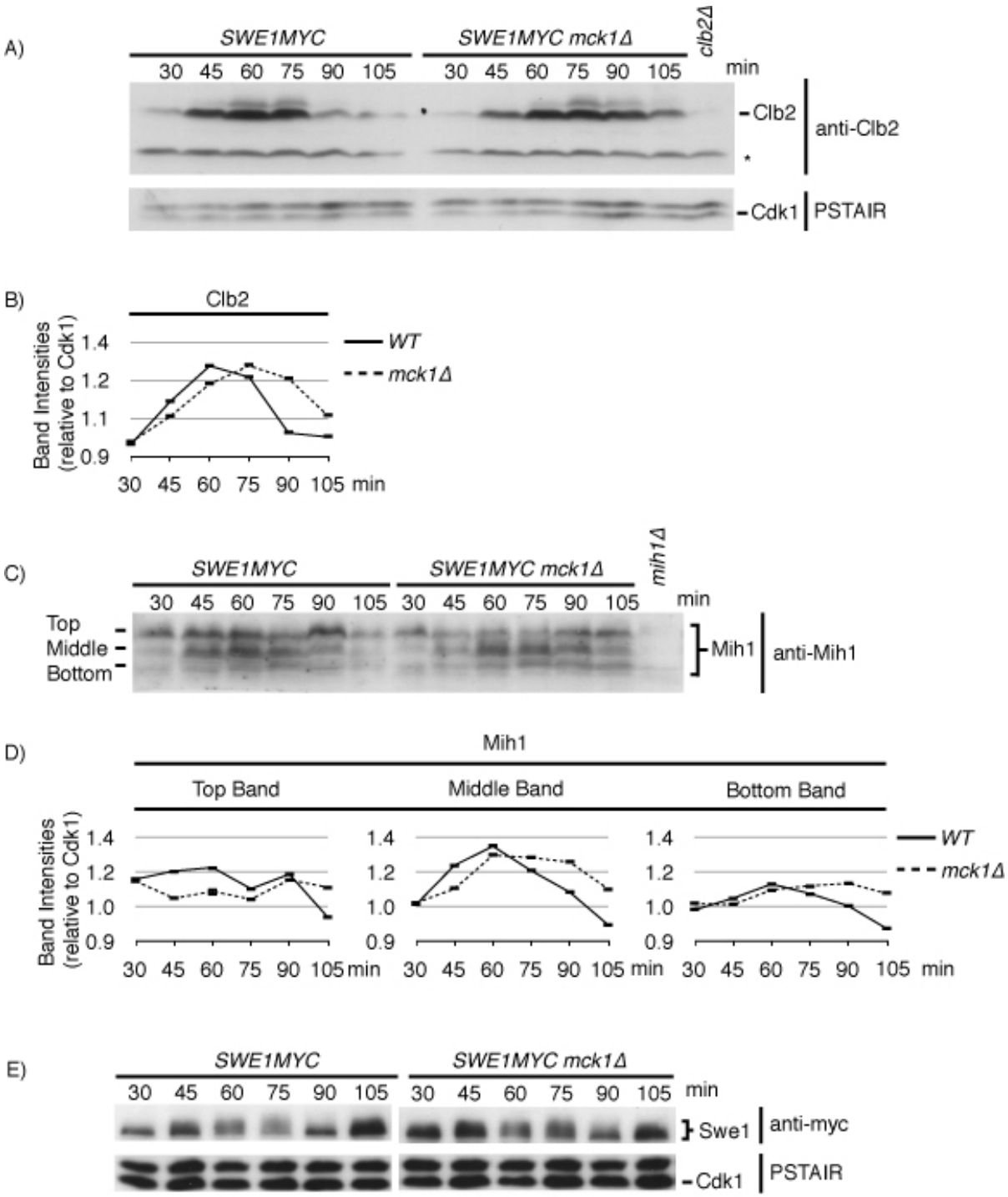
A)
SWE1MYC
SWE1MYC mck1Δ
clb2Δ
30 45 60 75 90 105
30 45 60 75 90 105
min
Clb2
anti-Clb2
*
Cdk1
PSTAIR
B)
Clb2
Band Intensities (relative to Cdk1)
1.4
1.2
1.1
0.9
WT
mck1Δ
30 45 60 75 90 105 min
C)
SWE1MYC
SWE1MYC mck1Δ
mih1Δ
30 45 60 75 90 105
30 45 60 75 90 105
min
Top
Middle
Bottom
Mih1
anti-Mih1
D)
Mih1
Top Band
Middle Band
Bottom Band
Band Intensities (relative to Cdk1)
1.4
1.2
1.0
0.9
WT
mck1Δ
30 45 60 75 90 105 min
E)
SWE1MYC
SWE1MYC mck1Δ
30 45 60 75 90 105
30 45 60 75 90 105
min
Swe1
anti-myc
Cdk1
PSTAIR

F)

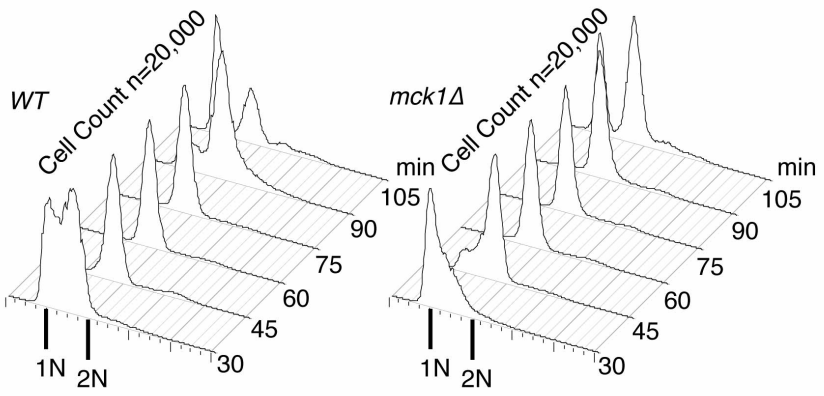

G)

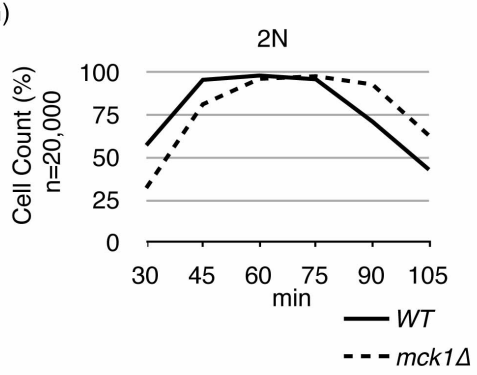

H)

WT	G1	S/G2	M	
			Dividing	Divided
45	3.6	96.4	0.0	0.0
60	0.4	87.2	11.1	1.3
75	3.7	35.8	11.1	49.5
90	46.2	16.0	0.6	37.2
105	60.9	25.5	0.9	12.8

mck1Δ	G1	S/G2	M	
			Dividing	Divided
45	18.3	80.9	0.0	0.8
60	3.0	93.2	3.4	0.4
75	1.4	61.9	14.1	22.7
90	5.3	28.2	9.1	57.4
105	25.1	7.8	1.2	65.8

I)

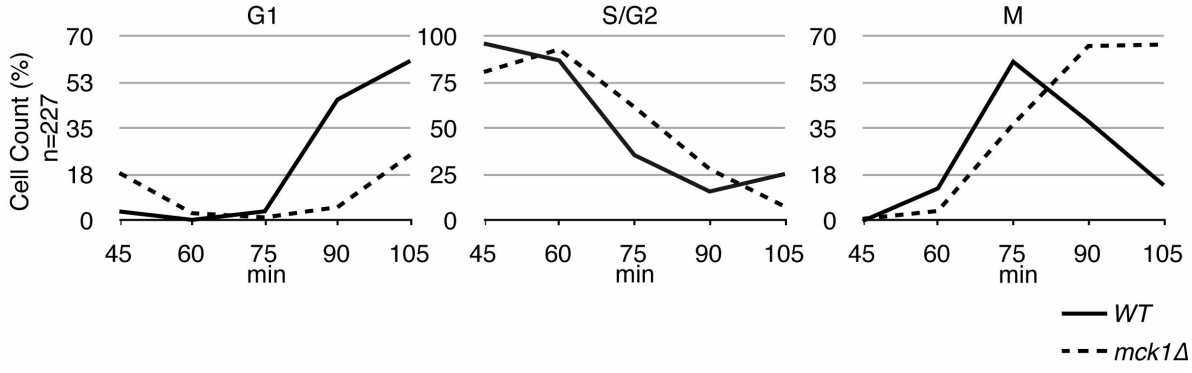

Figure 3-5 Mih1 phospho-isoforms are reduced and Clb2 degradation is delayed in *mck1*Δ strains.

Wild type **(***SWE1MYC*) and *mck1*Δ (*SWE1MYC mck1*Δ) strains were synchronized in G1 with mating factor. Time points were taken at 30, 45, 60, 75, 90 and 105 minutes after release and processed for western, FACS, and microscopy analysis. Cell cycle westerns were probed with (A) anti-Clb2 and anti- PSTAIR (loading control), (C) anti-Mih1, (E) anti-MYC antibodies. (*) Indicates background band. B and D) Plotted intensities of bands of interest relative to Cdk1 bands in (A) are plotted. Each band was counted three times and standard deviations are shown. F) DNA content profiles of WT and *mck1*Δ strains (from experiment in A and C) followed by FACS analysis. G) Percentage of 2N cells in WT and *mck1*Δ populations by gating FACS data. H) Microscopy cell cycle analysis of DAPI stained WT and *mck1*Δ cells (from experiment in A and B) as a percentage of total cells counted. I) Graphical representation of cell cycle microscopy analysis in (H).

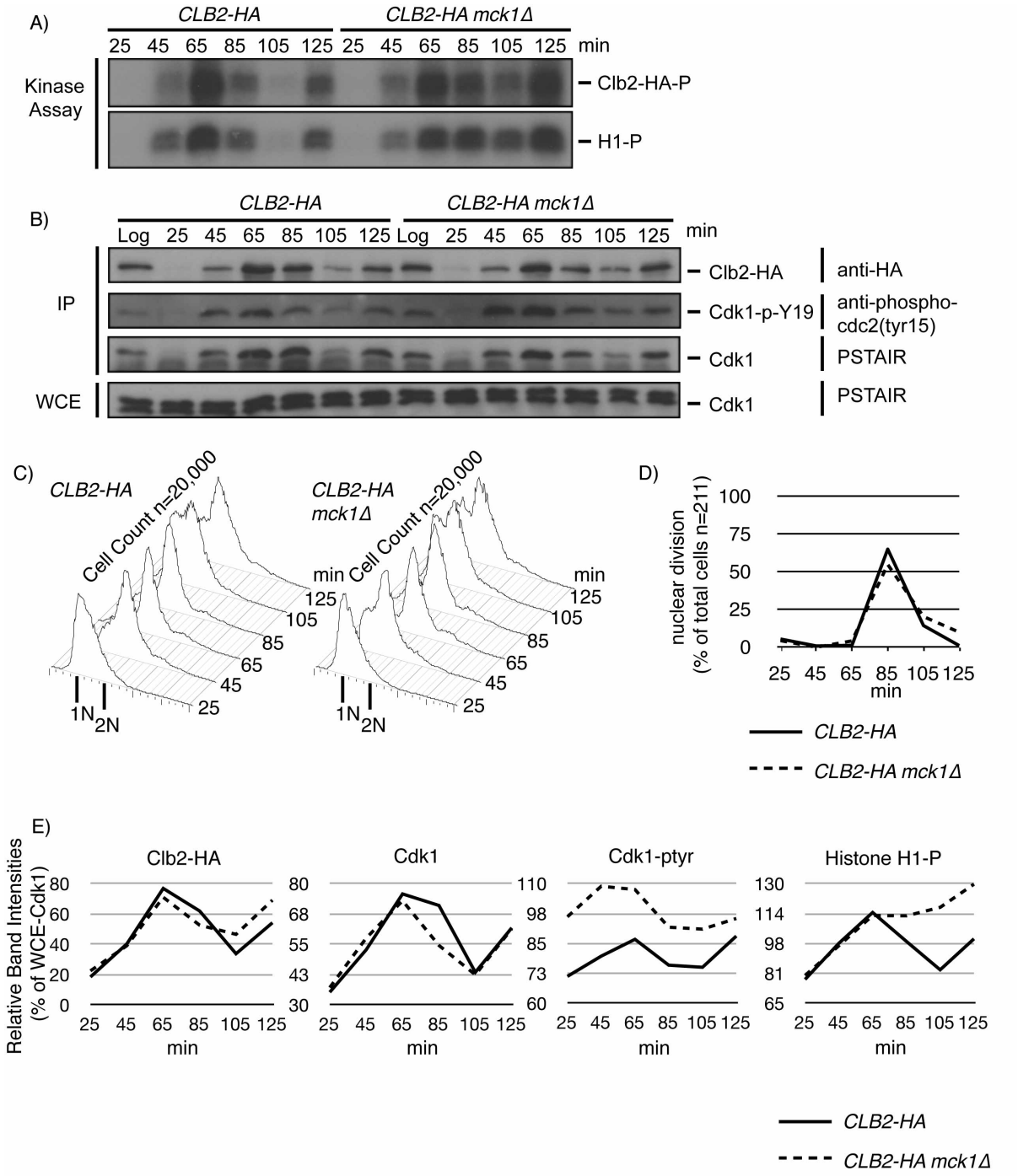
A)
CLB2-HA
CLB2-HA mck1Δ
25 45 65 85 105 125 25 45 65 85 105 125 min
Kinase Assay
Clb2-HA-P
H1-P
B)
CLB2-HA
CLB2-HA mck1Δ
Log 25 45 65 85 105 125 Log 25 45 65 85 105 125 min
IP
WCE
Clb2-HA
Cdk1-p-Y19
Cdk1
Cdk1
anti-HA
anti-phospho-cdc2(tyr15)
PSTAIR
PSTAIR
C)
CLB2-HA
Cell Count n=20,000
CLB2-HA mck1Δ
Cell Count n=20,000
min
125
105
85
65
45
25
1N
2N
D)
nuclear division (% of total cells n=211)
100
75
50
25
0
25 45 65 85 105 125
min
CLB2-HA
CLB2-HA mck1Δ
E)
Relative Band Intensities (% of WCE-Cdk1)
Clb2-HA
Cdk1
Cdk1-ptyr
Histone H1-P
min
CLB2-HA
CLB2-HA mck1Δ

Figure 3-6 Clb2-Cdk1 remains active post nuclear division in the absence of *MCK1*.

CLB2-HA and *CLB2-HA mck1*Δ strains were arrested in G1 with mating pheromone. Time points were taken at 25, 45, 65, 85, 105 and 125 minutes following release and processed for kinase assays (A), western blots (B), FACS (C) and microscopy analysis (D). A) Clb2-HA was IP'd from wild type (*CLB2-HA*) and *mck1*Δ (*CLB2-HA mck1*Δ) strains using anti-HA conjugated beads (Covance). Kinase assays were performed by incubating the IPs with γ-^{32}P-ATP and Histone H1. B) Western blot analysis of Clb2-HA IP and WCE probed with the following antibodies as indicated: anti-HA, anti-phospho-cdc2 (Tyr15) and anti-PSTAIR (Cdk1). C) DNA content profiles as monitored by FACS. (D) Cells from both the Clb2-HA and Clb2-HA *mck1*Δ time course were DAPI stained and nuclear division monitored by fluorescence microscopy. (E) Relative intensities of indicated bands relative to the WCE Cdk1 protein band in (B).

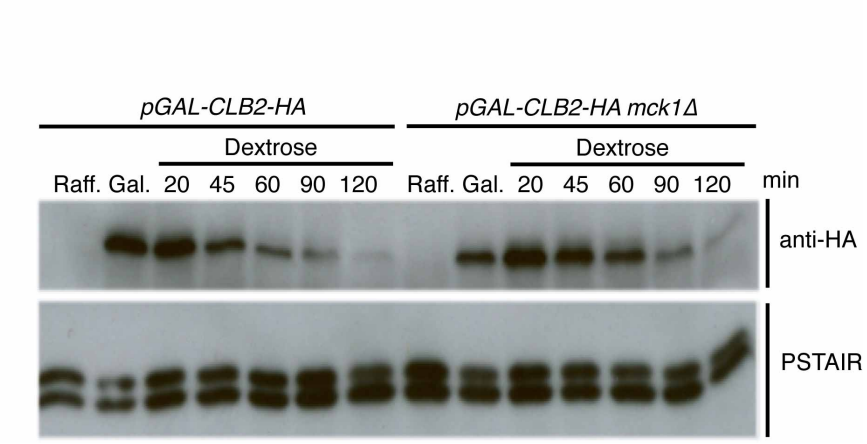

Figure 3-7 Clb2 degradation is unaltered in the absence of *MCK1*.

Wild type and *mck1*Δ strains carrying *CLB2-HA* on a plasmid under the control of the *GAL10* promoter (*pGAL-CLB2-HA*) were grown to logarithmic phase in SC^{-URA} 2% raffinose (Raff). Cultures were washed and resuspended in SC^{-URA} 2% galactose (Gal) for 30 minutes to induce *CLB2* expression. Cultures were then washed and re-suspended in SC^{-URA} 2% dextrose to stop *CLB2-HA* expression and samples were taken at indicated times (Dextrose). Clb2 degradation was followed by probing Western blots with anti-HA antibody. Anti-PSTAIR (Cdk1) antibody was used a loading control.

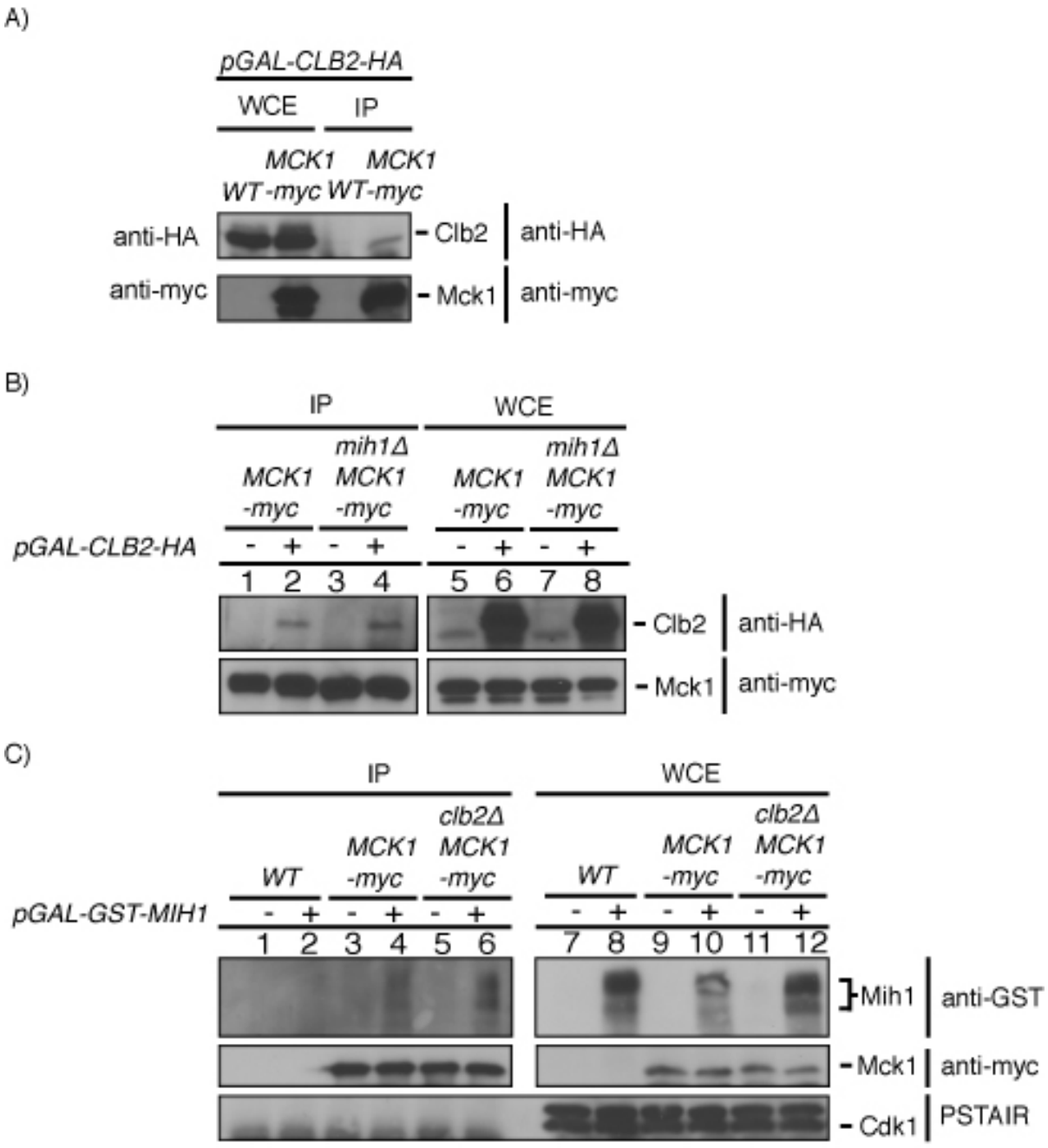

Figure 3-8 Mck1 co-immunoprecipitates with Clb2 and Mih1.

Myc tagged Mck1 in either wild type (A) and *mih1*Δ (B) or wild type and *clb2*Δ (C) strains were grown to mid-log phase in SC^{-URA} 2% raffinose media, washed and resuspended in SC^{-URA} 2% galactose to express either (A and B) *GAL-CLB2-HA* or (C) *GAL-GST-MIH1* for 1 hour. *Mck1-myc* was IP'd and protein interactions with Clb2 or Mih1 were detected by probing with anti-HA or anti-GST antibodies, respectively.

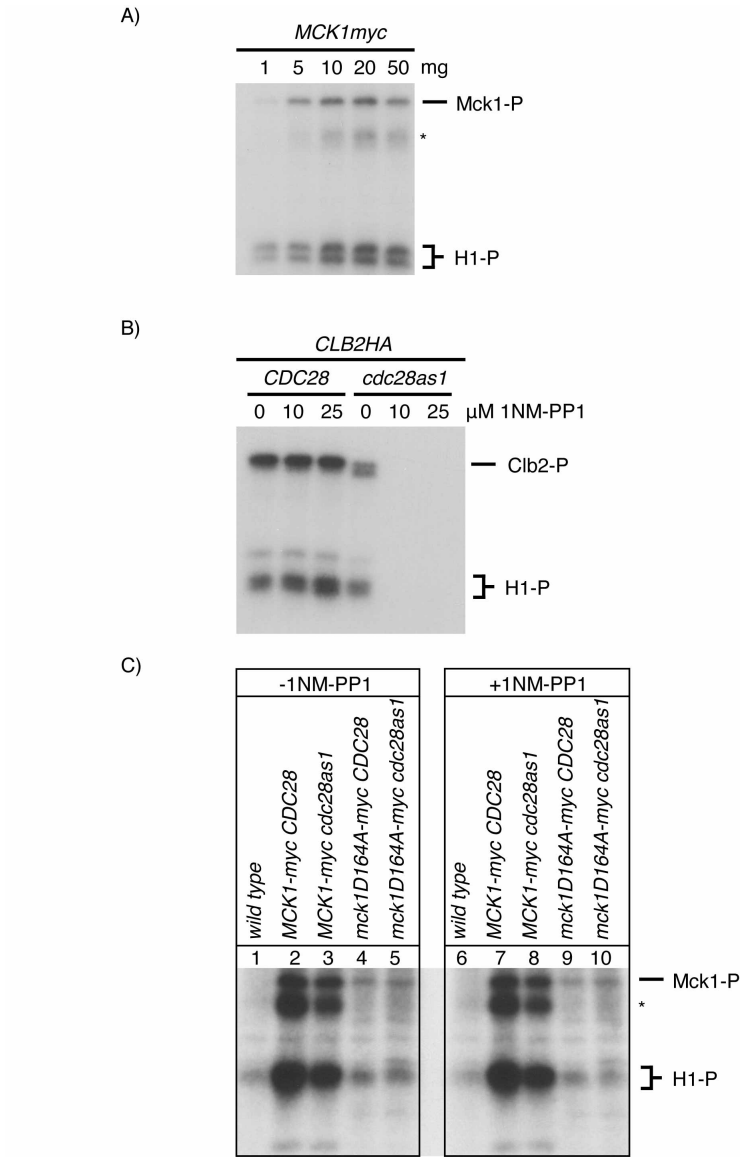

Figure 3-9 Mck1 does not co-immunoprecipitate with Cdk1 activity.

Kinase assays were performed with IPs from the indicated strains. A) Increasing amounts of lysate from a *MCK1-myc* strain were IP'd with equal portions of affinity matrix anti-myc beads. Kinase reactions were performed with addition of Histone H1 and γ-^{32}P-ATP. B) *CLB2-HA,* endogenously tagged in either a wild type (*CDC28)* or analog sensitive *cdc28as1* strain was IP'd with anti-HA Covance beads and split into 3 reactions. Each reaction was incubated with the indicated concentration of the inhibitor, 1NM-PP1. Kinase reactions were then performed with the addition of Histone H1 and γ-^{32}P-ATP. C) Mck1-myc or mck1D164A-myc (kinase dead) was IP'd from wild type (*CDC28)* or *cdc28as1* strains. IPs were split in half and incubated with 10 µM 1NM-PP1 or solvent control (DMSO). Kinase reactions were then performed with the addition of Histone H1 and γ-^{32}P-ATP. Asterisk (*) annotates contaminating band in the Histone H1 preparation.

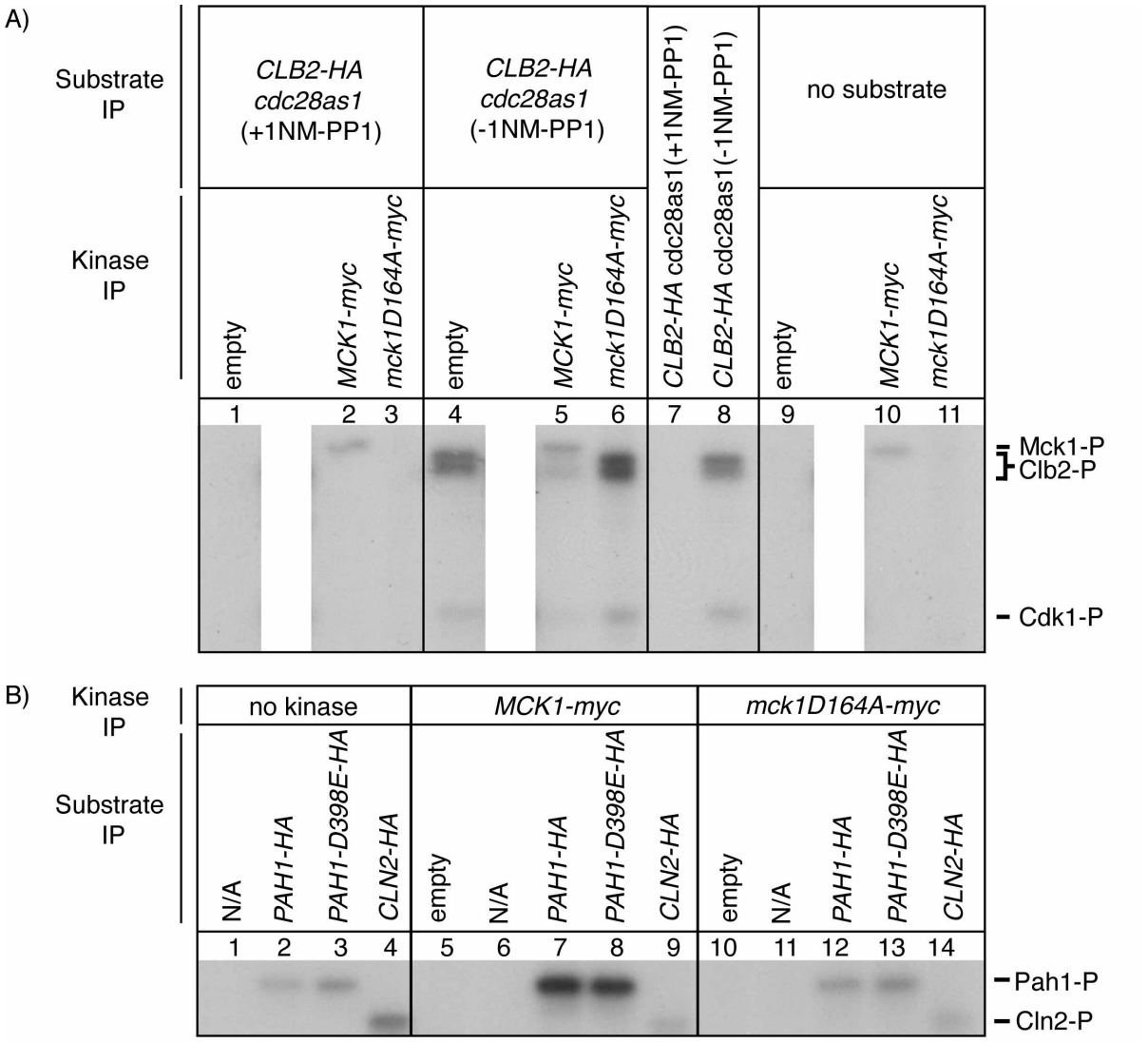

Figure 3-10 Mck1 kinase activity inhibits Clb2-Cdk1 activity and phosphorylates Pah1.

A) Clb2-HA was IP'd from the *cdc28as1* strain, split in half and incubated with either 1NM-PP1 or solvent control (DMSO). Mck1-myc and Mck1D164A-myc were IP'd and equivalent amounts of either inhibited Clb2-HA *cdc28as1* (+1NM-PP1) or uninhibited Clb2-HA *cdc28as1* (-1NM-PP1) were added to Mck1 kinase IPs, lanes 1-3 and lanes 4-6 respectively. Inhibited and uninhibited purified Clb2-HA *cdc28as1* is shown in lane 7 and 8 without addition of the Mck1 kinase. Mck1 kinase purifications with no added substrate are shown in Lane 9-11. B) HA tagged Pah1, a phosphatase inactive Pah1 mutant tagged with HA (Pah1D398E-HA) and Cln2-HA were IP'd and either incubated with γ-^{32}P-ATP (lanes 1-4) or mixed with IPs of Mck1-Myc (lanes 5-9) or mck1D164A-Myc (lanes 10-14), followed by addition of γ-^{32}P-ATP.

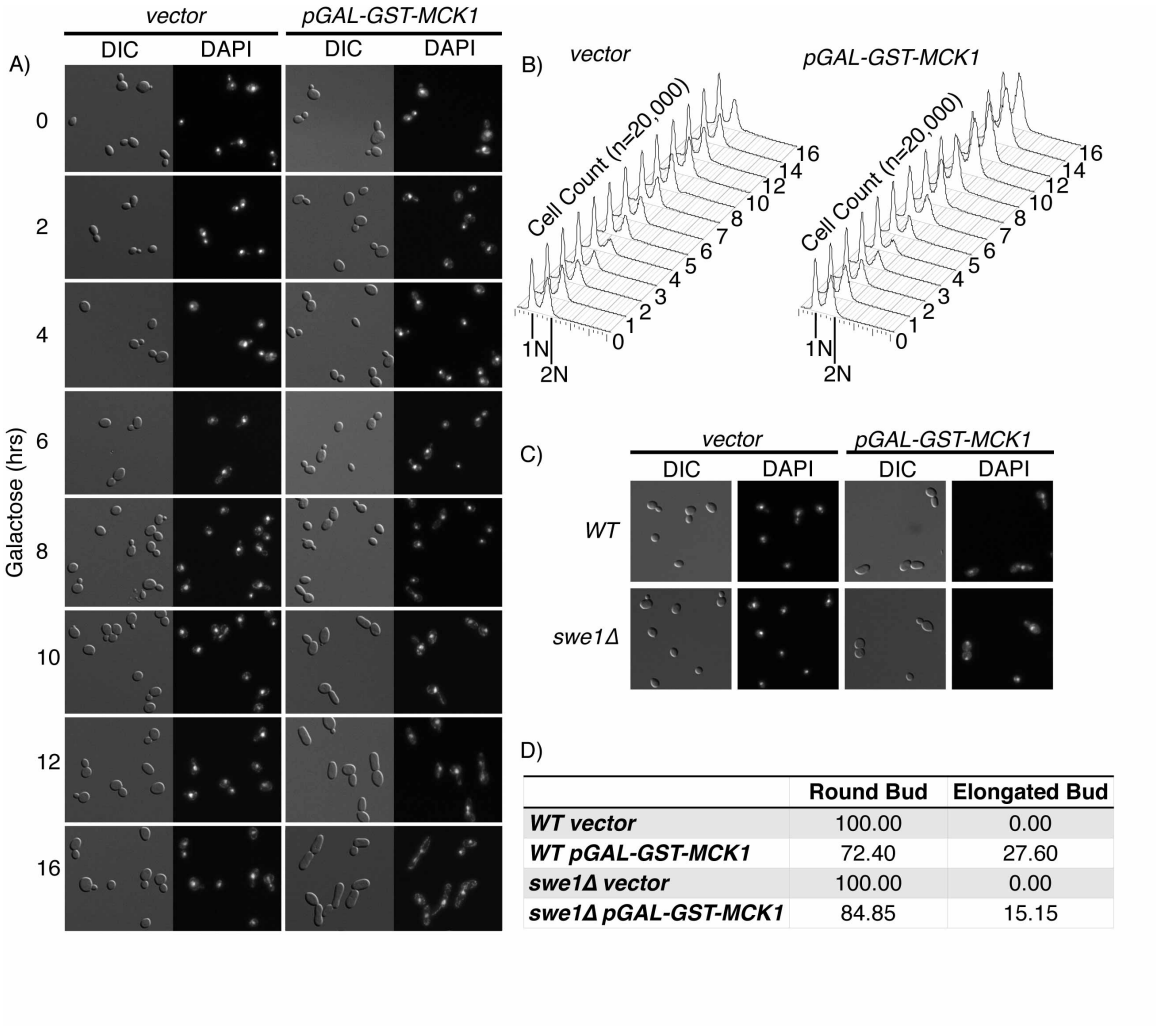

D)

	Round Bud	Elongated Bud
WT vector	100.00	0.00
WT pGAL-GST-MCK1	72.40	27.60
swe1Δ vector	100.00	0.00
swe1Δ pGAL-GST-MCK1	84.85	15.15

Figure 3-11 Expression of *pGAL-GST-MCK1* causes bud elongation that is partially rescued by the deletion of *SWE1*.

A) *pGAL-GST-MCK1* or vector alone were grown in wild type cells in SC^{-ura} 2%raffinose until early log phase then re-suspended into galactose media. Samples were taken for FACS and microscopy analysis every hour during galactose exposure until 8 hours and then again at 10, 12, 14 and 16 hours. (A) Representative microscopy images are shown for several time points. (B) FACs analysis representing DNA content profiles are shown. C) *pGAL-GST-MCK1* or vector alone were expressed in the presence or absence of *SWE1* for 16 hours. Representative microscopy images presented. D) Bud elongation defined as having a longer axis of growth versus width qualified by eye was counted for 224 cells. Percentages are displayed.

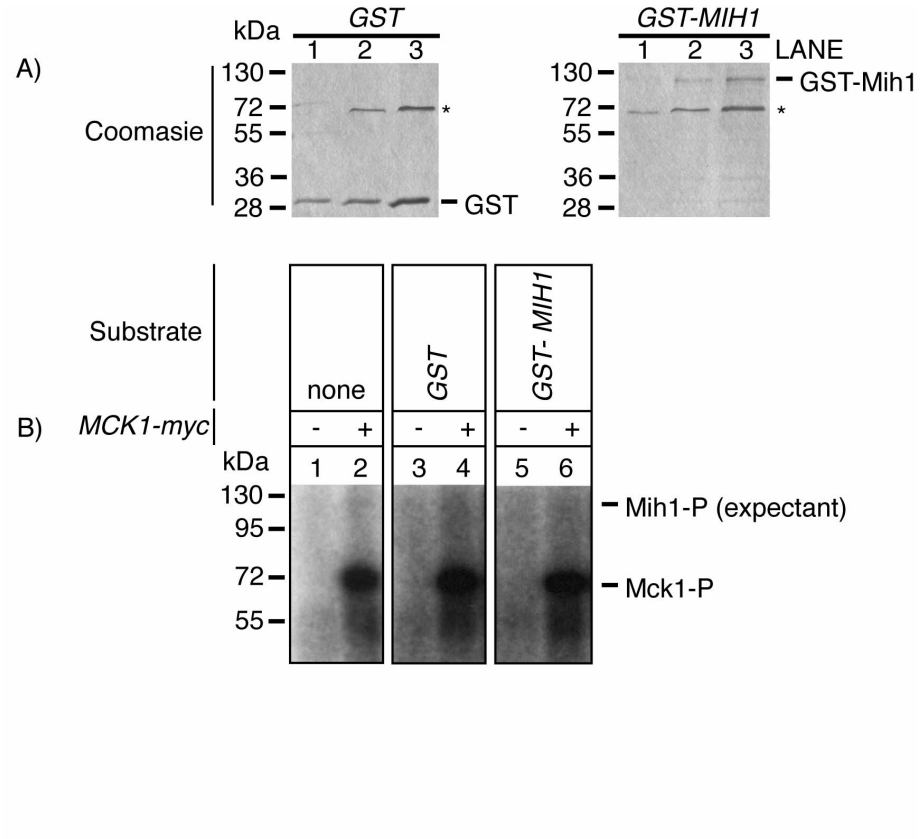

Figure 3-12 Mck1 does not phosphorylate purified Mih1 in vitro.

A) GST and GST-Mih1 were purified from *mck1*Δ *pGAL-GST* and *mck1*Δ *pGAL-GST-MIH1* strains respectively. Samples were taken from eluate 1 and eluate 2, (see Materials and Methods), and run on a coomassie gels. Lane1; 2 µl of eluate 1. Lane 2; 2 µl of eluate 2. Lane 3; 5 µl of eluate 2. GST and GST-Mih1 protein is indicated on respective gels. Asterisk (*) marks a background band. B) *MCK1-myc* and an untagged strain were incubated with affinity matrix anti-myc beads. Kinase reactions were performed by combining Mck1-myc immunoprecipitations, with either purified GST, GST-Mih1 or Histone H1, as well as γ-^{32}P-ATP.

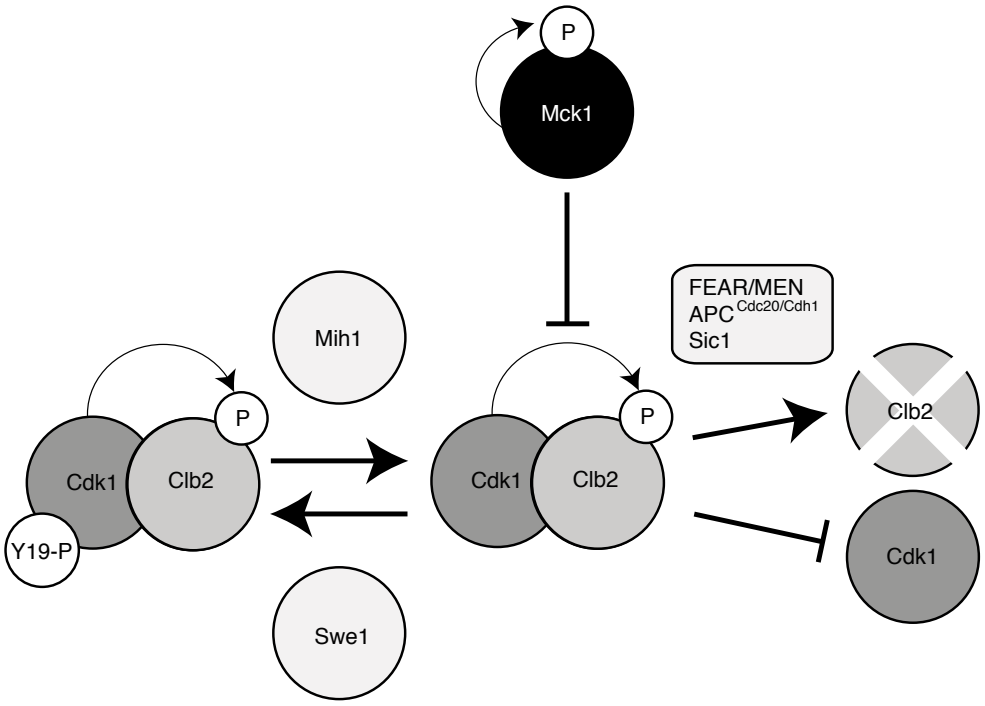

Figure 3-13 Model for control of Clb2-Cdk1 regulation.

Inhibitory phosphorylation of Cdk1 on tyrosine 19 is controlled by the phosphatase Mih1 and the kinase Swe1 prior to mitotic entry. Clb2 is targeted for degradation during mitotic exit by the $APC^{Cdc20/\ Cdh1}$, while the kinase activity of Cdk1 is inhibited by Sic1 and counteracted by the phosphatase Cdc14. The catalytic activity of Mck1 can inhibit the activity of Cdk1 towards Clb2, most likely through interactions with Clb2. Mck1 is not required but may contribute to the eventual degradation of Clb2.

Chapter 4: Survival in chronic DNA replication stress requires Mck1 kinase activity.

4.1 Introduction

Depletion of cellular dNTP's caused experimentally by the addition of HU, causes slowed or paused replication forks. The continued action of the MCM helicase, despite the lack of replication, unwinds DNA producing stretches of about 300 bp of ssDNA (Sogo et al., 2002) and a DNA replication checkpoint response, via Mec1 and Rad53 (Weinert et al., 1994). The DNA replication checkpoint responds in a multitude of ways to promote cell survival. A few of these mechanisms include the increase in transcription of genes involved in DNA repair and replication, promotion of replication fork stability and prevention of chromosomal segregation. The checkpoint induces the transcription of a large number of genes through the inhibition of the MBF transcriptional repressor Nrm1 (Travesa et al., 2012). Although the stability of the replication fork is still under intense study, a recent report suggests that the stability of the fork and presence of the replisome under HU treatment is independent of the checkpoint. The authors suggest instead that the replication fork is functionally regulated by the checkpoint (De Piccoli et al., 2012). As opposed to the response after DNA damage, the HU-induced DNA replication checkpoint does not trigger recruitment of DNA repair proteins to the site of stalled replication forks (Lisby et al., 2004). However, after chronic treatment of wild type cells with HU (>16 hours) or after short treatment of checkpoint deficient cells with HU, DNA repair foci (Mre11 and Rad52) are readily observed (Lisby et al., 2004). This suggests that HU stalled replication forks are not the site of DNA damage or repair until they eventually collapse. The initial observation that HU-treated checkpoint

deficient cells segregate DNA into the daughter cell, was interpreted as a role for the checkpoint in preventing mitotic entry (Weinert et al., 1994). In both *S. pombe* and higher eukaryotes it appears that the DNA replication checkpoint inhibits Cdk1 activity, thus preventing mitosis, through down regulating the phosphatase, Cdc25 (*S. cerevisiae Mih1*) which promotes Cdk1 activity (reviewed in (Diffley, 2004)). However, in *S. cerevisiae* it appears that HU-treated cells arrest with high Cdk1 activity (Bachant et al., 2005; Krishnan et al., 2004) and a mutation in the inhibitory Cdk1 phosphorylation site, which prevents phosphorylation does not lead to premature mitosis (Sorger and Murray, 1992). It has also been shown that checkpoint mutants segregate their chromosomes without entering mitosis as indicated by a lack of APC activation and Pds1 cleavage in checkpoint mutants (Bachant et al., 2005; Krishnan et al., 2004). It has been suggested that the DNA replication checkpoint controls spindle dynamics and centromere replication to create a bipolar spindle (Bachant et al., 2005; Krishnan et al., 2004; Liu et al., 2011). The high Cdk1 activity during DNA replication stress is essential to prevent the re-loading of replication forks and subsequent re-replication, which can lead to genomic instability (Kelly and Brown, 2000). Additionally, the activity of Clb5/Clb6-Cdk1 promotes sister chromatin cohesion during DNA replication stress that is independent of Pds1 activity (Hsu et al., 2011).

Mutants that are sensitive to HU-induced DNA replication stress fall into two categories, those that are checkpoint proficient and those that are checkpoint deficient. Mutants that are checkpoint proficient may be involved in recovery from HU arrest. The activity of Cdk1 is required for efficient recovery from HU arrest and prevention of mitotic catastrophe (Enserink et al., 2009). Additionally the Cdk1 inhibitor Swe1, accumulates during HU

response but is eventually hyperphosphorylated and degraded (Enserink et al., 2006). The ability to degrade Swe1 is an essential requirement for recovery from HU treatment and mutants defective in Swe1 degradation have elongated buds and a Swe1-dependent HU sensitivity (Liu and Wang, 2006; Matmati et al., 2009; Raspelli et al., 2011; Tripathi et al., 2011).

Mck1 is a *S. cerevisiae* GSK-3 protein kinase that has been identified in multiple genetic screens and thus has many known roles. Further characterization of its behavior during replication stress may have consequences for better understanding its human homologue GSK-3 that has been implicated in human cancers (Kang et al., 2008; Kastan and Bartek, 2004). There are three lines of evidence, which suggest Mck1 may be involved in the DNA replication checkpoint. Firstly, overexpression of *MCK1* rescues the HU sensitivity of the *spc24-9* kinetochore mutant. Secondly, along with established targets of the DNA replication checkpoint pathway such as *RNR1*, *MCK1* was identified in a screen for genes that rescued the lethality of the *rad53* and *mec1* checkpoint mutants. Thirdly, I have observed defects in replication of the *mck1*Δ strain during an unperturbed cell cycle as described in chapter 3.

The work presented here demonstrates that the kinase activity of Mck1 is required for cell viability during DNA replication stress, that *MCK1* deletion mutants are DNA replication checkpoint proficient, and that Mck1 is involved in proper recovery from HU treatment in a Swe1 independent manner.

4.2 Results

4.2.1 *MCK1* deletion mutants exhibit HU sensitivity.

To determine if the Mck1 protein kinase has a role in cell survival during DNA replication stress, I grew a *MCK1* deletion mutant strain (*mck1*Δ), wild type strain (WT) and the HU sensitive strain *spc24-9* in cultures and performed serial dilution assays on media with and without 0.1 M HU. Similar to the *spc24-9* mutant, the *mck1*Δ strain was unable to grow in the presence of 0.1 M HU (Figure 4-1A). I tested if the Mck1 catalytic activity or auto-phosphorylation site were required for HU viability by expressing the *MCK1* gene carrying point mutations on a plasmid in a *mck1*Δ strain (Rayner et al., 2002). The *MCK1* kinase dead (*pmck1D164A*) plasmid was unable to rescue the HU sensitivity of the *mck1*Δ strains (Figure 4-1B, compare *mck1*Δ *pmck1D164A* and *mck1*Δ *vector*), indicating that the Mck1 kinase activity is required for HU viability. In contrast, the auto-phosphorylation site (Y199) was not required for HU viability as the Y199 phosphorylation defective mutant (*pmck1Y199F*) was able to rescue the HU sensitivity (Figure 4-1B, compare *mck1*Δ *pmck1Y199F* and *mck1*Δ *vector*). Therefore, the Mck1 kinase activity, but not the tyrosine autophosphorylation of Mck1 on tyrosine 199, is required for viability during DNA replication stress induced by HU.

In order to determine if the *mck1*Δ strain is sensitive to additional forms of DNA stress, I performed a serial dilution assay with wild type, *mck1*Δ and the checkpoint mutant *mec1-1* on various concentrations of the DNA alkylating agent methyl methanesulfonate (MMS) and the topoisomerase I inhibitor camptothecin (CPT). MMS is an alkylating agent which causes the formation of N7- methylguanine and N3-methyladenine, that when encountered by replication forks can cause the formation of DNA double strand breaks and greatly slow the

replication fork (Groth et al., 2010; Vázquez et al., 2008). Like HU, MMS triggers the replication checkpoint. On the other hand, camptothecin (CPT) causes a checkpoint independent response. CPT inhibits through stabilization of the topoisomerase I (Topo I) complex, preventing the religation step, which results in a long-lived DNA-Topo I covalent complex. When a replication fork encouters such a lesion, DNA double strand breaks can occur which leads to fork collapse (Porter and Champoux, 1989). Although CPT-induced DNA damage can occur during S-phase, unlike HU and MMS induced DNA damage, the damage is not sensed and the arrest does not occur until G2/M (Redon et al., 2003). *MCK1* deletion mutants were only slightly sensitive to the highest concentration of MMS (Figure 4-1C). However, both the deletion mutant (*mck1*Δ) and the kinase dead allele (*mck1D164A-MYC*) were sensitive to CPT (Figure 4-1D). This is intriguing as HU, but not CPT, triggers the DNA replication checkpoint. *MCK1* deletion mutants are sensitive to particular genotoxic agents that suggest that its function is not directly linked to the DNA replication checkpoint nor is Mck1 part of a general genotoxic stress response.

4.2.2 The DNA replication checkpoint is functional in *mck1*Δ cells under HU stress.

The HU sensitivity of *mck1*Δ strains could be due to an inability of *mck1*Δ strains to arrest their cell cycle in response to HU stress. To determine if *MCK1* deletion mutants are DNA replication checkpoint proficient, I examined their morphology during HU treatment. Both wild type and *mck1*Δ strains arrested with large buds and undivided nuclei when treated with 0.1 M HU for 3 hours (Figure 4-2A). In contrast, mutants defective in the DNA replication checkpoint such as *mec1-1* failed to arrest and instead attempted to segregate their partially replicated DNA into the daughter cell (Figure 4-2A, (Krishnan et al., 2004)). It should be

noted that the percentage of *mck1*Δ cells that arrested in S/G2 with a large bud was lower than that of wild type (Figure 4-2B). However, this was not due to a defective checkpoint, as *mck1*Δ cells did not divide their nuclei as did the *mec1-1* cells, but instead, *mck1*Δ cells exhibited an increase in the G1 cell population (Figure 4-2B, G1: WT 0.75%, *mck1*Δ 22.55%, *mec1-1* 8.26%).

Strains that are not checkpoint proficient lose viability within a few hours of HU treatment as they attempt to divide their un-replicated chromosomes. I performed cell viability assays by treating wild type, *mck1*Δ and checkpoint defective *mec1-1* cells with 0.2 M HU for 0, 2, 3, 4, 5, 10 and 24 hours. I plated 50 cells on YPD plates and quantitated viability as the percentage of colonies in each mutant relative to wild type (Figure 4-2C). The checkpoint deficient cells (*mec1-1*) lost viability within 2 hours of HU treatment while *mck1*Δ cells did not start to lose viability until 8 hours of treatment and showed complete loss of viability after 24 hours (Figure 4-2C). Unlike checkpoint deficient cells, *mck1*Δ cells lose viability only upon prolonged exposure of HU.

Both the proper arrest morphology and viability upon short exposure (0-4 hours) of HU indicate that *MCK1* deletion mutants are checkpoint proficient. The activation of the DNA replication checkpoint results in the phosphorylation of the checkpoint protein Rad53 (reviewed in (Branzei and Foiani, 2009)). I examined Rad53 phosphorylation by analyzing the mobility shift of Rad53 in both wild type and *mck1*Δ strains upon HU exposure. Both wild type and *mck1*Δ demonstrated Rad53 phosphorylation upon HU exposure (Figure 4-2D). *MCK1* deletion mutants are checkpoint proficient and therefore Mck1 most likely does

not play a role in sensing replication defects and activation of the DNA replication checkpoint.

During the calcium stress response, mitosis is prevented through the action of Swe1 phosphorylating Cdk1-Y19 and thereby inhibiting Cdk1 activity. Swe1 itself is regulated by a series of kinases associated with the bud neck, which phosphorylate Swe1 thus targeting it for degradation. Upon calcium stress, Mck1 promotes the removal of one of these bud neck kinases, Hsl1, from the bud neck, therefore increasing Swe1 levels and preventing mitotic entry (Mizunuma et al., 2001). To determine if Mck1 played an equivalent role in response to HU, I examined the localization of both Hsl1 and the Cdc10 septin protein in HU treated cells. In response to HU, both Hsl1 and Cdc10 localized to the bud neck regardless of the presence or absence of *MCK1* (Figure 4-2E). My data confirms what has been previously reported; that the localization of Hsl1 does not play a role in mediating the HU response and the G2/M delay as seen in response to calcium (Liu and Wang, 2006). Furthermore, Mck1 does not have the same role in responding to calcium stress as it does in responding to DNA replication stress.

4.2.3 *MCK1* deletion mutants have defects in replication during HU treatment.

In an attempt to discover the cause of HU sensitivity of the *MCK1* deletion mutant, I monitored DNA replication in wild type and *mck1*Δ cells during HU treatment. During response to both 0.1 M and 0.2 M HU treatment, *mck1*Δ cells showed extended delays in replication when compared to wild type cells. With the lower concentration of HU (0.1 M), *MCK1* deletion mutants did not commence replication until about 4 hours of treatment

compared to 3 hours for wild type cells (Figure 4-3A). With the higher concentration of HU (0.2 M HU), even when wild type strains had almost completed replication by 8 hours of HU treatment, *mck1*Δ strains had not started replication. Instead, it appeared to take *mck1*Δ cells about 12 hours to complete replication (Figure 4-3B). To look at the role Mck1 may play in replication in more detail, I synchronized wild type and *mck1*Δ cells with mating factor and released into 0.2 M HU. While the wild type cell population showed a strong S/G2 accumulation at 60 minutes after release from mating factor, the same level of accumulation was lacking even after 120 minutes in *mck1*Δ cells (Figure 4-3C, S/G2 population). In the *mck1*Δ cell population, there was a larger proportion of cells that had not commenced replication as indicated by a lack of bud formation (Figure 4-3C, G1 population). This is similar to the phenotype observed in Figure 4-2B, where the *mck1*Δ strain shows an increased G1 population as compared to wild type. Mck1 appears to play a role in initiating or continuing replication during DNA replication stress.

4.2.4 *MCK1* is likely not involved in the transcriptional response to HU.

One of the ways that the DNA replication checkpoint maintains replication during replication stress is by inducing changes in the transcription profile to promote expression of genes involved in DNA replication and repair which are largely under control of the MBF transcriptional activator (as reviewed in (Branzei and Foiani, 2009)). A recent publication showed that in response to DNA replication stress, transcription from MBF-regulated promoters is induced. The induction is caused by checkpoint-dependent inhibition of Nrm1, an inhibitor of MBF activity (Travesa et al., 2012). As Nrm1 is regulated through phosphorylation and has a major effect on transcription during DNA replication stress, I wanted to determine if the Mck1 kinase played a role in Nrm1 inhibition. I hypothesized that

MCK1 deletion mutants would show an increased presence of Nrm1 on MBF promoters during HU treatment and that this caused the HU sensitivity. To test this I examined whether deletion of *NRM1* could rescue the HU sensitivity of *MCK1* deletion mutants. However, deletion of *NRM1* did not rescue *mck1*Δ strains' HU sensitivity (Figure 4-4A). In fact, removal of *NRM1* also caused sensitivity to HU, which is contradictory to findings in *S. pombe* (de Bruin et al., 2008). In conclusion, Mck1 does not play a role in Nrm1 regulation in response to DNA replication stress.

The Clb5 and Clb6 cyclins control Cdk1 activity during replication, and in response to HU treatment, they are both stabilized (Palou et al., 2010). To determine if Mck1 plays a role in Clb5 protein stability during HU response, I monitored the presence of endogenously tagged Clb5 in wild type and *mck1*Δ strains during HU treatment for four hours. Deletion of *MCK1* did not affect the stability of Clb5 over the time course (Figure 4-4B). The blot showed discrepancies in loading as indicated by the background band and thus cannot be used for fine qualitative comparisons between time points. The defects in replication observed in the absence of *MCK1* during HU response are not caused by the absence of the S-phase cyclin Clb5.

The action of *pGAL-MCK1* cannot compensate for DNA replication checkpoint mutants. *pGAL- MCK1* has been shown to weakly suppress both *mec1* and *rad53* lethality (Desany et al., 1998) as well as the *mec1-21* checkpoint defect during the DNA damage response induced by ssDNA at telomeres in the *cdc13-1* mutant (Searle et al., 2011). However, I was unable to demonstrate suppression of the HU sensitivity of either *mec1* or *rad53* mutants by

pGAL-MCK1 using a serial dilution growth assay (Figure 4-5). Instead, I found that overexpression of *MCK1* had a negative effect on the growth of *rad53-21* mutants (Figure 4-5). Since overexpression of *MCK1* cannot compensate for loss of the DNA replication checkpoint, it most likely that Mck1 does not have a role downstream of the DNA replication checkpoint that is a vital function of the checkpoint. This does not negate the possibility that *MCK1* could function downstream of the checkpoint but in a fashion that is unable to compensate for the loss of the checkpoint.

4.2.5 *MCK1* is required for proper recovery from the DNA replication checkpoint arrest.

MCK1 deletion mutants are checkpoint proficient as indicated by the viability upon short exposure to HU (Figure 4-2C), the proper arrest morphology (Figure 4-2A) and activation of Rad53 by phosphorylation (Figure 4-2D). Therefore, Mck1 may instead mediate recovery from the checkpoint arrest. I analyzed the recovery of wild type and *mck1*Δ strains from HU stress by treating cells with HU for three hours, washing the remaining HU away and resuspending cells in YPD. I monitored the cell cycle after HU wash out by analysis of DNA content by FACS. Both wild type and *mck1*Δ strains showed full arrest by three hours of HU treatment as indicated by a large 1N peak (Figure 4-6A, 180 minutes HU). By 60 minutes following HU treatment, most wild type cells had completed replication as indicated by the large 2N peak (Figure 4-6A, 60 minutes YPD). In contrast, *mck1*Δ cells are mid-way through DNA replication as demonstrated by the presence of both 1N and 2N peaks. After having completed replication, wild type cells subsequently divided their cells and accumulated 1N cells by 120 minutes (Figure 4-6A, 120 minutes YPD). *MCK1* deletion mutants despite an

accumulated 1N peak, maintained a large 2N peak throughout the rest of the time points (Figure 4-6A, 90-180 minutes YPD). This data suggests that following DNA replication stress, Mck1 promotes a timely cell cycle.

The mitotic Cdk1 inhibitor Swe1 has been shown to accumulate during HU response (Liu and Wang, 2006). In order for cells to recover from the transient arrest during HU treatment, Swe1 must be degraded (Enserink et al., 2006). In logarithmically growing cells, Swe1 is detected in both wild type and *mck1*Δ strains (Figure 4-6B). Upon four hours of HU treatment, Swe1 was no longer visible in the wild type cells, but maintained a strong presence in two *mck1*Δ strains (Figure 4-6B). The accumulation of Swe1 was not caused by mislocalization of Hsl1, as shown in Figure 4-2D. Interestingly, several genes involved in Swe1 degradation, including Hsl1, have been previously shown to be HU sensitive when mutated (Liu and Wang, 2006). Removal of *SWE1* was able to rescue these mutants and the authors proposed that the HU sensitivity of these mutants was due to elevated Swe1 levels preventing recovery from HU by inhibiting entry to mitosis (Liu and Wang, 2006). It is therefore a possibility that Mck1 may promote Swe1 degradation in response to HU, as well as calcium, which may explain the HU sensitivity in the *MCK1* deletion mutant. To see if the *mck1*Δ strain's HU sensitivity was due to high Swe1 levels, I examined the HU sensitivity upon removal of *SWE1* (Figure 4-6C). The *mck1*Δ*swe1*Δ double mutant was in fact more sensitive to HU than *mck1*Δ alone. Mck1 is involved in the degradation of Swe1 during HU treatment. This does not appear to be essential for preserving viability during DNA replication stress.

4.2.6 *MCK1*'s HU sensitivity is partially alleviated by removal of G1 cyclins.

Key cell cycle events are controlled by a variety of cyclins bound to the cyclin dependent kinase Cdk1. *MCK1* deletion mutants are synthetically lethal with *CLB5* deletion mutants (Ikui and Cross, 2009) and my studies in Chapter 3 demonstrated that Mck1 has a role in Clb2-Cdk1 inhibition. Therefore, I desired to know if *MCK1* showed any genetic interactions with cyclins during DNA replication stress. Growth of wild type (WT), cyclin mutants (*cyclin*Δ) and the double mutants (*cyclin*Δ*mck1*Δ) were analyzed by serial dilution assays with and without HU. Deletion of either the *CLN3* or *CLN2* G1 cyclins partially rescued the HU sensitivity of *mck1*Δ mutants, but removal of the G2 cyclins, *CLB3* or *CLB4* further enhanced *mck1*Δ's HU sensitivity (Figure 4-7A). This data suggests that the presence of Cln3-Cdk1 or Cln2-Cdk1 kinase activity is detrimental to cells lacking *MCK1* during replication stress whereas the presence of Clb3-Cdk1 or Clb4-Cdk1 is beneficial.

To further investigate the genetic interactions I utilized several cyclin overexpression plasmids (gifts from Mike Tyers) to examine the effect of overexpressing cyclins in *mck1*Δ strains. The plasmids were transformed into wild type and *mck1*Δ strains and serial dilution assays were performed on both dextrose (control) and galactose media. Overexpression of either *CLN3* or *CLN2* was detrimental, while overexpression of *CLN1* had no effect on the viability of *mck1*Δ strains either in the absence or presence of HU (Figure 4-7B). Both the B-type cyclins available for this study (*CLB2* and *CLB5*) were also detrimental to *mck1*Δ when overexpressed (Figure 4-7B). This data suggests that increasing the dosage of a subset of Cdk1 cyclins has a negative effect in cells lacking *MCK1*. The delays observed in replication in the absence of *MCK1* suggest that *MCK1* is a promoter of replication. The role

for Mck1 in promoting DNA replication may involve regulation of cyclin-Cdk1 activity during an unperturbed cell cycle and during the DNA replication checkpoint.

4.3 Discussion

4.3.1 A newly described role for Mck1 during HU induced DNA replication stress.

The discovery of a role for the Mck1 kinase in the DNA replication stress response caused by HU is in keeping with previously published works. It has been reported that *MCK1* is an overexpression suppressor of *rad53* and *mec1* deletion mutant lethality as well can mitigate the DNA damage stress response triggered by the *cdc13-1* mutant (Desany et al., 1998; Searle et al., 2011). I and members of the Measday lab previously identified *MCK1* as an overexpression suppressor of the HU sensitivity of the *spc24-9* kinetochore mutant (Ma et al., 2007). The work contained in this chapter is the first description of the requirement for the Mck1 kinase during HU induced DNA replication stress. There are five main findings in this work. Firstly, Mck1 kinase activity is required for cellular viability upon chronic exposure to HU (Figure 4-1B). Second, in response to HU, *mck1*Δ cells are DNA checkpoint proficient as indicated by viability upon short exposure to HU, wild type morphology, and Rad53 phosphorylation (Figure 4-2). Third, asynchronous *mck1*Δ cells have defects in replication upon acute exposure of HU (Figure 4-3A, 4-3B). Similarly, mating factor synchronized *mck1*Δ cells released into HU delayed in budding as compared to wild type (Figure 4-3C). Fourth, Mck1 does not influence Swe1 accumulation in HU arrested cells by way of Hsl1 delocalization from the bud neck, as it does in response to calcium (Figure 4-2E). Nor is the degradation of Swe1 an essential role for Mck1 during the DNA replication

checkpoint (Figure 4-6B, 4-6C). Lastly, the G1 cyclins *CLN3* and *CLN2* are partially responsible for the HU sensitivity of *mck1*Δ cells (Figure 4-7A).

4.3.2 Mck1's involvement in the HU response is most likely independent from its role in *cdc13-1* induced DNA damage.

Mck1 has been previously described as an inhibitor of the cAMP-dependent protein kinase (PKA) (Brazill et al., 1997; Rayner et al., 2002). The PKA complex is part of a nutrient sensing pathway utilized by the cell. Although direct binding and inhibition was observed between Mck1 and a catalytic subunit of the PKA complex (Tpk1), Mck1 was additionally determined to be required for the phosphorylation and relocalization of the PKA inhibitor, Bcy1 during heat stress (Griffioen et al., 2003; Rayner et al., 2002). At that time, relocalization of Bcy1 appeared to have no consequence towards the activity of PKA. Recently, PKA has been described to act in parallel with Chk1 and downstream to Mec1 in response to DNA damage caused by the *cdc13-1* mutant (Searle et al., 2004; Searle et al., 2011). This mutant strain causes a G2/M arrest that is characterized by large budded cells with undivided nuclei and high levels of Clb2 and Pds1. Proteins that regulate PKA, including Mck1, assist Mec1 in activating PKA towards Cdc20, thus inhibiting the APC^{Cdc20} and restraining mitosis (Searle et al., 2011). The authors go on to describe the ability of Mck1 to phosphorylate Bcy1 and the involvement of additional proteins in the relocalization of Bcy1 into the cytoplasm in response to DNA damage. Their findings suggest that Mck1 has a positive influence on PKA's activity, as *mck1*Δ cells, *bcy1* phosphorylation mutants and *tpk1*Δ cells behave similarly. This report raises the possibility that Mck1 may also act in a similar fashion within the context of HU stress. However, based of the data from Searle et al (Searle et al., 2011), MMS induces a phosphorylation on Bcy1, yet I did not observe the

*mck1*Δ strain to be as sensitive to MMS as HU (Figure 4-1). Additionally, the authors report a suppression of their *mec1* phenotype by overexpression of *MCK1*, which I did not observe during HU stress. During DNA damage response Mck1 plays a role in activating PKA and therefore inhibiting the APC^{Cdc20}. Accumulation of Cdc20 is observed in *cdc13-1* cells, but is not observed in HU treated wild type cells, therefore negating its need to be inhibited by Mck1-activated PKA (Clarke et al., 2003). This difference in Cdc20 accumulation is exemplified by work that shows that a target of APC^{Cdc20}, the microtubule motor protein Cin8, is capable of causing spindle elongation in HU treated cells when overexpressed, whereas it cannot during a *cdc13-1* DNA damage induced block (Krishnan et al., 2004). Most likely this inability to elongate the spindle is due to the presence of its inhibitor APC^{Cdc20} in *cdc13-1* cells but not in wild type HU treated cells. Additional experiments are required to determine if the PKA pathway has a role in HU response and if Mck1 functions through the PKA pathway to mediate DNA replication during HU treatment.

4.3.3 The requirement for Mck1 in HU response is independent of its role in Clb2-Cdk1 inhibition.

The inhibition of Clb2-Cdk1 by Mck1 as described in Chapter 3 does not appear to play a role in the S-phase DNA replication checkpoint, as removal of *CLB2* does not rescue HU sensitivity (Figure 4-7). Therefore, the high Clb2 levels that are observed post-mitosis in *mck1*Δ cells are of no consequence during HU response. In the M/G1 phase of the cell cycle, when Cdk1 activity is low, the pre-replication complex (pre-RC) is established at origins of replication. High Clb2-Cdk1 activity inhibits this process (Detweiler and Li, 1998). A possible consequence of high Clb2 levels in late mitosis as seen in *mck1*Δ cells could be a

delay in pre-RC establishment thus causing a delay in replication. However, it is important to note that if the replication delay observed in the *mck1*Δ strain is found to be dependent on *CLB2* and prevents pre-RC formation, this would still indicate that *MCK1* has an additional function in response to HU as the *CLB2* deletion does not rescue the *mck1*Δ strain's HU sensitivity.

4.3.4 Mck1 is involved in the promotion of replication.

DNA replication stress is not just caused by exogenous stresses such as HU but is a response provoked often during the normal progression of the cell cycle by endogenous cues (reviewed in (Branzei and Foiani, 2005)). Fittingly, I observed similar DNA replication defects in an unperturbed *mck1*Δ cell cycle (described in chapter 3) as I did during HU treatment of *mck1*Δ cells. It is unclear at this time whether Mck1 is involved in the initiation or maintenance of replication. Work from the lab of Fred Cross has established a genetic interaction between *MCK1* and *CLB5*. They confirmed synthetic lethality of the *mck1*Δ *clb5*Δ double mutant and further described synthetic lethality between *mck1*Δ and a mutation in the Clb5 binding domain of Orc6, *orc6-rxl* (Archambault et al., 2005; Ikui and Cross, 2009). Clb5 is known to be involved in triggering DNA replication as well as preventing re-replication (Schwob and Nasmyth, 1993; Wilmes et al., 2004). The Mck1 kinase may be involved in either preventing re-replication or triggering DNA replication in conjunction with *CLB5*.

4.3.5 The role of Mck1 in HU response is independent of its role in Swe1 degradation.

The work of Mizunuma *et al* (Mizunuma et al., 2001) revealed that in response to calcium stress, Hsl1 is delocalized from the bud neck in a *MCK1* dependent manner. The delocalization of Hsl1 is required for the G2/M arrest observed during calcium stress because Swe1 degradation is prevented, and thus Swe1 is free to inhibit mitotic Clb2-Cdk1 therefore producing a G2/M arrest. In response to HU induced replication stress, Swe1 also accumulates although its eventual degradation is required for recovery from the HU arrest (Enserink et al., 2006; Liu and Wang, 2006). Similar to arrest under calcium stress, the HU stress response also exhibited the hallmark signs of a G2/M arrest, a large bud and undivided nucleus. In *MCK1* deletion mutants Swe1 levels remain high after HU treatment, failing to diminish after 4 hours of treatment like wild type cells (Figure 4-6). Microscopy analysis revealed that stabilization of Swe1 is not due to delocalization of Hsl1 from the bud neck (Figure 4-2E). The increased level of Swe1 does not cause the HU sensitivity of *mck1*Δ strains since removal of *SWE1* does not rescue the HU sensitivity (Figure 4-6C). It is possible that *mck1*Δ strains only delay in Swe1 degradation and examining cells for a longer period of time would help elucidate this.

4.3.6 *CLN3* and *CLN2* are detrimental to *mck1*Δ cells.

The discovery that deletion of *CLN3* and *CLN2* but not *CLN1* can reduce *mck1*Δ HU sensitivity raises some interesting questions. Overexpression of either *CLN1* or *CLN2* has been previously described as reducing *RNR1* expression while their deletion increases *RNR1* expression (Vallen and Cross, 1999). This suggests that the rescue of *mck1*Δ strain's HU sensitivity by *CLN*2 deletion may be due to increasing *RNR1* expression and thus negating

the effects of HU. However, this does not take into account the inability of *CLN1* to rescue *mck1*Δ strains HU sensitivity, nor the effect of *CLN3*. Both the removal of *CLN3* and *CLN2* result in cells of larger size (Cross, 1988; Queralt and Igual, 2004). While the removal of *CLN3* delays the firing of replication origins (Barberis and Klipp, 2007), the removal of *CLN*2 delays bud emergence. The deletion of *CLN1* does not result in either a change in cell size, nor a cell cycle delay (Queralt and Igual, 2004). The specificity of the rescue of *mck1*Δ strains by the *CLN3* and *CLN2* deletions suggests that a delay at the beginning of the cell cycle is beneficial. This is interesting because *mck1*Δ cells exhibit a delay themselves. Perhaps *mck1*Δ cells acquire harmful lesions that are alleviated by a delay that permits more time for correction. Alternatively, Mck1 may regulate Cln3 or Cln2, in such a way that in the absence of Mck1, Cln3 or Cln2 are detrimental to the cell during HU response, and therefore their removal is beneficial. The detrimental effect of the overexpression of *CLN3* or *CLN2* in the presence or absence of HU supports either of these possibilities (Figure 4-7B). The involvement of these early G1 cyclins is additionally interesting as treatment with HU represses SBF-regulated transcripts, which includes *CLN2* (Travesa et al., 2012). Further studies are required to determine if the rescue of the *mck1*Δ strains growth defect by deletion of *CLN3* or *CLN2* is unique to HU and to explore the mechanism of their rescue.

This work has described a role for Mck1 in mitigating DNA replication stress. Further work is required to determine if Mck1 acts through known or novel pathways in this role, if Mck1 acts specifically in response to DNA replication stress, or has a role outside of the stress response in promoting DNA replication. Understanding the function of Mck1 during

replication stress may hold important insights to our understanding of the GSK-3 human homologue and its involvement in cancer development.

4.4 Materials and methods

4.4.1 Yeast strains, plasmids and media

Yeast strains and plasmids used in this study are described in Table 4-2. The wild type and *mck1*Δ strains were constructed in three different strain backgrounds - S288C/BY4742, S288C/YPH499 and W303. Figure 4-1 A, 4-1B, Figure 4-2 (A, B, C, D), Figure 4-3, Figure 4-5 and Figure 4-6 were all performed with S288C/YPH499 derived strains. For Figure 4-4A strains are all S288C/BY background. Figure 4-1C and 4-1D were performed with W303 strains. Genes were deleted or epitope tagged by using standard PCR-based homologous recombination yeast methods (Longtine et al., 1998). The plasmids with galactose inducible cyclins were generously provided by Dr. Mike Tyers and the *mck1D164A* and *mck1Y199F* plasmids were a gift from Dr. Jeremy Thorner. Standard methods for yeast culture and transformation were followed (Guthrie and R. Fink, 2004).

4.4.2 Yeast growth

Rich medium (YPD) and supplemental minimal medium (SC) were used (Amberg et al 2005). Cells were synchronized in G1 by mating factor (5 µg/ mL) for one hour, followed by another addition of mating factor (5 µg/ mL) for one hour. HU (Sigma- Aldrich) was stored in the -20 ˚C freezer at a 2 M concentration. Cells were treated with HU (Sigma-Aldrich) by growing in media containing either 0.1 M HU or 0.2 M HU. Dilution assays were performed by growing strains in either YPD [Figure 4-1(A, C, D), 4-4A, 4-6C, 4-7A] or minimal media

(Figure 4-1B, 4-5, 4-7B) to mid log phase. Serial dilutions were performed as described in chapter 3. CPT (Sigma-Aldrich) was diluted in DMSO to a stock concentration of 10 mM. MMS was from Sigma-Aldrich (64294 FLUKA).

4.4.3 Flow cytometry

Cells were fixed in 70% ethanol, 30% 1 M sorbitol overnight at 4 ˚C and processed for flow cytometry as described in chapter 3 before analysis with a Becton Dickinson FACScan machine and CellQuest software.

4.4.4 Microscopy

Cells were fixed in 3.7% formaldehyde for 10 minutes and processed for microscopy as described in chapter 3. Cells were imaged on a Zeiss Colibri LED illuminator with a Zeis Axiocam Ultra High Resolution Monochrome Digital Camera Rev3.0 and processed using Image J and Adobe Photoshop software. Graphs were produced using Numbers ’09 software (Apple Inc).

4.4.5 Western blots

Cells were grown to between OD_{600nm} 0.4 and 1.0, pelleted and supernatant removed. The cell pellet was lysed and equivalent protein amounts loaded per lane. The Rad53 protein was detected with anti-Rad53 antibody [Santa Cruz (yC19): sc6749]. Secondary antibody detection was performed with bovine anti-goat IgG-HRP. The Myc epitope tagged Clb5 protein was detected with anti-myc antibody. The Swe1protein was detected by anti-Swe1 antibody [Santa Cruz (y-311)].

Table 4-1 Yeast strains used in this study.

Strain	Genotype	Source
YJM561	BY4742/S288C, MATα *ura3Δ::NAT^{R}can1Δ::STE2pr-Sp_HIS5 lyp1Δ his3Δ1 leu2Δ0 ura3Δ0 met15Δ0 LYS2+*	Brenda Andrews, (Tong et al., 2001)
YJM562	BY4742/S288C, MATα *YNL307CΔNatR can1Δ::STE2pr-Sp_his5 lyp1Δ his3Δ1 leu2Δ0 ura3Δ0 met15Δ0 LYS2+*	Brenda Andrews (Tong et al., 2001)
YM1761	YPH499/S288C, MATa *his3Δ200 ade2-101 ura3-52 lys2-801 leu2Δ1 trp1-Δ63*	Phil Hieter
YJM336	YPH499/S288C, MATa *his3Δ200 ade2-101 ura3-52 lys2-801 leu2Δ1 trp1-Δ63, mck1Δ::KanMX6*	This study
YM2169 (DK186)	W303, MATa *leu2-3, 112 trp1-1 can1-100 ura3-1 ade2-1 his3-11,15 GAL+ bar1*	Doug Kellogg
YJM1155	W303, MATa *leu2-3, 112 trp1-1 can1-100 ura3-1 ade2-1 his3-11,15 GAL+ bar1 mck1:KanMX6*	This study
YJM1157	W303, MATa *leu2-3, 112 trp1-1 can1-100 ura3-1 ade2-1 his3-11,15 GAL+ bar1 MCK1-13myc:KanMX6*	This study
YJM1243A	W303, MATa *leu2-3, 112 trp1-1 can1-100 ura3-1 ade2-1 his3-11,15 GAL+ bar1 mck1D164A-13-myc*	This study
YVM1380	YPH499/S288C, MATa *his3Δ200 ade2-101 ura3-52 lys2-801 leu2Δ1 trp1-Δ63, spc24-9::KanMX6*	(Montpetit et al., 2005)
YLM53	YPH499/S288C, MATα *mec1-1 ura, trp1*	(Weinert et al., 1994)
YJM31	BY/ S288C, MATa *CDC10-GFP-HIS3MX his3Δ1 leu2Δ0 ura3Δ0 met15Δ0*	Brenda Andrews GFP collection
TBA [A]	YPH499/BY/S288C, MATa *CDC10-GFP-HIS3MX mck1ΔKanMX*	This study
YJM1215A	BY/ S288C, MATa *his3Δ1 leu2Δ0 ura3Δ0 met15Δ0, ura3Δ::NAT^R, HSL1-GFP-HIS3MX*	This study
YJM1217A	BY/S288C, MATa *his3Δ1 leu2Δ0 ura3Δ0 met15Δ0,* HSL1-GFP-*HIS3MX* mck1Δ*NAT^R*	This study
YJM764A	S288C/BY4742, MATa *his3Δ1 leu2Δ0 lys2Δ0 ura3Δ0 nrm1ΔkanMX6*	Open biosystems
YJM762A	S288C/BY4742, MATa *his3Δ1 leu2Δ0 lys2Δ0 ura3Δ0 nrm1ΔkanMX6 mck1ΔNAT^R*	This study
YJM1078A	W303, MATa *ura3Δ, trp1-1, ade2-1, his3-11, 15 Leu2-3 CLB5-9MYC:TRP*	This study
YJM1076A	W303, MATa *ura3Δ, trp1-1, ade2-1, his3-11, 15 Leu2-3 CLB5-9MYC:TRP, mck1ΔKAN*	This study
YLM438	W303, MATa*, Rad53-21, can1-100, his3-11, 15, ade2-1, trp1-1, ura3-1, leu2-3, 112*	Jeff Bachant (Desany et al., 1998)
YJM881A	BY4741/S288C, MATa *his3Δ1 leu2Δ0 met15Δ0 ura3Δ0 ura3Δ::NAT^R cln3ΔkanMX*	Open biosystems
YJM879A	BY4741/S288C, MATa *his3Δ1 leu2Δ0 met15Δ0 ura3Δ0 cln3ΔkanMX mck1ΔNAT^R*	This study

Strain	Genotype	Source
YJM945A	BY4741/S288C, MATa *his3Δ1 leu2Δ0 met15Δ0 ura3Δ0 ura3Δ::NAT^R cln1ΔkanMX*	Open biosystems
YJM947A	BY4741/S288C, MATa *his3Δ1 leu2Δ0 met15Δ0 ura3Δ0 cln1ΔkanMX mck1ΔNAT^R*	This study
YJM949A	BY4741/S288C, MATa *his3Δ1 leu2Δ0 met15Δ0 ura3Δ0 ura3Δ::NAT^R cln2ΔkanMX*	Open biosystems
YJM951A	BY4741/S288C, MATa *his3Δ1 leu2Δ0 met15Δ0 ura3Δ0 cln2ΔkanMX mck1ΔNAT^R*	This study
YJM875A	BY4741/S288C, MATa *his3Δ1 leu2Δ0 met15Δ0 ura3Δ0 ura3Δ::NAT^R clb6ΔkanMX*	Open biosystems
YJM877A	BY4741/S288C, MATa *his3Δ1 leu2Δ0 met15Δ0 ura3Δ0 clb6ΔkanMX mck1ΔNAT^R*	This study
YJM892A	BY4741/S288C, MATa *his3Δ1 leu2Δ0 met15Δ0 ura3Δ0 ura3Δ::NAT^R clb2ΔkanMX*	Open biosystems
YJM887A	BY4741/S288C, MATa *his3Δ1 leu2Δ0 met15Δ0 ura3Δ0 clb2ΔkanMX mck1ΔNAT^R*	This study
YJM953A	BY4741/S288C, MATa *his3Δ1 leu2Δ0 met15Δ0 ura3Δ0 ura3Δ::NAT^R clb3ΔkanMX*	Open biosystems
YJM955A	BY4741/S288C, MATa *his3Δ1 leu2Δ0 met15Δ0 ura3Δ0 clb3ΔkanMX mck1ΔNAT^R*	This study
YJM1080	BY4741/S288C, MATa *his3Δ1 leu2Δ0 met15Δ0 ura3Δ0 ura3Δ::NAT^R clb4ΔkanMX*	Open biosystems
YJM1082	BY4741/S288C, MATa *his3Δ1 leu2Δ0 met15Δ0 ura3Δ0 clb4ΔkanMX mck1ΔNAT^R*	This study

[A] These strains were created by mating a BY4742 strain to a YPH499 strain hence the precise genotype is not known.

Table 4-2 Plasmids used in this study.

Plasmid Name	Plasmid	Description	Source
BVM387/ MTID277	*2μ vector*	*pRS426: URA3 Amp*	Mike Tyers
BVM388/PMT41	*CLN3-HA*	*2μ, pGAL-CLN3: URA3*	Mike Tyers
BVM389/MTID273	*GAL-vector*	*pRS316, CEN, URA3*	Mike Tyers
BVM390/MTID485	*pGAL-CLN1*	*pGAL-CLN1-HA3, CEN, URA3*	Mike Tyers
BVM391/ MTID634	*pGAL-CLN2*	*pGAL-CLN2-HA, CEN, URA3*	Mike Tyers
BVM392/ MTID549	*pGAL-CLB2*	*pGAL10-CLB2-3HA, CEN, URA3*	Mike Tyers
BVM393/MTID550	*pGAL-CLB5*	*pGAL10-CLB5-3HA, CEN, URA3*	Mike Tyers
BLM21	*pMCK1*	*pRS202, 2μ, URA3, chrXIV 52447-58767 insert into BAMH1/BglII*	Lina Ma
BVM178/ pTRY MD164A MCK1	*pmck1D164A*	*pmck1D164A*	Jeremy Thorner (Rayner et al., 2002)
BVM180/ pTRYMUY199F	*pmck1Y199F*	*pmck1Y199F*	Jeremy Thorner (Rayner et al., 2002)
BVM245	*pGAL-MCK1:LEU*	*P415, CEN6/AMP/LEU GAL-MCK1*	This study

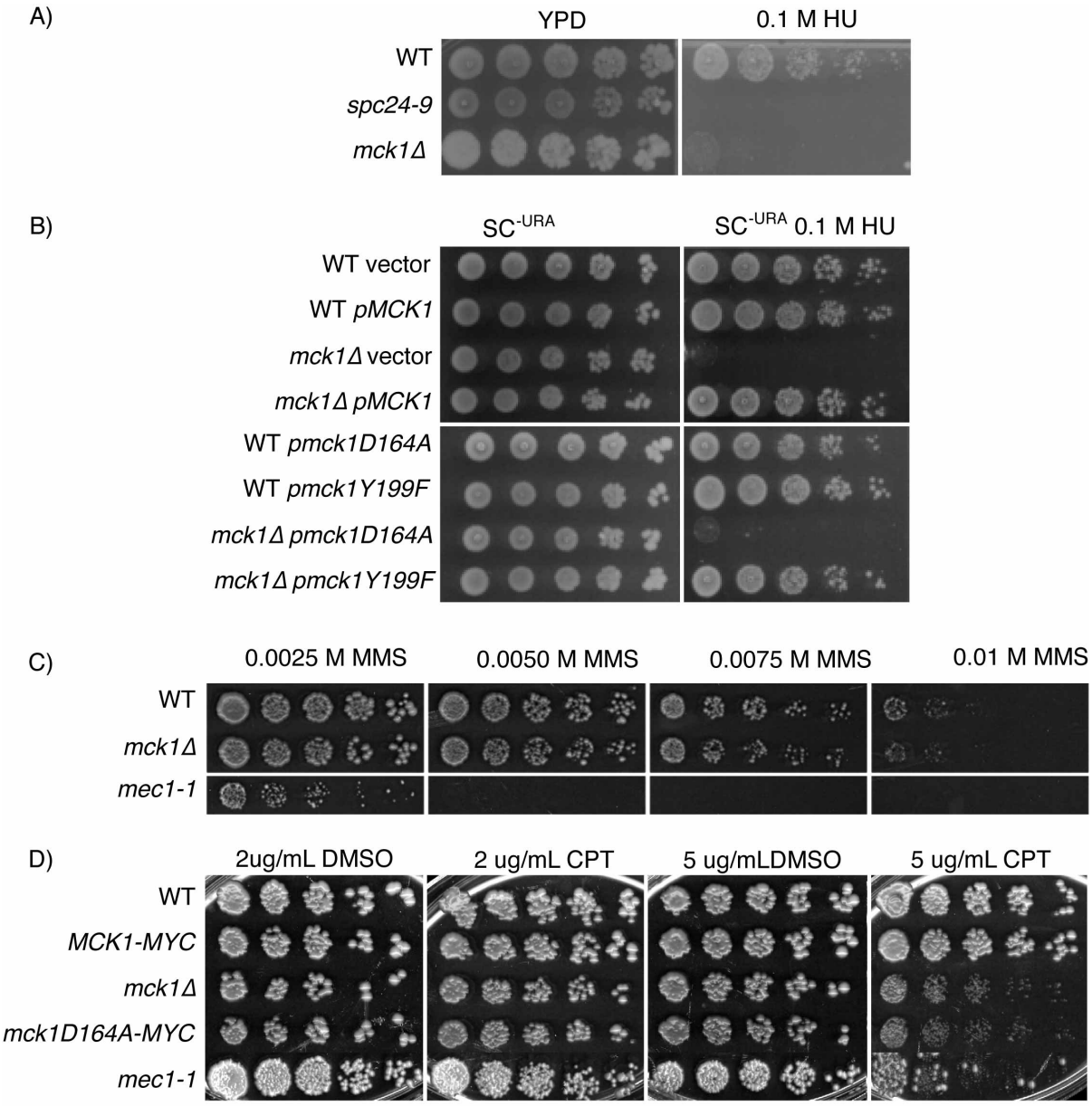

Figure 4-1 *MCK1* deletion mutants are sensitive to a subset of genotoxic stresses

The growth of various *MCK1* mutants on HU, MMS and CPT plates was compared to the HU sensitive strains, *spc24-9* and *mec1-1* by serial dilution assays at 30 ˚C. A) Wild type (*WT*), *MCK1* deletion mutant (*mck1*Δ) and the kinetochore mutant *spc24-9*, were grown on YPD and 0.1 M HU. B) Expression of active *MCK1* (*pMCK1*), kinase dead *MCK1* (*pmck1D164A)*, *MCK1* auto-phosphorylation site mutant (*pmck1Y199F*) or vector alone (vector) in WT or *mck1*Δ strains on SC^{-URA} or SC^{-URA} 0.1M HU plates. C) The growth of *WT*, *mck1*Δ and *mec1-1* strains on various concentrations of MMS. D) Growth compared between strains with wild type Mck1 function (*WT*, *MCK1myc*) and two mutant mck1 strains [*MCK1* deletion mutant (*mck1*Δ) and the catalytically dead strain (*mck1D164A-MYC*)] on various concentrations of CPT. DMSO is the negative control for CPT.

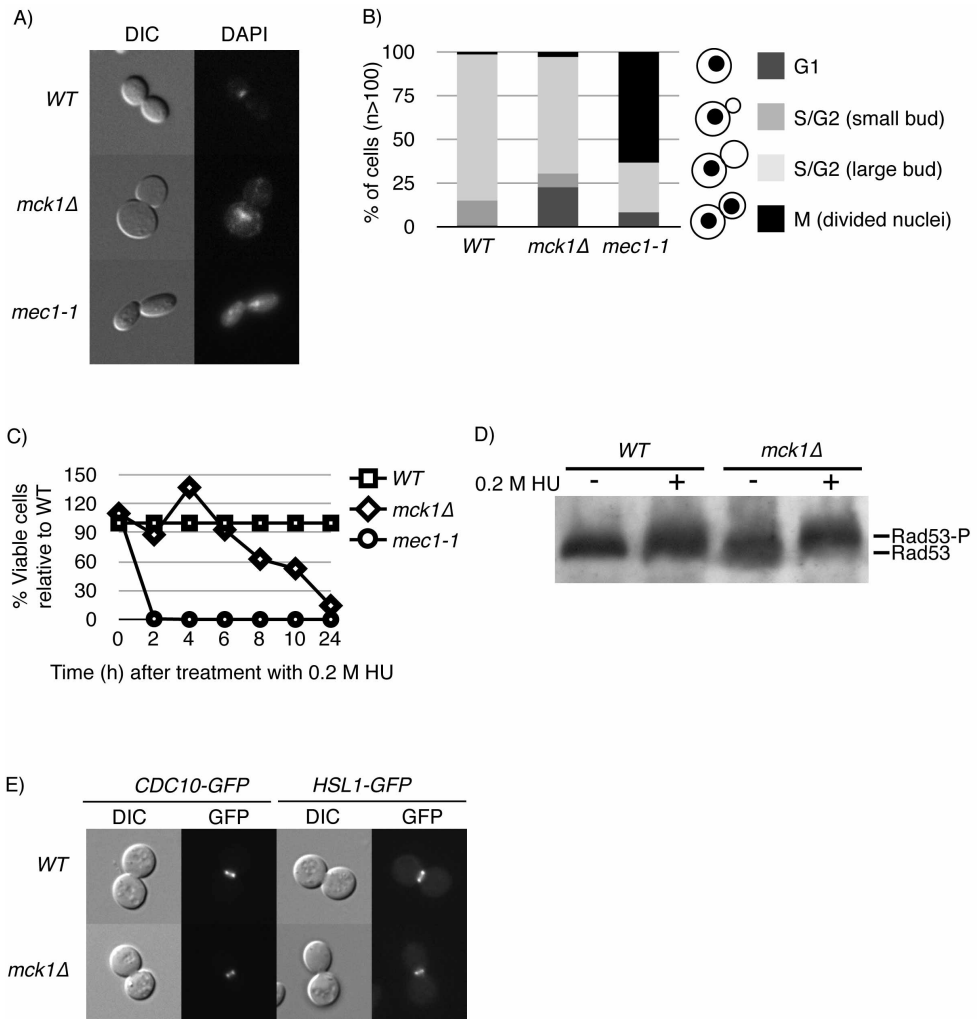

Figure 4-2 *MCK1* deletion mutants are DNA replication checkpoint proficient in response to HU stress.

A) *WT*, *mck1*Δ and *mec1-1* strains were treated with 0.1 M HU for 3 hours at 30˚C, fixed and stained with DAPI before examination by microscopy. B) The cell populations from the samples in (A) were counted and expressed as a percentage of total cell counts. C) *WT*, *mck1*Δ and *mec1-1* strains were treated with 0.2 M HU in liquid culture and every 2 hours 50 cells were plated onto YPD. The percentage of colonies relative to WT are represented. D) Western blot analysis of Rad53 phosphorylation in *WT* and *mck1*Δ strains treated with (+) and without (-) 0.2 M HU for 5 hours. Western blots were probed with Rad53 antibody. E) *WT* and *mck1D* strains carrying endogenously tagged *CDC10-GFP* and *HSL1-GFP* were imaged after treatment with 0.2 M HU for 5 hours.

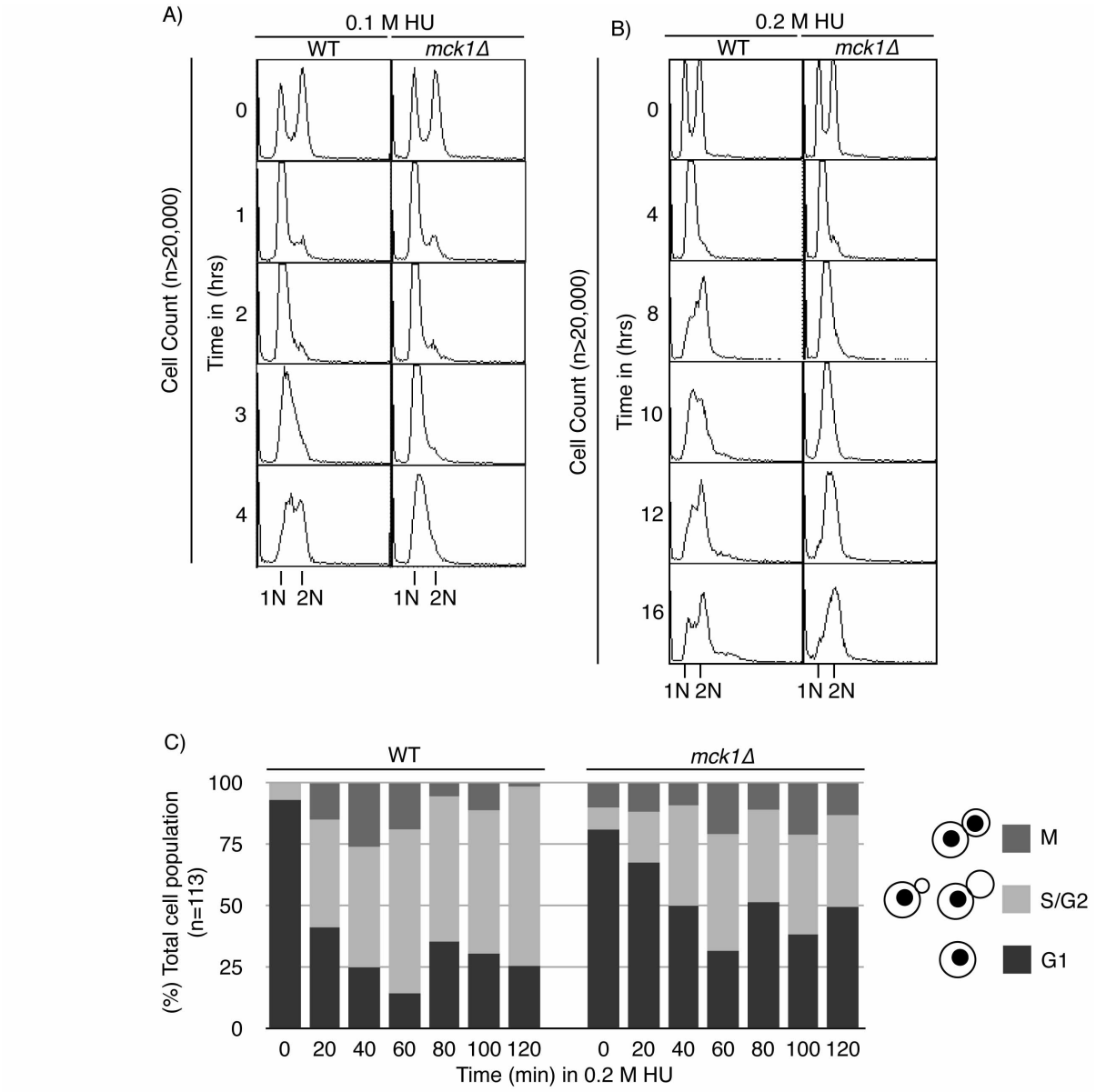

Figure 4-3 *MCK1* is required for the proper timing of replication during DNA replication stress.

A) *WT* and *mck1*Δ cultures were treated with 0.1 M HU and samples were taken for FACS analysis every hour for four hours. B) *WT* and *mck1*Δ cultures were treated with 0.2 M HU and samples taken for FACS analysis at 4, 8, 10, 12 and 16 hours. C) *WT* and *mck1*Δ strains were synchronized with mating pheromone and released into 0.2 M HU. Samples were taken every 20 minutes for 2 hours following release from HU arrest for microscopy analysis.

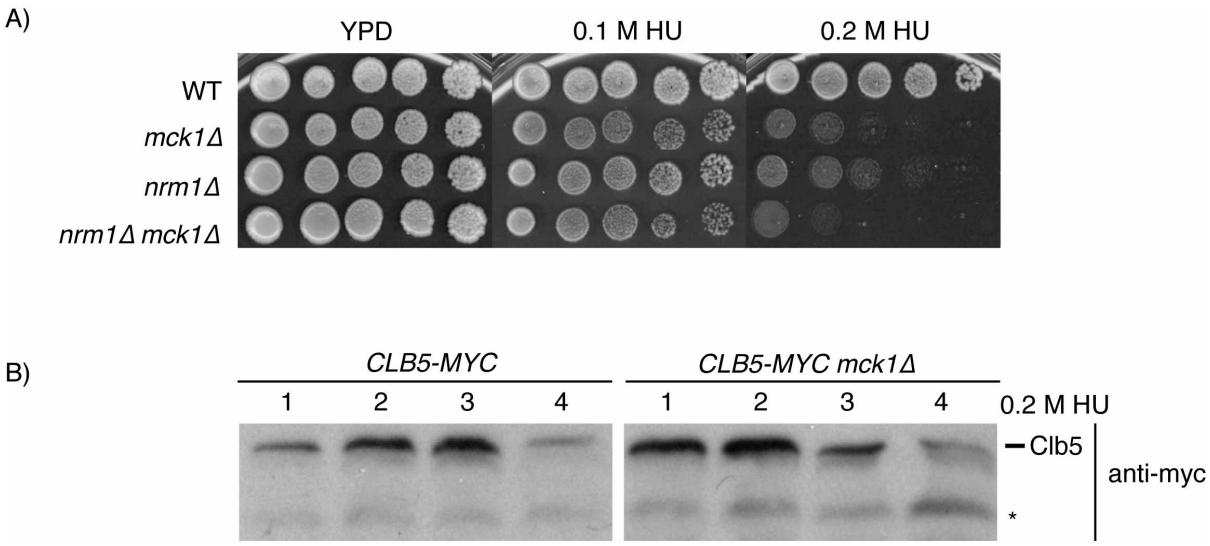

Figure 4-4 The *mck1*Δ mutant sensitivity to HU is not caused by the action of Nrm1 or lack of the Clb5 cyclin.

A) Growth analysis by serial dilution of wild type, *mck1*Δ, *nrm1*Δ and *nrm1*Δ*mck1*Δ strains on various concentrations of HU. B) Western blot analysis of endogenously tagged *CLB5-MYC* expressed in the presence or absence of *MCK1* during treatment with 0.2 M HU over four hours. Asterisk (*) indicates background band.

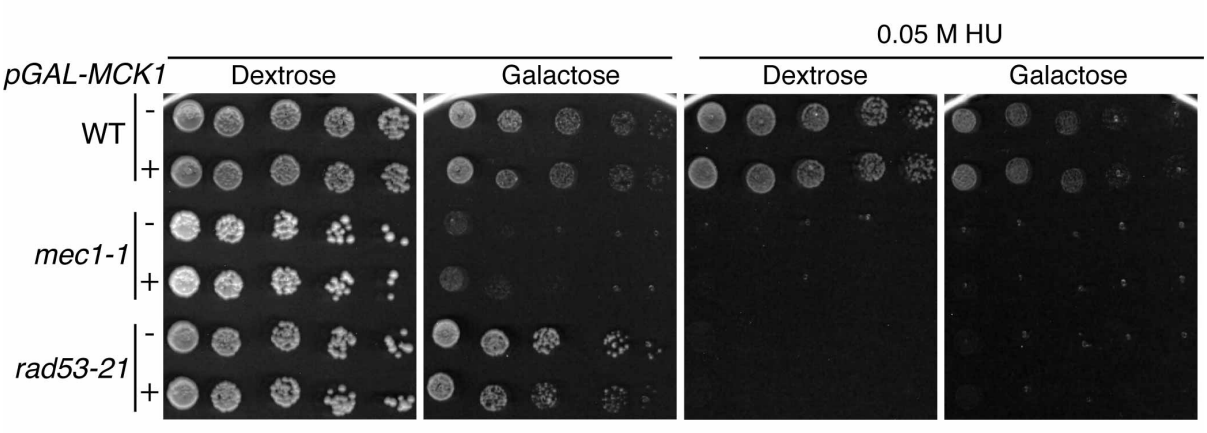

Figure 4-5 Over expression of *MCK1* cannot rescue the HU sensitivity of the *mec1-1* and *rad53-21* checkpoint mutants.

pGAL-MCK1 (+) or vector alone (-) was transformed into wild type, *mec1-1* and *rad53-21* strains and plated on repressing (dextrose) or inducing (galactose) media with and without HU.

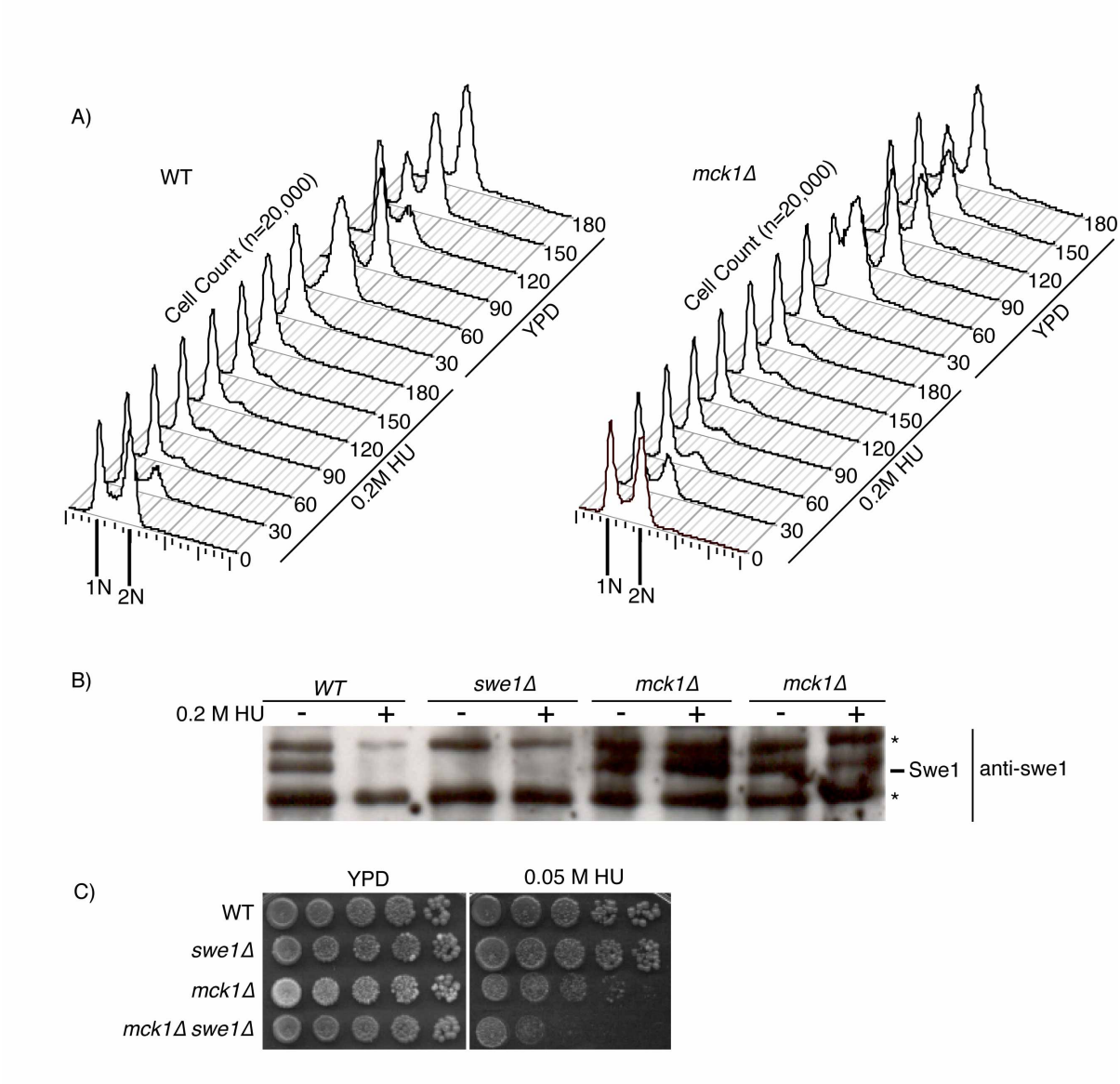

Figure 4-6 *MCK1* deletion mutants show defects in recovery from HU treatment.

A) WT and *mck1*Δ asynchronous cultures were treated with 0.2 M HU for 3 hours. HU was washed out and cultures released into fresh YPD. Samples were taken every 30 minutes for 3 hours and processed for FACS analysis. B) Western blot analysis of Swe1 protein levels in WT and *mck1*Δ strains with and without 0.2 M HU treatment for four hours. Anti-Swe1 (Santa Cruz) antibody was used to detect Swe1. *SWE1* deletion strain was used as a control for Swe1 protein detection. The asterisk (*) represents background bands. C) The growth of *WT, mck1*Δ*, swe1*Δ, and the double mutant *swe1*Δ*mck1*Δ was compared on 0.05M HU plates.

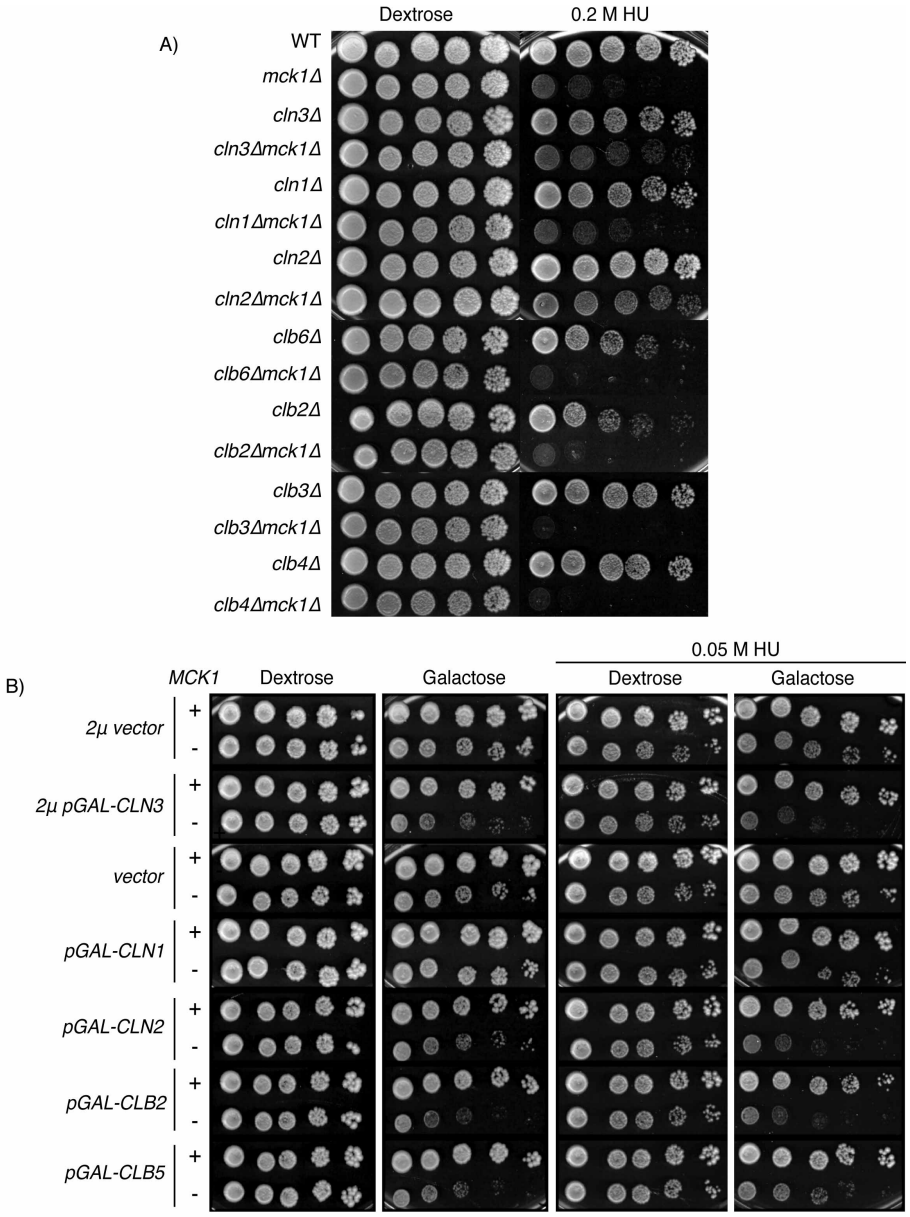

Figure 4-7 G1 cyclins are partially responsible for the HU sensitivity of *mck1*Δ strains.

A) The growth of wild type, *mck1*Δ, cyclin mutants (*cyclin*Δ) and the double mutants (*cyclin*Δ*mck1*Δ*)* was monitored with and without 0.2 M HU by serial dilution assay. B) Indicated plasmids were transformed into wild type (+ *MCK1*) and *MCK1* deletion mutants (- *MCK1*) and serially diluted onto dextrose and galactose medium with and without 0.05 M HU. The 2μ vector is the negative control for *pGAL-CLN3*, while vector is the negative control for *pGAL-CLN1*, *pGAL-CLN2*, *pGAL-CLB1*, *pGAL-CLB5*.

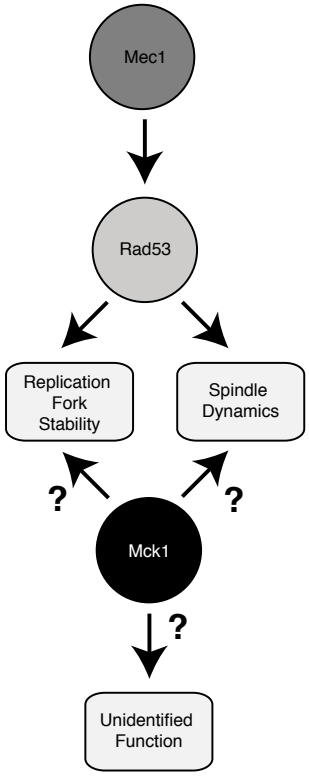

Figure 4-8 Model suggesting Mck1 role in the DNA replication checkpoint.

DNA replication stress triggers the checkpoint proteins Mec1 and Rad53, which amongst other roles, stabilize the replication fork and regulate spindle dynamics. Mck1 may play a role in replication fork stability as *mck1*Δ mutants exhibit replication delays. Overexpression of *MCK1* rescues spindle elongation of *spc24-9* mutants. Additional roles of Mck1 may include regulation of cyclin-Cdk1 regulation as deletion of *CLN3* and *CLN2* rescue *mck1*Δ strains HU sensitivity.

Chapter 5: Conclusion

5.1 Summary and perspectives

During DNA replication stress in *S. cerevisiae*, slowly replicating chromosomes must not be prematurely separated. In Chapter 2, I present work performed by Dr. Ma, Dr. Measday and myself that identified a particular kinetochore mutant (*spc24-9*) that, similar to DNA replication checkpoint mutants, fatally elongated its spindle during HU-induced DNA replication stress. Spindle elongation in DNA replication checkpoint mutants, such as *mec1* or *rad53* strains, occurs without the hallmark signs of mitosis such as activation of the APC or cohesin cleavage, suggesting an alternative means of spindle expansion (Bachant et al., 2005; Krishnan et al., 2004). A role for the kinetochore in prevention of spindle expansion during HU treatment had been previously mentioned (Bachant et al., 2005). Additionally, the DNA replication checkpoint had been suggested to regulate the levels of microtubule motor proteins such as Stu2 and Cin8 during HU treatment (Krishnan et al., 2004). Using a high copy suppressor screen several genes such as *MCK1* and a truncated version of *STU2,* were identified that could alleviate HU sensitivity and restrain spindle expansion in *spc24-9* cells. Interestingly, we found that when we combined a mutation in *STU2* (*stu2-10)* with *spc24-9*, spindle expansion was also restrained suggesting that the truncated version of *STU2* was acting in a dominant negative manner. Previous studies had localized Stu2 to the kinetochore during metaphase and the cytoplasmic side of the SPB and along the spindle MT's during anaphase (He et al., 2001; Kosco et al., 2001). Our study identified the localization of Stu2 to the kinetochore early in the cell cycle. As well, we found that Stu2 localization was dependent on functional Spc24 during an unperturbed cell cycle and during HU treatment. We also showed an inverse correlation between Stu2 spindle localization and spindle length.

After an hour of HU treatment, *spc24-9* mutant cells exhibited a diffuse Stu2 signal along the spindle of both short and long spindles, while in wild type cells Stu2 formed discrete foci. Through live cell imaging, we determined that the spindles of *spc24-9* mutants had a net expansion, but exhibited oscillations and demonstrated a loss of Stu2 from the spindle during HU treatment. It had been suggested that the DNA replication checkpoint prevents spindle elongation through ensuring bipolar attachment (Bachant et al., 2005). We were able to show that the *spc24-9* mutant exhibited wild type kinetics in attaining bipolar attachment during HU treatment. This suggested that spindle elongation is not prevented solely through establishment of a bipolar spindle.

Our identification of *MCK1* as a high copy suppressor of *spc24-9* lethality upon HU treatment, sparked further inquiry into its role in both DNA replication stress and cell cycle regulation in unperturbed conditions. The work presented in Chapter 3 describes the inhibition of the mitotic Clb2-Cdk1 complex by Mck1. This is of interest as the human GSK-3 protein kinases have been implicated in the degradation and reduced expression of a G1 cyclin, cyclin D1 (Takahashi-Yanaga and Sasaguri, 2008). Therefore, identification and dissection of similar functions in *S. cerevisiae* confirms homologous roles for the yeast and human GSK-3 kinases. Strains that are mutated for genes that regulate the degradation (*APC* mutants) or inhibition (*sic1*Δ) of Clb2-Cdk1 upon exit from mitosis are highly sensitive to increased levels of Clb2 and demonstrate persistent levels of Clb2 at the exit from mitosis (Cross et al., 2005; Kramer et al., 1998; Schwab et al., 1997; Toyn et al., 1997). Cells devoid of *MCK1* exhibit both of these phenotypes. Additionally, I have shown that Mck1 can co-immunoprecipitate with Clb2 and inhibit Clb2-Cdk1 activity *in vitro*. Known inhibitors of

Clb2-Cdk1 such as Cdh1 and Sic1 have been shown to both physically interact with Clb2 through co-immunoprecipitations (Archambault et al., 2004; Schwab et al., 2001). Addition of Sic1 to Clb2 IP's was also shown to reduce Clb2-Cdk1 activity (Schwob et al., 1994). Lastly, I demonstrated that overexpression of *MCK1* results in elongated buds, which is a hallmark sign of Clb2-Cdk1 inactivation (Barral et al., 1999). Mck1 has been previously identified during calcium stress as hindering the activity of Clb2-Cdk1 at G2/M through increased activation of Swe1 (Mizunuma et al., 2001). My work demonstrates a novel function for Mck1 in regulating Clb2-Cdk1 activity during an unstressed cell cycle that has implications not at G2/M but during mitotic exit. I was also able to show a physical interaction between Mck1 and Mih1, as well as reduced phospho-isoforms of Mih1 in the absence of *MCK1*. I was unable to show direct phosphorylation of Mih1 by Mck1. It has been previously noted that Clb2-Cdk1 can alter the phosphorylation status of Mih1, therefore I suspect that the effect of Mck1 on Clb2 activity can thus alter the Mih1 phospho-isoforms (Pal et al., 2008).

Previous reports have identified *MCK1* as an overexpression rescuer of the lethality of *mec1* and *rad53* DNA replication checkpoint mutants (Desany et al., 1998). In Chapter 4, I explored the role of Mck1 during HU-induced DNA replication stress. I found that the catalytic activity, but not the activation loop phosphorylation (auto-phosphorylation site), of Mck1 was required for viability on HU plates. I determined that *mck1*Δ cells are checkpoint proficient as they respond in a wild type manner to HU stress. HU sensitive mutants that are checkpoint proficient, such as *mck1*Δ, are most likely involved in the recovery from HU stress and include proteins that are required to establish bipolar attachment or degrade the

mitotic Clb2-Cdk1 inhibitor Swe1 (Enserink et al., 2006; Liu et al., 2011; Liu and Wang, 2006; Raspelli et al., 2011). I described a delay in replication during replication stress and following release from replication stress in *mck1*Δ cells. It is unknown at this time if the delay in replication observed in *mck1*Δ cells is the cause of the HU sensitivity. The replication delay is not specific to treatment with HU, as I also described a replication delay in *mck1*Δ mutants during an unperturbed cell cycle in Chapter 3. In *S. pombe*, *orp1-4* and *sna41-928* (*ORC1* and *CDC45* respectively) mutants show reduced replication and when combined with checkpoint mutants increase the checkpoint mutants sensitivity to replication stress (Nitani et al., 2006). Therefore, it is plausible that Mck1 has a role in establishing or maintaining replication and that this function is important for resuming replication after replication stress. During replication stress, cells arrest with high levels of Swe1, but eventually require degradation of Swe1 to resume their cell cycle (Enserink et al., 2006; Liu and Wang, 2006). Although *mck1*Δ cells demonstrated above wild type levels of Swe1 during an HU block, I found that the lethality of *mck1Δ* cells on HU plates is not due to the presence of Swe1. In response to calcium Mck1 is required for Hsl1 delocalization from the bud neck and therefore subsequent increase in Swe1 levels. I dismissed the possibility that Mck1 regulates Swe1 levels in HU in a manner similar to its mechanism in response to calcium stress, as Hsl1 maintains its localization at the budneck during HU treatment, and *mck1*Δ cells exhibit an increase in Swe1, not a decrease as would be expected. Interestingly, the HU sensitivity of *mck1*Δ mutants appeared to be partially dependent on the presence of *CLN3* and *CLN2* as their deletion partially rescues the HU sensitivity of *mck1Δ* strains. *CLN3* is the yeast homologue of cyclin D1, which is targeted for degradation by the activity of GSK-3 kinases (Takahashi-Yanaga and Sasaguri, 2008). Thus, it is reasonable that Mck1

could inhibit Cln3 and/or Cln2, and that increased Cln2-Cdk1 or Cln3-Cdk1 activity results in the HU sensitivity of *mck1Δ* strains. It is not clear how increased levels of Cln3 or Cln2 in the absence of *MCK1* would delay replication. This description of Mck1's role in the DNA replication checkpoint provides a foundation for more in depth study.

5.2 Future directions

5.2.1 Does Mck1 restrain spindle expansion in *spc24-9* mutants through regulation of microtubules?

The identification of *MCK1* as a high copy suppressor for *spc24-9* mutant cells, begs the question, by what mechanism does Mck1 rescue the kinetochore mutant? One hypothesis is that *MCK1* rescues *spc24-9* through regulation of spindle dynamics. The *spc24-9* mutant cells were shown to elongate their spindle in correlation with mislocalized Stu2. The human GSK-3 protein kinases have been shown to mediate phosphorylation of the microtubule stabilizing protein, tau (reviewed in (Hernández et al., 2009)). Hyper-phosphorylated tau is unable to bind microtubules and forms aggregates of microtubules which have been found in neuronal cells of Alzheimer's patients (reviewed in (Cohen and Frame, 2001)). The yeast Mck1 kinase can also phosphorylate purified tau protein *in vitro* (Lim et al., 1993). Although yeast lack a protein with shared homology to tau they do possess several microtubule stabilizing proteins such as Stu2 (Kosco et al., 2001). Examination of Stu2 localization upon *MCK1* overexpression in *spc24-9* cells would allow us to determine if *MCK1* rescued the *spc24-9* phenotype through promoting Stu2 association with the kinetochore. Interestingly, *MCK1* is required for viability in the absence of the microtubule plus end binding protein Bim1 or the microtubule motor proteins Cin8 or Kar3 (Pan et al., 2004; Tong et al., 2001;

Tong et al., 2004). This suggests that Mck1 may indeed play a role in regulating spindle dynamics in yeast. As the above genetic interactions were determined through high throughput techniques they would need to be confirmed. Thorough monitoring of spindle dynamics by live cell analysis in the absence of *MCK1* would be of great interest to gain insight into its possible role in regulating spindle dynamics.

5.2.2 Does Mck1 restrain spindle expansion in *spc24-9* mutants through reduction of PKA activity?

Recent work by the Measday lab has determined that *spc24-9* mutants trigger the PKA pathway (Ma et al., 2012 (in final revisions)). Their work has also shown that overexpression of inhibitors of the PKA pathway such as *BCY1* and *PDE2* improves viability of *spc24-9* mutants. Mck1 has a documented role in inhibition of the PKA pathway, therefore it is probable that overexpression of *MCK1* rescues *spc24-9* cells due to inhibition of the PKA pathway (Brazill et al., 1997; Rayner et al., 2002). If Mck1 and Bcy1 both function to inhibit PKA, their combined phenotype should not show synergistic growth effects. This could be performed through examination of the effects of overexpression of *MCK1* and *BCY1* on *spc24-9* viability. Under both high temperature stress and during G2/M DNA damage Mck1 has been implicated in the phosphorylation and localization of Bcy1 to the cytoplasm (Griffioen et al., 2003; Searle et al., 2011). This is not suspected to alter the activity of PKA, but instead assist in targeting PKA to particular substrates. To determine if Mck1 rescues the HU sensitivity of *spc24-9* strains through phosphorylation of Bcy1, the GSK-3 consensus sites of Bcy1 could be mutated to prevent phosphorylation in an *spc24-9* mutant, and the HU sensitivity tested with and without the overexpression of *MCK1*. Additionally, to see if the

overexpression of *MCK1* could reduce the high levels of PKA activity in *spc24-9* cells, I would look for a reduction in PKA substrate phosphorylation, such as on the transcription factor Msn2.

5.2.3 Is Mck1's involvement in the PKA pathway responsible for the *MCK1* deletion mutant's HU sensitivity?

The PKA pathway, including Mck1 has been suggested to prevent late nuclear division in the presence of DNA damage caused by the *cdc13-1* mutation, in an overlapping role with Mec1 by inhibition of APC^{Cdc20} (Searle et al., 2004). It would be interesting to test if the PKA pathway is required during DNA replication stress and if Mck1 has a similar role in HU as in *cdc13-1*. In order to determine if Mck1 regulates Bcy1 under HU stress, the cytoplasmic localization and phosphorylation of Bcy1 during HU treatment in the presence or absence of Mck1 should be examined. Likewise, the sensitivity of *tpk1*Δ*, tpk2*Δ and *tpk2*Δ strains could also be determined to provide insight into the function of PKA during DNA replication stress.

5.2.4 Does Mck1 inhibit Clb2-Cdk1 through either the FEAR or MEN pathways?

Mck1 may inhibit Clb2-Cdk1 activity through either the FEAR or MEN pathways. To determine if *mck1*Δ cells have defects in the FEAR pathway, Cdc14 release from the nucleolus can be monitored by indirect immunofluorescence and Net1 phosphorylation by western blotting. The FEAR pathway is required for efficient rDNA segregation in anaphase therefore rDNA segregation could be monitored by fluorescently labeling rDNA in wild type versus *mck1Δ* strains (Liang et al., 2009). Importantly, the FEAR pathway activates the

inhibitors of Clb2-Cdk1 activity, APC^{Cdh1} and Sic1, and both events can be monitored through western blot. The MEN is activated in late anaphase through several mechanisms; reduced Clb2-Cdk1 levels, the FEAR pathway, the spindle orientation checkpoint and unknown triggers. The activation of MEN results in the complete release of Cdc14 from the nucleolus, possibly through phosphorylation of the nuclear localization signal (NLS), complete degradation of Clb2, spindle disassembly and cytokinesis activation (reviewed in (de Gramont and Cohen-Fix, 2005). MEN activation can be followed through Dbf2-Histone H1 kinase assays as well as Cdc14 localization studies (Toyn and Johnston, 1994; Visintin and Amon, 2001). Phosphorylation protein chip studies have revealed that Mck1 can phosphorylate Cdc15 (Ptacek et al., 2005). Examination of Cdc15 reveals potential GSK-3 consensus sites (phosphoGRID, NetPhos). Confirmation of high throughput data that suggests Mck1 interacts with both Cdc14 and Net1 and phosphorylates Net1 and Cdc15 would also be essential next steps. To monitor difficulties in mitotic exit, both spindle and septin ring dynamics can be monitored through use of *TUB1-GFP* and *CDC10-GFP* strains. It is clear that Mck1 plays a role in Clb2-Cdk1 inhibition but determination of where this fits in the larger context of cellular pathways and responses requires further work.

5.2.5 Do *mck1*Δ strains contain an inappropriate level of Clb2-Cdk1 in G1 or S phase?

In Chapter 3, I demonstrated that Clb2-Cdk1 activity remains high after metaphase in *mck1Δ* cells but that no Clb2-Cdk1 activity was detected in S phase (Figure 2-6, Chapter 2). In order to synchronize cells in this experiment, cells were treated with mating factor, which causes reduced Clb2 levels through activation of APC^{Cdh1}. Therefore, my analysis of Clb2 levels

throughout the cell cycle may show a false decrease of Clb2 levels in *mck1Δ* cells in S phase. An alternative method of synchrony that does not rely on the use of adding drugs or peptides is to introduce cells into an elutriation rotor and isolate G1 cells. This method would be a better technique for analysis of Clb2 levels in early G1 cells although it is technically difficult to isolate sufficient quantities of cells for immunoprecipitation and kinase assays.

5.2.6 Does Mck1 interact with additional cyclins?

In Chapter 4, I showed that the HU sensitivity of *mck1Δ* cells is partially rescued by deletion of *CLN2* or *CLN3*, therefore it would be interesting to determine if Cln2-Cdk1 or Cln3-Cdk1 levels are altered in *mck1Δ* strains. Likewise, due to the difficulties that *mck1Δ* strains have in progression through S phase, Clb5-Cdk1 or Clb6-Cdk1 activity may be perturbed therefore it would be diligent to analyze their activity as well in the absence of Mck1.

5.2.7 Could the phosphorylation of Clb2 or Mih1 by Mck1 require a priming phosphorylation or a particular cellular condition?

Despite numerous attempts to determine if Mck1 phosphorylates Clb2 or Mih1 *in vitro*, I was unable to detect phosphorylation of these potential substrates even though Mih1 phospho-isoforms are clearly reduced in *mck1Δ* cells (Chapter 2, 2-5 and 2-12). One reason for the inability to detect phosphorylation could be that Mck1/GSK-3 substrates require a priming phosphorylation and the conditions by which Clb2 and Mih1 were purified did not allow for sufficient priming phosphorylation. Mck1 has recently been shown to phosphorylate Rpc53, a DNA Pol III subunit, upon inhibition of the TOR pathway, after priming phosphorylation by the LAMMER/Cdc-like kinase Kns1 (Lee et al., 2012). As well, the Type 1 casein

kinases, Yck1 and Yck2, phosphorylate Ubr1, thereby priming Ubr1 for phosphorylation by Mck1 (Hwang and Varshavsky, 2008). Therefore, phosphorylation of Clb2 or Mih1 by Mck1 may require priming phosphorylation by Kns1, Yck1 or Yck2. The type 1 casein kinases are likely possibilities for Mih1 priming phosphorylation because *yck2-2 yck1Δ* double mutants have reduced levels of Mih1 phosphorylation (Pal et al., 2008). Alternatively, Mck1 may phosphorylate Clb2 or Mih1 under conditions of DNA replication stress or nutrient starvation.

5.2.8 What is the cause of Mck1 replication defects?

The replication defects exhibited by *mck1*Δ mutants both with and without DNA replication stress, indicate an involvement with either the initiation or maintenance of replication. Analysis of the assembly of the pre-RC in the absence of *MCK1* could be performed through chromosomal immunoprecipitations (chIP). Examination of replication fork progression through 2D gel electrophoresis could also be carried out in both wild type and *mck1*Δ mutants. These experiments could be performed with or without treatment of HU. As Mck1 has several implicated roles such as in the inhibition of both Clb2-Cdk1 and PKA, it would therefore be of interest to determine if deletion of *CLB2* or *TPK1,2,3* could rescue the replication defect in *mck1*Δ cells.

The study of the protein kinase Mck1 is a worthwhile endeavor. Mck1 is involved in multiple pathways and likely phosphorylates a multitude of substrates. Analysis of Mck1 is ideal in a robust model organism such as *S. cerevisiae*, for its ease of genetic manipulation and genome wide screening. Identification of Mck1 substrates that are relevant to its cell cycle regulatory

function will help us better understand the GSK-3 human homologues, which are associated with a variety of diseases such as cancer where cell cycle regulation has gone awry.

Bibliography

Abraham, R.T. (2001). Cell cycle checkpoint signaling through the ATM and ATR kinases. Genes Dev *15*, 2177-2196.

Adams, I.R., and Kilmartin, J.V. (1999). Localization of core spindle pole body (SPB) components during SPB duplication in Saccharomyces cerevisiae. J Cell Biol *145*, 809-823.

Al-Bassam, J., Larsen, N.A., Hyman, A.A., and Harrison, S.C. (2007). Crystal Structure of a TOG Domain: Conserved Features of XMAP215/Dis1-Family TOG Domains and Implications for Tubulin Binding. Structure *15*, 355-362.

Al-Bassam, J., van Breugel, M., Harrison, S.C., and Hyman, A. (2006). Stu2p binds tubulin and undergoes an open-to-closed conformational change. J Cell Biol *172*, 1009-1022.

Alberghina, L., Rossi, R.L., Querin, L., Wanke, V., and Vanoni, M. (2004). A cell sizer network involving Cln3 and Far1 controls entrance into S phase in the mitotic cycle of budding yeast. J Cell Biol *167*, 433-443.

Albuquerque, C.P., Smolka, M.B., Payne, S.H., Bafna, V., Eng, J., and Zhou, H. (2008). A multidimensional chromatography technology for in-depth phosphoproteome analysis. Mol Cell Proteomics *7*, 1389-1396.

Alcasabas, A.A., Osborn, A.J., Bachant, J., Hu, F., Werler, P.J., Bousset, K., Furuya, K., Diffley, J.F., Carr, A.M., and Elledge, S.J. (2001). Mrc1 transduces signals of DNA replication stress to activate Rad53. Nat Cell Biol *3*, 958-965.

Allen, J.B., Zhou, Z., Siede, W., Friedberg, E.C., and Elledge, S.J. (1994). The SAD1/RAD53 protein kinase controls multiple checkpoints and DNA damage-induced transcription in yeast. Genes Dev *8*, 2401-2415.

Alvino, G.M., Collingwood, D., Murphy, J.M., Delrow, J., Brewer, B.J., and Raghuraman, M.K. (2007). Replication in hydroxyurea: it's a matter of time. Mol Cell Biol *27*, 6396-6406.

Amon, A. (1999). The spindle checkpoint. Curr Opin Genet Dev *9*, 69-75.

Amon, A., Surana, U., Muroff, I., and Nasmyth, K. (1992). Regulation of p34CDC28 tyrosine phosphorylation is not required for entry into mitosis in S. cerevisiae. Nature *355*, 368-371.

Amon, A., Tyers, M., Futcher, B., and Nasmyth, K. (1993). Mechanisms that help the yeast cell cycle clock tick: G2 cyclins transcriptionally activate G2 cyclins and repress G1 cyclins. Cell *74*, 993-1007.

Andoh, T., Hirata, Y., and Kikuchi, A. (2000). Yeast glycogen synthase kinase 3 is involved in protein degradation in cooperation with Bul1, Bul2, and Rsp5. Mol Cell Biol *20*, 6712-6720.

Archambault, V., Chang, E.J., Drapkin, B.J., Cross, F.R., Chait, B.T., and Rout, M.P. (2004). Targeted proteomic study of the cyclin-Cdk module. Mol Cell *14*, 699-711.

Archambault, V., Ikui, A.E., Drapkin, B.J., and Cross, F.R. (2005). Disruption of mechanisms that prevent rereplication triggers a DNA damage response. Mol Cell Biol *25*, 6707-6721.

Asano, S., Park, J.E., Sakchaisri, K., Yu, L.R., Song, S., Supavilai, P., Veenstra, T.D., and Lee, K.S. (2005). Concerted mechanism of Swe1/Wee1 regulation by multiple kinases in budding yeast. EMBO J *24*, 2194-2204.

Azzam, R., Chen, S.L., Shou, W., Mah, A.S., Alexandru, G., Nasmyth, K., Annan, R.S., Carr, S.A., and Deshaies, R.J. (2004). Phosphorylation by cyclin B-Cdk underlies release of mitotic exit activator Cdc14 from the nucleolus. Science *305*, 516-519.

Ba, A.N., and Moses, A.M. (2010). Evolution of characterized phosphorylation sites in budding yeast. Molecular biology and evolution *27*, 2027-2037.

Bachant, J., Jessen, S.R., Kavanaugh, S.E., and Fielding, C.S. (2005). The yeast S phase checkpoint enables replicating chromosomes to bi-orient and restrain spindle extension during S phase distress. J Cell Biol *168*, 999-1012.

Bailly, E., Cabantous, S., Sondaz, D., Bernadac, A., and Simon, M.-N. (2003). Differential cellular localization among mitotic cyclins from Saccharomyces cerevisiae: a new role for the axial budding protein Bud3 in targeting Clb2 to the mother-bud neck. J Cell Sci *116*, 4119-4130.

Barberis, M. (2012). Sic1 as a timer of Clb cyclins waves in the yeast cell cycle: design principle of not just an inhibitor. The FEBS journal.

Barberis, M., and Klipp, E. (2007). Insights into the network controlling the G1/S transition in budding yeast. Genome Inform *18*, 85-99.

Barral, Y., Jentsch, S., and Mann, C. (1995). G1 cyclin turnover and nutrient uptake are controlled by a common pathway in yeast. Genes Dev *9*, 399-409.

Barral, Y., Parra, M., Bidlingmaier, S., and Snyder, M. (1999). Nim1-related kinases coordinate cell cycle progression with the organization of the peripheral cytoskeleton in yeast. Genes Dev *13*, 176-187.

Bastos de Oliveira, F.M., Harris, M.R., Brazauskas, P., de Bruin, R.A.M., and Smolka, M.B. (2012). Linking DNA replication checkpoint to MBF cell-cycle transcription reveals a distinct class of G1/S genes. EMBO J.

Beranek, D.T. (1990). Distribution of methyl and ethyl adducts following alkylation with monofunctional alkylating agents. Mutat Res *231*, 11-30.

Biggins, S., and Murray, A.W. (2001). The budding yeast protein kinase Ipl1/Aurora allows the absence of tension to activate the spindle checkpoint. Genes Dev *15*, 3118-3129.

Bilsland-Marchesan, E., Arino, J., Saito, H., Sunnerhagen, P., and Posas, F. (2000). Rck2 kinase is a substrate for the osmotic stress-activated mitogen-activated protein kinase Hog1. Mol Cell Biol *20*, 3887-3895.

Bloom, J., and Cross, F.R. (2007). Multiple levels of cyclin specificity in cell-cycle control. Nat Rev Mol Cell Biol *8*, 149-160.

Bodenmiller, B., and Aebersold, R. (2010). Quantitative analysis of protein phosphorylation on a system-wide scale by mass spectrometry-based proteomics. Meth Enzymol *470*, 317-334.

Boekhorst, J., van Breukelen, B., Heck, A., Jr., and Snel, B. (2008). Comparative phosphoproteomics reveals evolutionary and functional conservation of phosphorylation across eukaryotes. Genome Biol *9*, R144.

Booher, R.N., Deshaies, R.J., and Kirschner, M.W. (1993). Properties of Saccharomyces cerevisiae wee1 and its differential regulation of p34CDC28 in response to G1 and G2 cyclins. EMBO J *12*, 3417-3426.

Boone, C., Bussey, H., and Andrews, B.J. (2007). Exploring genetic interactions and networks with yeast. Nat Rev Genet *8*, 437-449.

Bouck, D., and Bloom, K. (2005). The role of centromere-binding factor 3 (CBF3) in spindle stability, cytokinesis, and kinetochore attachment. Biochem Cell Biol *83*, 696-702.

Boutros, R., Dozier, C., and Ducommun, B. (2006). The when and wheres of CDC25 phosphatases. Curr Opin Cell Biol *18*, 185-191.

Bowdish, K.S., Yuan, H.E., and Mitchell, A.P. (1994). Analysis of RIM11, a yeast protein kinase that phosphorylates the meiotic activator IME1. Mol Cell Biol *14*, 7909-7919.

Branzei, D., and Foiani, M. (2005). The DNA damage response during DNA replication. Curr Opin Cell Biol *17*, 568-575.

Branzei, D., and Foiani, M. (2009). The checkpoint response to replication stress. DNA Repair (Amst) *8*, 1038-1046.

Brazill, D.T., Thorner, J., and Martin, G.S. (1997). Mck1, a member of the glycogen synthase kinase 3 family of protein kinases, is a negative regulator of pyruvate kinase in the yeast Saccharomyces cerevisiae. J Bacteriol *179*, 4415-4418.

Breitkreutz, A., Choi, H., Sharom, J.R., Boucher, L., Neduva, V., Larsen, B., Lin, Z.-Y., Breitkreutz, B.-J., Stark, C., Liu, G.*, et al.* (2010). A global protein kinase and phosphatase interaction network in yeast. Science *328*, 1043-1046.

Brown, J.L., Jaquenoud, M., Gulli, M.P., Chant, J., and Peter, M. (1997). Novel Cdc42-binding proteins Gic1 and Gic2 control cell polarity in yeast. Genes Dev *11*, 2972-2982.

Byun, T.S., Pacek, M., Yee, M.-c., Walter, J.C., and Cimprich, K.A. (2005). Functional uncoupling of MCM helicase and DNA polymerase activities activates the ATR-dependent checkpoint. Genes Dev *19*, 1040-1052.

Canman, C.E. (2001). Replication checkpoint: preventing mitotic catastrophe. Curr Biol *11*, R121-124.

Chee, M.K., and Haase, S.B. (2010). B-cyclin/CDKs regulate mitotic spindle assembly by phosphorylating kinesins-5 in budding yeast. PLoS Genet *6*, e1000935.

Cheeseman, I.M., Enquist-Newman, M., Muller-Reichert, T., Drubin, D.G., and Barnes, G. (2001). Mitotic spindle integrity and kinetochore function linked by the Duo1p/Dam1p complex. J Cell Biol *152*, 197-212.

Chen, G.C., Kim, Y.J., and Chan, C.S. (1997). The Cdc42 GTPase-associated proteins Gic1 and Gic2 are required for polarized cell growth in Saccharomyces cerevisiae. Genes Dev *11*, 2958-2971.

Chen, K.C., Csikasz-Nagy, A., Gyorffy, B., Val, J., Novak, B., and Tyson, J.J. (2000). Kinetic analysis of a molecular model of the budding yeast cell cycle. Mol Biol Cell *11*, 369-391.

Chen, S., and Bell, S.P. (2011). CDK prevents Mcm2-7 helicase loading by inhibiting Cdt1 interaction with Orc6. Genes Dev *25*, 363-372.

Chen, X.P., Yin, H., and Huffaker, T.C. (1998). The yeast spindle pole body component Spc72p interacts with Stu2p and is required for proper microtubule assembly. J Cell Biol *141*, 1169-1179.

Chi, A., Huttenhower, C., Geer, L.Y., Coon, J.J., Syka, J.E.P., Bai, D.L., Shabanowitz, J., Burke, D.J., Troyanskaya, O.G., and Hunt, D.F. (2007). Analysis of phosphorylation sites on proteins from Saccharomyces cerevisiae by electron transfer dissociation (ETD) mass spectrometry. Proc Natl Acad Sci USA *104*, 2193-2198.

Cid, V.J., Shulewitz, M.J., McDonald, K.L., and Thorner, J. (2001). Dynamic localization of the Swe1 regulator Hsl7 during the Saccharomyces cerevisiae cell cycle. Mol Biol Cell *12*, 1645-1669.

Clarke, D.J., Segal, M., Andrews, C.A., Rudyak, S.G., Jensen, S., Smith, K., and Reed, S.I. (2003). S-phase checkpoint controls mitosis via an APC-independent Cdc20p function. Nat Cell Biol *5*, 928-935.

Clarke, D.J., Segal, M., Jensen, S., and Reed, S.I. (2001). Mec1p regulates Pds1p levels in S phase: complex coordination of DNA replication and mitosis. Nat Cell Biol *3*, 619-627.

Cobb, J.A., Schleker, T., Rojas, V., Bjergbaek, L., Tercero, J.A., and Gasser, S.M. (2005). Replisome instability, fork collapse, and gross chromosomal rearrangements arise synergistically from Mec1 kinase and RecQ helicase mutations. Genes Dev *19*, 3055-3069.

Cohen, P., and Frame, S. (2001). The renaissance of GSK3. Nat Rev Mol Cell Biol *2*, 769-776.

Collins, S.R., Miller, K.M., Maas, N.L., Roguev, A., Fillingham, J., Chu, C.S., Schuldiner, M., Gebbia, M., Recht, J., Shales, M.*, et al.* (2007). Functional dissection of protein complexes involved in yeast chromosome biology using a genetic interaction map. Nature *446*, 806-810.

Connelly, C., and Hieter, P. (1996). Budding yeast SKP1 encodes an evolutionarily conserved kinetochore protein required for cell cycle progression. Cell *86*, 275-285.

Costanzo, M., Nishikawa, J.L., Tang, X., Millman, J.S., Schub, O., Breitkreuz, K., Dewar, D., Rupes, I., Andrews, B., and Tyers, M. (2004). CDK activity antagonizes Whi5, an inhibitor of G1/S transcription in yeast. Cell *117*, 899-913.

Crasta, K., and Surana, U. (2006). Disjunction of conjoined twins: Cdk1, Cdh1 and separation of centrosomes. Cell Div *1*, 12.

Cross, F.R. (1988). DAF1, a mutant gene affecting size control, pheromone arrest, and cell cycle kinetics of Saccharomyces cerevisiae. Mol Cell Biol *8*, 4675-4684.

Cross, F.R. (1995). Starting the cell cycle: what's the point? Curr Opin Cell Biol *7*, 790-797.

Cross, F.R., Schroeder, L., Kruse, M., and Chen, K.C. (2005). Quantitative characterization of a mitotic cyclin threshold regulating exit from mitosis. Mol Biol Cell *16*, 2129-2138.

Cross, F.R., Yuste-Rojas, M., Gray, S., and Jacobson, M.D. (1999). Specialization and targeting of B-type cyclins. Mol Cell *4*, 11-19.

Cuschieri, L., Miller, R., and Vogel, J. (2006). {gamma}-Tubulin Is Required for Proper Recruitment and Assembly of Kar9-Bim1 Complexes in Budding Yeast. Mol Biol Cell.

Dailey, D., Schieven, G.L., Lim, M.Y., Marquardt, H., Gilmore, T., Thorner, J., and Martin, G.S. (1990). Novel yeast protein kinase (YPK1 gene product) is a 40-kilodalton phosphotyrosyl protein associated with protein-tyrosine kinase activity. Mol Cell Biol *10*, 6244-6256.

Daniel, J.A., Keyes, B.E., Ng, Y.P., Freeman, C.O., and Burke, D.J. (2006). Diverse functions of spindle assembly checkpoint genes in Saccharomyces cerevisiae. Genetics *172*, 53-65.

Davies, B.W., Kohanski, M.A., Simmons, L.A., Winkler, J.A., Collins, J.J., and Walker, G.C. (2009). Hydroxyurea induces hydroxyl radical-mediated cell death in Escherichia coli. Mol Cell *36*, 845-860.

de Bruin, R.A., McDonald, W.H., Kalashnikova, T.I., Yates, J., and Wittenberg, C. (2004). Cln3 activates G1-specific transcription via phosphorylation of the SBF bound repressor Whi5. Cell *117*, 887-898.

de Bruin, R.A.M., Kalashnikova, T.I., Aslanian, A., Wohlschlegel, J., Chahwan, C., Yates, J.R., Russell, P., and Wittenberg, C. (2008). DNA replication checkpoint promotes G1-S transcription by inactivating the MBF repressor Nrm1. Proc Natl Acad Sci USA *105*, 11230-11235.

de Gramont, A., and Cohen-Fix, O. (2005). The many phases of anaphase. Trends Biochem Sci *30*, 559-568.

De Piccoli, G., Katou, Y., Itoh, T., Nakato, R., Shirahige, K., and Labib, K. (2012). Replisome stability at defective DNA replication forks is independent of s phase checkpoint kinases. Mol Cell *45*, 696-704.

Desany, B.A., Alcasabas, A.A., Bachant, J.B., and Elledge, S.J. (1998). Recovery from DNA replicational stress is the essential function of the S-phase checkpoint pathway. Genes Dev *12*, 2956-2970.

Deshaies, R.J. (1997). Phosphorylation and proteolysis: partners in the regulation of cell division in budding yeast. Curr Opin Genet Dev *7*, 7-16.

Deshaies, R.J., Chau, V., and Kirschner, M. (1995). Ubiquitination of the G1 cyclin Cln2p by a Cdc34p-dependent pathway. EMBO J *14*, 303-312.

Detweiler, C.S., and Li, J.J. (1998). Ectopic induction of Clb2 in early G1 phase is sufficient to block prereplicative complex formation in Saccharomyces cerevisiae. Proc Natl Acad Sci USA *95*, 2384-2389.

Dewar, H., Tanaka, K., Nasmyth, K., and Tanaka, T.U. (2004). Tension between two kinetochores suffices for their bi-orientation on the mitotic spindle. Nature *428*, 93-97.

Diffley, J.F., Bousset, K., Labib, K., Noton, E.A., Santocanale, C., and Tercero, J.A. (2000). Coping with and recovering from hydroxyurea-induced replication fork arrest in budding yeast. Cold Spring Harb Symp Quant Biol *65*, 333-342.

Diffley, J.F.X. (2004). Regulation of early events in chromosome replication. Curr Biol *14*, R778-786.

Diffley, J.F.X. (2010). The many faces of redundancy in DNA replication control. Cold Spring Harb Symp Quant Biol *75*, 135-142.

Doheny, K.F., Sorger, P.K., Hyman, A.A., Tugendreich, S., Spencer, F., and Hieter, P. (1993). Identification of essential components of the S. cerevisiae kinetochore. Cell *73*, 761-774.

Donaldson, A.D., Raghuraman, M.K., Friedman, K.L., Cross, F.R., Brewer, B.J., and Fangman, W.L. (1998). CLB5-dependent activation of late replication origins in S. cerevisiae. Mol Cell *2*, 173-182.

Donovan, J.D., Toyn, J.H., Johnson, A.L., and Johnston, L.H. (1994). P40SDB25, a putative CDK inhibitor, has a role in the M/G1 transition in Saccharomyces cerevisiae. Genes Dev *8*, 1640-1653.

Enserink, J.M., Hombauer, H., Huang, M.-E., and Kolodner, R.D. (2009). Cdc28/Cdk1 positively and negatively affects genome stability in S. cerevisiae. J Cell Biol *185*, 423-437.

Enserink, J.M., and Kolodner, R.D. (2010). An overview of Cdk1-controlled targets and processes. Cell division *5*, 11.

Enserink, J.M., Smolka, M.B., Zhou, H., and Kolodner, R.D. (2006). Checkpoint proteins control morphogenetic events during DNA replication stress in Saccharomyces cerevisiae. J Cell Biol *175*, 729-741.

Feng, W., Collingwood, D., Boeck, M.E., Fox, L.A., Alvino, G.M., Fangman, W.L., Raghuraman, M.K., and Brewer, B.J. (2006). Genomic mapping of single-stranded DNA in hydroxyurea-challenged yeasts identifies origins of replication. Nat Cell Biol *8*, 148-155.

Fernandes, L., Rodrigues-Pousada, C., and Struhl, K. (1997). Yap, a novel family of eight bZIP proteins in Saccharomyces cerevisiae with distinct biological functions. Mol Cell Biol *17*, 6982-6993.

Ficarro, S.B., McCleland, M.L., Stukenberg, P.T., Burke, D.J., Ross, M.M., Shabanowitz, J., Hunt, D.F., and White, F.M. (2002). Phosphoproteome analysis by mass spectrometry and its application to Saccharomyces cerevisiae. Nat Biotechnol *20*, 301-305.

Fiedler, D., Braberg, H., Mehta, M., Chechik, G., Cagney, G., Mukherjee, P., Silva, A.C., Shales, M., Collins, S.R., van Wageningen, S.*, et al.* (2009). Functional organization of the S. cerevisiae phosphorylation network. Cell *136*, 952-963.

Fiol, C.J., Mahrenholz, A.M., Wang, Y., Roeske, R.W., and Roach, P.J. (1987). Formation of protein kinase recognition sites by covalent modification of the substrate. Molecular mechanism for the synergistic action of casein kinase II and glycogen synthase kinase 3. J Biol Chem *262*, 14042-14048.

Fitch, I., Dahmann, C., Surana, U., Amon, A., Nasmyth, K., Goetsch, L., Byers, B., and Futcher, B. (1992). Characterization of four B-type cyclin genes of the budding yeast Saccharomyces cerevisiae. Mol Biol Cell *3*, 805-818.

Frame, S., and Cohen, P. (2001). GSK3 takes centre stage more than 20 years after its discovery. Biochem J *359*, 1-16.

Fraschini, R., Bilotta, D., Lucchini, G., and Piatti, S. (2004). Functional characterization of Dma1 and Dma2, the budding yeast homologues of Schizosaccharomyces pombe Dma1 and human Chfr. Mol Biol Cell *15*, 3796-3810.

Futcher, A.B. (1991). Saccharomyces cerevisiae cell cycle: cdc28 and the G1 cyclins. Semin Cell Biol *2*, 205-212.

Gard, D.L., Becker, B.E., and Josh Romney, S. (2004). MAPping the eukaryotic tree of life: structure, function, and evolution of the MAP215/Dis1 family of microtubule-associated proteins. Int Rev Cytol *239*, 179-272.

Gardner, R., Putnam, C.W., and Weinert, T. (1999). RAD53, DUN1 and PDS1 define two parallel G2/M checkpoint pathways in budding yeast. EMBO J *18*, 3173-3185.

Gardner, R.D., Poddar, A., Yellman, C., Tavormina, P.A., Monteagudo, M.C., and Burke, D.J. (2001). The spindle checkpoint of the yeast Saccharomyces cerevisiae requires kinetochore function and maps to the CBF3 domain. Genetics *157*, 1493-1502.

Ghiara, J.B., Richardson, H.E., Sugimoto, K., Henze, M., Lew, D.J., Wittenberg, C., and Reed, S.I. (1991). A cyclin B homolog in S. cerevisiae: chronic activation of the Cdc28 protein kinase by cyclin prevents exit from mitosis. Cell *65*, 163-174.

Gnad, F., de Godoy, L.M.F., Cox, J., Neuhauser, N., Ren, S., Olsen, J.V., and Mann, M. (2009). High-accuracy identification and bioinformatic analysis of in vivo protein phosphorylation sites in yeast. Proteomics *9*, 4642-4652.

Gnad, F., Forner, F., Zielinska, D.F., Birney, E., Gunawardena, J., and Mann, M. (2010). Evolutionary constraints of phosphorylation in eukaryotes, prokaryotes, and mitochondria. Mol Cell Proteomics *9*, 2642-2653.

Gorner, W., Durchschlag, E., Martinez-Pastor, M.T., Estruch, F., Ammerer, G., Hamilton, B., Ruis, H., and Schuller, C. (1998). Nuclear localization of the C2H2 zinc finger protein Msn2p is regulated by stress and protein kinase A activity. Genes Dev *12*, 586-597.

Goshima, G., and Yanagida, M. (2000). Establishing biorientation occurs with precocious separation of the sister kinetochores, but not the arms, in the early spindle of budding yeast. Cell *100*, 619-633.

Griffioen, G., Swinnen, S., and Thevelein, J.M. (2003). Feedback inhibition on cell wall integrity signaling by Zds1 involves Gsk3 phosphorylation of a cAMP-dependent protein kinase regulatory subunit. J Biol Chem *278*, 23460-23471.

Groth, P., Ausländer, S., Majumder, M.M., Schultz, N., Johansson, F., Petermann, E., and Helleday, T. (2010). Methylated DNA causes a physical block to replication forks independently of damage signalling, O(6)-methylguanine or DNA single-strand breaks and results in DNA damage. J Mol Biol *402*, 70-82.

Guthrie, C., and Fink, G.R. (1991). Guide to Yeast Genetics and Molecular Biology, Vol 194 (New York: Academic Press).

Guthrie, C., and R. Fink, G. (2004). Guide to yeast genetics and molecular and cell biology, Volume 1. 933.

Haase, S.B., and Lew, D.J. (1997). Flow cytometric analysis of DNA content in budding yeast. Methods Enzymol *283*, 322-332.

Hadwiger, J.A., Wittenberg, C., Richardson, H.E., de Barros Lopes, M., and Reed, S.I. (1989). A family of cyclin homologs that control the G1 phase in yeast. Proc Natl Acad Sci USA *86*, 6255-6259.

Han, G.S., Siniossoglou, S., and Carman, G.M. (2007). The cellular functions of the yeast lipin homolog PAH1p are dependent on its phosphatidate phosphatase activity. J Biol Chem *282*, 37026-37035.

Harrison, J.C., and Haber, J.E. (2006). Surviving the breakup: the DNA damage checkpoint. Annu Rev Genet *40*, 209-235.

Hartwell, L.H., and Weinert, T.A. (1989). Checkpoints: controls that ensure the order of cell cycle events. Science *246*, 629-634.

He, X., Asthana, S., and Sorger, P.K. (2000). Transient sister chromatid separation and elastic deformation of chromosomes during mitosis in budding yeast. Cell *101*, 763-775.

He, X., Rines, D.R., Espelin, C.W., and Sorger, P.K. (2001). Molecular analysis of kinetochore-microtubule attachment in budding yeast. Cell *106*, 195-206.

Henchoz, S., Chi, Y., Catarin, B., Herskowitz, I., Deshaies, R.J., and Peter, M. (1997). Phosphorylation- and ubiquitin-dependent degradation of the cyclin-dependent kinase inhibitor Far1p in budding yeast. Genes Dev *11*, 3046-3060.

Hernández, F., de Barreda, E.G., Fuster-Matanzo, A., Goñi-Oliver, P., Lucas, J.J., and Avila, J. (2009). The role of GSK3 in Alzheimer disease. Brain Res Bull *80*, 248-250.

Higuchi, T., and Uhlmann, F. (2005). Stabilization of microtubule dynamics at anaphase onset promotes chromosome segregation. Nature *433*, 171-176.

Hilioti, Z., Gallagher, D.A., Low-Nam, S.T., Ramaswamy, P., Gajer, P., Kingsbury, T.J., Birchwood, C.J., Levchenko, A., and Cunningham, K.W. (2004). GSK-3 kinases enhance calcineurin signaling by phosphorylation of RCNs. Genes Dev *18*, 35-47.

Hirata, Y., Andoh, T., Asahara, T., and Kikuchi, A. (2003). Yeast glycogen synthase kinase-3 activates Msn2p-dependent transcription of stress responsive genes. Mol Biol Cell *14*, 302-312.

Hoeflich, K.P., Luo, J., Rubie, E.A., Tsao, M.S., Jin, O., and Woodgett, J.R. (2000). Requirement for glycogen synthase kinase-3beta in cell survival and NF-kappaB activation. Nature *406*, 86-90.

Hoeijmakers, J.H. (2001). Genome maintenance mechanisms for preventing cancer. Nature *411*, 366-374.

Hofken, T., and Schiebel, E. (2004). Novel regulation of mitotic exit by the Cdc42 effectors Gic1 and Gic2. J Cell Biol *164*, 219-231.

Horak, C.E., Luscombe, N.M., Qian, J., Bertone, P., Piccirrillo, S., Gerstein, M., and Snyder, M. (2002). Complex transcriptional circuitry at the G1/S transition in Saccharomyces cerevisiae. Genes Dev *16*, 3017-3033.

Howell, A.S., and Lew, D.J. (2012). Morphogenesis and the cell cycle. Genetics *190*, 51-77.

Hsu, W.-S., Erickson, S.L., Tsai, H.-J., Andrews, C.A., Vas, A.C., and Clarke, D.J. (2011). S-phase cyclin-dependent kinases promote sister chromatid cohesion in budding yeast. Mol Cell Biol *31*, 2470-2483.

Hu, F., and Aparicio, O.M. (2005). Swe1 regulation and transcriptional control restrict the activity of mitotic cyclins toward replication proteins in Saccharomyces cerevisiae. Proc Natl Acad Sci USA *102*, 8910-8915.

Huang, D., Kaluarachchi, S., van Dyk, D., Friesen, H., Sopko, R., Ye, W., Bastajian, N., Moffat, J., Sassi, H., Costanzo, M.*, et al.* (2009). Dual regulation by pairs of cyclin-

dependent protein kinases and histone deacetylases controls G1 transcription in budding yeast. PLoS Biol *7*, e1000188.

Huang, M., Zhou, Z., and Elledge, S.J. (1998). The DNA replication and damage checkpoint pathways induce transcription by inhibition of the Crt1 repressor. Cell *94*, 595-605.

Hughes, K., Nikolakaki, E., Plyte, S.E., Totty, N.F., and Woodgett, J.R. (1993). Modulation of the glycogen synthase kinase-3 family by tyrosine phosphorylation. EMBO J *12*, 803-808.

Hwang, C.S., and Varshavsky, A. (2008). Regulation of peptide import through phosphorylation of Ubr1, the ubiquitin ligase of the N-end rule pathway. Proc Natl Acad Sci USA *105*, 19188-19193.

Hyland, K.M., Kingsbury, J., Koshland, D., and Hieter, P. (1999). Ctf19p: A novel kinetochore protein in Saccharomyces cerevisiae and a potential link between the kinetochore and mitotic spindle. J Cell Biol *145*, 15-28.

Ikui, A., and Cross, F. (2009). Specific Genetic Interactions Between Spindle Assembly Checkpoint Proteins and B-type Cyclins in Saccharomyces cerevisiae. Genetics.

Inoue, Y.H., do Carmo Avides, M., Shiraki, M., Deak, P., Yamaguchi, M., Nishimoto, Y., Matsukage, A., and Glover, D.M. (2000). Orbit, a novel microtubule-associated protein essential for mitosis in Drosophila melanogaster. J Cell Biol *149*, 153-166.

Jackson, L.P., Reed, S.I., and Haase, S.B. (2006). Distinct mechanisms control the stability of the related S-phase cyclins Clb5 and Clb6. Mol Cell Biol *26*, 2456-2466.

Janke, C., Ortiz, J., Lechner, J., Shevchenko, A., Shevchenko, A., Magiera, M.M., Schramm, C., and Schiebel, E. (2001). The budding yeast proteins Spc24p and Spc25p interact with Ndc80p and Nuf2p at the kinetochore and are important for kinetochore clustering and checkpoint control. Embo J *20*, 777-791.

Jaspersen, S.L., Charles, J.F., Tinker-Kulberg, R.L., and Morgan, D.O. (1998). A late mitotic regulatory network controlling cyclin destruction in Saccharomyces cerevisiae. Mol Biol Cell *9*, 2803-2817.

Jaspersen, S.L., and Morgan, D.O. (2000). Cdc14 activates cdc15 to promote mitotic exit in budding yeast. Curr Biol *10*, 615-618.

Jaspersen, S.L., and Winey, M. (2004). The budding yeast spindle pole body: structure, duplication, and function. Annu Rev Cell Dev Biol *20*, 1-28.

Jeoung, D.I., Oehlen, L.J., and Cross, F.R. (1998). Cln3-associated kinase activity in Saccharomyces cerevisiae is regulated by the mating factor pathway. Mol Cell Biol *18*, 433-441.

Jiang, W., and Koltin, Y. (1996). Two-hybrid interaction of a human UBC9 homolog with centromere proteins of Saccharomyces cerevisiae. Mol Gen Genet *251*, 153-160.

Jiang, W., Lim, M.Y., Yoon, H.J., Thorner, J., Martin, G.S., and Carbon, J. (1995). Overexpression of the yeast MCK1 protein kinase suppresses conditional mutations in centromere-binding protein genes CBF2 and CBF5. Mol Gen Genet *246*, 360-366.

Kaiser, C., Michaelis, S., and Mitchell, A. (1994). Methods in yeast genetics (Cold Spring Harbor, N.Y.: Cold Spring Harbor Laboratory Press).

Kaiser, P., Sia, R.A., Bardes, E.G., Lew, D.J., and Reed, S.I. (1998). Cdc34 and the F-box protein Met30 are required for degradation of the Cdk-inhibitory kinase Swe1. Genes Dev *12*, 2587-2597.

Kang, T., Wei, Y., Honaker, Y., Yamaguchi, H., Appella, E., Hung, M.-C., and Piwnica-Worms, H. (2008). GSK-3 beta targets Cdc25A for ubiquitin-mediated proteolysis, and GSK-3 beta inactivation correlates with Cdc25A overproduction in human cancers. Cancer Cell *13*, 36-47.

Kastan, M.B., and Bartek, J. (2004). Cell-cycle checkpoints and cancer. Nature *432*, 316-323.

Keaton, M.A., Bardes, E.S., Marquitz, A.R., Freel, C.D., Zyla, T.R., Rudolph, J., and Lew, D.J. (2007). Differential susceptibility of yeast S and M phase CDK complexes to inhibitory tyrosine phosphorylation. Curr Biol *17*, 1181-1189.

Keaton, M.A., and Lew, D.J. (2006). Eavesdropping on the cytoskeleton: progress and controversy in the yeast morphogenesis checkpoint. Curr Opin Microbiol *9*, 540-546.

Keaton, M.A., Szkotnicki, L., Marquitz, A.R., Harrison, J., Zyla, T.R., and Lew, D.J. (2008). Nucleocytoplasmic trafficking of G2/M regulators in yeast. Mol Biol Cell *19*, 4006-4018.

Kelly, T.J., and Brown, G.W. (2000). Regulation of chromosome replication. Annu Rev Biochem *69*, 829-880.

Khmelinskii, A., Lawrence, C., Roostalu, J., and Schiebel, E. (2007). Cdc14-regulated midzone assembly controls anaphase B. J Cell Biol *177*, 981-993.

Kim, S.-H., Gadiparthi, K., Kron, S.J., and Kitazono, A.A. (2009). A phosphorylation-independent role for the yeast cyclin-dependent kinase activating kinase Cak1. Gene *447*, 97-105.

Kishi, T., Ikeda, A., Nagao, R., and Koyama, N. (2007). The SCFCdc4 ubiquitin ligase regulates calcineurin signaling through degradation of phosphorylated Rcn1, an inhibitor of calcineurin. Proc Natl Acad Sci USA *104*, 17418-17423.

Kõivomägi, M., Valk, E., Venta, R., Iofik, A., Lepiku, M., Morgan, D.O., and Loog, M. (2011). Dynamics of Cdk1 substrate specificity during the cell cycle. Mol Cell *42*, 610-623.

Kolodner, R.D., Putnam, C.D., and Myung, K. (2002). Maintenance of genome stability in Saccharomyces cerevisiae. Science *297*, 552-557.

Kosco, K.A., Pearson, C.G., Maddox, P.S., Wang, P.J., Adams, I.R., Salmon, E.D., Bloom, K., and Huffaker, T.C. (2001). Control of microtubule dynamics by Stu2p is essential for spindle orientation and metaphase chromosome alignment in yeast. Mol Biol Cell *12*, 2870-2880.

Kramer, K.M., Fesquet, D., Johnson, A.L., and Johnston, L.H. (1998). Budding yeast RSI1/APC2, a novel gene necessary for initiation of anaphase, encodes an APC subunit. EMBO J *17*, 498-506.

Krishnan, V., Nirantar, S., Crasta, K., Cheng, A.Y., and Surana, U. (2004). DNA replication checkpoint prevents precocious chromosome segregation by regulating spindle behavior. Mol Cell *16*, 687-700.

Krishnan, V., and Surana, U. (2005). Taming the spindle for containing the chromosomes. Cell Cycle *4*, 376-379.

Labib, K. (2010). How do Cdc7 and cyclin-dependent kinases trigger the initiation of chromosome replication in eukaryotic cells? Genes Dev *24*, 1208-1219.

Labib, K., and De Piccoli, G. (2011). Surviving chromosome replication: the many roles of the S-phase checkpoint pathway. Philos Trans R Soc Lond, B, Biol Sci *366*, 3554-3561.

Landry, C.R., Levy, E.D., and Michnick, S.W. (2009). Weak functional constraints on phosphoproteomes. Trends Genet *25*, 193-197.

Lanker, S., Valdivieso, M.H., and Wittenberg, C. (1996). Rapid degradation of the G1 cyclin Cln2 induced by CDK-dependent phosphorylation. Science *271*, 1597-1601.

Le Masson, I., Saveanu, C., Chevalier, A., Namane, A., Gobin, R., Fromont-Racine, M., Jacquier, A., and Mann, C. (2002). Spc24 interacts with Mps2 and is required for chromosome segregation, but is not implicated in spindle pole body duplication. Mol Microbiol *43*, 1431-1443.

Lee, J., Moir, R.D., McIntosh, K.B., and Willis, I.M. (2012). TOR Signaling Regulates Ribosome and tRNA Synthesis via LAMMER/Clk and GSK-3 Family Kinases. Mol Cell *45*, 836-843.

Lee, S.E., Frenz, L.M., Wells, N.J., Johnson, A.L., and Johnston, L.H. (2001). Order of function of the budding-yeast mitotic exit-network proteins Tem1, Cdc15, Mob1, Dbf2, and Cdc5. Curr Biol *11*, 784-788.

Lengauer, C., Kinzler, K.W., and Vogelstein, B. (1998). Genetic instabilities in human cancers. Nature *396*, 643-649.

Lengronne, A., and Schwob, E. (2002). The yeast CDK inhibitor Sic1 prevents genomic instability by promoting replication origin licensing in late G(1). Mol Cell *9*, 1067-1078.

Lew, D.J. (2003). The morphogenesis checkpoint: how yeast cells watch their figures. Curr Opin Cell Biol *15*, 648-653.

Lew, D.J., and Burke, D.J. (2003). The spindle assembly and spindle position checkpoints. Annu Rev Genet *37*, 251-282.

Lew, D.J., and Reed, S.I. (1993). Morphogenesis in the yeast cell cycle: regulation by Cdc28 and cyclins. J Cell Biol *120*, 1305-1320.

Li, X., Gerber, S.A., Rudner, A.D., Beausoleil, S.A., Haas, W., Villén, J., Elias, J.E., and Gygi, S.P. (2007). Large-scale phosphorylation analysis of alpha-factor-arrested Saccharomyces cerevisiae. J Proteome Res *6*, 1190-1197.

Liang, F., Jin, F., Liu, H., and Wang, Y. (2009). The molecular function of the yeast polo-like kinase Cdc5 in Cdc14 release during early anaphase. Mol Biol Cell *20*, 3671-3679.

Lienhard, G.E. (2008). Non-functional phosphorylations? Trends Biochem Sci *33*, 351-352.

Lim, H.H., Goh, P.Y., and Surana, U. (1996). Spindle pole body separation in Saccharomyces cerevisiae requires dephosphorylation of the tyrosine 19 residue of Cdc28. Mol Cell Biol *16*, 6385-6397.

Lim, M.Y., Dailey, D., Martin, G.S., and Thorner, J. (1993). Yeast MCK1 protein kinase autophosphorylates at tyrosine and serine but phosphorylates exogenous substrates at serine and threonine. J Biol Chem *268*, 21155-21164.

Lin, H., de Carvalho, P., Kho, D., Tai, C.Y., Pierre, P., Fink, G.R., and Pellman, D. (2001). Polyploids require Bik1 for kinetochore-microtubule attachment. J Cell Biol *155*, 1173-1184.

Lisby, M., Barlow, J.H., Burgess, R.C., and Rothstein, R. (2004). Choreography of the DNA damage response: spatiotemporal relationships among checkpoint and repair proteins. Cell *118*, 699-713.

Lisby, M., and Rothstein, R. (2004). DNA damage checkpoint and repair centers. Curr Opin Cell Biol *16*, 328-334.

Liu, H., Jin, F., Liang, F., Tian, X., and Wang, Y. (2011). The Cik1/Kar3 motor complex is required for the proper kinetochore-microtubule interaction after stressful DNA replication. Genetics *187*, 397-407.

Liu, H., and Wang, Y. (2006). The function and regulation of budding yeast Swe1 in response to interrupted DNA synthesis. Mol Biol Cell *17*, 2746-2756.

Longhese, M.P., Neecke, H., Paciotti, V., Lucchini, G., and Plevani, P. (1996). The 70 kDa subunit of replication protein A is required for the G1/S and intra-S DNA damage checkpoints in budding yeast. Nucleic Acids Res *24*, 3533-3537.

Longtine, M.S., McKenzie, A., Demarini, D.J., Shah, N.G., Wach, A., Brachat, A., Philippsen, P., and Pringle, J.R. (1998). Additional modules for versatile and economical PCR-based gene deletion and modification in Saccharomyces cerevisiae. Yeast *14*, 953-961.

Longtine, M.S., Theesfeld, C.L., McMillan, J.N., Weaver, E., Pringle, J.R., and Lew, D.J. (2000). Septin-dependent assembly of a cell cycle-regulatory module in Saccharomyces cerevisiae. Mol Cell Biol *20*, 4049-4061.

Loog, M., and Morgan, D.O. (2005). Cyclin specificity in the phosphorylation of cyclin-dependent kinase substrates. Nature *434*, 104-108.

Lopes, M., Cotta-Ramusino, C., Pellicioli, A., Liberi, G., Plevani, P., Muzi-Falconi, M., Newlon, C.S., and Foiani, M. (2001). The DNA replication checkpoint response stabilizes stalled replication forks. Nature *412*, 557-561.

Luca, F.C., Mody, M., Kurischko, C., Roof, D.M., Giddings, T.H., and Winey, M. (2001). Saccharomyces cerevisiae Mob1p is required for cytokinesis and mitotic exit. Mol Cell Biol *21*, 6972-6983.

Ma, L., Ho, K., Piggott, N., Luo, Z., and Measday, V. (2012 (in final revisions)). Interactions between the kinetochore complex and the Protein Kinase A pathway in Saccharomyces cerevisiae. G3.

Ma, L., McQueen, J., Cuschieri, L., Vogel, J., and Measday, V. (2007). Spc24 and Stu2 promote spindle integrity when DNA replication is stalled. Molecular biology of the cell *18*, 2805-2816.

Maher, M., Cong, F., Kindelberger, D., Nasmyth, K., and Dalton, S. (1995). Cell cycle-regulated transcription of the CLB2 gene is dependent on Mcm1 and a ternary complex factor. Mol Cell Biol *15*, 3129-3137.

Malathi, K., Xiao, Y., and Mitchell, A.P. (1997). Interaction of yeast repressor-activator protein Ume6p with glycogen synthase kinase 3 homolog Rim11p. Mol Cell Biol *17*, 7230-7236.

Manning, G., Whyte, D.B., Martinez, R., Hunter, T., and Sudarsanam, S. (2002). The protein kinase complement of the human genome. Science *298*, 1912-1934.

Matmati, N., Kitagaki, H., Montefusco, D., Mohanty, B.K., and Hannun, Y.A. (2009). Hydroxyurea sensitivity reveals a role for ISC1 in the regulation of G2/M. J Biol Chem *284*, 8241-8246.

McAinsh, A.D., Tytell, J.D., and Sorger, P.K. (2003). Structure, function, and regulation of budding yeast kinetochores. Annu Rev Cell Dev Biol *19*, 519-539.

McInerny, C.J., Partridge, J.F., Mikesell, G.E., Creemer, D.P., and Breeden, L.L. (1997). A novel Mcm1-dependent element in the SWI4, CLN3, CDC6, and CDC47 promoters activates M/G1-specific transcription. Genes Dev *11*, 1277-1288.

McMillan, J.N., Longtine, M.S., Sia, R.A., Theesfeld, C.L., Bardes, E.S., Pringle, J.R., and Lew, D.J. (1999a). The morphogenesis checkpoint in Saccharomyces cerevisiae: cell cycle control of Swe1p degradation by Hsl1p and Hsl7p. Mol Cell Biol *19*, 6929-6939.

McMillan, J.N., Sia, R.A., Bardes, E.S., and Lew, D.J. (1999b). Phosphorylation-independent inhibition of Cdc28p by the tyrosine kinase Swe1p in the morphogenesis checkpoint. Mol Cell Biol *19*, 5981-5990.

McMillan, J.N., Sia, R.A., and Lew, D.J. (1998). A morphogenesis checkpoint monitors the actin cytoskeleton in yeast. J Cell Biol *142*, 1487-1499.

McMillan, J.N., Theesfeld, C.L., Harrison, J.C., Bardes, E.S., and Lew, D.J. (2002). Determinants of Swe1p degradation in Saccharomyces cerevisiae. Mol Biol Cell *13*, 3560-3575.

Measday, V., Hailey, D.W., Pot, I., Givan, S.A., Hyland, K.M., Cagney, G., Fields, S., Davis, T.N., and Hieter, P. (2002). Ctf3p, the Mis6 budding yeast homolog, interacts with Mcm22p and Mcm16p at the yeast outer kinetochore. Genes Dev *16*, 101-113.

Measday, V., and Hieter, P. (2002). Synthetic dosage lethality. Meth Enzymol *350*, 316-326.

Mendenhall, M.D. (1993). An inhibitor of p34CDC28 protein kinase activity from Saccharomyces cerevisiae. Science *259*, 216-219.

Mendenhall, M.D., and Hodge, A.E. (1998). Regulation of Cdc28 cyclin-dependent protein kinase activity during the cell cycle of the yeast Saccharomyces cerevisiae. Microbiol Mol Biol Rev *62*, 1191-1243.

Miranda, J.J., De Wulf, P., Sorger, P.K., and Harrison, S.C. (2005). The yeast DASH complex forms closed rings on microtubules. Nat Struct Mol Biol *12*, 138-143.

Mitchell, A.P., and Bowdish, K.S. (1992). Selection for early meiotic mutants in yeast. Genetics *131*, 65-72.

Miyakawa, T., and Mizunuma, M. (2007). Physiological roles of calcineurin in Saccharomyces cerevisiae with special emphasis on its roles in G2/M cell-cycle regulation. Biosci Biotechnol Biochem *71*, 633-645.

Mizunuma, M., Hirata, D., Miyaoka, R., and Miyakawa, T. (2001). GSK-3 kinase Mck1 and calcineurin coordinately mediate Hsl1 down-regulation by Ca2+ in budding yeast. EMBO J *20*, 1074-1085.

Mohl, D.A., Huddleston, M.J., Collingwood, T.S., Annan, R.S., and Deshaies, R.J. (2009). Dbf2-Mob1 drives relocalization of protein phosphatase Cdc14 to the cytoplasm during exit from mitosis. J Cell Biol *184*, 527-539.

Montpetit, B., Thorne, K., Barrett, I., Andrews, K., Jadusingh, R., Hieter, P., and Measday, V. (2005). Genome-wide synthetic lethal screens identify an interaction between the nuclear envelope protein, Apq12p, and the kinetochore in Saccharomyces cerevisiae. Genetics *171*, 489-501.

Morgan, D.O. (1997). Cyclin-dependent kinases: engines, clocks, and microprocessors. Annual review of cell and developmental biology *13*, 261-291.

Morgan, D.O. (2007). The cell cycle : principles of control (London
Sunderland, MA: Published by New Science Press in association with Oxford University Press ;
Distributed inside North America by Sinauer Associates, Publishers).

Morris, M.C., Kaiser, P., Rudyak, S., Baskerville, C., Watson, M.H., and Reed, S.I. (2003). Cks1-dependent proteasome recruitment and activation of CDC20 transcription in budding yeast. Nature *423*, 1009-1013.

Morrison, A.J., Kim, J.-A., Person, M.D., Highland, J., Xiao, J., Wehr, T.S., Hensley, S., Bao, Y., Shen, J., Collins, S.R.*, et al.* (2007). Mec1/Tel1 phosphorylation of the INO80 chromatin remodeling complex influences DNA damage checkpoint responses. Cell *130*, 499-511.

Myung, K., Datta, A., and Kolodner, R.D. (2001). Suppression of spontaneous chromosomal rearrangements by S phase checkpoint functions in Saccharomyces cerevisiae. Cell *104*, 397-408.

Nasmyth, K. (1996). At the heart of the budding yeast cell cycle. Trends Genet *12*, 405-412.

Nasmyth, K., and Dirick, L. (1991). The role of SWI4 and SWI6 in the activity of G1 cyclins in yeast. Cell *66*, 995-1013.

Nedelcheva, M.N., Roguev, A., Dolapchiev, L.B., Shevchenko, A., Taskov, H.B., Shevchenko, A., Stewart, A.F., and Stoynov, S.S. (2005). Uncoupling of unwinding from DNA synthesis implies regulation of MCM helicase by Tof1/Mrc1/Csm3 checkpoint complex. J Mol Biol *347*, 509-521.

Neigeborn, L., and Mitchell, A.P. (1991). The yeast MCK1 gene encodes a protein kinase homolog that activates early meiotic gene expression. Genes Dev *5*, 533-548.

Nevitt, T., Pereira, J., and Rodrigues-Pousada, C. (2004). YAP4 gene expression is induced in response to several forms of stress in Saccharomyces cerevisiae. Yeast *21*, 1365-1374.

Nitani, N., Nakamura, K., Nakagawa, C., Masukata, H., and Nakagawa, T. (2006). Regulation of DNA replication machinery by Mrc1 in fission yeast. Genetics *174*, 155-165.

Norden, C., Mendoza, M., Dobbelaere, J., Kotwaliwale, C.V., Biggins, S., and Barral, Y. (2006). The NoCut pathway links completion of cytokinesis to spindle midzone function to prevent chromosome breakage. Cell *125*, 85-98.

Ogas, J., Andrews, B.J., and Herskowitz, I. (1991). Transcriptional activation of CLN1, CLN2, and a putative new G1 cyclin (HCS26) by SWI4, a positive regulator of G1-specific transcription. Cell *66*, 1015-1026.

Oikonomou, C., and Cross, F.R. (2011). Rising cyclin-CDK levels order cell cycle events. PLoS ONE *6*, e20788.

Ozdemir, A., Spicuglia, S., Lasonder, E., Vermeulen, M., Campsteijn, C., Stunnenberg, H.G., and Logie, C. (2005). Characterization of lysine 56 of histone H3 as an acetylation site in Saccharomyces cerevisiae. J Biol Chem *280*, 25949-25952.

Pal, G., Paraz, M.T., and Kellogg, D.R. (2008). Regulation of Mih1/Cdc25 by protein phosphatase 2A and casein kinase 1. J Cell Biol *180*, 931-945.

Palou, G., Palou, R., Guerra-Moreno, A., Duch, A., Travesa, A., and Quintana, D.G. (2010). Cyclin regulation by the s phase checkpoint. J Biol Chem *285*, 26431-26440.

Pan, X., Ye, P., Yuan, D.S., Wang, X., Bader, J.S., and Boeke, J.D. (2006). A DNA Integrity Network in the Yeast Saccharomyces cerevisiae. Cell *124*, 1069-1081.

Pan, X., Yuan, D.S., Xiang, D., Wang, X., Sookhai-Mahadeo, S., Bader, J.S., Hieter, P., Spencer, F., and Boeke, J.D. (2004). A robust toolkit for functional profiling of the yeast genome. Mol Cell *16*, 487-496.

Papamichos-Chronakis, M., and Peterson, C.L. (2008). The Ino80 chromatin-remodeling enzyme regulates replisome function and stability. Nat Struct Mol Biol *15*, 338-345.

Pasqualone, D., and Huffaker, T.C. (1994). STU1, a suppressor of a beta-tubulin mutation, encodes a novel and essential component of the yeast mitotic spindle. J Cell Biol *127*, 1973-1984.

Paulovich, A.G., and Hartwell, L.H. (1995). A checkpoint regulates the rate of progression through S phase in S. cerevisiae in response to DNA damage. Cell *82*, 841-847.

Pearson, C.G., Maddox, P.S., Salmon, E.D., and Bloom, K. (2001). Budding yeast chromosome structure and dynamics during mitosis. J Cell Biol *152*, 1255-1266.

Pereira, J., Pimentel, C., Amaral, C., Menezes, R.A., and Rodrigues-Pousada, C. (2009). Yap4 PKA- and GSK3-dependent phosphorylation affects its stability but not its nuclear localization. Yeast *26*, 641-653.

Peter, M., and Herskowitz, I. (1994). Direct inhibition of the yeast cyclin-dependent kinase Cdc28-Cln by Far1. Science *265*, 1228-1231.

Pic-Taylor, A., Darieva, Z., Morgan, B.A., and Sharrocks, A.D. (2004). Regulation of cell cycle-specific gene expression through cyclin-dependent kinase-mediated phosphorylation of the forkhead transcription factor Fkh2p. Mol Cell Biol *24*, 10036-10046.

Pinsky, B.A., Kung, C., Shokat, K.M., and Biggins, S. (2006). The Ipl1-Aurora protein kinase activates the spindle checkpoint by creating unattached kinetochores. Nat Cell Biol *8*, 78-83.

Porter, S.E., and Champoux, J.J. (1989). The basis for camptothecin enhancement of DNA breakage by eukaryotic topoisomerase I. Nucleic Acids Res *17*, 8521-8532.

Pot, I., Knockleby, J., Aneliunas, V., Nguyen, T., Ah-Kye, S., Liszt, G., Snyder, M., Hieter, P., and Vogel, J. (2005). Spindle checkpoint maintenance requires Ame1 and Okp1. Cell Cycle *4*, 1448-1456.

Pot, I., Measday, V., Snydsman, B., Cagney, G., Fields, S., Davis, T.N., Muller, E.G., and Hieter, P. (2003). Chl4p and iml3p are two new members of the budding yeast outer kinetochore. Mol Biol Cell *14*, 460-476.

Pramila, T., Wu, W., Miles, S., Noble, W.S., and Breeden, L.L. (2006). The Forkhead transcription factor Hcm1 regulates chromosome segregation genes and fills the S-phase gap in the transcriptional circuitry of the cell cycle. Genes Dev *20*, 2266-2278.

Ptacek, J., Devgan, G., Michaud, G., Zhu, H., Zhu, X., Fasolo, J., Guo, H., Jona, G., Breitkreutz, A., Sopko, R.*, et al.* (2005). Global analysis of protein phosphorylation in yeast. Nature *438*, 679-684.

Putnam, C.D., Jaehnig, E.J., and Kolodner, R.D. (2009). Perspectives on the DNA damage and replication checkpoint responses in Saccharomyces cerevisiae. DNA Repair (Amst) *8*, 974-982.

Puziss, J.W., Hardy, T.A., Johnson, R.B., Roach, P.J., and Hieter, P. (1994). MDS1, a dosage suppressor of an mck1 mutant, encodes a putative yeast homolog of glycogen synthase kinase 3. Mol Cell Biol *14*, 831-839.

Queralt, E., and Igual, J.C. (2004). Functional distinction between Cln1p and Cln2p cyclins in the control of the Saccharomyces cerevisiae mitotic cycle. Genetics *168*, 129-140.

Queralt, E., Lehane, C., Novak, B., and Uhlmann, F. (2006). Downregulation of PP2A(Cdc55) phosphatase by separase initiates mitotic exit in budding yeast. Cell *125*, 719-732.

Rahal, R., and Amon, A. (2008). Mitotic CDKs control the metaphase-anaphase transition and trigger spindle elongation. Genes Dev *22*, 1534-1548.

Raspelli, E., Cassani, C., Lucchini, G., and Fraschini, R. (2011). Budding yeast Dma1 and Dma2 participate in regulation of Swe1 levels and localization. Mol Biol Cell.

Rayner, T.F., Gray, J.V., and Thorner, J.W. (2002). Direct and novel regulation of cAMP-dependent protein kinase by Mck1p, a yeast glycogen synthase kinase-3. J Biol Chem *277*, 16814-16822.

Redon, C., Pilch, D.R., Rogakou, E.P., Orr, A.H., Lowndes, N.F., and Bonner, W.M. (2003). Yeast histone 2A serine 129 is essential for the efficient repair of checkpoint-blind DNA damage. EMBO Rep *4*, 678-684.

Reid, B.J., and Hartwell, L.H. (1977). Regulation of mating in the cell cycle of Saccharomyces cerevisiae. J Cell Biol *75*, 355-365.

Rhind, N., Furnari, B., and Russell, P. (1997). Cdc2 tyrosine phosphorylation is required for the DNA damage checkpoint in fission yeast. Genes Dev *11*, 504-511.

Richardson, H., Lew, D.J., Henze, M., Sugimoto, K., and Reed, S.I. (1992). Cyclin-B homologs in Saccharomyces cerevisiae function in S phase and in G2. Genes Dev *6*, 2021-2034.

Richardson, H.E., Wittenberg, C., Cross, F., and Reed, S.I. (1989). An essential G1 function for cyclin-like proteins in yeast. Cell *59*, 1127-1133.

Rock, J.M., and Amon, A. (2011). Cdc15 integrates Tem1 GTPase-mediated spatial signals with Polo kinase-mediated temporal cues to activate mitotic exit. Genes Dev *25*, 1943-1954.

Roof, D.M., Meluh, P.B., and Rose, M.D. (1992). Kinesin-related proteins required for assembly of the mitotic spindle. J Cell Biol *118*, 95-108.

Ross, K.E., and Cohen-Fix, O. (2004). A role for the FEAR pathway in nuclear positioning during anaphase. Dev Cell *6*, 729-735.

Rubin-Bejerano, I., Mandel, S., Robzyk, K., and Kassir, Y. (1996). Induction of meiosis in Saccharomyces cerevisiae depends on conversion of the transcriptional represssor Ume6 to a positive regulator by its regulated association with the transcriptional activator Ime1. Mol Cell Biol *16*, 2518-2526.

Rudner, A.D., and Murray, A.W. (2000). Phosphorylation by Cdc28 activates the Cdc20-dependent activity of the anaphase-promoting complex. J Cell Biol *149*, 1377-1390.

Russell, I.D., Grancell, A.S., and Sorger, P.K. (1999). The unstable F-box protein p58-Ctf13 forms the structural core of the CBF3 kinetochore complex. J Cell Biol *145*, 933-950.

Russell, P., Moreno, S., and Reed, S.I. (1989). Conservation of mitotic controls in fission and budding yeasts. Cell *57*, 295-303.

Sakchaisri, K., Asano, S., Yu, L.-R., Shulewitz, M.J., Park, C.J., Park, J.-E., Cho, Y.-W., Veenstra, T.D., Thorner, J., and Lee, K.S. (2004). Coupling morphogenesis to mitotic entry. Proc Natl Acad Sci USA *101*, 4124-4129.

Sanchez, Y., Bachant, J., Wang, H., Hu, F., Liu, D., Tetzlaff, M., and Elledge, S.J. (1999). Control of the DNA damage checkpoint by chk1 and rad53 protein kinases through distinct mechanisms. Science *286*, 1166-1171.

Santocanale, C., and Diffley, J.F. (1998). A Mec1- and Rad53-dependent checkpoint controls late-firing origins of DNA replication. Nature *395*, 615-618.

Santocanale, C., Sharma, K., and Diffley, J.F. (1999). Activation of dormant origins of DNA replication in budding yeast. Genes Dev *13*, 2360-2364.

Sarin, S., Ross, K.E., Boucher, L., Green, Y., Tyers, M., and Cohen-Fix, O. (2004). Uncovering novel cell cycle players through the inactivation of securin in budding yeast. Genetics *168*, 1763-1771.

Schneider, B.L., Yang, Q.H., and Futcher, A.B. (1996). Linkage of replication to start by the Cdk inhibitor Sic1. Science *272*, 560-562.

Schwab, M., Lutum, A.S., and Seufert, W. (1997). Yeast Hct1 is a regulator of Clb2 cyclin proteolysis. Cell *90*, 683-693.

Schwab, M., Neutzner, M., Mocker, D., and Seufert, W. (2001). Yeast Hct1 recognizes the mitotic cyclin Clb2 and other substrates of the ubiquitin ligase APC. EMBO J *20*, 5165-5175.

Schwob, E., Böhm, T., Mendenhall, M.D., and Nasmyth, K. (1994). The B-type cyclin kinase inhibitor p40SIC1 controls the G1 to S transition in S. cerevisiae. Cell *79*, 233-244.

Schwob, E., and Nasmyth, K. (1993). CLB5 and CLB6, a new pair of B cyclins involved in DNA replication in Saccharomyces cerevisiae. Genes Dev *7*, 1160-1175.

Searle, J.S., Schollaert, K.L., Wilkins, B.J., and Sanchez, Y. (2004). The DNA damage checkpoint and PKA pathways converge on APC substrates and Cdc20 to regulate mitotic progression. Nat Cell Biol *6*, 138-145.

Searle, J.S., Wood, M.D., Kaur, M., Tobin, D.V., and Sanchez, Y. (2011). Proteins in the nutrient-sensing and DNA damage checkpoint pathways cooperate to restrain mitotic progression following DNA damage. PLoS Genet *7*, e1002176.

Segal, M. (2011). Mitotic exit control: a space and time odyssey. Curr Biol *21*, R857-859.

Segurado, M., and Tercero, J.A. (2009). The S-phase checkpoint: targeting the replication fork. Biol Cell *101*, 617-627.

Seufert, W., Futcher, B., and Jentsch, S. (1995). Role of a ubiquitin-conjugating enzyme in degradation of S- and M-phase cyclins. Nature *373*, 78-81.

Severin, F., Habermann, B., Huffaker, T., and Hyman, T. (2001). Stu2 promotes mitotic spindle elongation in anaphase. J Cell Biol *153*, 435-442.

Sharifpoor, S., van Dyk, D., Costanzo, M., Baryshnikova, A., Friesen, H., Douglas, A.C., Youn, J.-Y., VanderSluis, B., Myers, C.L., Papp, B.*, et al.* (2012). Functional wiring of the yeast kinome revealed by global analysis of genetic network motifs. Genome research.

Shero, J.H., and Hieter, P. (1991). A suppressor of a centromere DNA mutation encodes a putative protein kinase (MCK1). Genes Dev *5*, 549-560.

Shimada, K., Oma, Y., Schleker, T., Kugou, K., Ohta, K., Harata, M., and Gasser, S.M. (2008). Ino80 chromatin remodeling complex promotes recovery of stalled replication forks. Curr Biol *18*, 566-575.

Shimogawa, M.M., Graczyk, B., Gardner, M.K., Francis, S.E., White, E.A., Ess, M., Molk, J.N., Ruse, C., Niessen, S., Yates, J.R., 3rd*, et al.* (2006). Mps1 phosphorylation of dam1 couples kinetochores to microtubule plus ends at metaphase. Curr Biol *16*, 1489-1501.

Shirahige, K., Hori, Y., Shiraishi, K., Yamashita, M., Takahashi, K., Obuse, C., Tsurimoto, T., and Yoshikawa, H. (1998). Regulation of DNA-replication origins during cell-cycle progression. Nature *395*, 618-621.

Shirayama, M., Tóth, A., Gálová, M., and Nasmyth, K. (1999). APC(Cdc20) promotes exit from mitosis by destroying the anaphase inhibitor Pds1 and cyclin Clb5. Nature *402*, 203-207.

Shulewitz, M.J., Inouye, C.J., and Thorner, J. (1999). Hsl7 localizes to a septin ring and serves as an adapter in a regulatory pathway that relieves tyrosine phosphorylation of Cdc28 protein kinase in Saccharomyces cerevisiae. Mol Cell Biol *19*, 7123-7137.

Sia, R.A., Herald, H.A., and Lew, D.J. (1996). Cdc28 tyrosine phosphorylation and the morphogenesis checkpoint in budding yeast. Mol Biol Cell *7*, 1657-1666.

Skotheim, J.M., Di Talia, S., Siggia, E.D., and Cross, F.R. (2008). Positive feedback of G1 cyclins ensures coherent cell cycle entry. Nature *454*, 291-296.

Skowyra, D., Koepp, D.M., Kamura, T., Conrad, M.N., Conaway, R.C., Conaway, J.W., Elledge, S.J., and Harper, J.W. (1999). Reconstitution of G1 cyclin ubiquitination with complexes containing SCFGrr1 and Rbx1. Science *284*, 662-665.

Sogo, J.M., Lopes, M., and Foiani, M. (2002). Fork reversal and ssDNA accumulation at stalled replication forks owing to checkpoint defects. Science *297*, 599-602.

Song, S., and Lee, K.S. (2001). A novel function of Saccharomyces cerevisiae CDC5 in cytokinesis. J Cell Biol *152*, 451-469.

Sopko, R., Huang, D., Preston, N., Chua, G., Papp, B., Kafadar, K., Snyder, M., Oliver, S.G., Cyert, M., Hughes, T.R.*, et al.* (2006). Mapping pathways and phenotypes by systematic gene overexpression. Mol Cell *21*, 319-330.

Sorger, P.K., and Murray, A.W. (1992). S-phase feedback control in budding yeast independent of tyrosine phosphorylation of p34cdc28. Nature *355*, 365-368.

Stegmeier, F., Visintin, R., and Amon, A. (2002). Separase, polo kinase, the kinetochore protein Slk19, and Spo12 function in a network that controls Cdc14 localization during early anaphase. Cell *108*, 207-220.

Strickfaden, S.C., Winters, M.J., Ben-Ari, G., Lamson, R.E., Tyers, M., and Pryciak, P.M. (2007). A mechanism for cell-cycle regulation of MAP kinase signaling in a yeast differentiation pathway. Cell *128*, 519-531.

Stuart, D., and Wittenberg, C. (1995). CLN3, not positive feedback, determines the timing of CLN2 transcription in cycling cells. Genes Dev *9*, 2780-2794.

Sullivan, M., Higuchi, T., Katis, V.L., and Uhlmann, F. (2004). Cdc14 phosphatase induces rDNA condensation and resolves cohesin-independent cohesion during budding yeast anaphase. Cell *117*, 471-482.

Sullivan, M., and Morgan, D.O. (2007). Finishing mitosis, one step at a time. Nat Rev Mol Cell Biol *8*, 894-903.

Surana, U., Amon, A., Dowzer, C., McGrew, J., Byers, B., and Nasmyth, K. (1993). Destruction of the CDC28/CLB mitotic kinase is not required for the metaphase to anaphase transition in budding yeast. EMBO J *12*, 1969-1978.

Surana, U., Robitsch, H., Price, C., Schuster, T., Fitch, I., Futcher, A.B., and Nasmyth, K. (1991). The role of CDC28 and cyclins during mitosis in the budding yeast S. cerevisiae. Cell *65*, 145-161.

Sutherland, C. (2011). What Are the bona fide GSK3 Substrates? Int J Alzheimers Dis *2011*, 505607.

Takahashi-Yanaga, F., and Sasaguri, T. (2008). GSK-3beta regulates cyclin D1 expression: a new target for chemotherapy. Cell Signal *20*, 581-589.

Takahata, S., Yu, Y., and Stillman, D.J. (2009). The E2F functional analogue SBF recruits the Rpd3(L) HDAC, via Whi5 and Stb1, and the FACT chromatin reorganizer, to yeast G1 cyclin promoters. EMBO J *28*, 3378-3389.

Tan, C.S., Bodenmiller, B., Pasculescu, A., Jovanovic, M., Hengartner, M.O., Jorgensen, C., Bader, G.D., Aebersold, R., Pawson, T., and Linding, R. (2009). Comparative analysis reveals conserved protein phosphorylation networks implicated in multiple diseases. Sci Signal *2*, ra39.

Tanaka, K., Mukae, N., Dewar, H., van Breugel, M., James, E.K., Prescott, A.R., Antony, C., and Tanaka, T.U. (2005). Molecular mechanisms of kinetochore capture by spindle microtubules. Nature *434*, 987-994.

Tercero, J.A., and Diffley, J.F. (2001). Regulation of DNA replication fork progression through damaged DNA by the Mec1/Rad53 checkpoint. In Nature, pp. 553-557.

Tercero, J.A., Longhese, M.P., and Diffley, J.F.X. (2003). A central role for DNA replication forks in checkpoint activation and response. Mol Cell *11*, 1323-1336.

Thaminy, S., Newcomb, B., Kim, J., Gatbonton, T., Foss, E., Simon, J., and Bedalov, A. (2007). Hst3 is regulated by Mec1-dependent proteolysis and controls the S phase checkpoint

and sister chromatid cohesion by deacetylating histone H3 at lysine 56. J Biol Chem *282*, 37805-37814.

Tong, A.H., Evangelista, M., Parsons, A.B., Xu, H., Bader, G.D., Pagé, N., Robinson, M., Raghibizadeh, S., Hogue, C.W., Bussey, H.*, et al.* (2001). Systematic genetic analysis with ordered arrays of yeast deletion mutants. Science *294*, 2364-2368.

Tong, A.H., Lesage, G., Bader, G.D., Ding, H., Xu, H., Xin, X., Young, J., Berriz, G.F., Brost, R.L., Chang, M.*, et al.* (2004). Global mapping of the yeast genetic interaction network. Science *303*, 808-813.

Toyn, J.H., Johnson, A.L., Donovan, J.D., Toone, W.M., and Johnston, L.H. (1997). The Swi5 transcription factor of Saccharomyces cerevisiae has a role in exit from mitosis through induction of the cdk-inhibitor Sic1 in telophase. Genetics *145*, 85-96.

Toyn, J.H., and Johnston, L.H. (1994). The Dbf2 and Dbf20 protein kinases of budding yeast are activated after the metaphase to anaphase cell cycle transition. EMBO J *13*, 1103-1113.

Travesa, A., Kuo, D., de Bruin, R.A.M., Kalashnikova, T.I., Guaderrama, M., Thai, K., Aslanian, A., Smolka, M.B., Yates, J.R., Ideker, T.*, et al.* (2012). DNA replication stress differentially regulates G1/S genes via Rad53-dependent inactivation of Nrm1. EMBO J.

Tripathi, K., Matmati, N., Zheng, W.J., Hannun, Y.A., and Mohanty, B.K. (2011). Cellular morphogenesis under stress is influenced by the sphingolipid pathway gene ISC1 and DNA integrity checkpoint genes in Saccharomyces cerevisiae. Genetics *189*, 533-547.

Tyers, M., and Futcher, B. (1993). Far1 and Fus3 link the mating pheromone signal transduction pathway to three G1-phase Cdc28 kinase complexes. Mol Cell Biol *13*, 5659-5669.

Tyers, M., Tokiwa, G., and Futcher, B. (1993). Comparison of the Saccharomyces cerevisiae G1 cyclins: Cln3 may be an upstream activator of Cln1, Cln2 and other cyclins. EMBO J *12*, 1955-1968.

Tyers, M., Tokiwa, G., Nash, R., and Futcher, B. (1992). The Cln3-Cdc28 kinase complex of S. cerevisiae is regulated by proteolysis and phosphorylation. EMBO J *11*, 1773-1784.

Tytell, J.D., and Sorger, P.K. (2006). Analysis of kinesin motor function at budding yeast kinetochores. J Cell Biol *172*, 861-874.

Uhlmann, F., Lottspeich, F., and Nasmyth, K. (1999). Sister-chromatid separation at anaphase onset is promoted by cleavage of the cohesin subunit Scc1. Nature *400*, 37-42.

Vallen, E.A., and Cross, F.R. (1999). Interaction between the MEC1-dependent DNA synthesis checkpoint and G1 cyclin function in Saccharomyces cerevisiae. Genetics *151*, 459-471.

Vázquez, M.V., Rojas, V., and Tercero, J.A. (2008). Multiple pathways cooperate to facilitate DNA replication fork progression through alkylated DNA. DNA Repair (Amst) *7*, 1693-1704.

Verma, R., Annan, R.S., Huddleston, M.J., Carr, S.A., Reynard, G., and Deshaies, R.J. (1997). Phosphorylation of Sic1p by G1 Cdk required for its degradation and entry into S phase. Science *278*, 455-460.

Visintin, R., and Amon, A. (2001). Regulation of the mitotic exit protein kinases Cdc15 and Dbf2. Mol Biol Cell *12*, 2961-2974.

Visintin, R., Craig, K., Hwang, E.S., Prinz, S., Tyers, M., and Amon, A. (1998). The phosphatase Cdc14 triggers mitotic exit by reversal of Cdk-dependent phosphorylation. Mol Cell *2*, 709-718.

Visintin, R., Hwang, E.S., and Amon, A. (1999). Cfi1 prevents premature exit from mitosis by anchoring Cdc14 phosphatase in the nucleolus. Nature *398*, 818-823.

Visintin, R., Prinz, S., and Amon, A. (1997). CDC20 and CDH1: a family of substrate-specific activators of APC-dependent proteolysis. Science *278*, 460-463.

W. Caldecott, K. (2004). Eukaryotic DNA damage surveillance and repair. 161.

Wang, H., Carey, L.B., Cai, Y., Wijnen, H., and Futcher, B. (2009). Recruitment of Cln3 cyclin to promoters controls cell cycle entry via histone deacetylase and other targets. PLoS Biol *7*, e1000189.

Wang, H., Liu, D., Wang, Y., Qin, J., and Elledge, S.J. (2001). Pds1 phosphorylation in response to DNA damage is essential for its DNA damage checkpoint function. Genes Dev *15*, 1361-1372.

Wang, P.J., and Huffaker, T.C. (1997). Stu2p: A microtubule-binding protein that is an essential component of the yeast spindle pole body. J Cell Biol *139*, 1271-1280.

Wäsch, R., and Cross, F.R. (2002). APC-dependent proteolysis of the mitotic cyclin Clb2 is essential for mitotic exit. Nature *418*, 556-562.

Wei, R.R., Sorger, P.K., and Harrison, S.C. (2005). Molecular organization of the Ndc80 complex, an essential kinetochore component. Proc Natl Acad Sci U S A *102*, 5363-5367.

Weinert, T.A., and Hartwell, L.H. (1988). The RAD9 gene controls the cell cycle response to DNA damage in Saccharomyces cerevisiae. Science *241*, 317-322.

Weinert, T.A., Kiser, G.L., and Hartwell, L.H. (1994). Mitotic checkpoint genes in budding yeast and the dependence of mitosis on DNA replication and repair. Genes Dev *8*, 652-665.

Westermann, S., Avila-Sakar, A., Wang, H.W., Niederstrasser, H., Wong, J., Drubin, D.G., Nogales, E., and Barnes, G. (2005). Formation of a dynamic kinetochore- microtubule interface through assembly of the Dam1 ring complex. Mol Cell *17*, 277-290.

Westermann, S., Drubin, D.G., and Barnes, G. (2007). Structures and functions of yeast kinetochore complexes. Annu Rev Biochem *76*, 563-591.

Wigge, P.A., and Kilmartin, J.V. (2001). The Ndc80p complex from Saccharomyces cerevisiae contains conserved centromere components and has a function in chromosome segregation. J Cell Biol *152*, 349-360.

Wilmes, G.M., Archambault, V., Austin, R.J., Jacobson, M.D., Bell, S.P., and Cross, F.R. (2004). Interaction of the S-phase cyclin Clb5 with an "RXL" docking sequence in the initiator protein Orc6 provides an origin-localized replication control switch. Genes Dev *18*, 981-991.

Wittenberg, C., and Reed, S.I. (1988). Control of the yeast cell cycle is associated with assembly/disassembly of the Cdc28 protein kinase complex. Cell *54*, 1061-1072.

Wittenberg, C., and Reed, S.I. (2005). Cell cycle-dependent transcription in yeast: promoters, transcription factors, and transcriptomes. Oncogene *24*, 2746-2755.

Wolyniak, M.J., Blake-Hodek, K., Kosco, K., Hwang, E., You, L., and Huffaker, T.C. (2006). The regulation of microtubule dynamics in Saccharomyces cerevisiae by three interacting plus-end tracking proteins. Mol Biol Cell *17*, 2789-2798.

Wysocki, R., Javaheri, A., Kristjansdottir, K., Sha, F., and Kron, S.J. (2006). CDK Pho85 targets CDK inhibitor Sic1 to relieve yeast G1 checkpoint arrest after DNA damage. Nat Struct Mol Biol *13*, 908-914.

Xiao, Y., and Mitchell, A.P. (2000). Shared roles of yeast glycogen synthase kinase 3 family members in nitrogen-responsive phosphorylation of meiotic regulator Ume6p. Mol Cell Biol *20*, 5447-5453.

Xu, C., Kim, N.G., and Gumbiner, B.M. (2009). Regulation of protein stability by GSK3 mediated phosphorylation. Cell Cycle *8*, 4032-4039.

Yabuki, N., Terashima, H., and Kitada, K. (2002). Mapping of early firing origins on a replication profile of budding yeast. Genes Cells *7*, 781-789.

Yaglom, J., Linskens, M.H., Sadis, S., Rubin, D.M., Futcher, B., and Finley, D. (1995). p34Cdc28-mediated control of Cln3 cyclin degradation. Mol Cell Biol *15*, 731-741.

Yin, H., You, L., Pasqualone, D., Kopski, K.M., and Huffaker, T.C. (2002). Stu1p is physically associated with beta-tubulin and is required for structural integrity of the mitotic spindle. Mol Biol Cell *13*, 1881-1892.

Yu, V.P., Baskerville, C., Grünenfelder, B., and Reed, S.I. (2005). A kinase-independent function of Cks1 and Cdk1 in regulation of transcription. Mol Cell *17*, 145-151.

Yu, V.P., and Reed, S.I. (2004). Cks1 is dispensable for survival in Saccharomyces cerevisiae. Cell Cycle *3*, 1402-1404.

Zachariae, W., Schwab, M., Nasmyth, K., and Seufert, W. (1998). Control of cyclin ubiquitination by CDK-regulated binding of Hct1 to the anaphase promoting complex. Science *282*, 1721-1724.

Zachariae, W., Shin, T.H., Galova, M., Obermaier, B., and Nasmyth, K. (1996). Identification of subunits of the anaphase-promoting complex of Saccharomyces cerevisiae. Science *274*, 1201-1204.

Zegerman, P., and Diffley, J.F.X. (2010). Checkpoint-dependent inhibition of DNA replication initiation by Sld3 and Dbf4 phosphorylation. Nature *467*, 474-478.

Zhan, X.L., Hong, Y., Zhu, T., Mitchell, A.P., Deschenes, R.J., and Guan, K.L. (2000). Essential functions of protein tyrosine phosphatases PTP2 and PTP3 and RIM11 tyrosine phosphorylation in Saccharomyces cerevisiae meiosis and sporulation. Mol Biol Cell *11*, 663-676.

Zhang, T., Nirantar, S., Lim, H.H., Sinha, I., and Surana, U. (2009). DNA damage checkpoint maintains CDH1 in an active state to inhibit anaphase progression. Dev Cell *17*, 541-551.

Zhou, B.B., and Elledge, S.J. (2000). The DNA damage response: putting checkpoints in perspective. Nature *408*, 433-439.

Zhu, G., and Davis, T.N. (1998). The fork head transcription factor Hcm1p participates in the regulation of SPC110, which encodes the calmodulin-binding protein in the yeast spindle pole body. Biochim Biophys Acta *1448*, 236-244.

Zhu, G., Muller, E.G., Amacher, S.L., Northrop, J.L., and Davis, T.N. (1993). A dosage-dependent suppressor of a temperature-sensitive calmodulin mutant encodes a protein related to the fork head family of DNA-binding proteins. Mol Cell Biol *13*, 1779-1787.

Zou, L., and Elledge, S.J. (2003). Sensing DNA damage through ATRIP recognition of RPA-ssDNA complexes. Science *300*, 1542-1548.

Zou, L., Liu, D., and Elledge, S.J. (2003). Replication protein A-mediated recruitment and activation of Rad17 complexes. Proc Natl Acad Sci USA *100*, 13827-13832.